

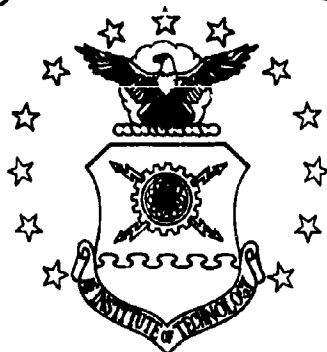
UNCLASSIFIED

AD NUMBER
AD875403
NEW LIMITATION CHANGE
TO Approved for public release, distribution unlimited
FROM Distribution authorized to U.S. Gov't. agencies and their contractors; Administrative/Operational Use; Jun 1970. Other requests shall be referred to Air Force Institute of Technology, Wright-Patterson AFB, Ohio 45433.
AUTHORITY
AFIT Memo, 22 Jul 1971

THIS PAGE IS UNCLASSIFIED

AD875403

# AIR FORCE INSTITUTE OF TECHNOLOGY



AIR UNIVERSITY  
UNITED STATES AIR FORCE

AD No. \_\_\_\_\_  
DDG FILE COPY

SYNTHESIS OF A SUBOPTIMAL  
GUIDANCE LAW TO MINIMIZE THE  
TERMINAL ERROR OF AN ENTRY VEHICLE

THESIS

Richard E. Holdeman  
Civ. USAF

Michael W. Wynne  
Capt. USAF

GGC/EE/70-10

SCHOOL OF ENGINEERING

RECEIVED  
OCT 25 1970  
RECEIVED

WRIGHT-PATTERSON AIR FORCE BASE, OHIO

A

184

SYNTHESIS OF A SUBOPTIMAL  
GUIDANCE LAW TO MINIMIZE THE  
TERMINAL ERROR OF AN ENTRY VEHICLE

THESIS

Richard E. Holdeman  
Civ. USAF

GCC/EE/70-10

Michael W. Wynne  
Capt. USAF

This document is subject to special export controls and each transmittal to foreign governments or foreign nationals may be made only with prior approval of the Dean of Engineering, Air Force Institute of Technology (AFIT-SE), Wright Patterson Air Force Base, Ohio, 45433.

SYNTHESIS OF A SUBOPTIMAL GUIDANCE LAW TO MINIMIZE  
THE TERMINAL ERROR OF AN ENTRY VEHICLE

THESIS

Presented to the Faculty of the School of Engineering of  
the Air Force Institute of Technology

Air University

in Partial Fulfillment of the

Requirements for the

Master of Science Degree

in Electrical Engineering

by

Richard E. Holdeman, B.S.  
Civ. USAF

Michael W. Wynne, B.S.  
Capt. USAF

Graduate Guidance and Control

June 1970

This document is subject to special export controls and each transmittal to foreign governments or foreign nationals may be made only with prior approval of the Dean of Engineering, Air Force Institute of Technology (AFIT-SE), Wright Patterson Air Force Base, Ohio, 45433.



Preface

This thesis, suggested by a term problem by Capt. J. Henry and Mr. R. Ringo, AFIT-SE, GCC-69, concerns the use of optimal control techniques for sensitivity coefficient minimization for a non-thrusting entry vehicle. A simulation of an optimal implicit guidance scheme including a Kalman filter is accomplished to verify the results.

We wish to express our appreciation to Lt. Col. Roger W. Johnson, AFIT-SE, our sponsor and advisor. This topic was originally suggested by Lt. Col. Johnson based on the results of his doctoral dissertation (Ref. 1). His continued assistance and encouragement proved invaluable throughout this investigation. We are also indebted to Lt. Col. R. A. Hannen, AFIT-SE, for his advice and instruction in the fields of optimal control and state estimation. Discussions at considerable length with Capt. T. R. Filiatreau, a contemporary student and co-author of a thesis on Kalman filtering applied to orbit determination, are also gratefully acknowledged.

Finally, to our wives, Judith Holdeman and Barbara Wynne, who typed, edited, and translated the thesis while their husbands were at the computer center, we express our deepest appreciation and thanks. Without their continued assistance and understanding, this thesis would not be.

Any errors or oversites in the body of this thesis are the complete and total responsibility of the other author.

Table Of Contents

Preface .....	II
List of Figures .....	V
List of Tables .....	VII
Abstract .....	VIII
I. Introduction .....	1
Background .....	1
Purpose .....	1
Assumptions .....	2
Approach to the Problem .....	3
II. Optimization Techniques .....	5
Statement of the General Optimal Control Problem .....	5
Summary of the Pontryagin Maximum Principle .....	6
Open-Loop Optimal Control Methods .....	9
First Variation Gradient Technique .....	9
First Variation Terminal Error Function Technique .....	10
Second Variation Technique .....	13
Suboptimal Closed-Loop Control Methods .....	22
Optimal State Estimation .....	25
Initial Estimate of the Error Covariance Matrix .....	31
III. Derivation of Basic Entry Equations .....	35
State Vector Equations of Motion .....	35
Sensitivity Coefficient Equations .....	39
Lumped-Parameter Control Equations .....	41
IV. Optimization Equations for the Entry Problem .....	46
The Criterion Function .....	46
The Necessary Conditions for Optimality .....	47
Second Variation Equations .....	50
Numerical Applications of the Optimization Algorithms .....	52
General Discussion of Algorithms .....	52
First Variation Numerical Considerations .....	54
Second Variation Numerical Considerations .....	56
V. Trajectory Solutions .....	59
Unconstrained Control Solutions .....	60
Solutions With Lift and Drag Control Constraints .....	72
Solution With Drag Control Constraints Only .....	79
Discussion of Trajectory Solutions .....	83

VI.	Optimal Implicit Guidance Simulation for the Entry Problem .	89
	Definition of Optimal Implicit Guidance .....	89
	Assumptions .....	90
	Entry Feedback Equations .....	91
	Digital Computer Simulation .....	93
VII.	Simulation Results .....	98
VIII.	Conclusions .....	144
IX.	Reccommendations .....	147
	References .....	150
	Appendix A: Open-Loop Optimal Control Equations for the Entry Problem .....	152
	Appendix B: Parameters for Sample Trajectory .....	169
Vita:	Richard Eugene Holdeman .....	170
Vita:	Michael Walter Wynne .....	171

List Of Figures

<u>Figure</u>	<u>Page</u>
1. Neighboring Trajectory for Linear Feedback Scheme .....	24
2. Block Diagram for Implementing Feedback Gains .....	24
3. Entry Geometry .....	35
4. Shock Wave Geometry .....	43
5. Solution Flow Diagram .....	53
6. States .....	61
7. Sensitivity Coefficients .....	61
8. Optimal Controls .....	62
9. Lift/Drag .....	62
10-13. Same as Case 1 .....	64-65
14-17. Same as Case 1 .....	67-68
18-21. Same as Case 1 .....	70-71
22-25. Same as Case 1 .....	73-74
26-29. Same as Case 1 .....	77-78
30-33. Same as Case 1 .....	81-82
34. Optimal Implicit Guidance Block Diagram .....	90
35. Simulation Indexing Method .....	94
36-37. Control Gains for Case 1 .....	100
38. Position Error .....	101
39. Velocity Error .....	102
40. Flight Angle Error .....	103
41-42. Error Covariance Terms .....	104
43-47. Same as Case 1.1 .....	105-108
48-52. Same as Case 1.1, without noise .....	109-112

	Case 1.4	
53-57.	Same as Case 1.1 .....	113-116
	Case 1.5	
58-62.	Same as Case 1.1 .....	117-120
63-64.	Control Gains for Case 7 .....	121
	Case 7.1	
65-69.	Same as Case 1.1 .....	122-125
	Case 7.2	
70-74.	Same as Case 1.1 .....	126-129
	Case 7.3	
75-79.	Same as Case 1.1, without noise .....	130-133
	Case 7.4	
80-84.	Same as Case 1.1 .....	134-137
	Case 7.5	
85-89.	Same as Case 1.1 .....	138-141

List Of Tables

<u>Table</u>	<u>Page</u>
I. Constraints on Variables .....	8
II. Boundary Conditions for the Entry Problem .....	50
III. Known Boundary Conditions for Gradient Algorithm .....	55
IV. Summary of Trajectory Solutions .....	85

Abstract

The objective of this thesis is to minimize the terminal position error of an entry vehicle. To do this, the concept of minimizing the position sensitivity coefficients is employed. With this in mind, two purposes are established: first, to investigate a set of optimal solutions minimizing a criterion function of sensitivity coefficients; and, second, to form a suboptimal guidance law for these trajectories. The trajectories are generated by using a type of control which includes parameters describing the vehicle configuration and attitude. This is called a lumped parameter control. Due to the use of a lumped parameter control, a Valentine's procedure is employed to restrict the range to a set of realistic design values. A closed-loop optimal implicit guidance scheme including a state estimator is used in a simulation of selected trajectories to test the validity of the feedback gains determined for the trajectories.

The minimum sensitivity coefficient trajectory appears to be one in which the vehicle first levels out to nearly horizontal flight and then dives to achieve the desired terminal flight path angle. The values of the radius and flight path angle sensitivity coefficients for this type of trajectory are about an order of magnitude lower than for other types considered, while the maximum velocity sensitivity coefficient remains about the same.

For most of the cases considered, there appears to be a definite relationship between the sensitivity coefficients and range angle and rate of change of flight path angle. For all cases but one, the flight path angle sensitivity coefficient is nearly a linear function of

range angle.

The simulation results using a set of feedback gains and assuming noisy observations drives the system to within 5 m, 2 mps, and 0.2 deg at the terminal point with initial errors of 5000 m, 100 mps, and 1.0 deg in position, velocity, and flight path angle respectively.



SYNTHESIS OF A SUBOPTIMAL GUIDANCE LAW TO MINIMIZE  
THE TERMINAL ERROR OF AN ENTRY VEHICLE

I. Introduction

Background

When a vehicle enters the earth's atmosphere, any error in its position vector or velocity vector will cause a subsequent position error at the desired terminal point. The quantities which describe the sensitivity of the position error at the terminal point are called sensitivity coefficients or influence coefficients. One method of minimizing the position error at the terminal point is to minimize these sensitivity coefficients. A trajectory which minimized the sensitivity coefficients is also the trajectory which provides the minimum position error at the terminal point. This concept was first considered by Johnson in his dissertation (Ref. 1).

Purpose

The basic objectives of this thesis are as follows:

A. To synthesize and analyze a set of optimal open-loop trajectories for an entry problem which will minimize a function of the sensitivity coefficients described above.

B. To generate a set of suboptimal feedback gains which will drive the vehicle to the desired terminal point in the presence of small errors in the vehicle position and velocity vectors at any time during entry.

In theory, the use of a set of feedback gains would appear to invalidate the objective of minimizing the sensitivity coefficients, since with perfect measurements and an optimal feedback scheme, the

terminal conditions would be analytically satisfied. However, in practice, neither of the two assumptions are valid. First, consider the environment; the measurements are extracted from an Inertial Measurement Unit, which is in turn adjusted by the overall attitude of the vehicle. Errors from the environment, then, can be additive, and, at present, must be compensated for. Consider, also, the feedback scheme; the ideal controller would require some nonlinear relationship between the control vector and the position and velocity vectors. Since, in an entry, control must be applied in near real time, the nonlinear relationship is impractical. Thus a linear relationship, valid for a small region about a nominal trajectory, is used, and the errors inherent in an approximation are, again significant. In practice, then, there is ample motivation to seek a trajectory where the influence of these errors on the terminal position will be minimized.

The open-loop controller which achieves the desired optimal trajectory is defined to include all possible parameters of the non-thrusting entry vehicle controller and all the parameters which describe the vehicle configuration. This is done for the purpose of allowing the vehicle designer maximum flexibility in choosing a combination of parameters which meet the control requirements and which also fall within reasonable design limits. This type of control is called lumped parameter control.

#### Assumptions

It is assumed that the entry control vector synthesized yields a planar trajectory with respect to a spherical, non-rotating earth. Since the control used here is a lumped parameter control, it is nec-

essary to restrict the range of control to realistic design limits. The specific limits used herein are given in Chapter III.

In constructing the feedback control schema, it is assumed that a linear relation between the control vector and the vectors for position and velocity can be used. It is further assumed that the use of the position and velocity vectors alone in the feedback scheme, with no use being made of the sensitivity coefficients, is sufficient to drive the vehicle to the desired terminal conditions. It is necessary to make this assumption because the errors in the sensitivity coefficients cannot be computed onboard the vehicle.

#### Approach To The Problem

The optimal open-loop trajectory and the control required are found by first variation optimization techniques based on the calculus of variations. Using this trajectory and control as a set of nominal values a set of linear perturbation equations are solved to refine the values such that the terminal conditions are precisely satisfied. These linear perturbation equations are solved using a second variation optimization technique based on the calculus of variations.

Once an open-loop trajectory and control are generated that satisfy the terminal conditions, a set of linear perturbation equations are solved to produce a set of feedback gains for the trajectory. In order to observe the effects of implementing the feedback control in a practical situation with measurement errors and noise present, a computer simulation is accomplished using the previously determined nominal optimal control and the feedback gains. A Kalman filter is therefore applied to the nonlinear trajectory state equations of motion

to estimate the position and velocity vectors in the presence of noise.

The techniques used in both the open- and closed-loop optimization problem are presented in brief in Chapter II. Also in Chapter II an outline for the implementation of the Kalman filter, and a method for analytically generating the initial error covariance matrix for the filter are presented and discussed. The model equations to be used for the problem of minimizing sensitivity coefficients, and a transformation of independent variables is accomplished in Chapter III. In Chapter III, the derivation of the lumped parameter control is also presented in depth. The application of the techniques given in Chapter II to the equations from Chapter III is found in Chapters IV and VI. In Chapter IV, the open-loop equations are derived using the optimal theory from Chapter II, and some computation difficulties occurring during the application of optimal open-loop algorithms are discussed. In Chapter VI, a closed-loop simulation algorithm, implementing the theory for the Kalman filter is presented. Also in Chapter VI, a derivation for the closed-loop feedback scheme is presented. The results of the open-loop part of this thesis are presented and observations made in Chapter V, while the results for the closed-loop part are presented and discussed in Chapter VIII, and recommendations concerning this problem as well as areas of further study are given in Chapter IX.

## II. Optimization Techniques

The purpose of this chapter is to present a summary of general optimal control techniques and of optimal state estimation techniques. The Pontryagin maximum principle and the necessary conditions for optimality associated with it will be discussed as well as numerical methods for satisfying these necessary conditions to determine an open-loop control. The general equations for an optimal linear feedback control will be derived and the limitations of this control will be discussed. The equations for a Kalman state estimator applied to a nonlinear system will be summarized and a general computational algorithm presented.

### Statement Of The General Optimal Control Problem

The mathematical model describing the dynamics of a controllable process can generally be expressed as a set of first-order, nonlinear, vector differential equations as follows:

$$\dot{\underline{x}} = \underline{f}(\underline{x}, \underline{u}, t) \quad (2-1)$$

where the vector  $\underline{x}$  includes all the quantities which are necessary to describe the dynamics of the system (e.g., position, velocity, and flight path angle for an entry vehicle), and the vector  $\underline{u}$  includes all the system control variables (e.g., lift control and drag control for an entry vehicle). The vector  $\underline{x}$  is referred to as a state vector. The initial conditions on the state vector are denoted as follows:

$$\underline{x}(t_0) \triangleq \underline{x}^0 \quad (2-2)$$

The final conditions are denoted by:

$$\underline{x}(t_f) \triangleq \underline{x}^f \quad (2-3)$$

The problem under consideration is that of choosing a control, from some acceptable class of controls, which best satisfies some selected criterion. The criterion selected is in general to minimize some function of the state variables and the control. This function will be referred to as the criterion function and will be defined as a scalar. The control which minimizes the criterion is the optimal control and is denoted  $\underline{u}^*$ . The selection of the criterion function is a vital part of the problem since it specifies the desired performance of the system. The general criterion function treated here is called the Lagrange form and is expressed as follows:

$$J = \int_{t_0}^{t_f} \phi[\underline{x}(\tau), \underline{u}(\tau), \tau] d\tau \quad (2-4)$$

The next section discusses the conditions under which  $J$  is a minimum (or a maximum). The variable  $\phi$  is some function of the states and controls. The derivation of the conditions is discussed in additional detail in references 10 and 11.

#### Summary Of The Pontryagin Maximum Principle

The function  $\phi$  is assumed to be continuous and differentiable through the second order with respect to the components of the state vector  $\underline{x}$  and with respect to the components of the control vector  $\underline{u}$ . By using Lagrange multipliers as adjoint variables, the criterion function is augmented as follows:

$$J = \int_{t_0}^{t_f} \{ \phi[\underline{x}(\tau), \underline{u}(\tau), \tau] + \underline{\lambda}^T(\tau) [ \underline{f}[\underline{x}(\tau), \underline{u}(\tau), \tau] - \dot{\underline{x}}(\tau) ] \} d\tau \quad (2-5)$$

It should be noted that this equation is basically no different from the original criterion function, Eq(2-4). Since the factor multiplying the Lagrange multiplier in Eq(2-5) is identically equal to zero from Eq(2-1).

From Eq(2-5), a scalar function called the Hamiltonian is defined as follows:

$$H[\underline{x}(t), \underline{u}(t), \underline{\lambda}(t), t] = \phi[\underline{x}(t), \underline{u}(t), t] + \underline{\lambda}^T(t) \underline{f}[\underline{x}(t), \underline{u}(t), t] \quad (2-6)$$

Substituting this into Eq(2-5) gives:

$$J = \int_{t_0}^{t_f} \{H[\underline{x}(\tau), \underline{u}(\tau), \underline{\lambda}(\tau), \tau] - \underline{\lambda}^T(\tau) \dot{\underline{x}}(\tau)\} d\tau \quad (2-7)$$

When Eq(2-7) is integrated by parts, the result is:

$$J = - \underline{\lambda}^T(\tau) \underline{x}(\tau) \Big|_{t_0}^{t_f} + \int_{t_0}^{t_f} \{H[\underline{x}(\tau), \underline{u}(\tau), \underline{\lambda}(\tau), \tau] - \dot{\underline{\lambda}}^T(\tau) \underline{x}(\tau)\} d\tau \quad (2-8)$$

When Eq(2-8) is minimized, the original criterion function is minimized and the state vector equality constraints, Eq(2-1) are satisfied. In order to minimize Eq(2-8), a small variation is made in both the state vector and the control vector and the limit is taken as the small variation approaches zero.

When the small variations in state and control are made, the following equation is obtained (dropping functional notation):

$$\delta J = [\delta \underline{x}^T(-\underline{\lambda})] \Big|_{t_0}^{t_f} + \int_{t_0}^{t_f} \{ \delta \underline{x}^T \left[ \frac{\partial H}{\partial \underline{x}} + \dot{\underline{\lambda}} \right] + \delta \underline{u}^T \frac{\partial H}{\partial \underline{u}} \} d\tau \quad (2-9)$$

When the limit is taken as the small variations approach zero, each of the terms in Eq(2-9) must approach zero. This gives the following necessary conditions for optimality:

$$[\delta \underline{x}^T(-\lambda)] \Big|_t^{t_f} = 0 \quad (2-10)$$

$$\dot{\lambda} = - \frac{\partial H}{\partial \underline{x}} \quad (2-11)$$

$$\dot{\underline{x}} = \frac{\partial H}{\partial \underline{\lambda}} = \underline{f}(\underline{x}, \underline{u}, t) \quad (2-12)$$

$$\frac{\partial H}{\partial \underline{u}} = \underline{0} \quad (2-13)$$

where Eq(2-10) is the transversality condition (i.e., boundary condition), Eq(2-11) is the set of adjoint equations, Eq(2-12) is the original set of state equations, and Eq(2-13) is the gradient equation. This set of equations constitutes the necessary conditions for optimality, but they are not sufficient. Solution of these equations leads to a local extremum which may be either a maximum or a minimum but cannot be considered a global minimum.

The transversality condition, Eq(2-10), must be considered for two separate cases. When the initial or final condition on any component of the state vector  $\underline{x}$  is specified, the first variation of the component at that point is identically zero. When the initial or final condition on any component of the state vector is unspecified, the corresponding adjoint variable at that point must be identically zero and the first variation in the state component is then unconstrained. This is illustrated in Table I.

Table I. Constraints On Variables

State, $\underline{x}$	Specified	Unspecified
Adjoint, $\lambda$	Unconstrained	0
Variation, $\delta \underline{x}$	0	Unconstrained



Open-Loop Optimal Methods

First Variation Gradient Technique. The gradient procedure discussed here inherently satisfies the state and adjoint differential equations, and satisfies the gradient equation, Eq(2-13), by an iterative procedure. The procedure also inherently satisfies the transversality conditions. From Eq(2-9), and assuming that Eq(2-10) through Eq(2-12) are satisfied, the following relationship may be obtained:

$$\delta J = \int_{t_0}^{t_f} \delta \underline{u}^T \frac{\partial H}{\partial \underline{u}} dt \quad (2-14)$$

The objective of this procedure, then, is to drive the gradient to zero. To achieve this goal, a gradient  $\partial H / \partial \underline{u}$  is computed and a change in control  $\delta \underline{u}$  calculated. The new control is then used to compute a new gradient and the process is repeated until  $\delta \underline{u}$  approaches zero. When  $\delta \underline{u}$  is sufficiently small, the gradient is near zero and the last necessary condition of optimality is considered satisfied.

The sign of the required change in control can be found from the sign of the gradient, but the magnitude is more difficult to determine. The magnitude is generally determined by searching over a range of magnitudes until one is found which minimized the criterion function. The gradient technique is derived and described in more detail in references 7 and 11.

Assuming that all state components are specified at the initial time and unspecified at the final time, a typical computation algorithm for implementing the gradient technique is as follows:

- Step 1. Guess an initial control versus time,  $\underline{u}$ .
- Step 2. Integrate the state equations forward from the

given initial conditions and store the final values.

Step 3. Using zero as the final condition on the adjoints and the final conditions on the states from step 2, integrate the state and adjoint equations backward and store the computed gradient versus time. The sign on the gradient provides the sign for the control change.

Step 4. Perform a one-dimensional search over different magnitudes of  $\delta u$  until a  $\delta u$  is found which minimizes the first variation of the criterion function ( $\delta J$ ).

Step 5. Construct a new control versus time,  $u_{\text{new}} = u_{\text{old}} + \delta u$ .

Step 6. Go back to step 2 with the new control values and continue until the gradient is sufficiently small or until the change in either the control or the criterion function is sufficiently small.

First Variation Terminal Error Function Technique. The gradient algorithm described above always satisfies the state, adjoint, and transversality equations and works to satisfy the gradient equation. The terminal error function technique always satisfies the state, adjoint, and gradient equations and works to satisfy the transversality equation.

At each end of the problem, there are  $2n$  boundary conditions where  $n$  is the number of states. Of these,  $n$  conditions are specified and  $n$  are unconstrained. For the  $n$  that are specified, two vectors are formed,  $\underline{z}$  and  $\underline{z}_D$ , where  $\underline{z}$  is the actual value of the states or adjoints at the boundary and  $\underline{z}_D$  is the desired or specified value. A new criterion function,  $Q$ , is defined as follows:

$$Q = [\underline{z} - \underline{z}_D]^T [\underline{z} - \underline{z}_D] \quad (2-15)$$

where  $Q$  is called the terminal error function. When this function is minimized, the transversality conditions are considered satisfied. Since the state and adjoint equations and the gradient equation are always satisfied, every solution is an optimal control for the particular end conditions achieved.

To implement this technique, the states and adjoints are integrated simultaneously from either end of the problem. The integration is performed using the given boundary conditions for those variables which are specified and estimated or guessed values for those variables at the other end of the problem, the estimated values are changed and the process is repeated until the integration terminates with the desired boundary conditions. This is equivalent to transforming the two-point-boundary-value problem (TPBVP) into either an initial value problem or a final value problem.

A necessary condition for the use of this method is that the control be completely removed from the problem. For this to be done the second partial of the Hamiltonian with respect to the control vector must be non-singular. That is:

$$\left| \frac{\partial^2 H}{\partial \underline{u}^2} \right| \neq 0 \quad (2-16)$$

If the determinant is not zero, the control can be expressed as:

$$\underline{u} = \underline{h}(\underline{x}, \underline{\lambda}, t) \quad (2-17)$$

A substitution for the control in the state equations can be accomplished.

Once the unconstrained boundary conditions are estimated and the boundary conditions at the other end of the problem are found to be in

error, a gradient is computed for the criterion function with respect to the estimated boundary conditions,  $E_1$ , as follows:

$$\nabla Q_1 = \frac{Q(E_1 + \Delta E_1) - Q(E_1)}{\Delta E_1} \quad (2-18)$$

The computation of this gradient provides a search direction for the change in boundary conditions which will satisfy the boundary conditions at the other end.

A computational algorithm for the terminal error function procedure is as follows:

Step 1. Construct a terminal error criterion function,  $Q$ , corresponding to one end of the problem.

Step 2. At the opposite end of the problem, guess the  $n$  unspecified values.

Step 3. Integrate both the state and adjoint differential equations using the specified and guessed boundary conditions as a starting point.

Step 4. Determine the value of  $Q$ .

Step 5. Numerically differentiate  $Q$  with respect to the guessed boundary conditions to form  $\nabla Q$ .

Step 6. Perform a one-dimensional search over the guessed boundary conditions in the direction of  $-\nabla Q$  to minimize  $Q$ .

Step 7. With new guessed boundary conditions from Step 6, go back to Step 3 and continue until  $Q$  is sufficiently small.

The only difference between this method and that of the second variation is that in the terminal error function, a linear search is performed based on the first variation equations; whereas, in the second variation procedure, numerical perturbation differential

equations are solved during the integration of the state and adjoint equations to determine the necessary changes in the guesses. The terminal error function technique described here is due to Trushell and Birta given in Reference 6.

Second Variation Technique. In the open-loop optimal control technique based on the second variation of the Hamiltonian, it is assumed that all necessary conditions for optimality are identically satisfied with the exception of the boundary conditions. This technique transforms a two-point-boundary-value problem (i.e., a problem in which some conditions are known and some are unknown at each end of the trajectory) into an initial-value or final-value problem (i.e., a problem in which all of the conditions are known at either one end of the trajectory or the other).

Since the gradient is defined to be identically zero, it is assumed here that the control vector can be expressed as an explicit analytical function of the state and adjoint variables. Based on this assumption, the control function can be substituted into the state and adjoint differential equations to completely remove control from the problem. Then, once the boundary conditions have been satisfied, the final open-loop control versus time can be computed from the functional relationship.

Based on these assumptions, the state and adjoint equations are integrated starting at either end of the trajectory. Errors in known values at the end indicate the initial unknown boundary conditions are in error and must be changed. The entire purpose of this procedure is to determine the magnitude of these unknown boundary conditions such

that the known boundary conditions at the other end of the trajectory are satisfied. This is done by solving a set of perturbation differential equations simultaneously with the state and adjoint differential equations. The solution to this set of perturbation equations provides the sensitivity of errors in the specified values at one end of the trajectory to changes in the estimated values at the other end. These sensitivities are then used in a Newton-Raphson procedure to change the estimated values.

The sensitivity quantities provided by this method will be referred to in this thesis as boundary value partials to avoid confusion with the position sensitivity coefficients which are being minimized. The boundary value partials are sensitivity coefficients, but the sensitivity coefficients being minimized relate deviations in position along the trajectory to errors in states at the terminal point, whereas, the boundary value ratios relate errors in all of the known state and adjoint variables at one end of the trajectory to changes in the unconstrained state and adjoint variables at the other end.

To illustrate the Newton-Raphson procedure, an example is considered in which the first  $q$  states of a total of  $n$  states are assumed to be specified at the initial point and all  $n$  states are specified at the final point. Two separate cases must be considered for this example. One case deals with the procedure when backward integration is selected to satisfy the initial boundary conditions, the other with the procedure when forward integration is selected to satisfy the final boundary conditions.

In the case of backward integration for this case, the unconstrained adjoints at the final point are iteratively adjusted to satisfy

the specified boundary conditions at the initial point. The specified boundary conditions at the final point are satisfied because these conditions are used to begin the backward integration. The Newton-Raphson equation for this case may be expressed as:

$$\begin{bmatrix} \underline{\delta\psi}(t_0) \\ \underline{\delta\omega}(t_0) \end{bmatrix} = \begin{bmatrix} \frac{\partial \underline{\psi}(t_0)}{\partial \underline{\lambda}(t_f)} \\ \frac{\partial \underline{\omega}(t_0)}{\partial \underline{\lambda}(t_f)} \end{bmatrix} \underline{\delta\lambda}(t_f) \quad (2-19)$$

which may be rewritten as:

$$\underline{\delta\lambda}(t_f) = \begin{bmatrix} \frac{\partial \underline{\psi}(t_0)}{\partial \underline{\lambda}(t_f)} \\ \frac{\partial \underline{\omega}(t_0)}{\partial \underline{\lambda}(t_f)} \end{bmatrix}^{-1} \begin{bmatrix} \underline{\delta\psi}(t_0) \\ \underline{\delta\omega}(t_0) \end{bmatrix} \quad (2-20)$$

where  $\underline{\delta\psi}(t_0)$  = a q-vector of the deviations of the initial states  $[\underline{x}(t_0)]$  from the specified values.

$\underline{\delta\omega}(t_0)$  = an (n-q) vector of the deviations of the initial adjoints  $[\underline{\lambda}(t_0)]$  from zero. These adjoints are specified to be zero at the initial point because the corresponding states are completely unconstrained.

$\underline{\delta\lambda}(t_f)$  = the necessary change in the unconstrained adjoint variables at the final point to satisfy the initial boundary conditions.

Eq(2-20) may be written in terms of an iterative equation as follows:

$$\underline{\lambda}(t_f)^{n+1} = \underline{\lambda}(t_f)^n + \begin{bmatrix} \frac{\partial \underline{\psi}(t_0)}{\partial \underline{\lambda}(t_f)} \\ \frac{\partial \underline{\omega}(t_0)}{\partial \underline{\lambda}(t_f)} \end{bmatrix}^{-1} \begin{bmatrix} \underline{\psi}^0 - \underline{\psi}^n(t_0) \\ \underline{0} - \underline{\omega}^n(t_0) \end{bmatrix} \quad (2-21)$$

where  $\psi^0$  is the vector of specified initial states,  $\psi(t_0)$  is the vector of actual initial states from the backward integration and  $\omega(t_0)$  is the vector of actual initial adjoints. The quantities in the matrix to be inverted may be derived by performing a Taylor series expansion on three of the necessary equations of optimality. These equations are

$$\dot{\underline{x}} = \underline{f}(\underline{x}, \underline{u}) \quad (2-22)$$

$$\dot{\underline{\lambda}} = - \frac{\partial \underline{H}}{\partial \underline{x}} \quad (2-23)$$

and 
$$\frac{\partial \underline{H}}{\partial \underline{u}} = \underline{0} \quad (2-24)$$

The partial derivatives of these three equations with respect to  $\underline{\lambda}(t_f)$  are:

$$\left[ \frac{\partial \dot{\underline{x}}(t)}{\partial \underline{\lambda}(t_f)} \right] = \frac{d}{dt} \left[ \frac{\partial \underline{x}(t)}{\partial \underline{\lambda}(t_f)} \right] = \left[ \frac{\partial \underline{f}(\underline{x}, \underline{u})}{\partial \underline{\lambda}(t_f)} \right] \quad (2-25)$$

$$\left[ \frac{\partial \dot{\underline{\lambda}}(t)}{\partial \underline{\lambda}(t_f)} \right] = \frac{d}{dt} \left[ \frac{\partial \underline{\lambda}(t)}{\partial \underline{\lambda}(t_f)} \right] = - \frac{\partial}{\partial \underline{\lambda}(t_f)} \left[ \frac{\partial \underline{H}}{\partial \underline{x}(t)} \right] \quad (2-26)$$

and 
$$\frac{\partial}{\partial \underline{\lambda}(t_f)} \left[ \frac{\partial \underline{H}}{\partial \underline{u}(t)} \right] \Delta \left[ \frac{\partial \underline{G}(t)}{\partial \underline{\lambda}(t_f)} \right] = 0 \quad (2-27)$$

Performing a Taylor series expansion on these three equations gives:

$$\frac{d}{dt} \left[ \frac{\partial \underline{x}(t)}{\partial \underline{\lambda}(t_f)} \right] = \left[ \frac{\partial \underline{f}(\underline{x}, \underline{u})}{\partial \underline{x}(t)} \right] \left[ \frac{\partial \underline{x}(t)}{\partial \underline{\lambda}(t_f)} \right] + \left[ \frac{\partial \underline{f}(\underline{x}, \underline{u})}{\partial \underline{u}(t)} \right] \left[ \frac{\partial \underline{u}(t)}{\partial \underline{\lambda}(t_f)} \right] \quad (2-28)$$

$$\frac{d}{dt} \left[ \frac{\partial \underline{\lambda}(t)}{\partial \underline{\lambda}(t_f)} \right] = \left[ \frac{\partial \dot{\underline{\lambda}}(\underline{x}, \underline{u}, \underline{\lambda})}{\partial \underline{x}(t)} \right] \left[ \frac{\partial \underline{x}(t)}{\partial \underline{\lambda}(t_f)} \right] + \left[ \frac{\partial \dot{\underline{\lambda}}(\underline{x}, \underline{u}, \underline{\lambda})}{\partial \underline{\lambda}(t)} \right] \left[ \frac{\partial \underline{\lambda}(t)}{\partial \underline{\lambda}(t_f)} \right] + \left[ \frac{\partial \dot{\underline{\lambda}}(\underline{x}, \underline{u}, \underline{\lambda})}{\partial \underline{u}(t)} \right] \left[ \frac{\partial \underline{u}(t)}{\partial \underline{\lambda}(t_f)} \right] \quad (2-29)$$



and:

$$\left[ \frac{\partial G(\underline{x}, \underline{u}, \lambda)}{\partial \underline{x}(t)} \right] \left[ \frac{\partial \underline{x}(t)}{\partial \lambda(t_f)} \right] + \left[ \frac{\partial G(\underline{x}, \underline{u}, \lambda)}{\partial \lambda(t)} \right] \left[ \frac{\partial \lambda(t)}{\partial \lambda(t_f)} \right] + \left[ \frac{\partial G(\underline{x}, \underline{u}, \lambda)}{\partial \underline{u}(t)} \right] \left[ \frac{\partial \underline{u}(t)}{\partial \lambda(t_f)} \right] = 0 \quad (2-30)$$

where the final conditions are specified as:

$$\left[ \frac{\partial \underline{x}(t_f)}{\partial \lambda(t_f)} \right] = 0 \quad (2-31)$$

and

$$\left[ \frac{\partial \lambda(t_f)}{\partial \lambda(t_f)} \right] = I \quad (2-32)$$

The last equation can be solved for  $[\partial \underline{u}(t)/\partial \lambda(t_f)]$  analytically and substituted into Eq(2-28) and Eq(2-29) to eliminate the quantity from the equations. The solution to Eq(2-28) and Eq(2-29) provides the boundary value partials to be used to form the Newton-Raphson matrix in Eq(2-21). An algorithm for implementing this method is presented at the end of this section.

In the case of the forward integration for this example, the unspecified states and adjoints at the initial point are iteratively adjusted to satisfy the specified states at the final point. The Newton-Raphson equation for this case is:

$$\delta \underline{x}(t_f) = \left[ \frac{\partial \underline{x}(t_f)}{\partial \underline{u}(t_0)} \middle| \frac{\partial \underline{x}(t_f)}{\partial \underline{\psi}(t_0)} \right] \left[ \frac{\delta \underline{u}(t_0)}{\delta \underline{\psi}(t_0)} \right] \quad (2-33)$$

which may be rewritten as:

$$\left[ \frac{\delta \underline{u}(t_0)}{\delta \underline{\psi}(t_0)} \right] = \left[ \frac{\partial \underline{x}(t_f)}{\partial \underline{u}(t_0)} \middle| \frac{\partial \underline{x}(t_f)}{\partial \underline{\psi}(t_0)} \right]^{-1} \delta \underline{x}(t_f) \quad (2-34)$$

where for this case:

$\delta \underline{x}(t_f)$  = an n-vector of the deviations of the final states from the specified values.

$\delta \underline{\omega}(t_0)$  = a q-vector of the necessary changes to the unconstrained initial adjoints.

$\delta \underline{\psi}(t_0)$  = an (n-q)-vector of the necessary changes to the unspecified initial states.

The recursive equation for this case is:

$$\begin{bmatrix} \underline{\omega}(t_0) \\ \underline{\psi}(t_0) \end{bmatrix}^{n+1} = \begin{bmatrix} \underline{\omega}(t_0) \\ \underline{\psi}(t_0) \end{bmatrix}^n + \begin{bmatrix} \frac{\partial \underline{x}(t_f)}{\partial \underline{\omega}(t_0)} & \frac{\partial \underline{x}(t_f)}{\partial \underline{\psi}(t_0)} \end{bmatrix}^{-1} [\underline{x}^f - \underline{x}^n(t_f)] \quad (2-35)$$

The perturbation equations for the terms in the matrix in the above equation will not be presented here but have the same form as the equations derived for the case of backward integration presented earlier.

In order to satisfy control constraints for a bounded control problem in the second variation method, Valentine's constraint procedure is used (Ref. 2). In Valentine's procedure, a new constraint is added to the problem and is of the form:

$$\underline{w}(\underline{u}) \geq \underline{0} \quad (2-36)$$

It is assumed that the control constraint is:

$$\underline{B}_L \leq \underline{u} \leq \underline{B}_T \quad (2-37)$$

or

$$\underline{u} - \underline{B}_L \geq \underline{0} \quad (2-38)$$

and

$$\underline{B}_T - \underline{u} \geq \underline{0} \quad (2-39)$$

These two inequalities can be combined as:

$$\underline{w}(\underline{u}) = \begin{bmatrix} (u_1 - B_{L1}) & (B_{T1} - u_1) \\ \vdots \\ (u_j - B_{Lj}) & (B_{Tj} - u_j) \end{bmatrix} \geq \underline{0} \quad (2-40)$$

This constraint is added to the Hamiltonian with a new Lagrange multiplier,  $\underline{\mu}$ . If the new Hamiltonian is denoted  $H'$ , then:

$$H' = H + \underline{\mu}^T \underline{w}(u) \quad (2-41)$$

To satisfy the original problem, the new term must always be identically zero. When a particular control component is on one of the boundaries then that component of  $\underline{w}(u)$  is zero. If the control component is not on a boundary, then the multiplier must be identically zero. A new gradient equation is formed as:

$$\underline{G}' \triangleq \frac{\partial H'}{\partial \underline{u}} = \frac{\partial H}{\partial \underline{u}} + \left[ \frac{\partial \underline{w}(u)}{\partial \underline{u}} \right]^T \underline{\mu} = \underline{0} \quad (2-42)$$

or

$$\underline{G}' = \underline{G} + \left[ \frac{\partial \underline{w}(u)}{\partial \underline{u}} \right]^T \underline{\mu} = \underline{0} \quad (2-43)$$

Where  $\underline{G}$  is the original gradient without constraints. If a control is on a boundary,  $\underline{\mu}$  must be computed such that the gradient equation is zero. The fact that:

$$\underline{\mu}^T \underline{w}(u) = 0 \quad (2-44)$$

is not a sufficient condition for:

$$\left[ \frac{\partial \underline{w}(u)}{\partial \underline{u}} \right]^T \underline{\mu} = \underline{0} \quad (2-45)$$

For this reason, when a control  $u_j$  is on a boundary,  $\mu_j$  is computed from the corresponding gradient equation:

$$\mu_j = \frac{-\frac{\partial H}{\partial u_j}}{B_{Lj} + B_{Tj} - 2u_j} \quad (2-46)$$

When the control is on the lower boundary

$$\mu_j = \frac{-\frac{\partial H}{\partial u_j} |_{B_{Lj}}}{B_{Tj} - B_{Lj}} \quad (2-47)$$

and

$$\frac{\partial H}{\partial u_j} |_{B_{Lj}} \geq 0 \quad ; \quad (B_{Tj} - B_{Lj}) \geq 0 \quad (2-48)$$

which implies that  $\mu_j$  is negative on the lower boundary. When the control is on the upper boundary

$$\mu_j = \frac{\frac{\partial H}{\partial u_j} |_{B_{Tj}}}{B_{Tj} - B_{Lj}} \quad (2-49)$$

and

$$\frac{\partial H}{\partial u_j} |_{B_{Lj}} \leq 0 \quad ; \quad (B_{Tj} - B_{Lj}) \geq 0 \quad (2-50)$$

which implies that  $u_j$  is negative. Then  $\mu_j$  is always negative when the control is on either boundary. The term in the numerator is positive because the original gradient equation, with no constraints, is of the form

$$u_j - h_j(\underline{x}, \lambda) = 0 \quad (2-51)$$

when the control is on the lower boundary:

$$u_j = B_{Lj} \quad (2-52)$$

But  $h_j(\underline{x}, \lambda)$  is the value the control would be if no boundary were present and is consequently less than  $B_{Lj}$ . This implies that  $u_j - h_j(\underline{x}, \lambda)$  is greater than zero. When the control is on the upper boundary

$$u_j = B_{Tj} \quad (2-53)$$

But, in this case,  $h_j(\underline{x}, \lambda)$  is larger than the boundary and  $u_j - h_j(\underline{x}, \lambda)$

is less than zero.

When the control is on a boundary, then changes in control at that point are not functions of changes in either the state or adjoint variables at  $t_0$  or  $t_f$  and

$$\begin{aligned} \left[ \frac{\partial u_j(t)}{\partial \lambda(t_f)} \right] = 0 & ; \left[ \frac{\partial u_j(t)}{\partial \underline{x}(t_f)} \right] = 0 \\ \left[ \frac{\partial u_j(t)}{\partial \lambda(t_0)} \right] = 0 & ; \left[ \frac{\partial u_j(t)}{\partial \underline{x}(t_0)} \right] = 0 \end{aligned} \quad (2-54)$$

at that point.

When the control is not on a boundary, then

$$\mu_j = 0 \quad (2-55)$$

and the control is computed as if the boundary on control did not exist.

An algorithm for implementing the second variation procedure with control inequality constraints and using backward integration follows. The method for forward integration is similar.

Step 1. An initial set of estimates are made for the terminal adjoint variables.

Step 2. The control is computed at  $t_f$  from the gradient Eq(2-43). If it is within bounds go to Step 3; otherwise, go to Step 5.

Step 3. The state and adjoint equations are integrated backward for one increment of time.

Step 4. The control is computed at this point from Eq(2-43). If it is within bounds go to Step 6; otherwise go to Step 5.

Step 5. Let the control equal  $B_T$  or  $B_L$  and compute from Eq(2-47). Set  $[\partial u_j(t)/\partial \lambda(t_f)]$  equal to zero and go to Step 7.

Step 6. Set  $\mu = 0$  and continue.

Step 7. Solve the perturbation equations backward in time to the same point as the states and adjoints.

Step 8. If the initial time has been reached go to Step 9; otherwise go to Step 3.

Step 9. Compute new estimates of the terminal adjoints from Eq(2-22) by inverting the  $n \times n$  matrix and go back to Step 2 and continue until the boundary conditions converge to within a tolerance of the specified values.

#### Suboptimal Closed-Loop Control Methods

The basic purpose of using a closed-loop control in conjunction with an optimal problem is to form a practical, near optimal, guidance law for use in a real time adaptive controller. If this suboptimal law is used with perfect measurements, the feedback elements derived herein will satisfy the final boundary conditions established in the optimal solution. The solution of the open-loop optimal control problem determines a nominal trajectory and control set which satisfy the boundary conditions at both ends of the trajectory. However, when the optimal control is applied as a forcing function during a mission, the actual initial conditions may not be identical to the nominal initial conditions for the optimal trajectory. Also, due to perturbations along the trajectory, the actual trajectory may deviate from the nominal optimal trajectory by a small amount. For a mission such as entry into the earth's atmosphere, there still exists a

requirement to reach a particular target with a set of specified final states. An optimal closed-loop control scheme corrects for these deviations by continually computing a new optimal trajectory to arrive at the specified boundary conditions. However, the computation of an optimal control at every point in time to satisfy the final boundary conditions requires the complete solution of the original optimal control problem from the actual initial conditions at each point to the final point.

An alternative to solving the entire problem at each point is to define a linear functional relationship between small deviations in the states from the nominal and small changes in control from the nominal to achieve the desired final boundary conditions. This functional relationship is only valid in a linear range about the nominal, but allows a practical compensation for small errors. This functional relationship is given in reference 1 as:

$$\delta \underline{u}(t) = \left[ \frac{\partial \underline{u}(t)}{\partial \underline{x}(t)} \right] \delta \underline{x}(t) \quad (2-56)$$

where  $\delta \underline{u}(t)$  is the required change in control vector to correct for small errors  $\delta \underline{x}(t)$  in the state vector. The matrix is computed from quantities available from the original solution of the optimal open-loop control problem. It should be noted that the change in control generated does not immediately correct the trajectory to the nominal. Instead, it allows the states to follow a neighboring path to the specified final conditions. This is illustrated in Figure 1. In order to accomplish this, the matrix  $[\partial \underline{u}(t) / \partial \underline{x}(t)]$  is computed backward in time, relating all variables to the final specified conditions. This matrix is referred to as the feedback gain matrix.

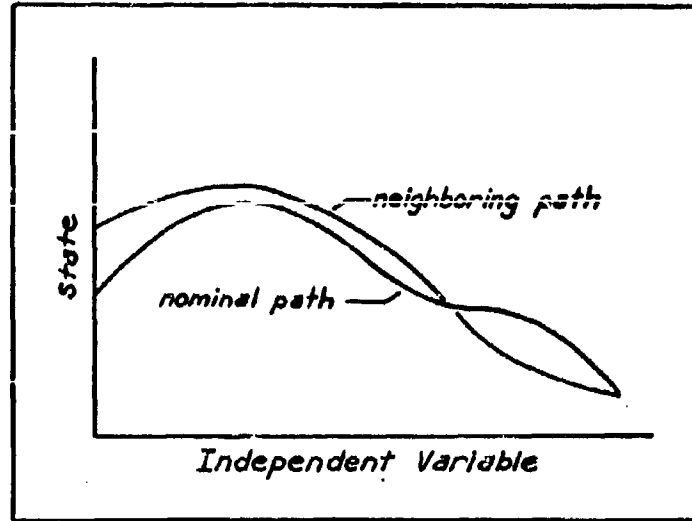


Figure 1. Neighboring Trajectory for Linear Feedback Scheme

The block diagram in Figure 2 illustrates an example of the implementation of a linear feedback scheme.

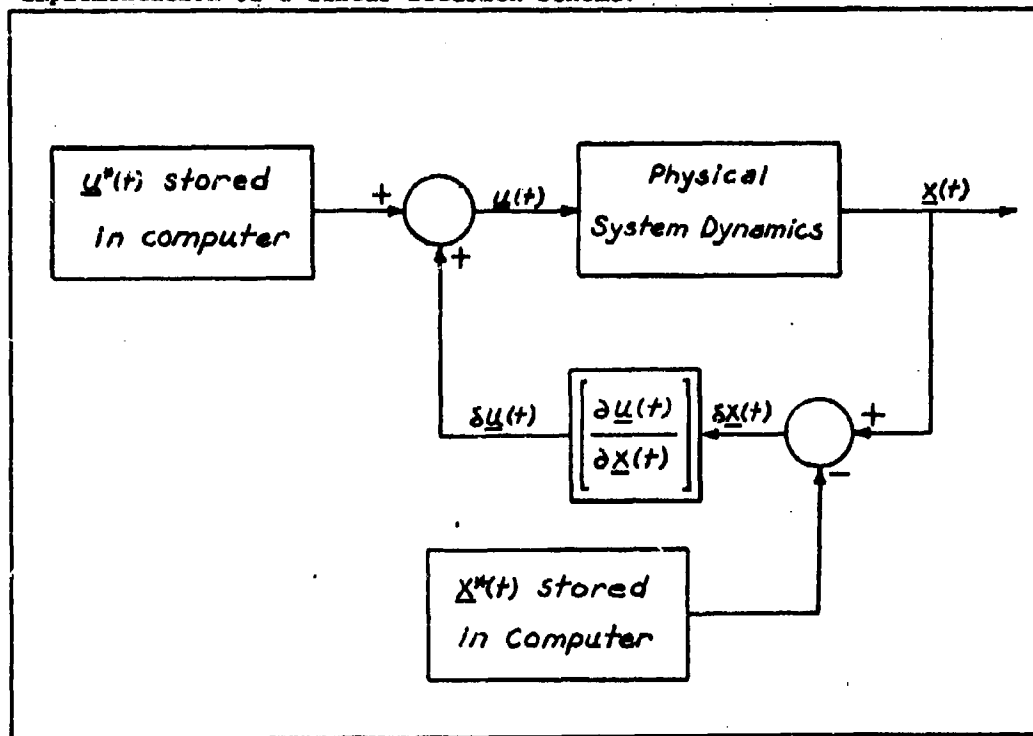


Figure 2. Block Diagram for Implementing Feedback Gains



The quantity which must be derived is the relationship for the feedback gain matrix. The equation for defining this matrix as derived by Johnson in Reference 1 is:

$$\begin{bmatrix} \frac{\partial \underline{u}(t)}{\partial \underline{x}(t)} \end{bmatrix} = - \begin{bmatrix} \frac{\partial G(t)}{\partial \underline{u}(t)} \end{bmatrix}^{-1} \left\{ \begin{bmatrix} \frac{\partial G(t)}{\partial \underline{x}(t)} \end{bmatrix} + \begin{bmatrix} \frac{\partial G(t)}{\partial \underline{\lambda}(t)} \end{bmatrix} \begin{bmatrix} \frac{\partial \underline{\lambda}(t)}{\partial \underline{\lambda}(t_f)} \end{bmatrix} \begin{bmatrix} \frac{\partial \underline{x}(t)}{\partial \underline{\lambda}(t_f)} \end{bmatrix}^{-1} \right\} \quad (2-57)$$

where  $\underline{G}(t)$  is the gradient and

$$\begin{bmatrix} \frac{\partial \underline{\lambda}(t)}{\partial \underline{\lambda}(t_f)} \end{bmatrix} \quad \text{and} \quad \begin{bmatrix} \frac{\partial \underline{x}(t)}{\partial \underline{\lambda}(t_f)} \end{bmatrix}$$

are computed by solving the perturbation equations, Eq(2-28), Eq(2-29), and Eq(2-30) in the previous section. This equation is only valid for the case in which the states are specified at both ends of the trajectory. It is not practical to force the change in control to be a function of errors in the adjoint variables since these errors cannot be generally computed during an actual entry mission.

The algorithm for computing the feedback gains simply consists of integrating the three perturbation equations backward in time, substituting the quantities into Eq(2-58), and storing the resulting gain values at each point in time. It should be noted that these gain values cannot be computed from forward integration because the final specified boundary conditions do not directly enter into the integration.

#### Optimal State Estimation

The optimal state estimator used in this thesis is the discrete Kalman filter. The Kalman filter is a minimum variance, unbiased, linear estimator. The classical least squares estimator is a special

case of the Kalman filter. When no plant noise is present and the plant differential equations are uncoupled, the Kalman filter and the unweighted least squares estimator are equivalent. The discrete Kalman filter is expressed as a set of recursive equations just as the least squares estimator can be. A derivation of the filter equations will not be presented here but is well described in Ref. 5, 12, and 13.

When the plant and observation noise are independent, white Gaussian vectors and the plant and observation equations are linear, the Kalman filter provides the optimal Bayesian estimate of the state vector. When the noise is not Gaussian, the Kalman filter still provides the optimal linear estimate of the state vector. When the plant or observation vector equations are non-linear, the optimal Bayesian estimate is given by a non-linear filter which must be derived for each problem individually whether the noise vectors are white Gaussian vectors or not. For most non-linear problems, the most practical approach is to linearize the equations and apply the Kalman filter to the small deviations within a linear range. The following basic procedure is generally followed in applying the Kalman filter to a non-linear set of equations:

A. The non-linear plant and observation equations are linearized either about a precomputed nominal set of values of the state vector or about the current optimal linear estimates of the state vector. In this thesis, only linearization about the current optimal linear estimates are considered.

B. The Kalman filter is applied to the linear set of deviations from the nominal or estimated states to form the optimal

estimates of the deviations.

C. The optimal estimates of the deviations are added to the precomputed nominal states or to the best estimate of the states given all information except the current observation vector values. This provides the optimal linear estimate of the state values.

The system model (i.e., plant model, message model) equation and the observation equation are defined as follows:

$$\dot{\underline{x}} = \underline{f}(\underline{x}, \underline{\xi}, \underline{u}) \quad (2-58)$$

$$\underline{y} = \underline{g}(\underline{x}, \underline{\eta}) \quad (2-59)$$

where  $\underline{x}$  = state vector to be estimated  
 $\underline{y}$  = observation vector  
 $\underline{u}$  = control vector  
 $\underline{\xi}$  = Gaussian white system noise  
 $\underline{\eta}$  = Gaussian white observation noise

In order to establish a discrete, recursive set of equations, the system and observation equations are written in the following discrete form:

$$\frac{\underline{x}_{i+1} - \underline{x}_i}{H} = \underline{f}(\underline{x}_i, \underline{\xi}_i, \underline{u}_i) \quad (2-60)$$

or 
$$\underline{x}_{i+1} = \underline{x}_i + H \cdot \underline{f}(\underline{x}_i, \underline{\xi}_i, \underline{u}_i) \triangleq \underline{F}(\underline{x}_i, \underline{\xi}_i, \underline{u}_i) \quad (2-61)$$

and 
$$\underline{y}_i = \underline{g}(\underline{x}_i, \underline{\eta}_i) \triangleq \underline{G}(\underline{x}_i, \underline{\eta}_i) \quad (2-62)$$

where H is the integration step size for a linear approximation. When the discrete system and observation equations are expanded in a Taylor series about the optimal estimates  $\hat{\underline{x}}_i$ ,  $\hat{\underline{\xi}}_i$ ,  $\hat{\underline{u}}_i$  and  $\hat{\underline{\eta}}_i$  the following equations are obtained:

$$\begin{aligned}
\mathbf{x}_{i+1} &= \mathbf{F}(\mathbf{x}_i, \hat{\mathbf{E}}_i, \hat{\mathbf{u}}_i) + \left[ \frac{\partial \mathbf{F}(\mathbf{x}_i, \mathbf{E}_i, \mathbf{u}_i)}{\partial \mathbf{x}_i} \right]_{\mathbf{x}_i = \hat{\mathbf{x}}_i} (\mathbf{x}_i - \hat{\mathbf{x}}_i) \\
&+ \left[ \frac{\partial \mathbf{F}(\mathbf{x}_i, \mathbf{E}_i, \mathbf{u}_i)}{\partial \mathbf{E}_i} \right]_{\mathbf{E}_i = \hat{\mathbf{E}}_i} (\mathbf{E}_i - \hat{\mathbf{E}}_i) \\
&+ \left[ \frac{\partial \mathbf{F}(\mathbf{x}_i, \mathbf{E}_i, \mathbf{u}_i)}{\partial \mathbf{u}_i} \right]_{\mathbf{u}_i = \hat{\mathbf{u}}_i} (\mathbf{u}_i - \hat{\mathbf{u}}_i) \quad (2-63)
\end{aligned}$$

$$\begin{aligned}
\mathbf{y}_i &= \mathbf{G}(\mathbf{x}_i, \hat{\mathbf{n}}_i) + \left[ \frac{\partial \mathbf{G}(\mathbf{x}_i, \mathbf{n}_i)}{\partial \mathbf{x}_i} \right]_{\mathbf{x}_i = \hat{\mathbf{x}}_i} (\mathbf{x}_i - \hat{\mathbf{x}}_i) \\
&+ \left[ \frac{\partial \mathbf{G}(\mathbf{x}_i, \mathbf{n}_i)}{\partial \mathbf{n}_i} \right]_{\mathbf{n}_i = \hat{\mathbf{n}}_i} (\mathbf{n}_i - \hat{\mathbf{n}}_i) \quad (2-64)
\end{aligned}$$

If  $\mathbf{E}$  and  $\mathbf{n}$  have zero mean then

$$\hat{\mathbf{E}}_i = \mathbf{E}(\hat{\mathbf{E}}_i) = \mathbf{0} \quad (2-65)$$

and

$$\hat{\mathbf{n}}_i = \mathbf{E}(\hat{\mathbf{n}}_i) = \mathbf{0} \quad (2-66)$$

where  $\mathbf{E}(\cdot)$  is the expected value of the quantity in the parentheses.

If the control vector is assumed to be a forcing function (i.e., not a function of the states) then:

$$\hat{\mathbf{u}}_i = \mathbf{u}_i \quad (2-67)$$

When these relations are substituted into Eq(2-63) the final linearized equations can be expressed as:

$$\begin{aligned}
\mathbf{x}_{i+1} &= \mathbf{F}(\hat{\mathbf{x}}_i, \mathbf{0}, \mathbf{u}_i) + \left[ \frac{\partial \mathbf{F}(\mathbf{x}_i, \mathbf{E}_i, \mathbf{u}_i)}{\partial \mathbf{x}_i} \right]_{\mathbf{x}_i = \hat{\mathbf{x}}_i} (\mathbf{x}_i - \hat{\mathbf{x}}_i) \\
&+ \left[ \frac{\partial \mathbf{F}(\mathbf{x}_i, \mathbf{E}_i, \mathbf{u}_i)}{\partial \mathbf{E}_i} \right]_{\mathbf{E}_i = \mathbf{0}} \mathbf{E}_i \quad (2-68)
\end{aligned}$$

$$y_i = G(\hat{x}_i, 0) + \left[ \frac{\partial G(x_i, \Omega_i)}{\partial x_i} \right]_{x_i = \hat{x}_i} (x_i - \hat{x}_i) + \left[ \frac{\partial G(x_i, \Omega_i)}{\partial \Omega_i} \right]_{\Omega_i = 0} \Omega_i \quad (2-69)$$

The Kalman filter may be used with these equations in two ways. Both are equivalent. One method involves applying the linear filter equations to the deviations from the optimal estimate to find the optimal estimate of the deviations and then adding the result to the best estimate of the states. The other method consists of modifying the filter equations to include the best estimates of the states. The latter procedure will be followed here. The best estimate of  $x_{i+1}$  given only  $y_i$  and all preceding observations is denoted  $x(i+1|i)$ . The best estimate may be computed by solving Eq(2-58) as:

$$\dot{x}(j|i) = f[x(j|i), 0, u_j] \quad 1 \leq j \leq i+1 \quad (2-70)$$

where, the integration begins at:

$$x(i|i) = \hat{x}_i \quad (2-71)$$

and ends when  $j = i+1$ .

The recursive relations to be computed for the filter are as follows:

A. Kalman Gain:

$$K_{i+1} = \Gamma(i+1|i) G_x(i+1)^T [G_x(i+1) \Gamma(i+1|i) G_x(i+1)^T + W_{i+1}]^{-1} \quad (2-72)$$

B. Best Estimate Of Error Covariance Given  $y_i$ :

$$\Gamma(i+1|i) = F_{xi} \Gamma_i F_{xi}^T + V_i \quad (2-73)$$

This quantity may be computed by propagating over small intervals with

the state transition matrices  $F_x$  and  $F$  at the same time  $x(i+1|i)$  is computed.

C. Error Covariance Given  $y_{i+1}$ :

$$\Gamma_{i+1} = [I - K_{i+1}G_x(i+1)] \Gamma(i+1|i) [I - K_{i+1}G_x(i+1)]^T + K_{i+1}W_{i+1}K_{i+1}^T \quad (2-74)$$

D. Optimal Estimate:

$$\hat{x}_{i+1} = \hat{x}(i+1|i) + K_{i+1} y_{i+1} - G[\hat{x}(i+1|i), 0] \quad (2-75)$$

In the four sets of equations above:

$K_{i+1}$  = Kalman gains at measurement point (i+1).

$\Gamma(i+1|i)$  = Best estimate of error covariance at measurement point (i+1) given  $y_i$ .

$\Gamma_{i+1}$  = Error covariance at measurement point (i+1) given  $y_{i+1}$

$\hat{x}(i+1|i)$  = Best estimate of state vector at measurement point (i+1) given  $y_i$ .

$\hat{x}_i$  = Optimal estimate of state vector at measurement point (i+1) given  $y_{i+1}$ .

$$G_x(i+1) = \left[ \frac{\partial G(\hat{x}_{i+1}, 0)}{\partial \hat{x}_{i+1}} \right]_{\hat{x}_{i+1} = \hat{x}(i+1|i)}$$

$$F_{xi} = \left[ \frac{\partial F(\hat{x}_i, 0, u_i)}{\partial \hat{x}_i} \right]_{\hat{x}_i = \hat{x}_i}$$

$$V_i = E(v_i v_i^T)$$

where

$$v_i = \left[ \frac{\partial F(\hat{x}_i, \xi_i, u_i)}{\partial \xi_i} \right]_{\xi_i=0} \xi_i$$

$$W_1 = E(W_1 W_1^T)$$

where

$$W_1 = \left[ \frac{\partial G(x_1, n_1)}{\partial n_1} \right]_{n_1=0} n_1$$

A specific algorithm for implementing the Kalman filter will be presented in Chapter VI on Optimal Implicit Guidance. These equations will form the basis for the optimal estimation in the entry guidance law formulation.

Initial Estimate Of The Error Covariance Matrix. In this section, a set of equations will be derived for computing the initial error covariance matrix,  $\Gamma_0$ , when certain assumptions are satisfied. It will be shown that it is not, in general, necessary to guess an initial estimate  $\Gamma_0$ . It may be computed instead. It is assumed here that the problem begins at the first measurement point. Theoretically, for a linear system and linear observations, given a long enough sequence of measurements, any estimate of the initial error covariance matrix should produce the same steady state errors. In actual practice with non-linear systems, given non-linear observations and a finite sample time, this does not occur. This is illustrated by Elliott and Filiatreau in Ref. 17. They investigated the effects of variations in the initial estimate of the error covariance matrix in conjunction with an orbit determination problem.

The steady state errors are sometimes critically dependent on the initial estimate of  $\Gamma_0$ . If the estimate is much smaller than the initial observation noise covariance matrix,  $W(0)$ , the variables may not

reach steady state values at all. If the estimate is larger than  $W(0)$ , the variables in some cases reach steady state values in a much shorter time than for lower estimates. When the estimate is much larger than  $W(0)$ , the reference cited above indicates a tendency for the variables also not to reach steady state values as in the case in which the estimate is much smaller than  $W(0)$ .

The equation for the optimal estimate, Eq(2-75), is:

$$\hat{\underline{x}}_{i+1} = \underline{x}(i+1|1) + K_{i+1} [Y_{i+1} - G(\underline{x}(i+1|1), 0)] \quad (2-76)$$

For the initial observation point this equation becomes:

$$\hat{\underline{x}}_0 = \underline{x}^0 + K_0 [Y_0 - G(\underline{x}^0, 0)] \quad (2-77)$$

where  $\underline{x}^0$  is defined as the best estimate of the initial state vector given no observations, and  $\hat{\underline{x}}_0$  is the optimal estimate of the initial state vector given the initial observation. Thus,  $\underline{x}^0$  can be based only on a priori information. The following assumptions are now made:

- A.  $\underline{x}^0$  is an arbitrary a priori estimate of the initial state vector.
- B.  $K_0$  is an arbitrary a priori estimate of the initial Kalman gain matrix. The value of  $K_0$  will be determined by the confidence level of the a priori  $\underline{x}^0$  as compared to the confidence level of the observation vector  $Y_0$  as given by  $W(0)$ .

The equation for the initial Kalman gain from Eq(2-72) is:

$$K_0 = \Gamma^0 G_x(0)^T [G_x(0) \Gamma^0 G_x(0)^T + W(0)]^{-1} \quad (2-78)$$

where  $\Gamma^0$  is defined as the best estimate of the initial error covariance matrix given no measurements. The optimal estimate of the initial error covariance matrix given the first measurement will be denoted  $\Gamma^0$ . Solving Eq(2-78) for  $\Gamma^0$  gives:

$$\Gamma^0 = [I - K_0 G_x(0)]^{-1} K_0 W(0) G_x(0)^{-T} \quad (2-79)$$



The equation for the optimal estimate of the initial error covariance matrix,  $\Gamma_0$ , from Eq(2-74) is:

$$\Gamma^0 = [I - K_0 G_x(0)] \Gamma^0 [I - K_0 G_x(0)]^T + K_0 W(0) K_0^T \quad (2-80)$$

Substituting Eq(2-79):

$$\Gamma_0 = [I - K_0 G_x(0)] [I - K_0 G_x(0)]^{-1} K_0 W(0) G_x(0)^{-T} [I - K_0 G_x(0)]^T + K_0 W(0) K_0^T \quad (2-81)$$

or:

$$\Gamma_0 = K_0 W(0) G_x(0)^{-T} [I - K_0 G_x(0)]^T + K_0 W(0) K_0^T \quad (2-82)$$

Simplifying this equation gives:

$$\Gamma_0 = K_0 W(0) \{ G_x(0)^{-T} - G_x(0)^{-T} [K_0 G_x(0)]^T + K_0^T \} \quad (2-83)$$

or:

$$\Gamma_0 = K_0 W(0) G_x(0)^{-T} \quad (2-84)$$

where:

$$G_x(0) = \left[ \frac{\partial G(x,0)}{\partial x} \right]_{x=x^0} \quad (2-85)$$

Eq(2-84) defines the optimal estimate of the initial error covariance matrix,  $\Gamma_0$ , once  $\hat{x}_0$  has been computed using arbitrarily selected values for  $x^0$  and  $K_0$ .

A special solution of this problem will now be considered in which:

$$K_0 \triangleq I \quad (2-87)$$

and:

$$x^0 = G(x^0, 0) \quad (2-88)$$

In the case in which the observation vector is a linear function of the state vector or:

$$y_i = x_i + n_i \quad (2-89)$$

Eq(2-88) is satisfied by any value of  $x^0$  and Eq(2-85) and Eq(2-84) give

$$G_x(0) = I \quad (2-90)$$

and:

$$\Gamma_0 = W(0) \quad (2-91)$$

The special case described above is the one which will be applied in the optimal implicit guidance simulation for this thesis.

Eq(2-84) provides a relationship which allows the following initial estimate algorithm to be constructed:

Step 1. By some arbitrary method, select an  $\underline{x}^0$  and  $K_0$  such that:

$$\hat{\underline{x}}_0 = \underline{x}^0 + K_0 [y_0 - G(\underline{x}, 0)] \quad (2-92)$$

provides the desired relationship for  $\hat{\underline{x}}_0$  (such as  $\underline{x}^0 = \underline{0}$  and  $K_0 = I$ )

Step 2. Evaluate:

$$G_x(0)^T = \left[ \frac{G(\underline{x}, 0)}{\underline{x}} \right]_{\underline{x}=\underline{x}^0}^T \quad (2-93)$$

and invert the matrix to form  $G_x(0)^{-T}$ .

Step 3. Compute the initial error covariance matrix from:

$$\Gamma_0 = K_0 W(0) G_x(0)^{-T} \quad (2-94)$$

This method of estimating the initial error covariance matrix and a further development of the case to which it is applied are presented in Chapter VI. The following chapter shall develop the model equations for the optimal open-loop control problem.

### III. Derivation Of Basic Entry Equations

In this chapter the basic equations of motion for an entry body will be established along with the equations for the position sensitivity coefficients to be minimized. The lumped parameter control containing parameters for vehicle configuration and attitude will be defined and the characteristics and effects of the atmosphere will be discussed.

#### State Vector Equations Of Motion

Figure 3 below shows the geometry and sign conventions to be used for the entry problem. The motion of the entry vehicle can be described by a set of four coupled differential equations. The solution of these equations provides position with respect to the center of the earth ( $r$ ), velocity ( $v$ ), areal velocity ( $w$ ), and range angle ( $\sigma$ ). For

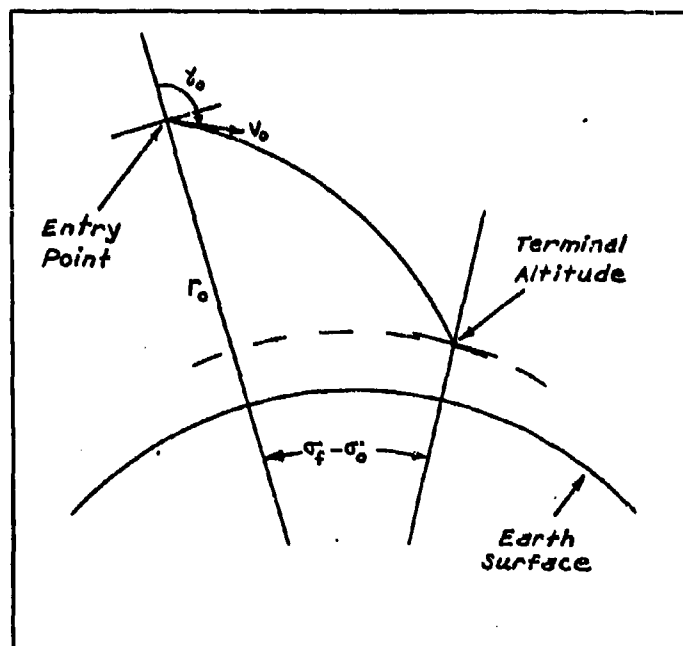


Figure 3. Entry Geometry

this problem a transformation of the independent variable is made such that the range angle,  $\sigma$ , is the independent variable instead of time. This reduces the number of equations to three. A transformation is also made from the areal velocity,  $w$ , to flight path angle,  $\gamma$ .

The equations of motion for a planar trajectory with respect to a spherical, non-rotating earth with ablation effects neglected as developed by Johnson in reference 1 are:

$$\dot{r} = \frac{v}{r} \quad (3-1)$$

$$\dot{v} = -\frac{wv}{r^2} - D \quad (3-2)$$

$$\dot{w} = v^2 - \frac{L}{r} - D r \cos(\gamma) + L r \sin(\gamma) \quad (3-3)$$

$$\dot{\sigma} = \frac{v \sin(\gamma)}{r} \quad (3-4)$$

Where  $r$  = displacement with respect to the center of the earth.

$v$  = velocity.

$\gamma$  = angle of the velocity vector measured from the local vertical. This is always a positive quantity.

$\sigma$  = range angle. The range angle is a positive quantity and assumed to be a monotonic function of time.

$w$  = areal velocity. This quantity is defined by the relation  $w = rv \cos(\gamma)$ .

$D$  = drag. The drag is dependent on the coefficient of drag and the square of the velocity and is normalized to be drag force per unit mass.

$L$  = lift. The lift is dependent on the coefficient of lift and the square of the velocity and is normalized to be lift force per unit mass.

$\mu$  = universal gravitational constant times the mass of the earth.

This quantity is the earth's gravitational constant.

The areal velocity,  $w$ , is used to improve the stability of the model, for large variations in  $\gamma$ . Since only a thirty degree maximum variation in  $\gamma$  is expected, it is not necessary to use the areal velocity. Also the computation of  $w$  onboard an entry vehicle would require a continual computation of  $(\cos \gamma)$  throughout the flight. The quantity  $\gamma$ , is available onboard from the gimbal resolvers in the Inertial Measuring Unit (IMU). For these reasons a new set of equations will be derived to replace  $w$  with  $\gamma$ .

The relationship between  $w$  and  $\gamma$  is:

$$w = rv \cos \gamma \quad (3-5)$$

When the time derivative of  $w$  is computed, the result is:

$$\dot{w} = \dot{r}v \cos \gamma + r\dot{v} \cos \gamma - rv\dot{\gamma} \sin \gamma \quad (3-6)$$

Substituting the equations for  $\dot{r}$  and  $\dot{v}$  from Eq(3-1) and Eq(3-2) gives:

$$\dot{w} = \frac{wv \cos \gamma}{r} - \frac{\mu w \cos \gamma}{vr^2} - rD \cos \gamma - rv\dot{\gamma} \sin \gamma \quad (3-7)$$

or

$$\dot{\gamma} \sin \gamma = \frac{w \cos \gamma}{r^2} - \frac{\mu w \cos \gamma}{v^2 r^3} - \frac{D \cos \gamma}{v} - \frac{\dot{w}}{rv} \quad (3-8)$$

Substituting for  $\dot{w}$  from Eq(3-3) and for  $w$  from Eq(3-5), combining terms and dividing by  $\sin \gamma$  gives:

$$\dot{\gamma} = -\frac{v \sin \gamma}{r} - \frac{\mu \sin \gamma}{r^2 v} - \frac{L}{v} \quad (3-9)$$

A new set of state equations may now be written as follows:

$$\dot{r} = v \cos \gamma \quad (3-10)$$

$$\dot{v} = -\frac{\mu \cos \gamma}{r^2} - D \quad (3-11)$$

$$\dot{\gamma} = -\frac{v \sin \gamma}{r} + \frac{u \sin \gamma}{r^2 v} - \frac{L}{v} \quad (3-12)$$

$$\dot{\sigma} = \frac{u \sin \gamma}{r} \quad (3-13)$$

The independent variable in the above equations is time, which is monotonic and measurable. It is assumed that range angle is also monotonic. To simplify the model equations, the independent variable, time, is replaced with range angle  $\sigma$ . It is important, however, to compute time versus range angle, to be able to revert to a time base at the conclusion of the problem.

Dividing Eq(3-11) through Eq(3-13) by  $\dot{\sigma}$  yields the following set of dynamic equations:

$$r' \triangleq \frac{dr}{d\sigma} = \frac{r}{\tan \gamma} \quad (3-14)$$

$$v' \triangleq \frac{dv}{d\sigma} = -\frac{u}{rv \tan \gamma} - \frac{rD}{v \sin \gamma} \quad (3-15)$$

$$\gamma' \triangleq \frac{d\gamma}{d\sigma} = -1 + \frac{u}{rv^2} - \frac{rL}{v^2 \sin \gamma} \quad (3-16)$$

To determine the time,  $t$ , at any point on the trajectory, the reciprocal of Eq(3-13) can be used, which is:

$$t' \triangleq \frac{dt}{d\sigma} = \frac{r}{v \sin(\gamma)} \quad (3-17)$$

Introducing state space notation to the model equations derived above gives:

$$\underline{x}^T = [x_1, x_2, x_3] \triangleq [r, v, \gamma] \quad (3-18)$$

Substituting Eq(3-18) into Eq(3-17), the dynamic equations of state are:

$$x_1' = \frac{x_1}{\tan x_3} \quad \Delta F_1 \quad (3-19)$$

$$x_2' = - \frac{u}{x_1 x_2 \tan x_3} - \frac{x_1 D}{x_2 \sin x_3} \quad \Delta F_2 \quad (3-20)$$

$$x_3' = - 1 + \frac{u}{x_1 x_2^2} - \frac{x_1 L}{x_2^2 \sin x_3} \quad \Delta F_3 \quad (3-21)$$

Eq(3-19) through Eq(3-21) are the state equations of motion which will be used throughout the report.

Sensitivity Coefficient State Equations

This report is concerned with the minimization of position sensitivity coefficients, which give the sensitivity of the position error at the terminal point to an error in the position or velocity vector at any point along the trajectory.

The matrix differential equation describing all the sensitivity coefficients for the three states described in Eq(3-19), Eq(3-20) and Eq(3-21) is:

$$\frac{d}{d\sigma} \left[ \frac{\partial x}{\partial x} (\sigma_f) \right] = - \left[ \frac{\partial x}{\partial x} (\sigma) \right] \left[ \frac{\partial F(\sigma)}{\partial x(\sigma)} \right] \quad (3-22)$$

This equation has been derived by Johnson (Ref. 2). In state space notation, Eq(3-22) may be written as:

$$\frac{d}{d\sigma} \begin{bmatrix} x_4 & x_5 & x_6 \\ \hline x_7 & x_8 & x_9 \\ \hline x_{10} & x_{11} & x_{12} \end{bmatrix} = - \begin{bmatrix} x_4 & x_5 & x_6 \\ \hline x_7 & x_8 & x_9 \\ \hline x_{10} & x_{11} & x_{12} \end{bmatrix} \begin{bmatrix} \frac{\partial F_1}{\partial x_1} & \frac{\partial F_1}{\partial x_2} & \frac{\partial F_1}{\partial x_3} \\ \hline \frac{\partial F_2}{\partial x_1} & \frac{\partial F_2}{\partial x_2} & \frac{\partial F_2}{\partial x_3} \\ \hline \frac{\partial F_3}{\partial x_1} & \frac{\partial F_3}{\partial x_2} & \frac{\partial F_3}{\partial x_3} \end{bmatrix} \quad (3-23)$$

The partials of  $F_1$ ,  $F_2$ , and  $F_3$  from Eq(3-19), Eq(3-20), and Eq(3-21) are:

$$\frac{\partial F_1}{\partial x_1} = \frac{1}{\tan x_3} \quad (3-24)$$

$$\frac{\partial F_1}{\partial x_2} = 0 \quad (3-25)$$

$$\frac{\partial F_1}{\partial x_3} = -\frac{x_1}{\sin^2 x_3} \quad (3-26)$$

$$\frac{\partial F_2}{\partial x_1} = \frac{\mu}{x_1^2 x_2 \tan x_3} - \frac{D}{x_2 \sin x_3} - \frac{x_1}{x_2 \sin x_3} \frac{\partial D}{\partial x_1} \quad (3-27)$$

$$\frac{\partial F_2}{\partial x_2} = \frac{\mu}{x_1 x_2^2 \tan x_3} + \frac{x_1 D}{x_2^2 \sin x_3} - \frac{x_1}{x_2 \sin x_3} \frac{\partial D}{\partial x_2} \quad (3-28)$$

$$\frac{\partial F_2}{\partial x_3} = \frac{\mu}{x_1 x_2 \sin^2 x_3} + \frac{x_1 D \cos x_3}{x_2 \sin^2 x_3} \quad (3-29)$$

$$\frac{\partial F_3}{\partial x_1} = -\frac{\mu}{x_1^2 x_2^2} - \frac{L}{x_2^2 \sin x_3} - \frac{x_1}{x_2^2 \sin x_3} \frac{\partial L}{\partial x_1} \quad (3-30)$$

$$\frac{\partial F_3}{\partial x_2} = -\frac{2\mu}{x_1 x_2^3} + \frac{2x_1 L}{x_2^3 \sin x_3} - \frac{x_1}{x_2^2 \sin x_3} \frac{\partial L}{\partial x_2} \quad (3-31)$$

$$\frac{\partial F_3}{\partial x_3} = \frac{x_1 L \cos x_3}{x_2^2 \sin^2 x_3} \quad (3-32)$$

Nine sensitivity coefficients result from the solution of Eq(3-23) through Eq(3-32). These describe the sensitivity of errors in all three states at the terminal time. In this report, however, only the position error is considered. Position is determined by the radius and the range angle. Since the range angle is the independent variable for the model, there is no range angle error at the terminal point, by definition. Therefore, only the sensitivity coefficients relating the error in radius,  $x_1$ , at the terminal point, to errors in the three states during the flight are considered. In Eq(3-23), each row of the matrix on the left hand side is uncoupled from the remaining rows, such that for errors only in position, the following equation suffices:



$$\frac{d}{d\sigma} \left[ \frac{\partial x_1(\sigma_f)}{\partial x(\sigma)} \right] = \frac{d}{d\sigma} \left[ \frac{\partial x_1(\sigma_f)}{\partial x_1(\sigma)}, \frac{\partial x_1(\sigma_f)}{\partial x_2(\sigma)}, \frac{\partial x_1(\sigma_f)}{\partial x_3(\sigma)} \right] \quad (3-33)$$

Based on this and Eq(3-23):

$$\frac{d}{d\sigma} \left[ x_4, x_5, x_6 \right] = - \left[ x_4, x_5, x_6 \right] \begin{bmatrix} \frac{\partial f_1}{\partial x_1} & \frac{\partial f_1}{\partial x_2} & \frac{\partial f_1}{\partial x_3} \\ \frac{\partial f_2}{\partial x_1} & \frac{\partial f_2}{\partial x_2} & \frac{\partial f_2}{\partial x_3} \\ \frac{\partial f_3}{\partial x_1} & \frac{\partial f_3}{\partial x_2} & \frac{\partial f_3}{\partial x_3} \end{bmatrix} \quad (3-34)$$

where the partials are defined in Eq(3-24) through Eq(3-32).

#### Lumped Parameter Control Equations

The design of a passive control restricts the control available to atmospheric forces. In this section the equations for drag and lift shall be functionally separated into two parts. The first part shall contain parameters related to vehicle configuration and attitude and shall be defined as a lumped parameter control. The second part shall contain parameters related to mach number.

The equations for lift and drag are:

$$D = \frac{AC_D^I(\alpha)}{m} \times \frac{\rho v^2 C_{ps}}{2} \quad (3-35)$$

$$L = \frac{SC_L^I(\alpha)}{m} \times \frac{\rho v^2 C_{ps}}{2} \quad (3-36)$$

where  $\rho$  = density

$v$  = velocity

$C_{ps}$  = coefficient of pressure at the stagnation point, a function of mach number

$A$  = cross-section area perpendicular to velocity vector

$S$  = planform area perpendicular to both the velocity vector and the radius vector

$m$  = mass (a constant)

$C_D'(\alpha)$  = a drag coefficient which is a function of angle of attack,  $\alpha$

$C_L'(\alpha)$  = a lift coefficient which is a function of angle of attack,  $\alpha$

Two controls will be defined as follows:

$$u_D \triangleq \frac{AC_D'(\alpha)}{m} \quad (3-37)$$

$$u_L \triangleq \frac{SC_L'(\alpha)}{m} \quad (3-38)$$

The values which the controls are allowed to take on are limited by practical considerations of vehicle design, thus the lumped control problem is a bounded control problem. The boundaries are as follows:

$$2.76 \times 10^{-5} \leq u_D \leq 2.22 \times 10^{-3}$$

$$-1.6 u_D \leq u_L \leq 1.6 u_D$$

These boundaries on the controls correspond to:

$$250 \leq \frac{W}{C_D A} \leq 20,000 \text{ Kg/meters}^2$$

$$-1.6 \leq L/D \leq 1.6$$

Substituting the control relations into Eq(3-35) and Eq(3-36) gives:

$$D = \frac{\rho v^2 C_{ps}}{2} u_D \quad (3-39)$$

$$L = \frac{\rho v^2 C_{ps}}{2} u_L \quad (3-40)$$

The term  $C_{ps}$ , the coefficient of stagnation pressure in the above equations is a function of mach number, which in turn is a function of altitude, pressure, density, and velocity. This term is derived using

the following assumptions:

- A. Perfect Gas
- B. Isentropic Flow
- C. Adiabatic Flow
- D. The shock is locally normal

In Fig. 4 below,  $P_{01}$  and  $P_{02}$  are the stagnation pressures at points 1 and 2;  $P_1$  and  $P_2$  are the pressures at the two points, and  $M$  is mach number. Using assumptions A, C, and D, the following

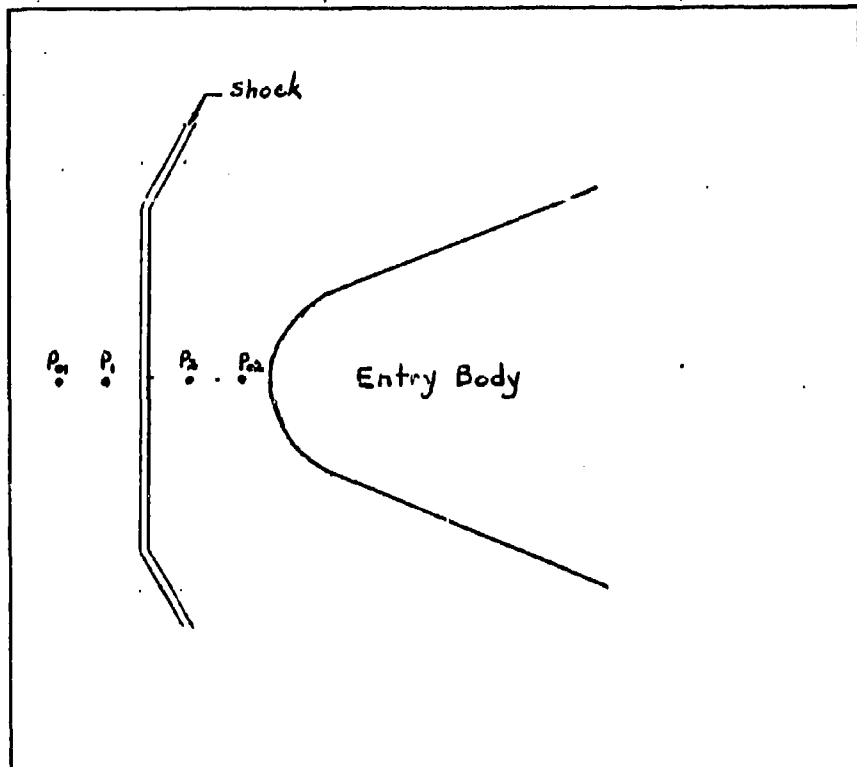


Figure 4. Shock Wave Geometry

relations are obtained (Ref. 15):

$$C_{ps} = C_{p02} = \frac{2}{M_1^2 \gamma} \left[ \frac{P_{02}}{P_1} - 1 \right] \quad (3-41)$$

and

$$\frac{P_{02}}{P_{01}} = \left[ 1 + \frac{2\gamma}{\gamma+1} (M_1^2 - 1) \right]^{-\frac{1}{\gamma-1}} \left[ \frac{(\gamma+1)M_1^2}{(\gamma-1)M_1^2 + 2} \right]^{\frac{\gamma}{\gamma-1}} \quad (3-42)$$

From assumption B:

$$\frac{P_{01}}{P_1} = \left[ 1 + \frac{\gamma-1}{2} M_1^2 \right]^{\frac{\gamma}{\gamma-1}} \quad (3-43)$$

Multiplying Eq(3-42) and Eq(3-43) together and substituting the result for the quantity  $P_{02}/P_1$  in Eq(3-41)

$$C_{ps} = \frac{2}{\gamma} \left[ \frac{\gamma+1}{2\gamma - \frac{\gamma-1}{M_1^2}} \right]^{\frac{1}{\gamma-1}} \left[ \frac{\gamma+1}{2} \right]^{\frac{\gamma}{\gamma-1}} - \frac{2}{\gamma M_1^2} \quad (3-44)$$

For air,  $\gamma=1.4$ , which when substituted into Eq(3-44) provides the final relation for  $C_{ps}$ .

$$C_{ps} = \frac{238.87872M^5}{7(2.8M^2-0.4)^2} \left[ \frac{1}{2(2.8M^2-0.4)} \right]^{\frac{1}{2}} - \frac{10}{7M^2} \quad (3-45)$$

The above equation is valid for velocities above Mach 2. The density  $\rho$  is interpolated numerically from the 1959 ARDC Standard Atmospheric Tables.

Substituting the expressions of Eq(3-39) and Eq(3-40), for drag and lift respectively, into the state equations, Eq(3-19) through (3-21) the final state equations are:

$$x_1' = \frac{x_1}{\tan x_3} \quad \Delta F_1 \quad (3-46)$$

$$\dot{x}_2 = -\frac{\mu}{x_1 x_2 \tan x_3} - \frac{x_1 x_2 C_{DM}}{2 \sin x_3} u_D \quad \Delta F_2 \quad (3-47)$$

$$\dot{x}_3 = -1 + \frac{\mu}{x_1 x_2^2} - \frac{x_1 \rho C_{DM}}{2 \sin x_3} u_L \quad \Delta F_3 \quad (3-48)$$

$$\dot{x}_4 = -x_4 \frac{\partial F_1}{\partial x_1} - x_5 \frac{\partial F_2}{\partial x_1} - x_6 \frac{\partial F_3}{\partial x_1} \quad \Delta F_4 \quad (3-49)$$

$$\dot{x}_5 = -x_4 \frac{\partial F_1}{\partial x_2} - x_5 \frac{\partial F_2}{\partial x_2} - x_6 \frac{\partial F_3}{\partial x_2} \quad \Delta F_5 \quad (3-50)$$

$$\dot{x}_6 = -x_4 \frac{\partial F_1}{\partial x_3} - x_5 \frac{\partial F_2}{\partial x_3} - x_6 \frac{\partial F_3}{\partial x_3} \quad \Delta F_6 \quad (3-51)$$

These are the basic model equations to be used in the optimal control problem to be discussed in the following chapter.

#### IV. The Maximum Principle Applied To The Entry Problem

In Chapter II, it was established that an arbitrary criterion could be satisfied along with a set of non-linear plant equations provided a set of necessary optimal conditions are met. In Chapter III, mathematical model equations were derived for the entry problem. The quantities to be used in the criterion function, the position sensitivity coefficients, were also explained in concept and derived in Chapter III. In this chapter, the criterion function is established for the entry model along with a set of necessary optimal conditions such that the model equations are satisfied.

##### Criterion Function

The criterion function is a scalar valued function which contains all the elements to be minimized. For this problem, the criterion function must contain a convex function of the errors at the terminal point due to errors at any point of the entry trajectory. The position influence coefficients, as developed in Chapter III, describe these errors, and therefore serve as elements of the criterion function. The remaining elements of the function are the lift and drag control quantities. Since control requires an expenditure of energy, it is generally minimized with respect to zero. In this problem, the control vector is in a lumped-parameter form containing parameters defining the vehicle configuration and a variable function of angle of attack. It is desirable to minimize the control quantities about nominal mean values to satisfy practical limitations on the vehicle configuration. This allows for control deviations from the nominal

design values as well as determines the optimal control based on trajectory considerations. The criterion function is:

$$J = \frac{1}{2} \int_{\sigma_0}^{\sigma_f} [ \underline{Y}^T R \underline{Y} + \underline{V}^T S \underline{V} ] d\sigma \quad (4-1)$$

$$\text{where: } \underline{Y} = \begin{bmatrix} x_4 \\ x_5 \\ x_6 \end{bmatrix} ; \quad \underline{V} = \begin{bmatrix} u_D - M_{u_D} \\ u_L - M_{u_L} \end{bmatrix} \quad (4-2)$$

and R and S are positive definite diagonal weighting matrices.

#### Necessary Conditions For Optimality

The necessary conditions for optimality are established by formulating the Hamiltonian and applying the appropriate conditions. The state vector  $\underline{X}$  includes the state of the entry model and the position influence coefficients derived in Chapter III. The minimization problem is stated as:

$$\text{minimize } J = \frac{1}{2} \int_{\sigma_0}^{\sigma_f} \phi d\sigma \text{ subject to } \underline{x}' = \underline{f}(\underline{x}, \underline{u}) \quad (4-3)$$

The state equations from Chapter III are:

$$x_1' = \frac{x_1}{\tan x_3} \quad \triangleq F_1 \quad (4-4)$$

$$x_2' = \frac{\mu}{x_1 x_2 \tan x_3} - \frac{C_D x_1}{x_2 \sin x_3} u_D \quad \triangleq F_2 \quad (4-5)$$

$$x_3' = -1 + \frac{\mu}{x_1 x_2^3} - \frac{C_L x_1}{x_2^2 \sin x_3} u_L \quad \triangleq F_3 \quad (4-6)$$

$$\dot{x}_4 = -x_4 \frac{\partial F_1}{\partial x_1} - x_5 \frac{\partial F_2}{\partial x_1} - x_6 \frac{\partial F_3}{\partial x_1} \quad \Delta F_4 \quad (4-7)$$

$$\dot{x}_5 = -x_4 \frac{\partial F_1}{\partial x_2} - x_5 \frac{\partial F_2}{\partial x_2} - x_6 \frac{\partial F_3}{\partial x_2} \quad \Delta F_5 \quad (4-8)$$

$$\dot{x}_6 = -x_4 \frac{\partial F_1}{\partial x_3} - x_5 \frac{\partial F_2}{\partial x_3} - x_6 \frac{\partial F_3}{\partial x_3} \quad \Delta F_6 \quad (4-9)$$

The complete equations of the necessary conditions for optimality are not developed here, but are included in Appendix A. For the development in this section, a set of equations only at a functional level is given.

Given the formulation of the minimization problem in Eq(4-3), the Hamiltonian is as follows:

$$H = \phi + \sum_{i=1}^6 \lambda_i F_i \quad (4-10)$$

where

$F_i$  = state derivatives

$\lambda_i$  = adjoint variables

With the Hamiltonian defined, the four sets of necessary conditions may be stated for the entry problem by referring to Eq(2-10) through Eq(2-13) in Chapter II.

The State Equations. The state equations have been stated in Eq(4-4) through Eq(4-9), and are given by:

$$\frac{\partial H}{\partial \lambda_i} = \dot{x}_i = F_i \quad (4-11)$$



Adjoint Equations. The adjoint equations are derived from:

$$\frac{\partial H}{\partial x_i} = -\lambda'_i \quad (4-12)$$

These are expanded as follows:

$$-\lambda'_i = \lambda_1 \frac{\partial F_1}{\partial x_i} + \lambda_2 \frac{\partial F_2}{\partial x_i} + \lambda_3 \frac{\partial F_3}{\partial x_i} + \lambda_4 \frac{\partial F_4}{\partial x_i} + \lambda_5 \frac{\partial F_5}{\partial x_i} + \lambda_6 \frac{\partial F_6}{\partial x_i} \quad (i = 1, 2, 3) \quad (4-13)$$

$$-\lambda'_j = x_j R_{kk} + \lambda_4 \frac{\partial F_4}{\partial x_j} + \lambda_5 \frac{\partial F_5}{\partial x_j} + \lambda_6 \frac{\partial F_6}{\partial x_j} \quad (j = 4, 5, 6; K = j-3) \quad (4-14)$$

Gradient Equations. The gradient equations are derived from:

$$\frac{\partial H}{\partial u_i} = g(u_i, \underline{x}, \underline{\lambda}, \sigma) = 0 \quad (i = 1, 2) \quad (4-15)$$

They are expanded as follows:

$$G_{u_D} = S_{11} (u_1 - M_{u_D}) + \lambda_2 \frac{\partial F_2}{\partial u_1} + \lambda_4 \frac{\partial F_4}{\partial u_1} + \lambda_5 \frac{\partial F_5}{\partial u_1} + \lambda_6 \frac{\partial F_6}{\partial u_1} \quad (4-16)$$

$$G_{u_D} = S_{22} (u_2 - M_{u_D}) + \lambda_3 \frac{\partial F_3}{\partial u_2} + \lambda_4 \frac{\partial F_4}{\partial u_2} + \lambda_5 \frac{\partial F_5}{\partial u_2} + \lambda_6 \frac{\partial F_6}{\partial u_2} \quad (4-17)$$

Transversality Conditions. The transversality (boundary) conditions are established according to:

$$\begin{bmatrix} \delta x \lambda \end{bmatrix} \begin{matrix} \sigma_f \\ \sigma_0 \end{matrix} = 0 \quad (4-18)$$

This leads to the following table:

Table II. Boundary Conditions For The Entry Problem

	$\sigma_0$	$\sigma_f$
$x_i$ (i = 1,2,3)	specified	specified
$\lambda_i$ (i = 1,2,3)	unconstrained	unconstrained
$x_j$ (j = 4,5,6)	unconstrained	specified (1,0,0)
$\lambda_j$ (j = 4,5,6)	0	unconstrained

When all four conditions are satisfied, the optimal problem is solved. To accomplish this, the numerical procedures described in Chapter II are used. The application of the algorithms to the optimal entry problem is discussed in the following section.

#### Second Variation Equations

The complete perturbation equations for the second variation procedure are not presented here but are included in Appendix A. For the entry problem, it is assumed that position, velocity, and flight angle are specified at the initial point and the sensitivity coefficients are unspecified. It is also assumed that all six states are specified at the terminal point. Thus for backward integration, iterative estimates are made on all six terminal adjoint values. The Newton-Raphson equation for this case is:



or

$$\begin{bmatrix} \delta \lambda (\sigma_0) \\ \delta \underline{x} (\sigma_0) \end{bmatrix} = B^{-1} \delta \underline{x} (\sigma_f)$$

These equations are equivalent to Eq(2-33) and Eq(2-34) in Chapter II.

#### Numerical Application Of The Optimization Algorithms

The application of the numerical optimization techniques of Chapter II to the problem derived in the previous section is shown in flow chart form in Fig. 5, on the following page. A discussion of the solution flow is presented, with the considerations given for the choice of each algorithm.

General Discussion Of Algorithms. To start the solution, the gradient technique is employed. The determining factor for this choice is that since the gradient is not defined to be zero, the largest convergence envelope is obtained. A set of controls are chosen to initialize the gradient and the algorithm proceeds until the criterion for convergence is satisfied. At this point, the state and adjoint values at the boundaries are stored for use as initial estimates in the terminal error function technique.

The terminal error function technique is used as an intermediate technique due to the complexity of the problem. The preliminary investigation into other problems where both first and second variation techniques were used brought out one major common problem. The convergence of the gradient had to be accurate to almost ten significant figures before convergence could be obtained in the second variation technique. The complexity of the problems surveyed appeared to be less than the complexity of the problem under discussion here,

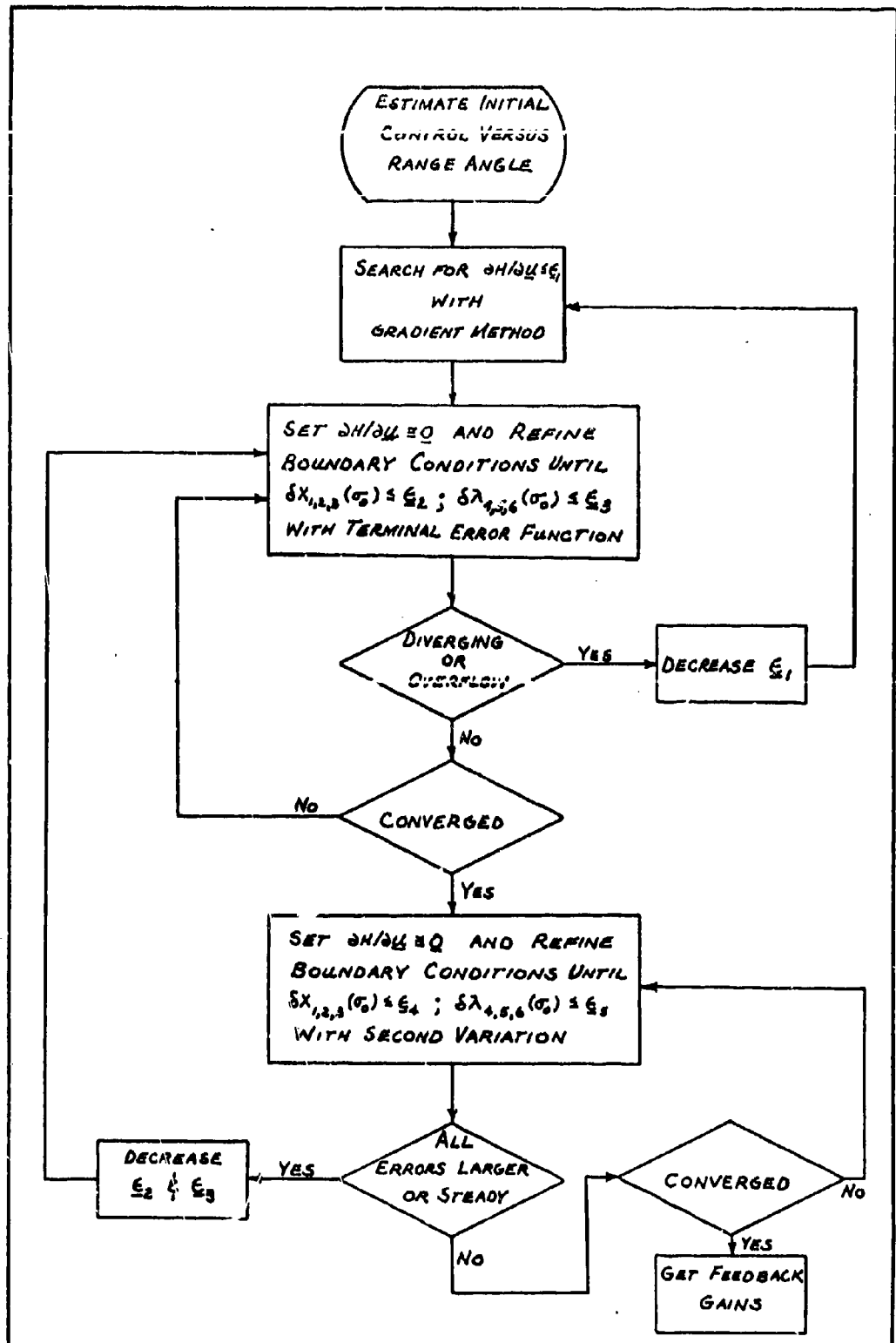


Figure 5. Solution Flow Diagram

therefore, the apparent solution was to develop an intermediate technique which has all the characteristics of the second variation but none of the perturbation equations. These contain the higher order effects, and are the most sensitive to an incompletely converged control. The method of converging to the boundary conditions improves the rate of convergence from a distance, but is sluggish when the desired conditions are nearly attained. This property complements the second variation convergence property very well.

The boundary conditions on one end of the problem are employed as an initial guess for the terminal error function, these are refined in an iterative fashion until the second variation technique accepts them. The complementary convergence property is employed if the convergence in the second variation appears sluggish. An arbitrary indicator of this is the weighting value with the Newton-Raphson matrix.

The second variation procedure is used to refine further the boundary conditions. The procedure will, in general, converge in fewer iterations than the other techniques since it is a second order method. However, linear assumptions are made and the initial estimates to start the procedure must be accurate enough to prevent divergence. When the method converges, the convergence is generally to within eight significant digits in less than thirty iterations.

Some numerical considerations unique to each of the techniques are discussed in the following sections.

First Variation Numerical Considerations. During the thesis, there occurred several areas where the computational solution was inhibited or assisted by the numerical method used. Here, some of the major numerical considerations shall be discussed.

In the gradient algorithm there exists a problem in the integration. In a typical optimal control problem, there are two integrations performed, one forward for the states, and one backwards for the adjoints. Here, there are four integrations. These are necessitated because of the sensitivity coefficients under consideration, and the nature of an entry. The functional relationship is a cumulative one, such that all sets of equations functionally related to the one being integrated must be integrated simultaneously. The table below indicates the four distinct sets of equations, the order in which they are integrated, and the location of the boundary conditions.

Table III  
Known Boundary Conditions For Gradient Algorithm

Integration Order	Equation Set	Known Boundaries
1	State	Initial
2	Sensitivity Coefficients	Final
3	Sensitivity Coefficient Adjoint	Initial
4	State Adjoints	Final

The method of successive integration sweeps is extremely time consuming, therefore to cut down a large amount of this time, the alpha search in the gradient uses only the first two integration sweeps. From these sweeps the cost can be fully determined, and the alpha search can proceed in minimum time. There is a pitfall, which occurred often enough to warrant a check in the computation scheme. The adjoint equations are never consulted during the alpha search,

and sometimes overflow the computer due to the large changes in the control. This occurs primarily in the sensitivity coefficient adjoint equations, which are third order equations. When this occurs, the nearest value of alpha, for which a gradient could be calculated, is used. With this part of the algorithm streamlined, a great amount of computation time is saved.

In the terminal error function, the major problem area is in the convergence. This problem occurs as a direct result of the functional relation discussed in the gradient algorithm. The convergence is in general slow when all criterion elements are balanced, such that each boundary condition error carries a similar weight. The convergence is much improved by converging on each element in turn, saving the adjoint variables until last. The terminal error function in this problem converges very quickly to the state boundaries, at the expense of the adjoint boundaries. This convergence problem will be further discussed when the results are presented.

Second Variation Numerical Considerations. In using the second variation method, the computer time required becomes of primary concern. In the entry problem presented in this report, it is necessary to solve 162 differential equations. For integration of a trajectory with 100 integration intervals using a fourth order Runge-Kutta integration scheme, approximately one and one-half minutes of computer execution time on an IBM 7040 is required. If 30 to 40 iterations with the Newton-Raphson matrix are required, a total execution time of about 45 to 60 minutes results. This problem is the most difficult to overcome. If all nine position sensitivity coefficients are included



in the problem, it is necessary to solve 24 state and adjoint equations and 576 perturbation equations resulting in a large time increase.

Depending on the nature of the state and adjoint equations, the second variation procedure may converge in fewer iterations using backward integration than using forward integration. However, in order to reduce the terminal velocity by several thousand meters per second and the terminal flight angle by several degrees while holding the initial conditions constant, it is more desirable to use forward integration. This allows the Newton-Raphson procedure to slowly lower the terminal conditions.

For the entry problem considered, the second variation procedure may be started without initial estimates from either the gradient or terminal error function procedures. This requires a visual examination of the control equations with the purpose of determining the proper signs on each variable estimated to cause the trajectory to proceed in the desired direction. The magnitudes can be determined by testing the program with any arbitrary magnitudes and subsequently reducing the estimated values until no overflow condition exists in the computer. This does not produce an acceptable trajectory, but does produce a beginning trajectory to allow the final conditions to be satisfied by the Newton-Raphson procedure. The magnitudes of the estimates for one example case are presented in Appendix B. This heuristic approach is not mathematically based but allows maximum use of engineering judgement to start the procedure.

The Newton-Raphson matrix for the entry problem is a  $6 \times 6$  matrix and must be inverted with double precision arithmetic in the computer to allow convergence. No measures of ill-condition for this matrix have

been computed, but the elements for the entry problem range from  $10^{+14}$  to  $10^{-19}$ . It is possible that the matrix is highly ill-conditioned because of this. However, on some of the trajectories considered backward integration produced convergence to within  $10^{-8}$  m in position,  $10^{-8}$  mps in velocity, and  $10^{-5}$  deg in flight angle.

### V. Trajectory Solutions

In order to analyze the form and magnitude of the sensitivity coefficients, a set of solutions to the optimal entry problem is produced, each of which minimized the sensitivity coefficients for a given set of parameters and control constraints. In this chapter, the results of these solutions are presented and discussed.

The optimal problem is cast into the following four general forms:

- A. Unconstrained control with a drag control bias
- B. Unconstrained control without a drag control bias
- C. Constrained control with a drag control bias
- D. Constrained control without a drag control bias

Within each of these forms, the boundary conditions are varied to produce variations in the lift and drag controls and in the trajectories. The bias value represents the results of defining an arbitrary vehicle configuration. The concept of designing the controls to contain all the vehicle parameters is described in Chapter III. The bias chosen is the mean of the control boundaries. For the drag control element the bias value is:

$$M_{UD} \Delta \frac{u_{Dmax} + u_{Dmin}}{2} = 0.00014688 \quad (5-1)$$

The lift control is bounded symmetrically about zero; thus, no bias is necessary.

The trajectory solutions are presented in the first portion of this chapter, and are discussed in the latter portion. Seven cases are considered.

Unconstrained Control Solutions

Four trajectories are discussed here, each with a different control and terminal boundary value limitation. The first two cases do not include the arbitrary configuration bias parameter. The second two include a defined configuration and also an attempt to achieve nearly horizontal flight with a terminal velocity of about Mach 5 at a terminal altitude of 10 Km.

Case 1. Free Terminal Velocity And Flight Path Angle And A Range Angle Of 1.71 Degrees. In the first trajectory considered, the following boundary conditions are defined:

Range Angle	Radius (r)	Velocity (v)	Flight Angle ( $\gamma$ )
$\sigma_0$	120 Km	7420 mps	120 degrees
$\sigma_f$	9 Km	unconstrained	unconstrained

The results for this trajectory are shown in Fig. 6 through Fig. 9. The maximum change in flight angle for this trajectory is 0.13 deg. and its terminal value is 119.88 deg. The velocity increases monotonically from the initial value to a terminal value of 7563 mps (meters per second). The reasons for the nearly constant acceleration are found by examining the values of the lift and drag controls. As the vehicle enters the most dense portion of the atmosphere, the controls begin to change from the zero level. The drag control becomes more negative so as to cause constant acceleration of the vehicle. The trajectory for this case has a nearly constant flight path angle indicating that the velocity sensitivity coefficient,  $[\partial r(\sigma_f)/\partial v(\sigma)]$ , is minimized by forcing the trajectory to be as near a straight line in space as possible. For a fixed  $\sigma_f$ , the control for this type of

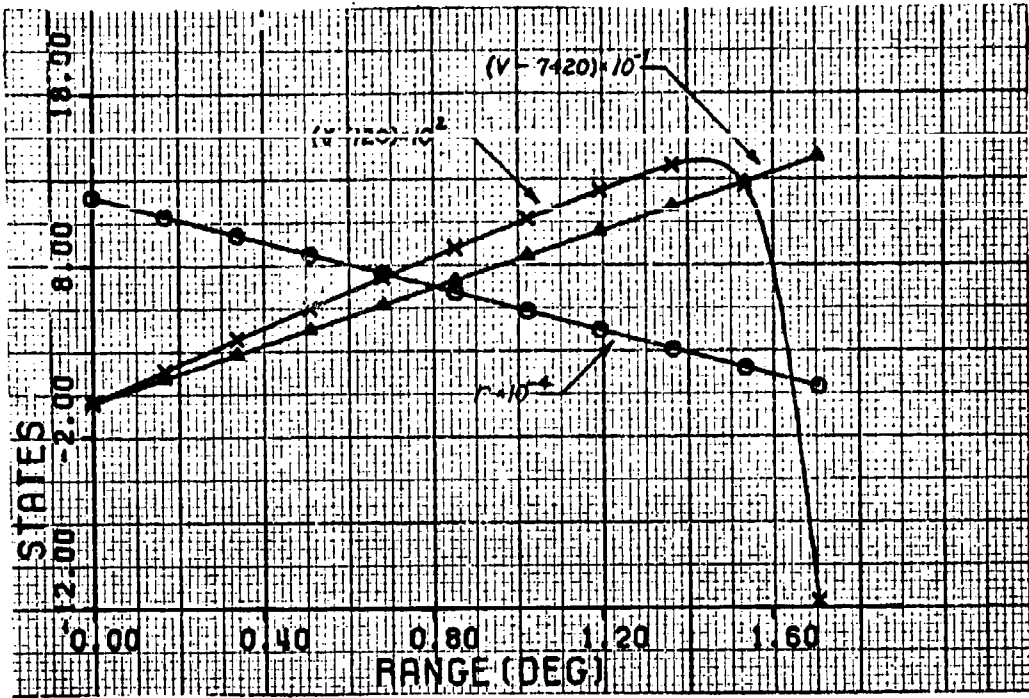


Figure 6. Case 1 - States

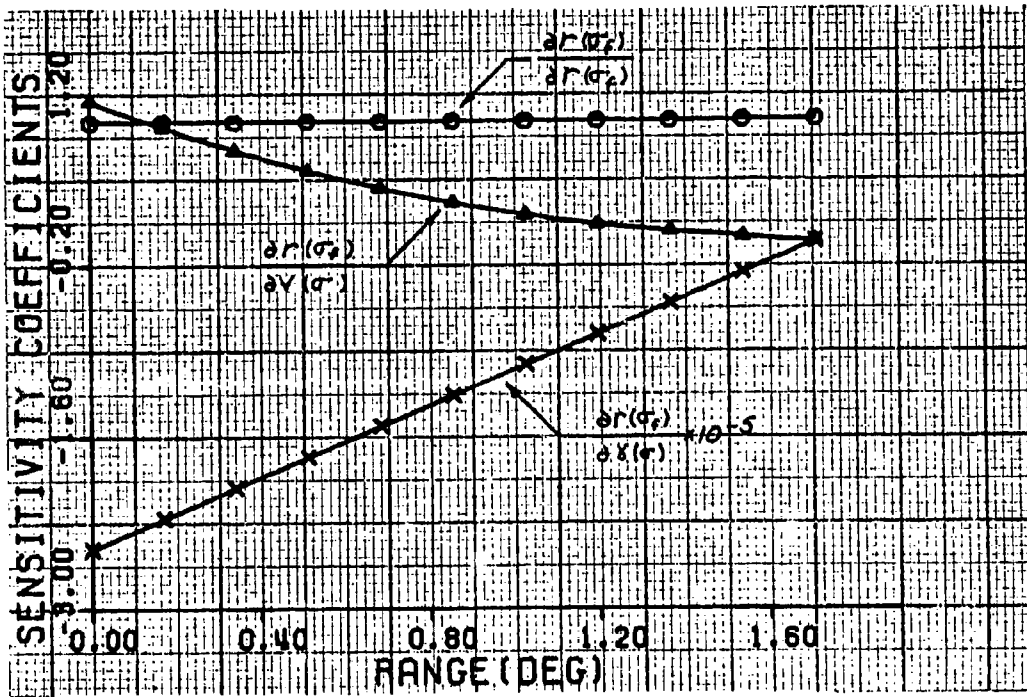


Figure 7. Case 1 - Sensitivity Coefficients

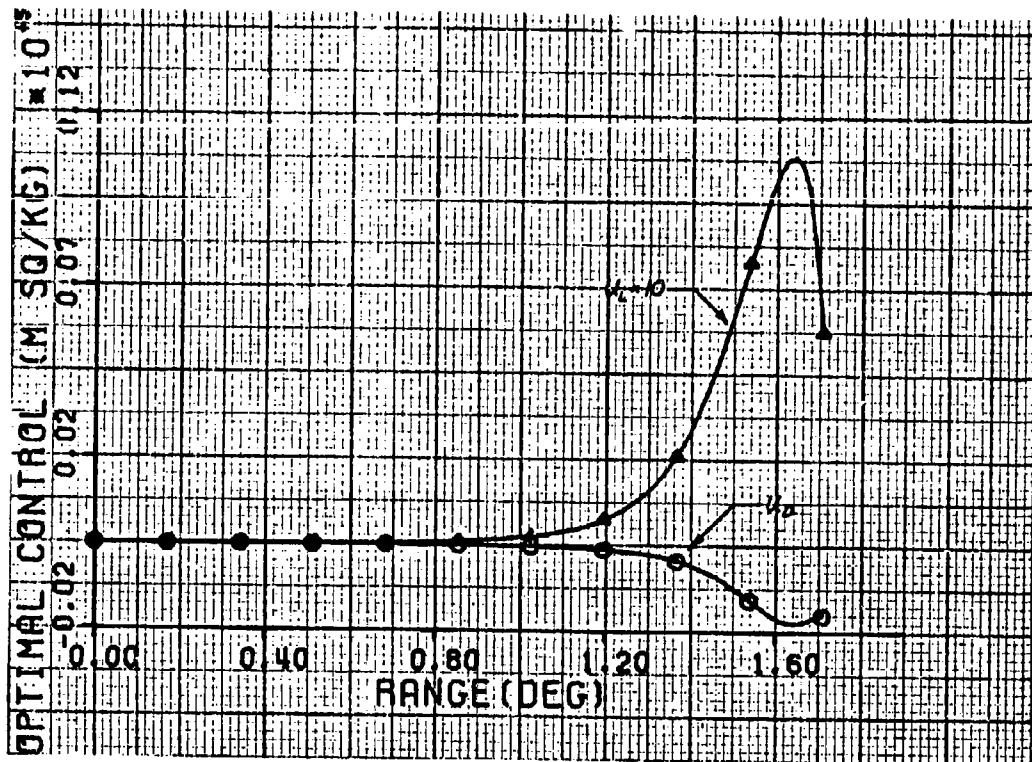


Figure 8. Case 1 - Optimal Controls

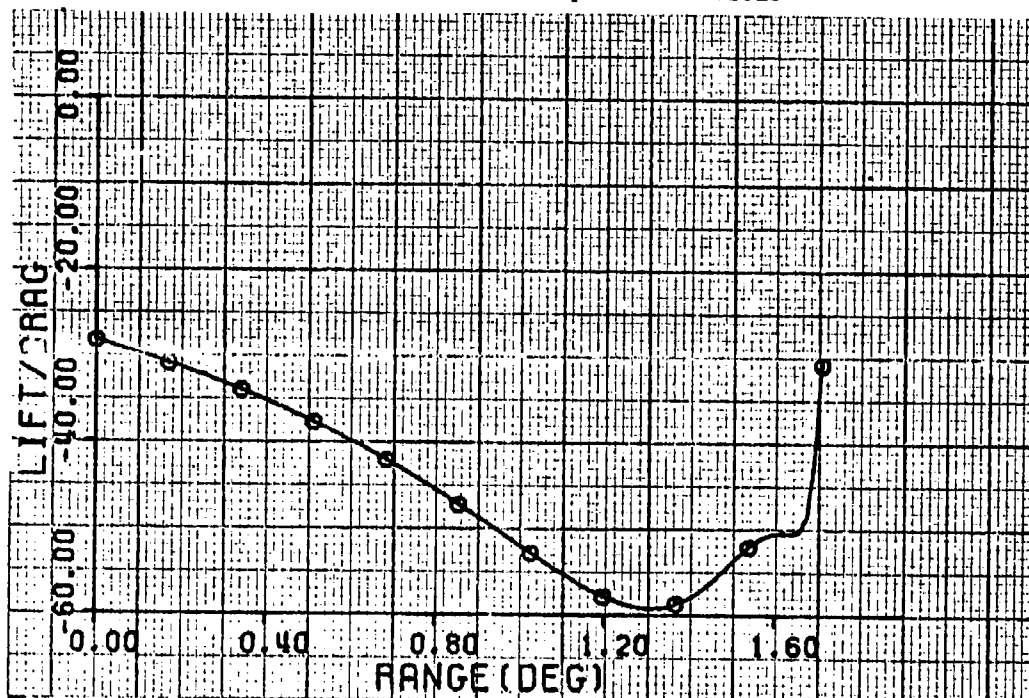


Figure 9. Case 1 - Lift/Drag

trajectory produces smaller sensitivity coefficients than for most of the other cases. However, the nature of the trajectory limits its practical use because a thrust capability is required to produce the negative drag profile.

Case 2. Specified Terminal States And A Range Angle Of 1.71 Degrees. The second trajectory considered is constrained to meet terminal boundary conditions on all three states. The conditions are as follows:

Range Angle	Radius (r)	Velocity (v)	Flight Angle ( $\gamma$ )
$\sigma_0$	120 Km	7420 mps	120 degrees
$\sigma_f$	9 Km	6500 mps	119.88 degrees

The results of this case are shown in Fig. 10 through Fig. 13. This trajectory resembles the previous case in that the flight angle profiles for the two cases are similar. The effect of the lower velocity at the terminal point is reflected in the drag control. The drag control for this case is positive throughout the trajectory. Above the altitude of 12.3 Km, the control is below the range of most practical non-thrusting entry body controllers.

In this trajectory the controls do not deviate from zero until the dense portion of the atmosphere is entered, at approximately 35 Km, and nearly all of the controlling is done in the last one-sixth of the trajectory. This is reflected in the velocity profile, which remains nearly constant until the end of the trajectory. The drag control is dominant in this case as shown by the lift to drag ratio. The form and magnitude of the sensitivity coefficients is similar to that of Case 1.

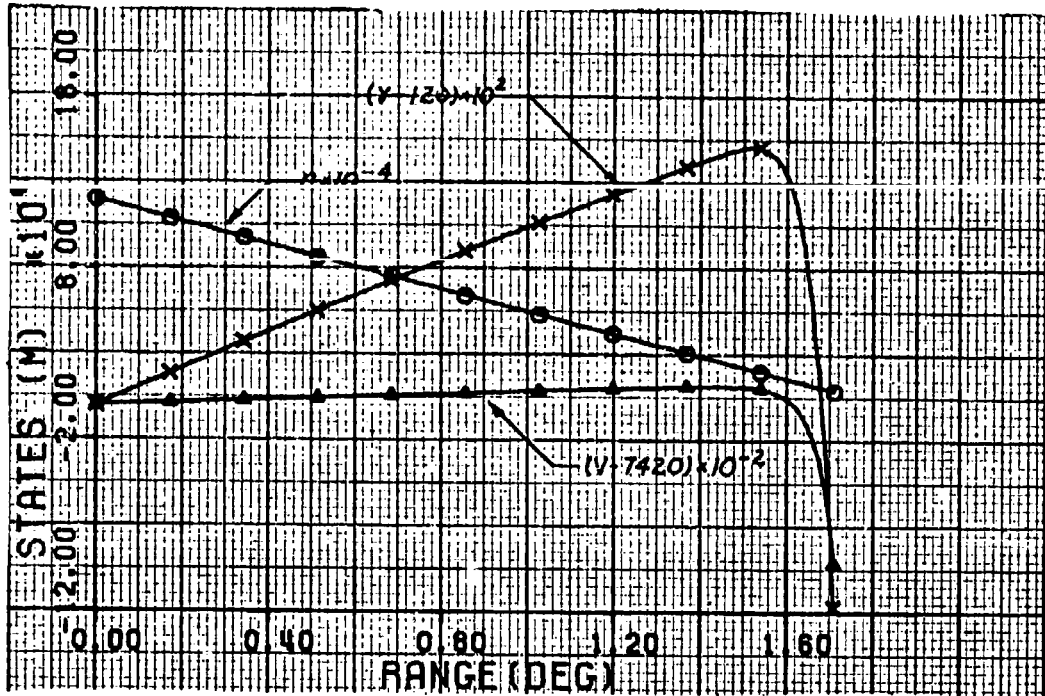


Figure 10. Case 2 - States

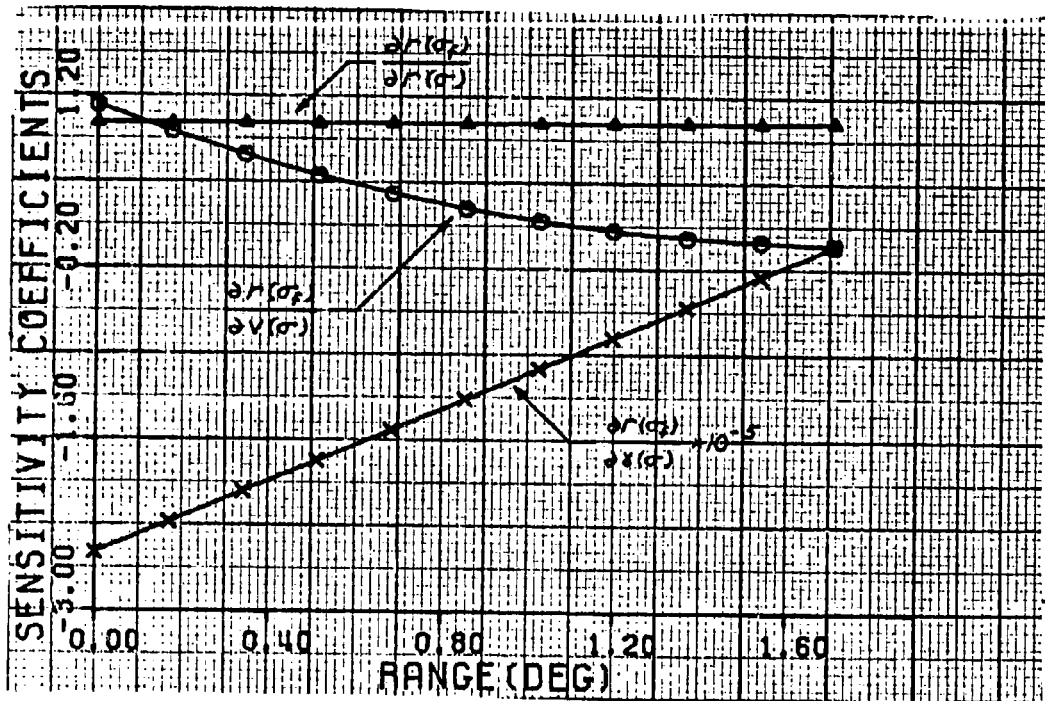


Figure 11. Case 2 - Sensitivity Coefficients



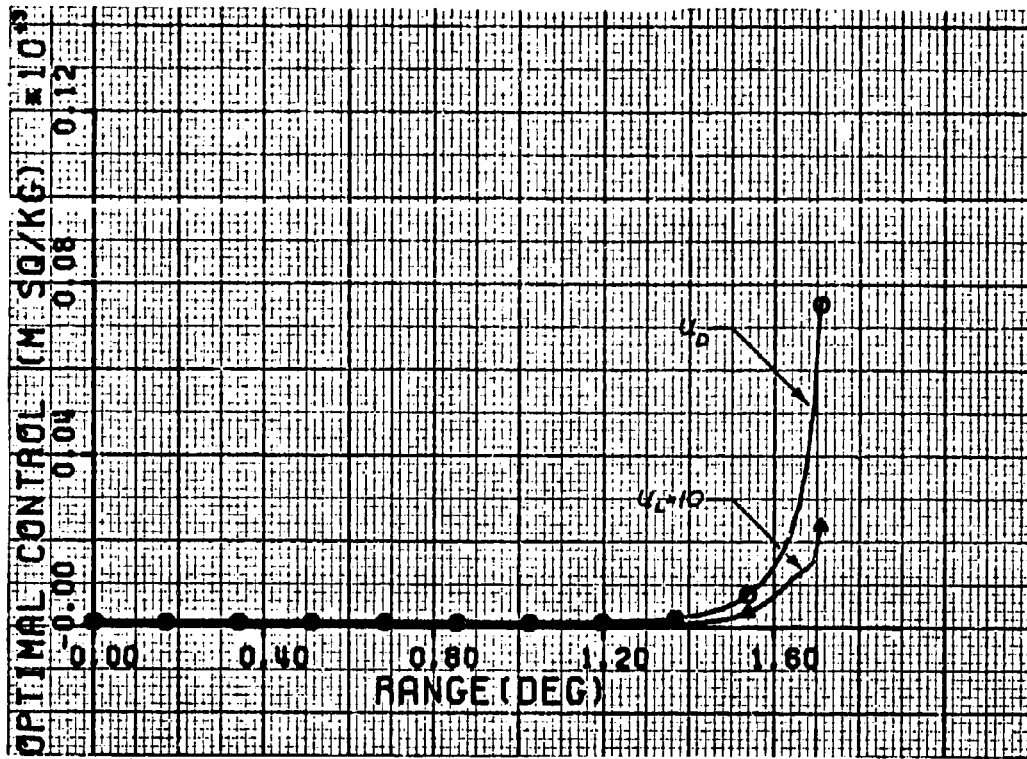


Figure 12. Case 2 - Optimal controls

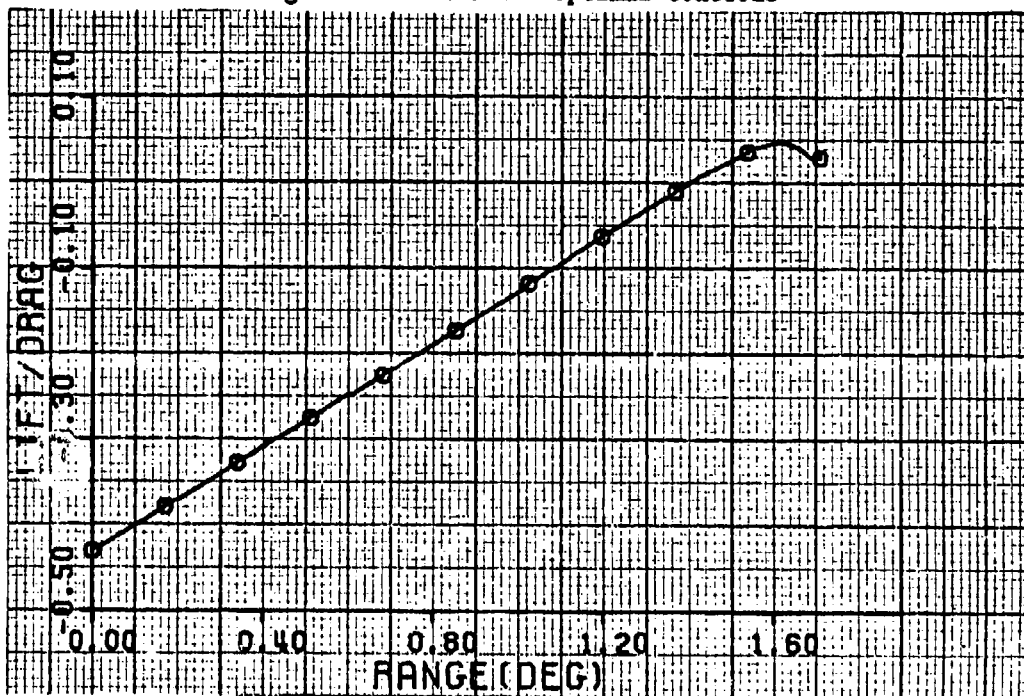


Figure 13. Case 2 - Lift/Drag

The maximum deceleration for this case is 138 G's during the final portion of the trajectory. The high terminal velocity and low drag profile in this case limits its practical use.

Case 3. Specified Terminal States With A Control Mean And A Range Angle Of 3.16 Degrees. The two trajectories discussed previously are limited due to drag control values below the boundaries of a non-thrusting controller. To eliminate this limitation, two additional elements are considered. First a drag control bias is placed in the criterion function to allow for drag control about a constant value. Second, the terminal conditions of the problem are changed such that a reasonably flat terminal flight angle and a terminal velocity of approximately Mach 5, are obtained.

The trajectory for this case has the following boundary conditions:

Range Angle	Radius (r)	Velocity (v)	Flight Angle ( $\gamma$ )
$\sigma_0$	120 Km	7240 mps	108.0 degrees
$\sigma_f$	8.1 Km	1650 mps	98.9 degrees

As shown in Fig. 14 through Fig. 17, the controls are relatively constant until the vehicle enters the most dense portion of the atmosphere when large changes begin to occur in the velocity and  $\gamma$  profiles. The controls reach maximum values at the maximum dynamic pressure point which is at 10.5 Km. The lift to drag ratio is also a maximum at this point. The changes in control are reflected in the sensitivity coefficients, especially in the velocity sensitivity coefficient.

A secondary objective of this trajectory is to reduce the amount of deceleration of the vehicle by obtaining a flatter trajectory and by inducing additional drag throughout the entry. This reduction in

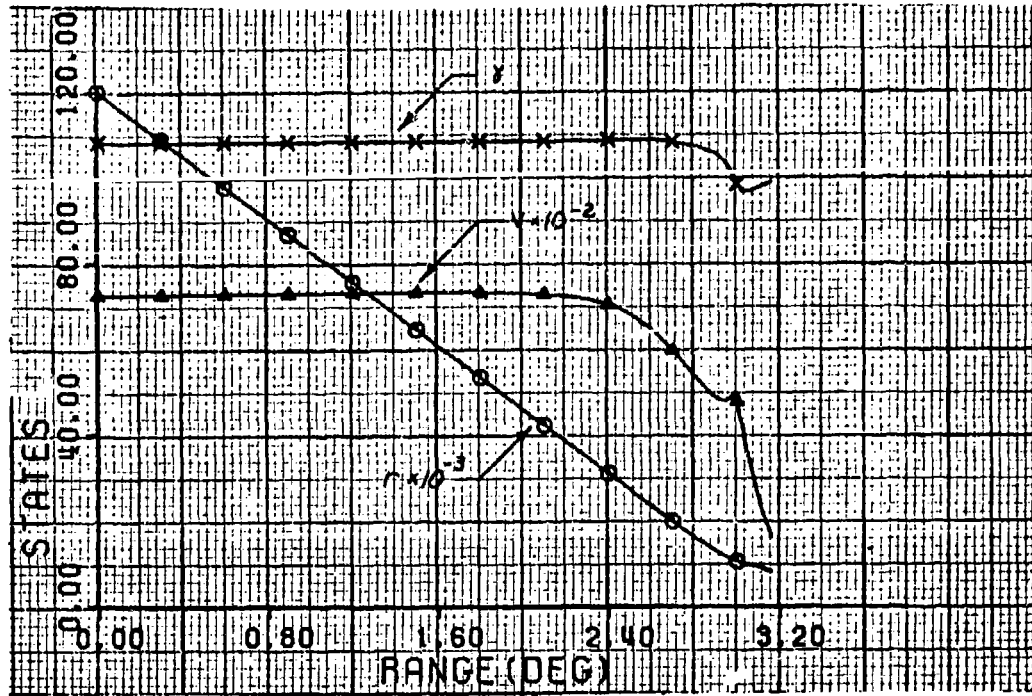


Figure 14. Case 3 - States

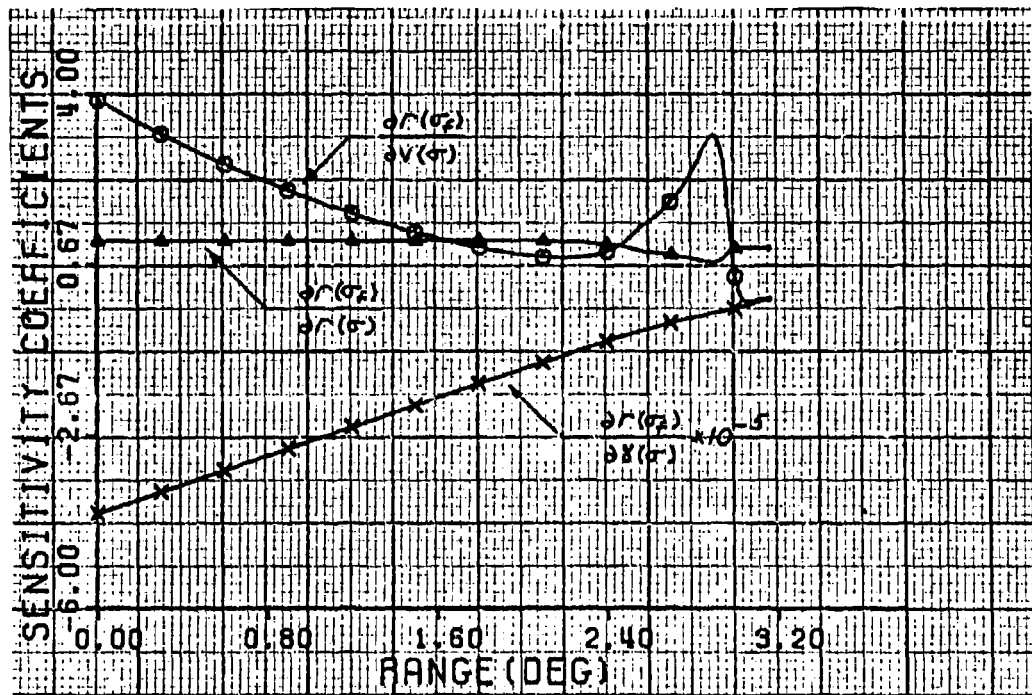


Figure 15. Case 3 - Sensitivity Coefficients

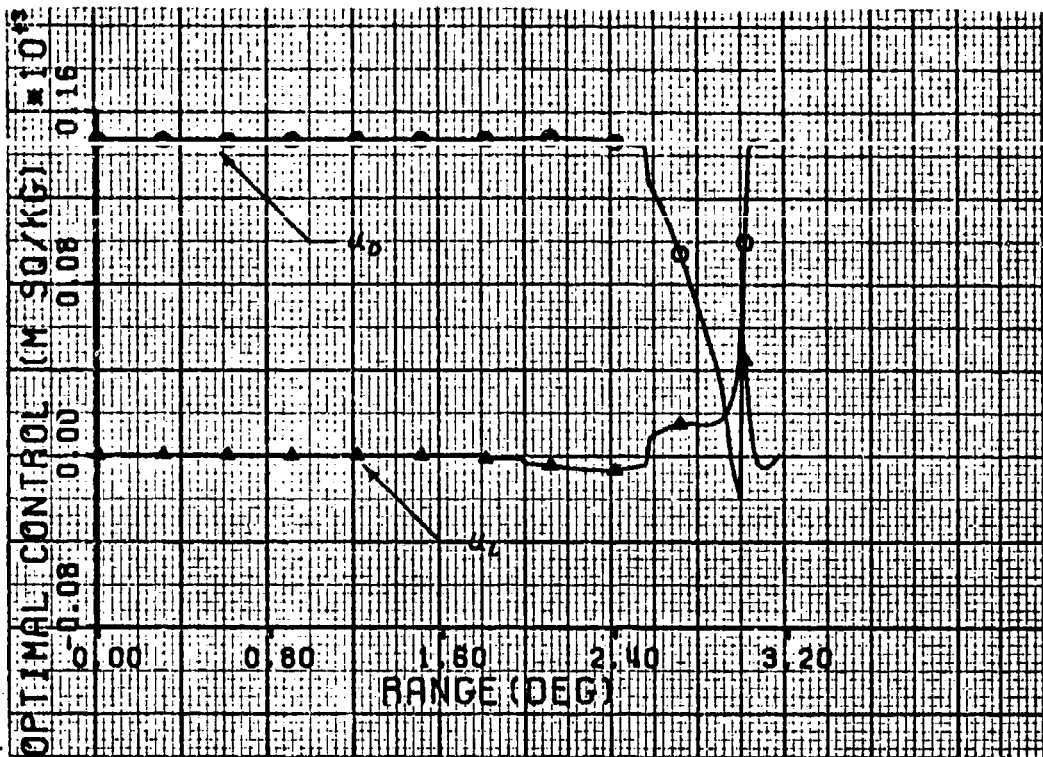


Figure 16. Case 3 - Optimal Controls

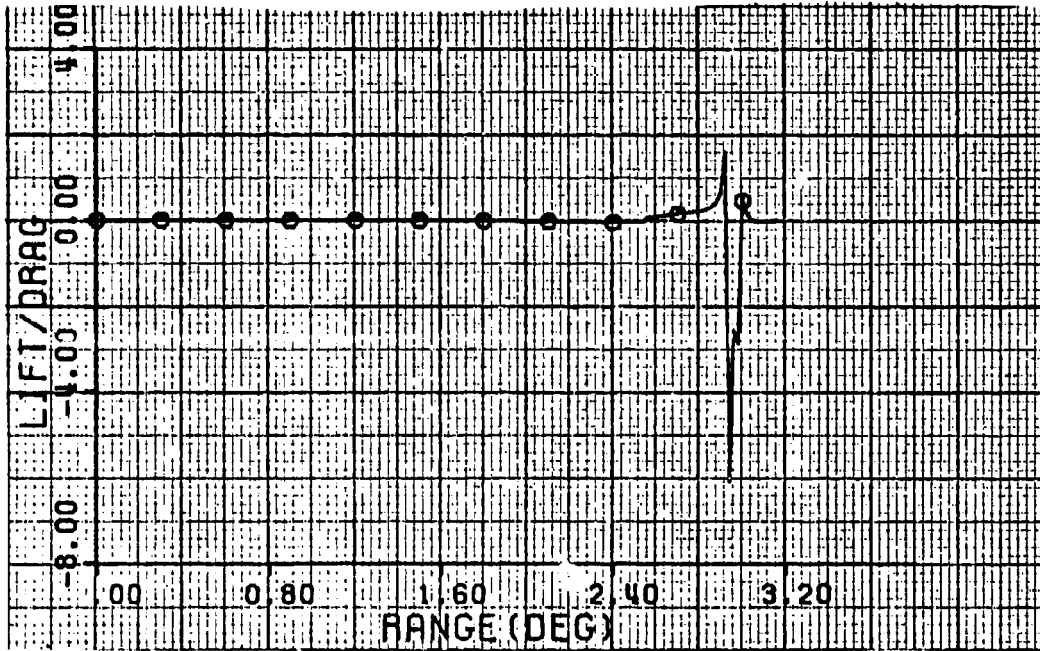


Figure 17. Case 3 - Lift/Drage

drag deceleration in this case is offset by the lift spike shown in the graph of the controls resulting in a high total deceleration at the end of the trajectory. Also, during the highest deceleration, the drag control falls below acceptable limits, and even becomes negative. The negative drag requires a thrusting vehicle, and thus limits its use. Once again the two control elements do not change significantly from the initial values until the last portion of the trajectory in the most dense part of the atmosphere. The maximum deceleration is 101 G's which occurs at approximately the point of maximum dynamic pressure.

Case 4. Specified Terminal States With A Control Mean And A Range Angle Of 3.32 Degrees. In the previous case, the sensitivity coefficients appear to be simply a function of the range angle. To investigate this relationship, as well as to generate a flatter trajectory, an additional case is defined. The boundary conditions for this case are defined as follows:

Range Angle	Radius (r)	Velocity (v)	Flight Angle ( $\gamma$ )
$\sigma_0$	120 Km	6780 mps	107.0 degrees
$\sigma_f$	8.1 Km	1650 mps	98.8 degrees

The results of this case are shown in Fig. 18 through Fig. 21. The trajectory obtained is similar to that of Case 3. The controls for these two cases differ only slightly in both form and magnitude. The sensitivity of radius with respect to velocity for this case rises sharply; whereas, the sensitivity of the radius with respect to flight angle and the sensitivity of radius with respect to radius appear to continue to vary linearly with range angle as in the first three cases.

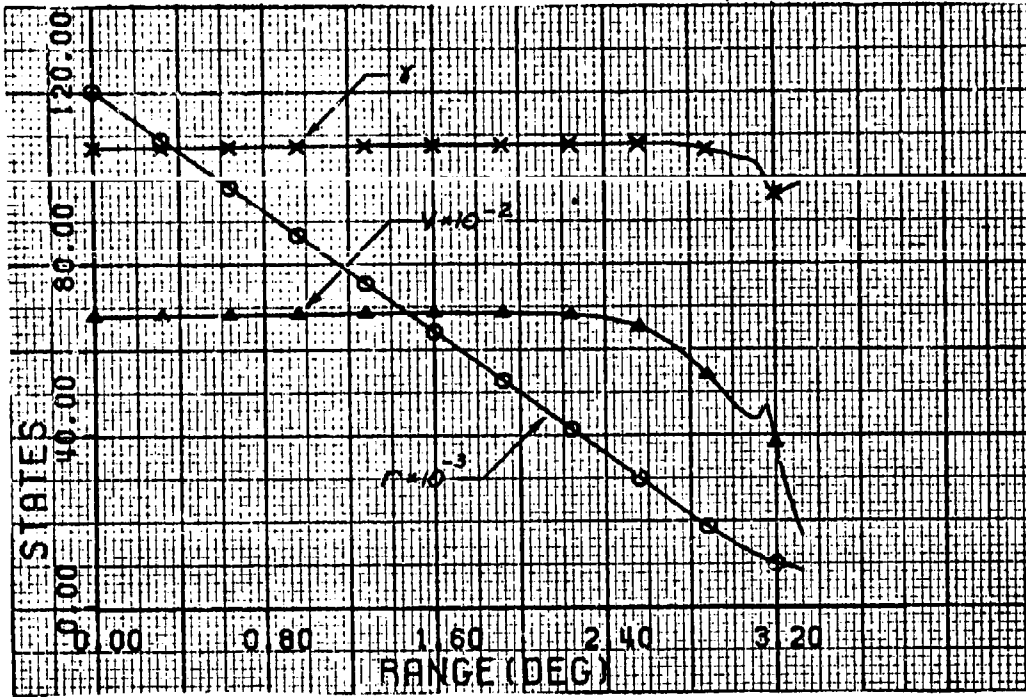


Figure 18. Case 4 - States

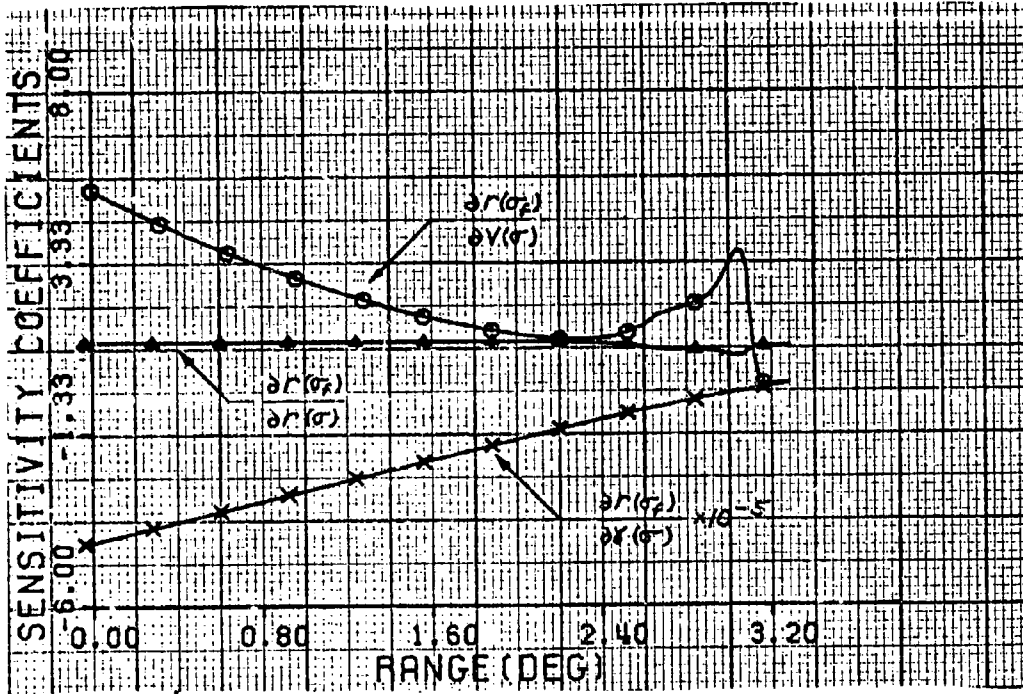


Figure 19. Case 4 - Sensitivity Coefficients

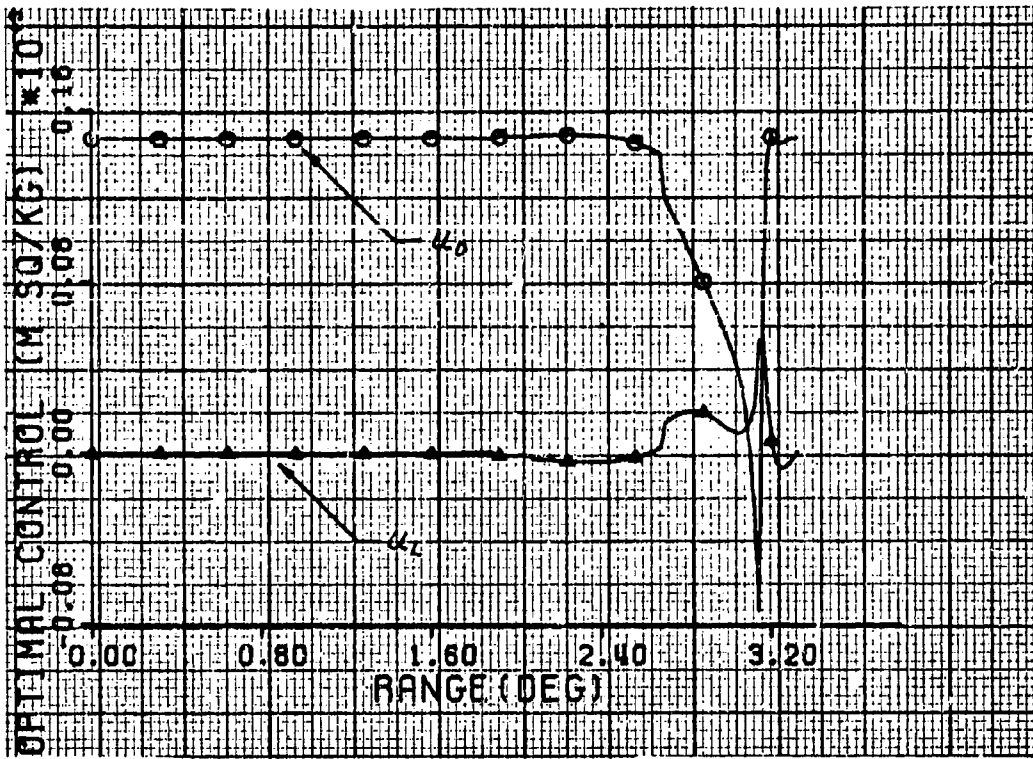


Figure 20. Case 4 - Optimal Controls

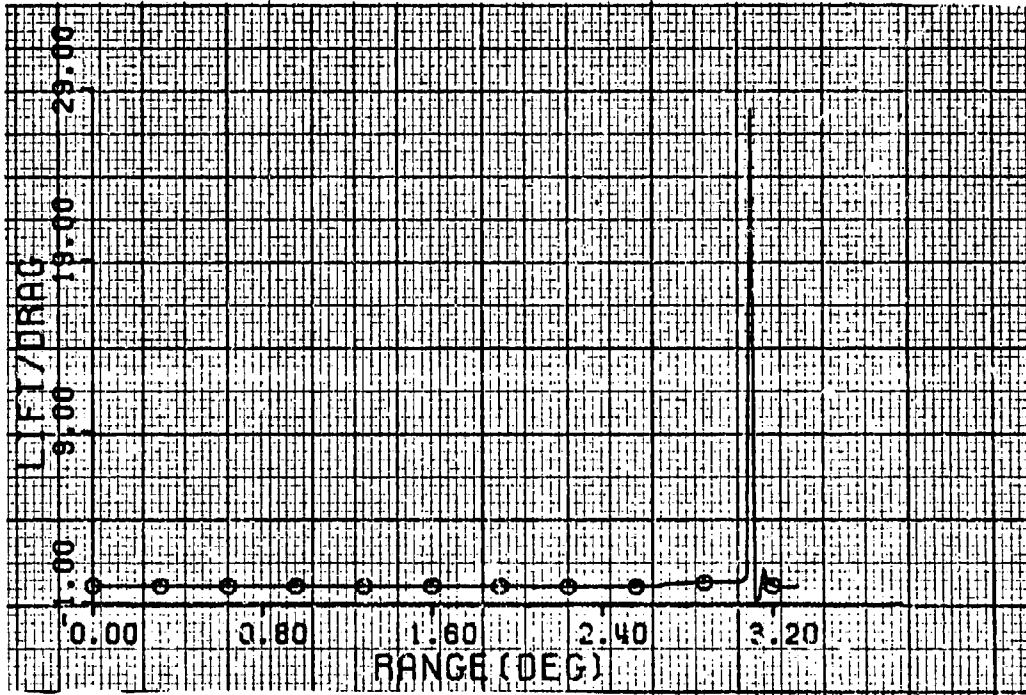


Figure 21. Case 4 - Lift/Drag

For the secondary objective of reducing the deceleration, it is shown that along with the increase in one sensitivity coefficient a lower maximum deceleration is attained. The maximum deceleration for this trajectory is 97.0 G's occurring again at approximately the point of maximum dynamic pressure.

#### Solutions With Lift And Drag Control Constraints

All of the four previous cases satisfy the necessary conditions of the optimal entry problem. However, none satisfy the practical requirement that the controls remain within physical limits. Even in the cases with a drag control bias, the control boundaries were violated. To correct for this, Valentine's procedure for a bounded control solution is used for the entry problem in the second variation optimization method.

Two trajectories are determined in the following cases; one which employs the drag control bias, and one which does not. In both cases the control constraints are as follows:

$$2.76 \times 10^{-5} \leq u_D \leq 2.20 \times 10^{-3}$$

$$-1.6u_D \leq u_L \leq 1.6u_D$$

The lift constraint simply limits the lift to drag ratio.

Case 5. Specified Terminal States And A Range Angle Of 2.0 Degrees. This trajectory is obtained by an investigation of the effects of lower starting altitude, velocity, and flight angle on the sensitivity coefficients. The conditions for this case are as follows:

Range Angle	Radius (r)	Velocity (v)	Flight Angle ( $\gamma$ )
$\sigma_0$	115 Km	6115 mps	115.5 degrees
$\sigma_f$	7 Km	5000 mps	114.5 degrees



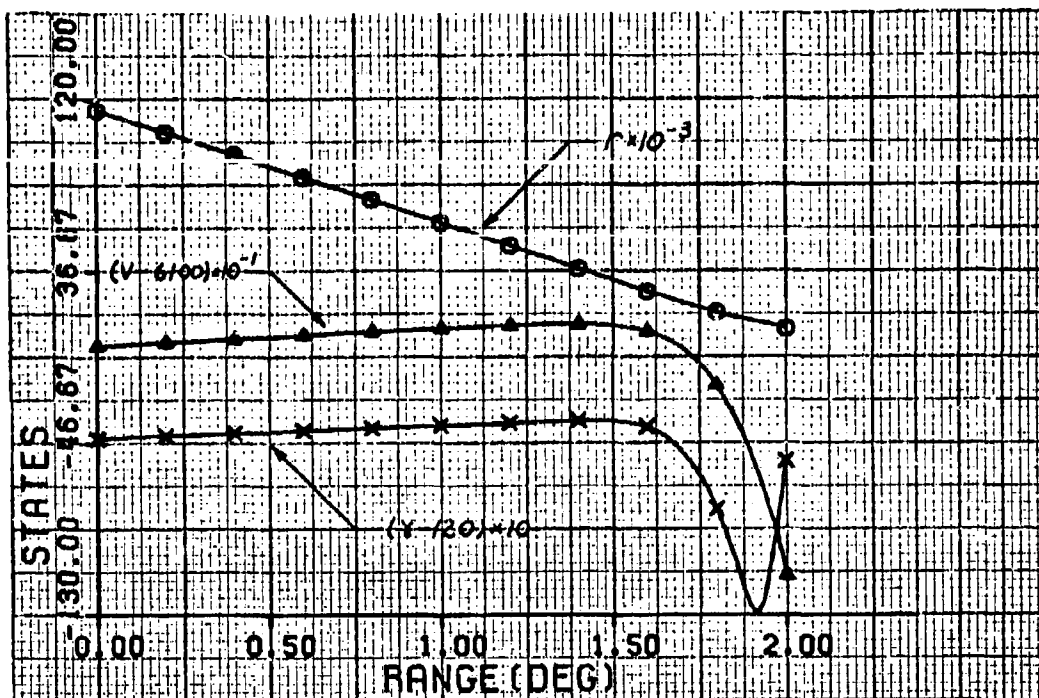


Figure 22. Case 5 - States

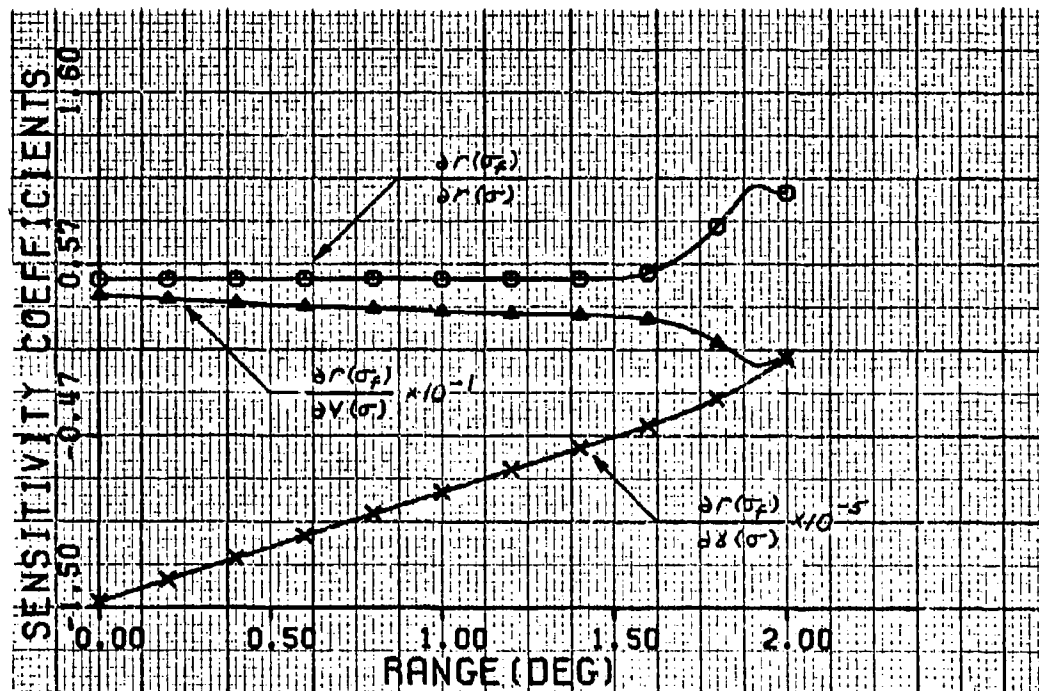


Figure 23. Case 5 - Sensitivity Coefficients

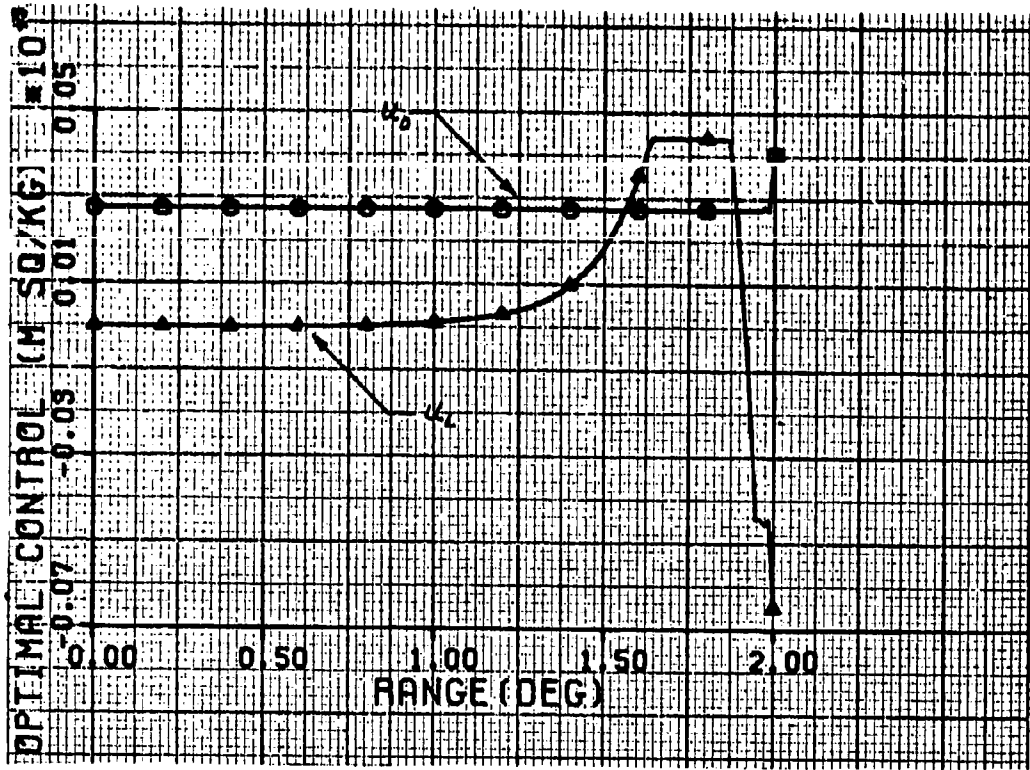


Figure 24. Case 5 - Optimal Controls

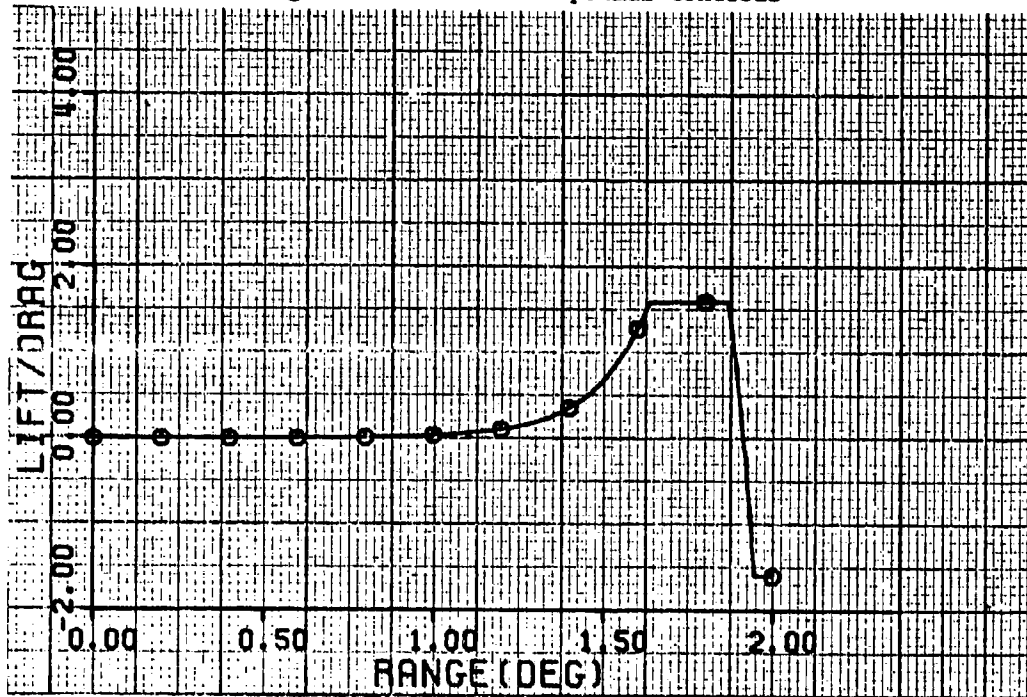


Figure 25. Case 5 - Lift/Drage

As the Fig. 22 through Fig. 25 show, this trajectory results in large changes of the flight angle during the entry. These changes are reflected by the control curves, which show that nearly all the maneuvering is done by the lift control, while the drag control remains on the lower boundary. The lift control begins to significantly deviate from zero at about the midpoint of the trajectory. However, this does not significantly affect the velocity and flight angle until the last quarter of the trajectory. At this point, lift becomes the dominant control, and begins to directly affect the flight angle,  $\gamma$ . Referring to the graph of the lift to drag ratio, dominant lift control does not occur until the lift to drag ratio approaches unity. The lift control reduces the flight angle to well below the terminal value and the drag control increases at the very last of the trajectory to satisfy the terminal velocity condition and to give to the terminal flight angle condition.

The drag control remains on the lower boundary until the terminal phase of the trajectory. With drag remaining at a minimum for nearly all of the trajectory, the lift control maneuvers the flight of the vehicle.

The effect of the control constraint is evident by the smooth changes in the flight angle. The lift control is more uniformly distributed during the flight than in the previous cases. The lift and drag controls are within acceptable practical limits throughout the trajectory.

This trajectory resembles those of Case 3 and Case 4 with respect to the form of the sensitivity coefficients. In each of these, the sensitivity coefficients appear to be smooth curves until changes in

the flight angle occur. At that point the radial and velocity sensitivity coefficients change significantly. This effect shall be discussed in the latter portion of the chapter.

This trajectory is the most practical yet discussed. However, due to the high terminal velocity and the high deceleration resulting from the high drag control at the last of the trajectory, its use is also limited. The maximum deceleration is 83 G's and occurs at the terminal point of the trajectory.

Case 6. Specified Terminal States With A Control Mean And A Range Angle Of 2.06 Degrees. This case contains similar boundary conditions to those of Cases 3 and 4, but with a smaller total range angle. The boundary conditions for this case are as follows:

Range Angle	Radius (r)	Velocity (v)	Flight Angle ( $\gamma$ )
$\sigma_0$	120 Km	7667 mps	118.4 degrees
$\sigma_f$	8.1 Km	1600 mps	97.0 degrees

The trajectory for this case is very similar to those found in Cases 3 and 4. The results are illustrated in Fig. 26 through Fig. 29. The effect of the control constraint is evident by examining the portion of the trajectory during which the flight angle changes. The use of the Valentine procedure keeps the controls within bounds; however, this alone is not a sufficient practical constraint. The rate of change of the lift to drag ratio caused by the sudden change in the magnitude of the drag control cannot be duplicated in any practical vehicle.

The sensitivity coefficients generally resemble those from Cases 3 and 4; however, there are some notable differences between these.

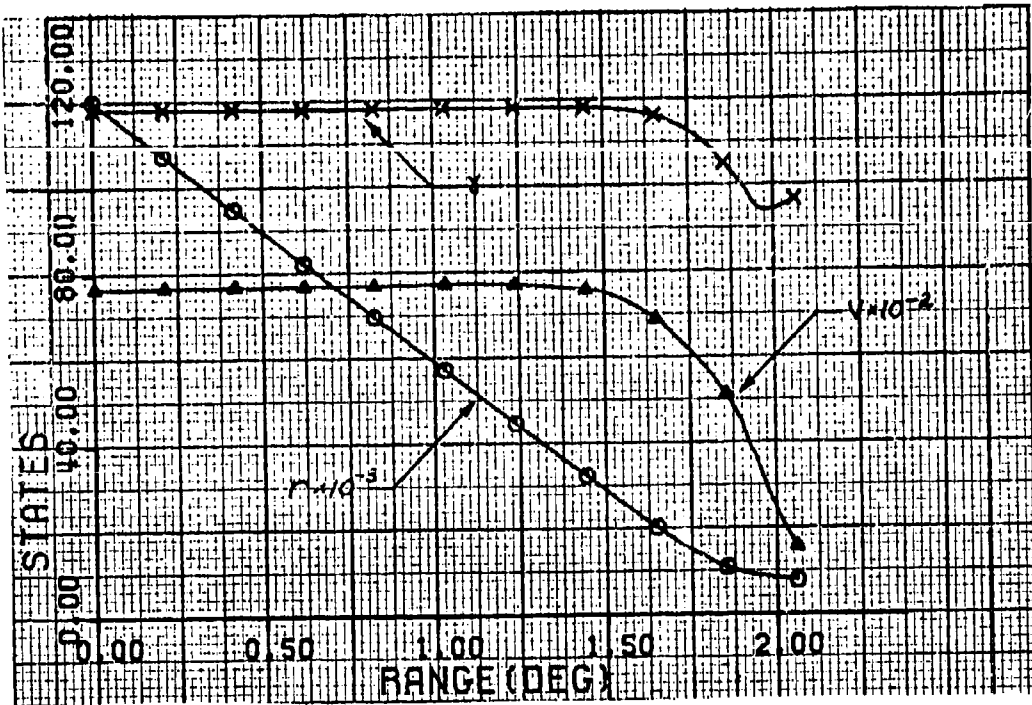


Figure 26. Case 6 - States

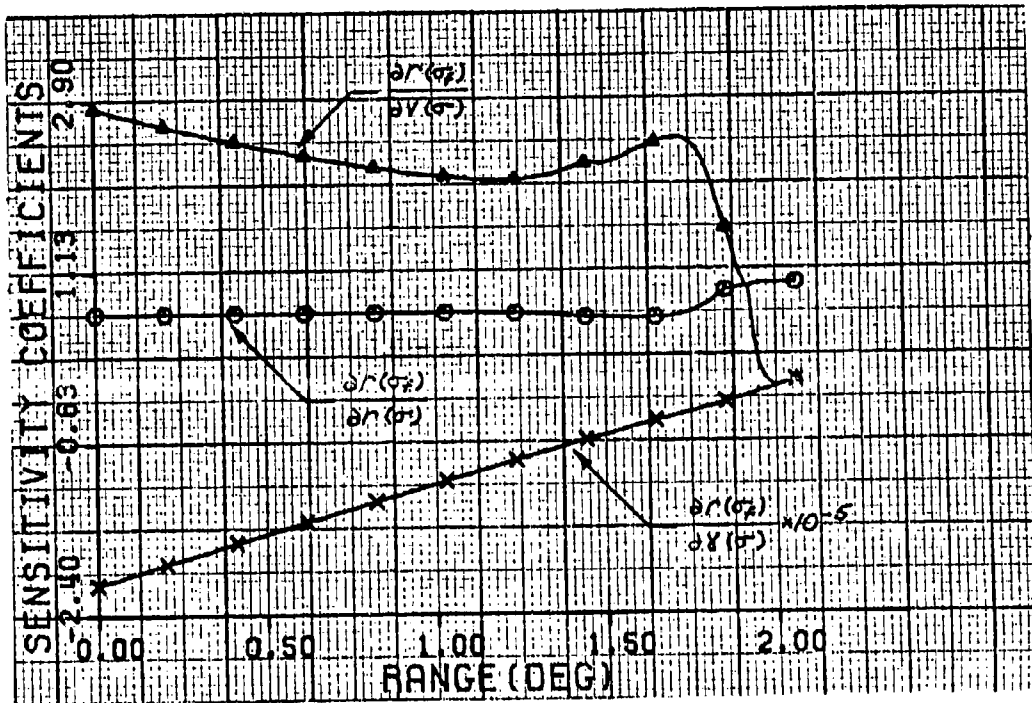


Figure 27. Case 6 - Sensitivity Coefficients

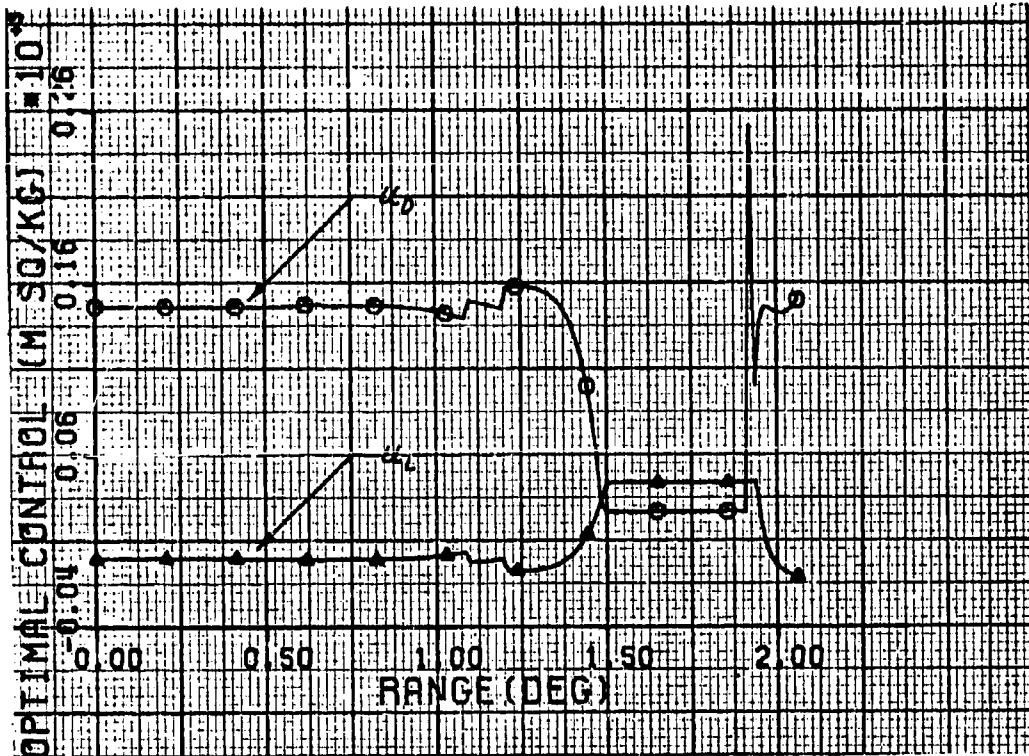


Figure 28. Case 6 - Optimal Controls

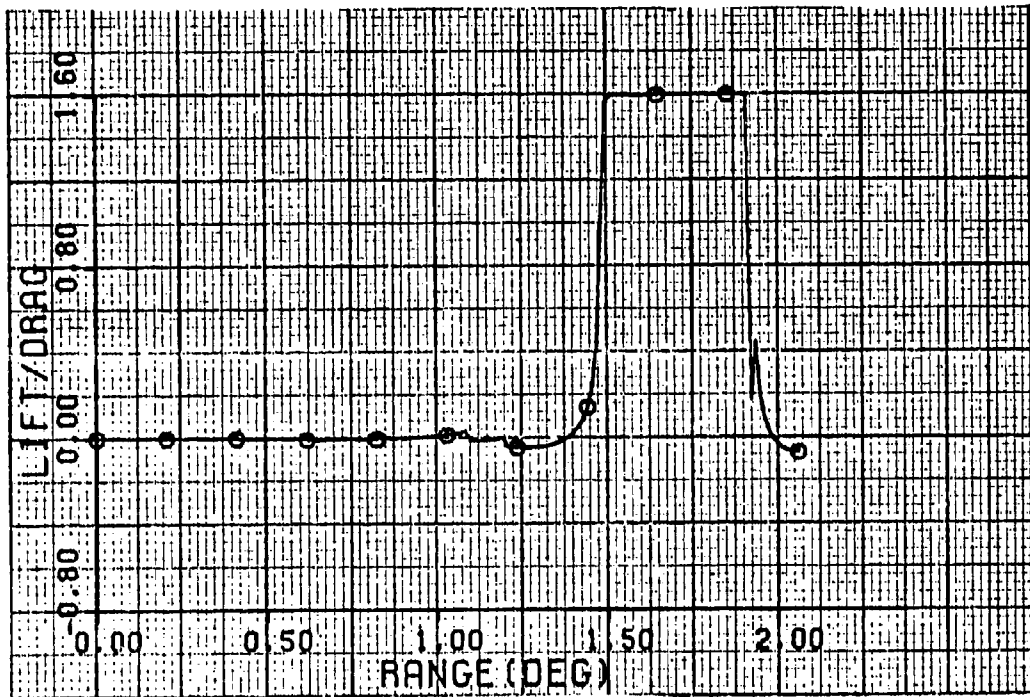


Figure 29. Case 6 - Lift/Drag

First, due to changes in flight angle earlier in the trajectory than previously noted, the radial and velocity sensitivity coefficients begin to deviate from a smooth curve earlier in the trajectory than in Case 5. Second, they appear to be displaced by a constant value from the extrapolated end points of the smooth curves. The flight angle sensitivity coefficient remains a nearly linear function of range angle. There is also in each instance where a flight angle change occurs an abrupt change in slope in the flight angle sensitivity coefficient curve. In Cases 3, 4, and 6, the change is from a positive slope to a less negative slope, while in Case 5 the change is from a positive slope to a more negative slope. A more detailed discussion of these tendencies and other aspects of the minimum sensitivity coefficients will be presented in the last section of this chapter.

This trajectory is impractical due to the rate of change of the lift to drag ratio. The maximum deceleration is 162 G's. This occurs at the point of maximum control change, which is past the point of maximum dynamic pressure. It is evident that to produce a practical trajectory, it is not only necessary to constrain the change in control, but also the rate of change of control.

#### Solution With Drag Control Constraints Only

It has been previously noted that when drag control dominates the entry trajectory, as it does when a drag control bias is used, the changes in slope of the sensitivity coefficients are opposite to the changes in slope when a bias is not used. These changes in slope occur only when the flight angle changes radically during the trajectory. Before discussing the one remaining case, it should be noted

that the sensitivity coefficient equations are final value equations and are integrated in reverse time. For this reason changes in the sensitivity coefficients are more easily interpreted by considering them beginning at the final range angle and ending with the initial range angle. Use will be made of this interpretation method in the discussion of Case 7.

Case 7. Specified Terminal States, Drag Control Constrained; Range Angle Of 1.86 Degrees. The results of the trajectory for this case are illustrated by Fig. 30 through Fig. 33. The boundary conditions are as follows:

Range Angle	Radius (r)	Velocity (v)	Flight Angle ( $\gamma$ )
$\sigma_0$	120 Km	6700 mps	120.3 degrees
$\sigma_f$	9 Km	5000 mps	114.5 degrees

The trajectory states shown in the figures resemble those of Case 5, with two significant differences. First, the amount of maximum change in the flight path angle is twice that of Case 5 due to the dominance of the lift control. Second, the maximum velocity change is increased by 700 meter/second.

The lift and drag profiles of the two cases are similar if magnitudes are ignored. In this case the lift control does not deviate significantly zero until near the last quarter of the trajectory. The drag control remains on the lower boundary until the last integration interval of the trajectory. Thus, this trajectory consists predominately of lift control.

The form and magnitude of the radial and flight angle sensitivity coefficients for this case are different from those of all the other



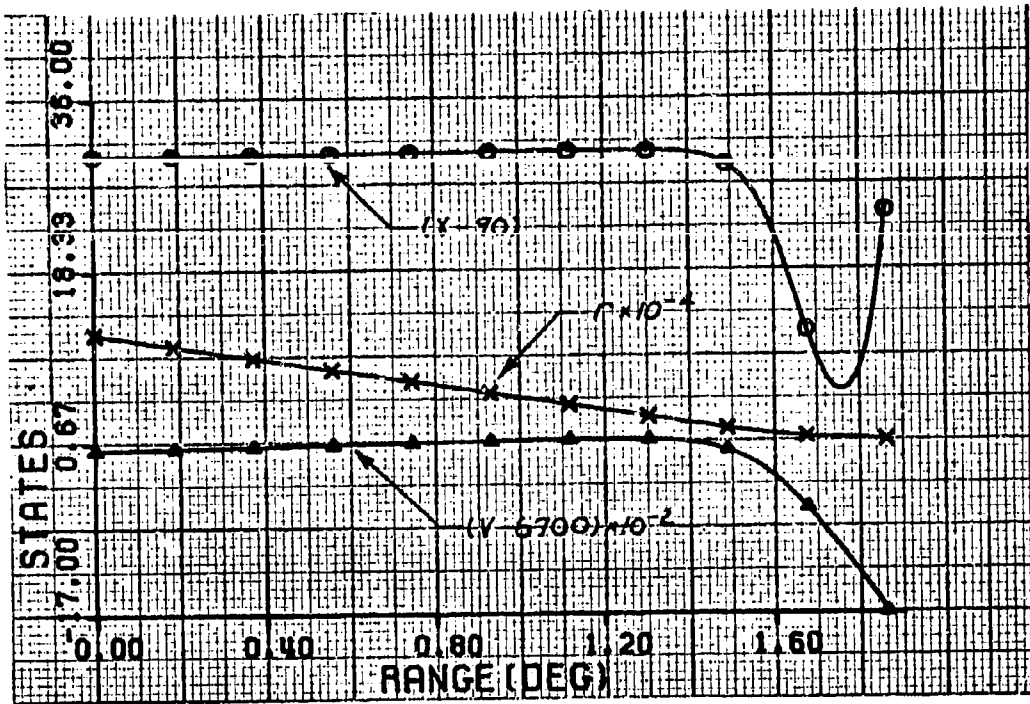


Figure 30. Case 7 - States

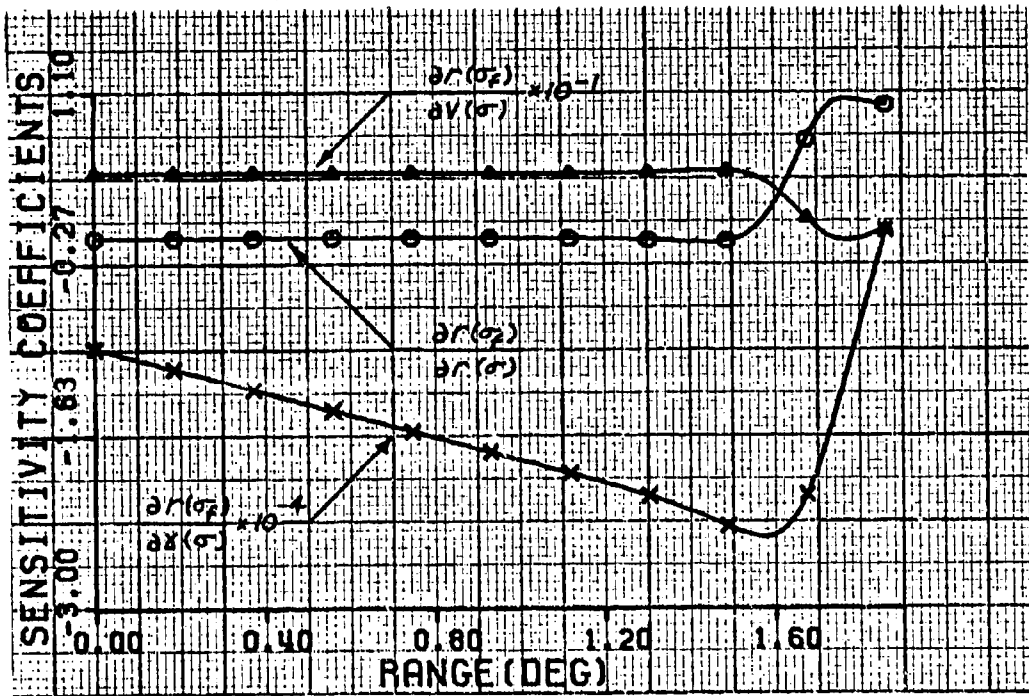


Figure 31. Case 7 - Sensitivity Coefficients

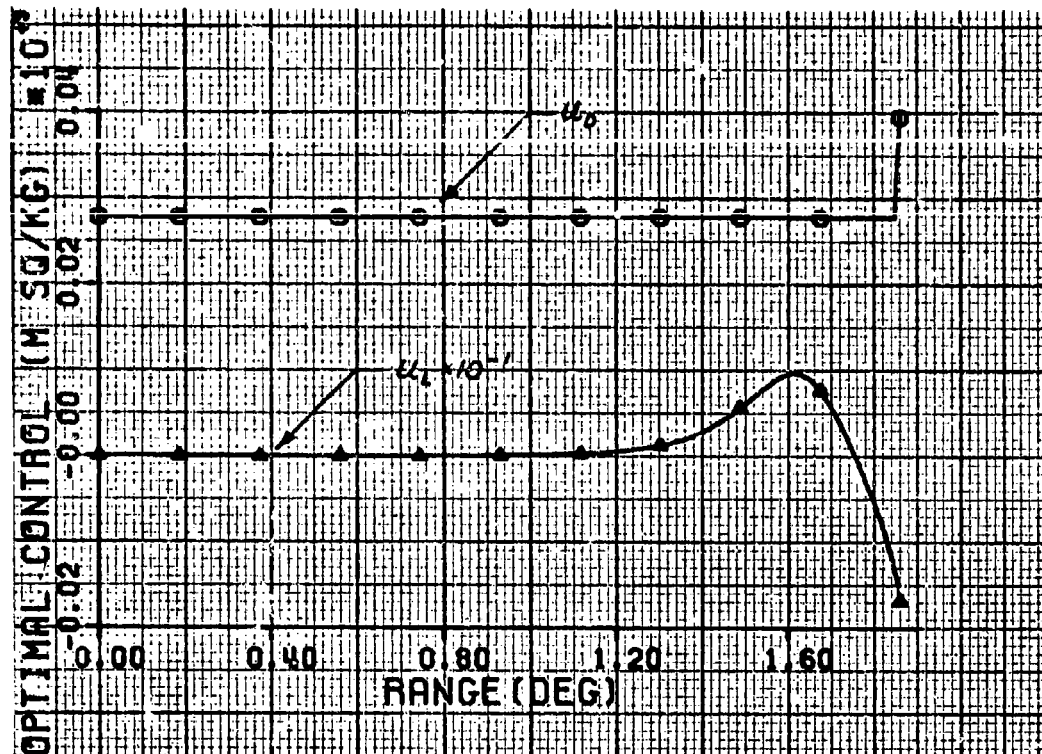


Figure 32. Case 7 - Optimal Controls

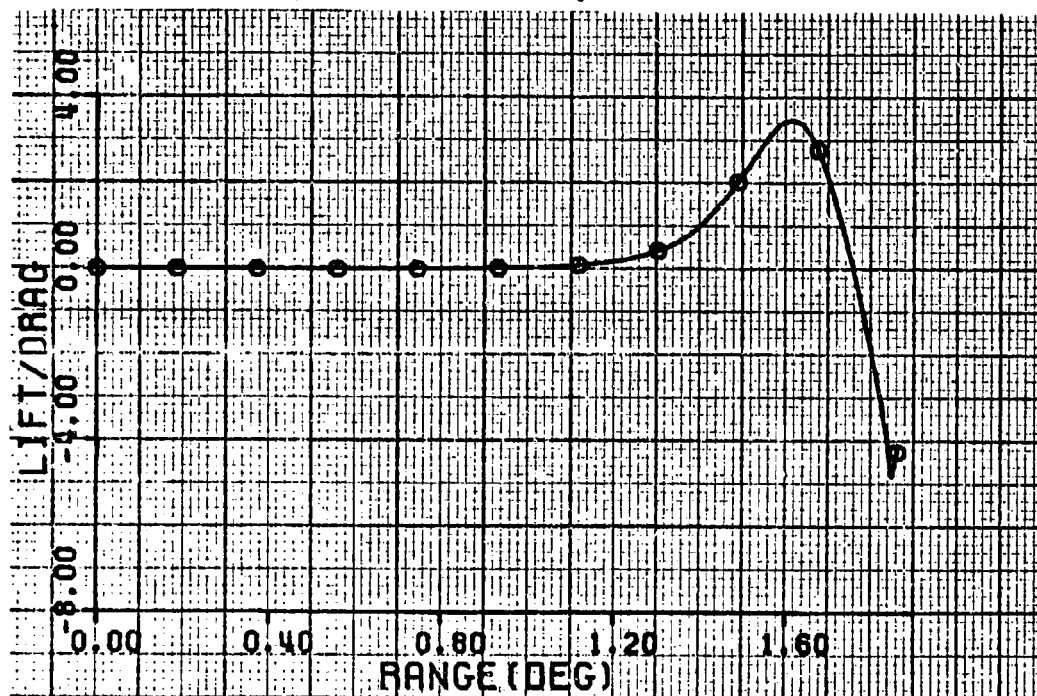


Figure 33. Case 7 - Lift/Drag

cases considered. The radial sensitivity coefficient,  $[\partial r(\sigma_f)/\partial r(\sigma)]$ , has a value of unity at the terminal point and, examining the coefficient backward in range angle, decreases to a value of about -0.05 and remains at this value until the initial range angle of zero is reached. The flight angle coefficient,  $[\partial r(\sigma_f)/\partial \gamma(\sigma)]$ , starts with a value of zero at the terminal point, decreases to about -23000 and then increases to about -9000 at the initial point. The velocity sensitivity coefficient,  $[\partial r(\sigma_f)/\partial v(\sigma)]$  for this case is similar in form to those of Case 5. The coefficient increases from zero at the terminal point to a value of about +4.6 and remains at this value until the initial range angle is reached.

This trajectory results in significantly lower range and flight angle sensitivity coefficients than for any of the other cases. The velocity sensitivity coefficient for this case is higher than for all other cases except Case 4.

The maximum deceleration for this trajectory is 188 G's at the terminal point of the trajectory. This large deceleration is primarily due to the change in control during the dive maneuver during the last part of the trajectory.

#### Discussion Of Trajectory Solutions

In the previous section, seven solutions to the optimal problem formulated in Chapter IV were presented. In each case, different parameters were varied to allow for the maximum variation among the solutions. Although the solutions varied, there were some general trends which were noticeable throughout. In this section, several observations will be presented and substantiated. The observations

will concern the curves formed by the integration of the sensitivity coefficients. As the observations shall be substantiated by examples from the cases, a summary of the salient points from each case are given in Table IV. The observations are as follows:

Observation 1: The sensitivity coefficient solutions may be separated into two distinct portions during each trajectory. This observation is substantiated by the appearance of a break point in the three sensitivity coefficient curves in all cases after Case 2. Referring to Case 3, there is a smooth curve down to the last quarter of the trajectory, then the curves diverge significantly. The first portion of the trajectory shall be defined as the non-aerodynamic portion. The second part shall be defined as the aerodynamic portion.

Observation 2: The non-aerodynamic portion of the trajectory is characterized by a drag dominance, and small changes in flight angle. This observation is substantiated by Cases 1 and 2 which are non-aerodynamic trajectories. Both of these exhibit a drag dominance in the lift to drag ratio, and have a small change in flight angle. All other cases exhibit this same tendency throughout the non-aerodynamic portion.

Observation 3: The sensitivity coefficient curves, in the non-aerodynamic portion are either functions of range angle, or constant. This tendency is common throughout the cases. This observation shall be substantiated for each sensitivity coefficient. The radial sensitivity coefficient  $[\partial r(\sigma_F)/\partial r(\sigma)]$ , in each case is a near constant with respect to range angle. For example, in Case 6, the value is .7 from  $\sigma_0$  to the break point. The velocity sensitivity coefficient,

Table 4  
Summary of Trajectory Solutions

CASE	DRAG CONSTRAINT	LIFT CONSTRAINT	INITIAL $v^*$ (mps)	FINAL $v^*$ (mps)	INITIAL $\gamma$ (Deg)	FINAL $\gamma$ (Deg)	MAXIMUM CHANGE IN $v^*$	MAXIMUM CHANGE IN $\gamma$	$\frac{\partial r(\sigma_2)}{\partial r(\sigma_0)}$	$\frac{\partial r(\sigma_2)}{\partial v^*(\sigma_1)}$	$\frac{\partial r(\sigma_2)}{\partial \gamma(\sigma_1)}$
1	No	No	7420	7563	120.00	119.88	163.	0.3	0.97	1.14	-251401.
2	No	No	7420	6500	120.00	119.88	1036.	0.3	0.98	1.13	-252630.
3	No	No	7420	1650	108.00	98.90	5588.	9.8	1.15	4.19	-428544.
4	No	No	6780	1650	107.00	98.80	5204.	9.2	1.12	5.30	-435782.
5	Yes	Yes	6115	5000	115.50	114.50	1120.	9.3	0.48	3.82	-446298.
6	Yes	Yes	7667	1600	118.40	97.00	6137.	21.4	0.71	2.82	-208221.
7	Yes	No	6700	5000	120.30	114.50	1793.	23.9	-0.05	4.60	-9387.

$[\partial r(\sigma_f)/\partial v(\sigma)]$ , in all cases, excluding Case 7, is observed to be some exponential function of range angle. In Case 7, the value appears to remain near constant; however, from Cases 5 and 6 there appears to be a second function which determines the magnitude of the exponential function of range angle. This function remains constant throughout the non-aerodynamic portion of the trajectory. The flight angle sensitivity coefficient,  $[\partial r(\sigma_f)/\partial \gamma(\sigma)]$ , is a linear function of range angle. In all cases, except Case 7, the slope is positive. In all cases, however, there is a definite linear relation to range angle. It is apparent, from the cases which both have different slope change at the break point, that there is some function which sets the value of  $\frac{\partial}{\partial \sigma}[\partial r(\sigma_f)/\partial \gamma(\sigma)]$  equal to a constant at the break point. Since the sensitivity coefficients are integrated in reverse time, as final value equations, the conditions for the constant value of  $[\partial r(\sigma_f)/\partial r(\sigma)]$ , the constant multiplier in  $\partial r/\partial v$  and the first derivative of  $[\partial r(\sigma_f)/\partial \gamma(\sigma)]$  are set at the break point as final values for the reverse time integration. These conditions shall be further discussed after the observations concerning the aerodynamic portion of the trajectory have been stated.

Observation 4: The aerodynamic portion of the trajectory is characterized by changes in both flight angle and velocity; and dominance by the lift control.

This observation is substantiated by the fact that in each case which has two distinct portions of the trajectory, the break point of all of the sensitivity coefficient curves occur at a given range angle. at that range angle, in the profile of velocity and flight angle for the same case, a similar break point can be found. In forward time at

the break point, the velocity and flight angle profiles diverge from their previously near constant state. Also at the range angle, for the same case, the lift drag ratio passes through approximately .5. This shows a definite dominance by lift until the last part of the aerodynamic portion of the trajectory.

Observation 5: In the aerodynamic portion of the trajectory, the  $[\partial r(\sigma_f)/\partial r(\sigma)]$  and  $[\partial r(\sigma_f)/\partial \gamma(\sigma)]$  curves are a function of the rate of change of velocity and  $\gamma$ . The  $[\partial r(\sigma_f)/\partial \gamma(\sigma)]$  curve is a function of the rate of change of lift with respect to  $\sigma$ .

The first part of this observation is substantiated by correlating the curves for  $[\partial r(\sigma_f)/\partial r(\sigma)]$  and  $[\partial r(\sigma_f)/\partial \gamma(\sigma)]$  with the velocity and flight angle curves. For example, in Case 6, when  $[\partial \gamma/\partial \sigma]=0$ , there is also a zero slope achieved by the  $[\partial r(\sigma_f)/\partial r(\sigma)]$  and  $[\partial r(\sigma_f)/\partial v(\sigma)]$  curves. Also in this same case there is a pulse in the velocity curve at a range angle of 1.96, and a corresponding pulse in both the radial and velocity sensitivity coefficient curves. Additional examples are found by correlating the curves of Cases 3 and 4.

The second part of this observation is substantiated by correlating the lift curve slope and the  $[\partial r(\sigma_f)/\partial \gamma(\sigma)]$  curve. For example, in Case 7, which best shows the correlation, the slope of the flight angle sensitivity coefficient curve undergoes a change, here from a positive slope to a negative slope at the same range angle that lift undergoes a slope change. In other cases the  $[\partial r(\sigma_f)/\partial \gamma(\sigma)]$  slope change is not as dramatic as in Case 7, however the slope change can be closely correlated in a similar fashion with the lift slope.

Observation 6: There exists some relation between the aerodynamic portion of the trajectories and the conditions during the

non-aerodynamic portion for the following:

1. The constant that describes the radial sensitivity coefficient  $[\partial r(\sigma_f)/\partial r(\sigma)]$ .
2. The constant which multiplies the exponential function that describes the velocity sensitivity coefficient  $[\partial r(\sigma_f)/\partial v(\sigma)]$ .
3. The slope (sign and magnitude of the first derivative) of the linear function which describes the flight angle sensitivity coefficient  $[\partial r(\sigma_f)/\partial \gamma(\sigma)]$ .

Observation 7: There exists some relation between the control boundaries and the aerodynamic portion of the trajectory.

Observation 6 and 7 are existential only and are substantiated by the different cases. For observation 6, it is necessary only to note the variations in the aerodynamic portion among Cases 3 through 7, with respect to the non-aerodynamic portion of the trajectory. To substantiate observation 7, a comparison of the sensitivity coefficients for Cases 3 and 4 with those for Cases 5, 6, and 7 shows some relation exists. No further extrapolations can be made for observations 6 and 7 due to a lack of data for correlation.

These observations are intended as a basis for conclusions to be drawn concerning the general problem of minimizing the sensitivity coefficients. These shall not be drawn here, but shall be drawn following the implicit guidance simulation presented in the succeeding chapters.



## VI. Optimal Implicit Guidance Simulation For The Entry Problem

In the guidance of astronomical vehicles, there are two basic philosophies which can be used. One philosophy is called explicit guidance and the other implicit guidance. These guidance philosophies are described in considerable detail in reference 2. This chapter will define implicit guidance and optimal implicit guidance and will outline the procedures for simulating the optimal implicit guidance philosophy on a high speed digital computer. The purpose of such a simulation is to investigate the validity and limitations of the solution to the optimal open-loop and closed-loop control problems in a practical situation with arbitrary initial errors in the trajectory states and white Gaussian distributed, zero mean observation noise present.

### Definition Of Optimal Implicit Guidance

In order to define implicit guidance, it is desirable to also define explicit guidance. In the philosophy of explicit guidance, it is assumed that an approximate closed form solution of the guidance equation exists which will explicitly relate the current control vector to the terminal boundary conditions. This involves, for the entry problem, the solution of a set of transcendental equations at each control point. A Newton-Raphson algorithm is generally used to solve these transcendental equations. However, since this must be done at each control point, a significant amount of computer time is necessary. For this reason, another scheme, which determines the control vector as an implicit function of the terminal boundary conditions is generally used.

In implicit guidance, it is assumed that a nominal trajectory and

control are computed before the beginning of the mission (or simulation in this case). The procedure then consists of applying a linear theory to errors or deviations from the nominal trajectory in order to satisfy the terminal boundary conditions. In optimal implicit guidance the nominal trajectory and control are the precomputed open-loop optimal trajectory and control. The linear theory in optimal implicit guidance consists of applying a set of precomputed linear feedback gains to the deviations from the nominal trajectory so that a neighboring optimal path is followed to the specified terminal boundary conditions. When the actual values of the states are observed with observation noise present, a Kalman filter (described in Chapter II) may be used to obtain optimal estimates of the actual values of the states at each control point. This philosophy is illustrated in the block diagram in Figure 34, below. In the diagram,  $\underline{y}$  is the observation noise vector.

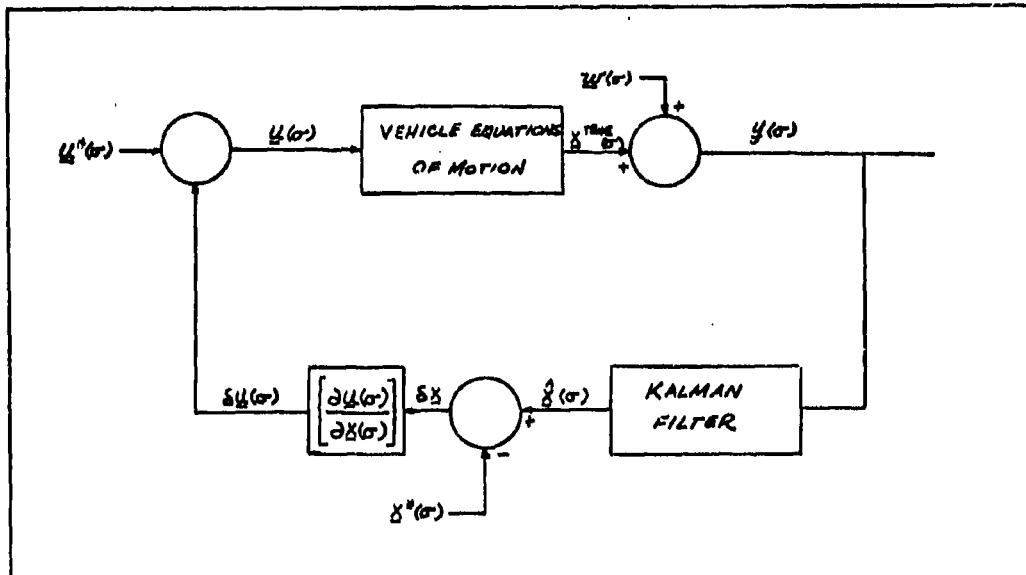


Figure 34. Optimal Implicit Guidance Block Diagram

Assumptions

The optimal implicit guidance philosophy is based on the following

## assumptions:

- A. The deviations of the actual states from the nominal states are within the linear range of the feedback gains.
- B. The nominal optimal control and trajectory are continuous and not adjacent to any boundaries. If this assumption is not made, the required change in control computed from the feedback gains could cause either the control or the states to exceed boundary limitations.
- C. The observation noise vector consists of white Gaussian noise with a known mean and covariance matrix.
- D. The vehicle dynamics can be described by a set of non-linear, coupled, first-order differential equations with deterministic coefficients.

Entry Feedback Equations

The linear feedback scheme uses the following equation:

$$\delta \underline{u}(\sigma) = \left[ \frac{\partial \underline{u}(\sigma)}{\partial \underline{x}(\sigma)} \right] \delta \underline{x}(\sigma) \quad (6-1)$$

where the matrix  $[\partial \underline{u}(\sigma) / \partial \underline{x}(\sigma)]$  is derived such that the trajectory follows a neighboring path to the specified terminal conditions. If all six states of the entry problem are considered, then the matrix is of dimension  $2 \times 6$  as there are two control components. However, onboard a practical vehicle, the errors in the sensitivity coefficients cannot be computed. For this reason, the feedback scheme uses errors in the states only. It is assumed, and shall be demonstrated that with no measurement error, the feedback scheme will satisfy the position, velocity, and flight angle terminal conditions. If there are errors

in measurement, the use of a minimum sensitivity coefficient nominal trajectory will aid in minimizing these errors. This, however, shall not be demonstrated.

The equations for the entry problem are:

$$\begin{bmatrix} \delta u_D(\sigma) \\ \delta u_L(\sigma) \end{bmatrix} = \begin{bmatrix} \frac{\partial u_D(\sigma)}{\partial x_1(\sigma)} & \frac{\partial u_D(\sigma)}{\partial x_2(\sigma)} & \frac{\partial u_D(\sigma)}{\partial x_3(\sigma)} \\ \frac{\partial u_L(\sigma)}{\partial x_1(\sigma)} & \frac{\partial u_L(\sigma)}{\partial x_2(\sigma)} & \frac{\partial u_L(\sigma)}{\partial x_3(\sigma)} \end{bmatrix} \begin{bmatrix} \delta x_1(\sigma) \\ \delta x_2(\sigma) \\ \delta x_3(\sigma) \end{bmatrix} \quad (6-2)$$

where the 2x3 matrix above is found from:

$$\left[ \frac{\partial \underline{u}(\sigma)}{\partial \underline{x}(\sigma)} \right] = - \left[ \frac{\partial \underline{G}(\sigma)}{\partial \underline{u}(\sigma)} \right]^{-1} \left\{ \left[ \frac{\partial \underline{G}(\sigma)}{\partial \underline{x}(\sigma)} \right] + \left[ \frac{\partial \underline{G}(\sigma)}{\partial \underline{\lambda}(\sigma)} \right] \left[ \frac{\partial \underline{\lambda}(\sigma)}{\partial \underline{\lambda}(\sigma_F)} \right] \left[ \frac{\partial \underline{x}(\sigma)}{\partial \underline{\lambda}(\sigma_F)} \right]^{-1} \right\} \quad (6-3)$$

and where:

$$\left[ \frac{\partial \underline{G}(\sigma)}{\partial \underline{u}(\sigma)} \right]^{-1} = \begin{bmatrix} \frac{1}{K_{UD}} & 0 \\ 0 & \frac{1}{K_{UL}} \end{bmatrix} \quad (6-4)$$

$$\left[ \frac{\partial \underline{G}(\sigma)}{\partial \underline{x}(\sigma)} \right] = \begin{bmatrix} \frac{\partial G_1(\sigma)}{\partial x_1(\sigma)} & \frac{\partial G_1(\sigma)}{\partial x_2(\sigma)} & \frac{\partial G_1(\sigma)}{\partial x_3(\sigma)} \\ \frac{\partial G_2(\sigma)}{\partial x_1(\sigma)} & \frac{\partial G_2(\sigma)}{\partial x_2(\sigma)} & \frac{\partial G_2(\sigma)}{\partial x_3(\sigma)} \end{bmatrix} \quad (6-5)$$

$$\left[ \frac{\partial \underline{G}(\sigma)}{\partial \underline{\lambda}(\sigma)} \right] = \begin{bmatrix} \frac{\partial G_1(\sigma)}{\partial \lambda_1(\sigma)} & \frac{\partial G_1(\sigma)}{\partial \lambda_2(\sigma)} & \frac{\partial G_1(\sigma)}{\partial \lambda_3(\sigma)} \\ \frac{\partial G_2(\sigma)}{\partial \lambda_1(\sigma)} & \frac{\partial G_2(\sigma)}{\partial \lambda_2(\sigma)} & \frac{\partial G_2(\sigma)}{\partial \lambda_3(\sigma)} \end{bmatrix} \quad (6-6)$$

$$\left[ \frac{\partial \underline{\lambda}(\sigma)}{\partial \underline{\lambda}(\sigma_f)} \right] = \begin{bmatrix} \frac{\partial \lambda_1(\sigma)}{\partial \lambda_1(\sigma_f)} & \frac{\partial \lambda_1(\sigma)}{\partial \lambda_2(\sigma_f)} & \frac{\partial \lambda_1(\sigma)}{\partial \lambda_3(\sigma_f)} \\ \frac{\partial \lambda_2(\sigma)}{\partial \lambda_1(\sigma_f)} & \frac{\partial \lambda_2(\sigma)}{\partial \lambda_2(\sigma_f)} & \frac{\partial \lambda_2(\sigma)}{\partial \lambda_3(\sigma_f)} \\ \frac{\partial \lambda_3(\sigma)}{\partial \lambda_1(\sigma_f)} & \frac{\partial \lambda_3(\sigma)}{\partial \lambda_2(\sigma_f)} & \frac{\partial \lambda_3(\sigma)}{\partial \lambda_3(\sigma_f)} \end{bmatrix} \quad (6-7)$$

$$\left[ \frac{\partial \underline{x}(\sigma)}{\partial \underline{\lambda}(\sigma_f)} \right] = \begin{bmatrix} \frac{\partial x_1(\sigma)}{\partial \lambda_1(\sigma_f)} & \frac{\partial x_1(\sigma)}{\partial \lambda_2(\sigma_f)} & \frac{\partial x_1(\sigma)}{\partial \lambda_3(\sigma_f)} \\ \frac{\partial x_2(\sigma)}{\partial \lambda_1(\sigma_f)} & \frac{\partial x_2(\sigma)}{\partial \lambda_2(\sigma_f)} & \frac{\partial x_2(\sigma)}{\partial \lambda_3(\sigma_f)} \\ \frac{\partial x_3(\sigma)}{\partial \lambda_1(\sigma_f)} & \frac{\partial x_3(\sigma)}{\partial \lambda_2(\sigma_f)} & \frac{\partial x_3(\sigma)}{\partial \lambda_3(\sigma_f)} \end{bmatrix} \quad (6-8)$$

$K_{UD}$  and  $K_{UD}$  are the weighting factors on control in the criterion function and the elements of the matrices are found by choosing the proper elements from the solutions to the perturbation equations in Chapter IV and Appendix A. The matrices above are written out to show that they are not the 6x6 matrices from the perturbation equations but only 3x3 partitions of those matrices.

#### Digital Computer Simulation

For the entry problem, two simplifying assumptions are made in addition to those made in the previous section. These are as follows:

A. No system (i.e., plant or message) noise is present. System noise could be considered by including several additional terms in the filter equations.

B. The observation vector is a linear function of the state vector and contains linear-additive zero mean noise with a constant covariance matrix.

The purpose of this section is to present the algorithm used to simulate the optimal implicit guidance scheme on a high speed digital computer. Fig. 35 shows the basic indexing method used for simulating the true (i.e., nominal) system and for applying the Kalman filter.

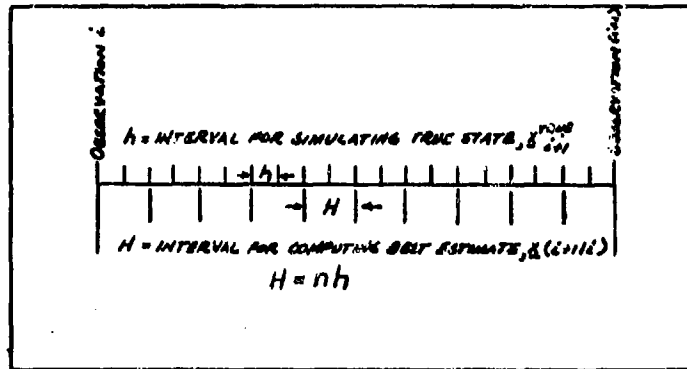


Figure 35. Simulation Indexing Method

In order to simulate the guidance scheme, the problem must first be put into discrete form for the digital computer. In the algorithm, presented below, it is assumed that the gain matrices, control values and nominal states for each point of the trajectory are put out on binary tape by the program which generates them.

Step 1. Based on a priori knowledge, estimate the constant observation noise covariance matrix,  $W$ .

Step 2. Based on the first observation,  $y_1 (i = 0)$ , and some arbitrary scheme, estimate the initial optimal estimate  $\hat{x}_0$ . For linear observations,  $\hat{x}_0$  is estimated from

$$\hat{x}_0 \triangleq y_0 \quad (6-9)$$

Step 3. Compute the initial error covariance matrix,  $\Gamma_0$ . For linear observations, this is

$$\Gamma_0 = W \quad (6-10)$$

This is computed rather than estimated since the equation which defines  $\underline{x}_0$  specifies the initial Kalman gain matrix,  $K_0$  (see Chapter II on initial error covariance).

Step 4. Using the precomputed values of control and the known initial nominal trajectory conditions, integrate the state equations forward in time to the terminal range angle to define a new nominal trajectory. This is done because when the discrete control values are used as forcing functions in the state equations. A linear interpolation must be used in the Runge-Kutta integration routine, resulting in a slightly different nominal trajectory from the precomputed one.

Step 5. Simulate the initial observation with

$$\underline{y}_0 = \underline{x}_0^{\text{true}} + \underline{w}_0 \quad (6-11)$$

where  $\underline{w}_0$  is an independent zero mean Gaussian noise vector.

Step 6. Integrate the true state (from  $\underline{x}_0^{\text{true}}$ ) to the (i+1) observation point using a step size h by solving:

$$\dot{\underline{x}}^{\text{true}} = \underline{F}(\underline{x}^{\text{true}}, \underline{u}) \quad (6-12)$$

where

$$\underline{u} = \underline{u}^{\text{nom}} + \delta \underline{u} \quad (6-13)$$

and

$$\delta \underline{u} = [\text{gain}] \delta \underline{x} \quad (6-14)$$

and

$$\delta \underline{x} = \underline{x}^{\text{true}} - \underline{x}^{\text{nom}} \quad (6-15)$$

It is assumed here that the gain at any point will be associated with the complete interval immediately following that point.

Step 7. Simulate the observation noise at the (i+1) observation point as:

$$\underline{y}_{i+1} = \underline{x}_{i+1}^{\text{true}} + \underline{w}_{i+1} \quad (6-16)$$

Step 8. Propagate optimal estimate  $\hat{\underline{x}}_i$  and error covariance

$\Gamma_i$  to (i+1) observation point to form the best estimates  $\underline{x}(i+1|i)$  and  $\Gamma(i+1|i)$  given everything except  $y_{i+1}$ . The subscript j will denote the intervals between i and (i+1). A step size of H is used for these subintervals. The steps in this procedure are as follows:

- A.  $j = 0$
- B. Define  $\underline{x}(j|j) = \underline{x}_1$  and  $\Gamma(j|j) = \Gamma_1$
- C. Solve the following equations to obtain the best estimates at the (j+1) subinterval:

$$A(j+1, j) = \frac{\partial F[\underline{x}(j|j), \underline{u}_j]}{\partial \underline{x}(j|j)} \times H + I \quad (6-17)$$

$$\Gamma(j+1|j) = A(j+1, j)\Gamma(j|j)A(j+1, j)^T \quad (6-18)$$

$$\underline{x}'(j+1|j) = F[\underline{x}(j+1|j), \underline{u}_{j+1}] \quad (6-19)$$

where

$$\delta \underline{u}_{j+1} = [\text{gain}]_{j+1} \delta \underline{x}_{j+1} \quad (6-20)$$

$$\underline{u}_{j+1} = \underline{u}_{j+1}^{\text{nom}} + \delta \underline{u}_{j+1} \quad (6-21)$$

$$\delta \underline{x}_j = \underline{x}(j+1|j) - \underline{x}_j^{\text{nom}} \quad (6-22)$$

- D. Go back to C with  $j=j+1$  noting that  $\Gamma(j|j) = \Gamma(j|j-1)$ .

Continue the solution until the (i+1) observation point is reached.

At this point:

$$\underline{x}(i+1|i) = \underline{x}(j+1|j) \quad (6-23)$$

and

$$\Gamma(i+1|i) = \Gamma(j+1|j) \quad (6-24)$$

Step 9. Compute the following quantities at the (i+1)

observation point:

- A. Kalman Gain Matrix:

$$K_{i+1} = \Gamma(i+1|i) [\Gamma(i+1|i) + w]^{-1} \quad (6-25)$$



## B. Error Covariance Matrix:

$$\Gamma_{i+1} = [I - K_{i+1}] \Gamma(i+1|i) [I - K_{i+1}]^T + K_{i+1} \Gamma(i+1|i) K_{i+1}^T \quad (6-26)$$

## C. Optimal Estimate:

$$\hat{x}_{i+1} = \underline{x}(i+1|i+1) = \underline{x}(i+1|i) + K_{i+1} [y_{i+1} - \underline{x}(i+1|i)] \quad (6-27)$$

Step 10. Compute the observation error and estimation errors with respect to the nominal by:

$$\Delta y_{i+1} \triangleq y_{i+1} - \underline{x}_{i+1}^{\text{nom}}$$

$$\Delta \hat{x}_{i+1} \triangleq \hat{x}_{i+1} - \underline{x}_{i+1}^{\text{nom}}$$

Step 11.  $i = i+1$

Step 12. Go back to Step 6 and continue until the final range angle is reached.

### VII. Simulation Results

Simulation results for two of the open-loop trajectories considered in Chapter V are selected for presentation here. These are for Case 1 and Case 7. Since no graphical analysis can be performed directly on the estimated states because of the magnitudes of the numbers involved, only deviations from the nominal optimal trajectory are presented. The observation and estimation error quantities are defined as follows:

$$\Delta \underline{y}(\sigma) \triangleq \underline{y}(\sigma) - \underline{x}^*(\sigma) = [\underline{x}^{\text{true}}(\sigma) - \underline{x}^*(\sigma)] + \underline{w}(\sigma) \quad (7-1)$$

and

$$\Delta \underline{x}(\sigma) \triangleq \underline{x}(\sigma) - \underline{x}^*(\sigma) \quad (7-2)$$

These are the errors in the observation vector and in the optimal estimate with respect to the nominal optimal trajectory.

For each case, two basic sets of results are presented. These are as follows:

A. Initial trajectory errors of +1000 m, +50 mps, and +0.2 deg. (+0.4 deg. for Case 7) in  $r$ ,  $v$ , and  $\gamma$  respectively with observation noise present.

B. Initial trajectory errors of -1000 m, -50 mps, and -0.2 deg. (-0.4 deg. for Case 7) in  $r$ ,  $v$ , and  $\gamma$  respectively with observation noise present.

C. Initial trajectory errors of +5000 m, +100 mps, and +1.0 deg. in  $r$ ,  $v$ , and  $\gamma$  respectively both with and without observation noise present.

D. Initial trajectory errors of -5000 m, -100 mps, and -1.0 deg. in  $r$ ,  $v$ , and  $\gamma$  respectively with observation noise present.

The gain matrix elements for each trajectory are presented in Figures 36 and 37 and in Figures 63 and 64.

The unconstrained control results for the cases with terminal velocities of 1650 mps and 1600 mps are not considered here because of large amplitude, high frequency variations in the gain matrix elements during the final portion of the trajectory. Due to the discrete nature of the optimal implicit guidance scheme, a smaller integration step size would be necessary to produce usable gains for these cases.

It should be noted that the trajectory of Case 7 is generated with Valentine's procedure in the second variation program for a drag control constraint. This fact violates the assumption made in the previous chapter that the control quantities could not be adjacent to any boundaries. However, since this trajectory produces the lowest sensitivity coefficients, it is worthwhile to examine the properties in a feedback loop.

Fig. 38 through Fig. 62 show the errors with respect to the nominal trajectory and the error covariance matrix ( $\Gamma$ ) elements for Case 1. Fig. 65 through Fig. 89 show the corresponding quantities for Case 7. In the graphs, sigma is the same as the range angle and has no relation to the standard deviation of the noise.

In all examples, the graphs show that the feedback gains have no effect on velocity and flight angle until the last few points in the trajectory. In Case 1, 100 gain values are used and in Case 7, 150 gain values are used. Virtually all the effect of the gain values occurs during the last two-tenths of a degree of range angle. If the last gain value is not used, observations have shown that the terminal values are in error by as much or more than the initial error values.

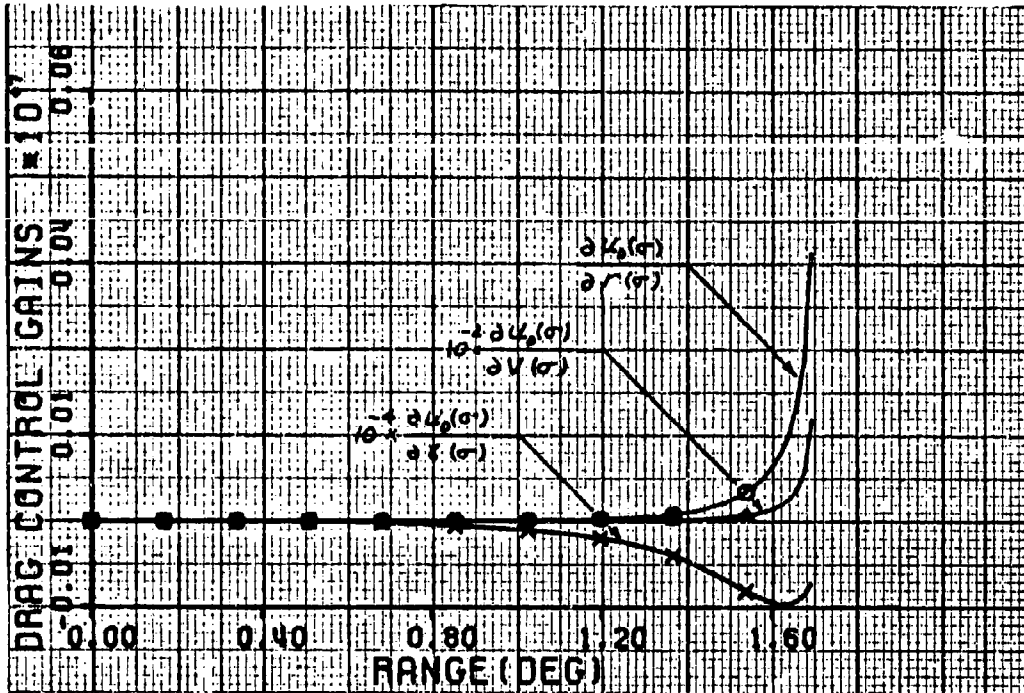


Figure 36. Case 1 - Drag Control Gains

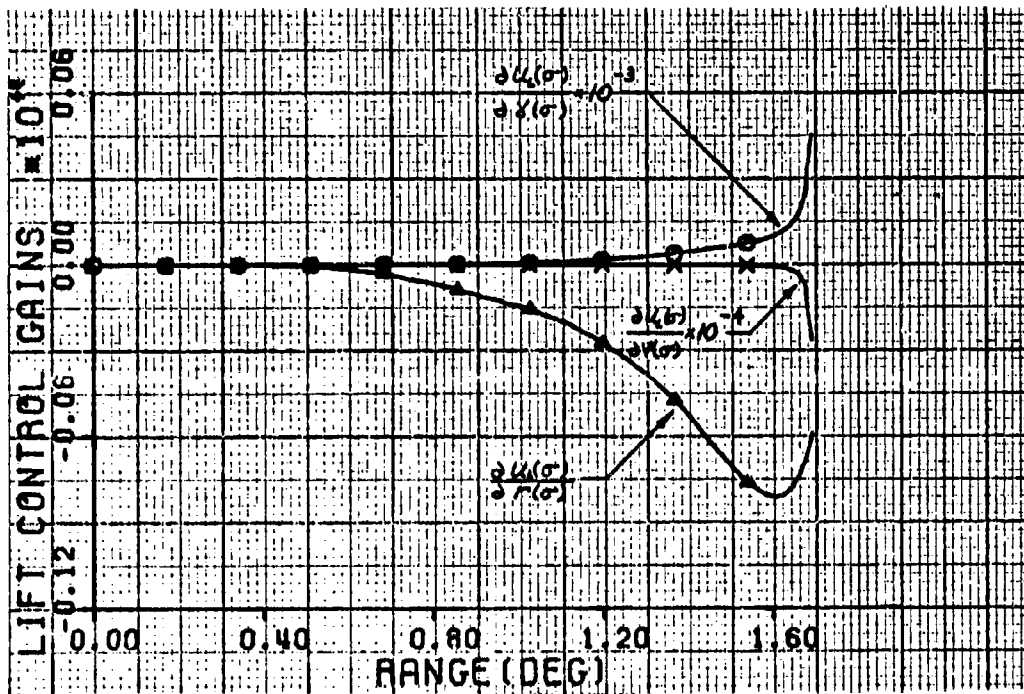


Figure 37. Case 1 - Lift Control Gains

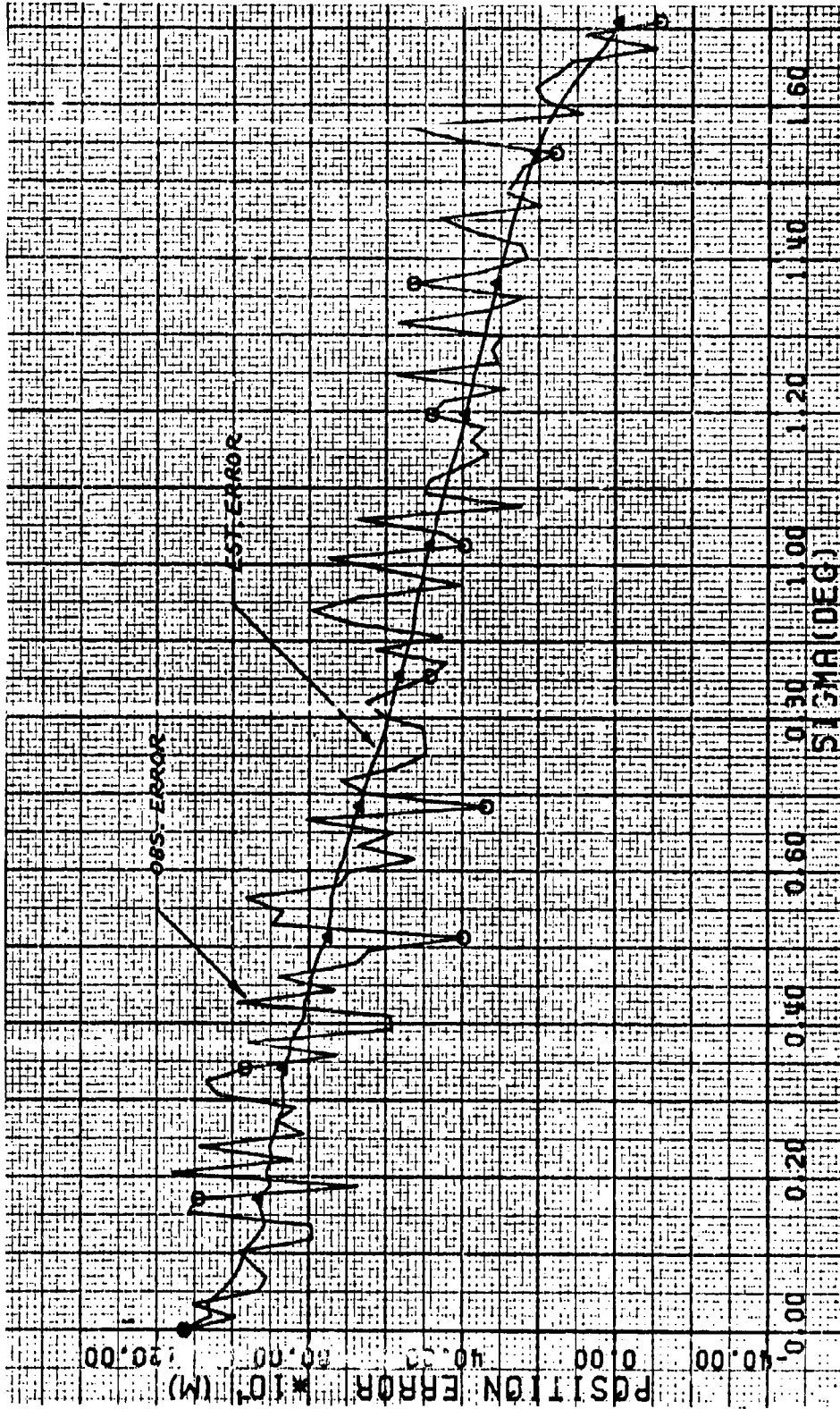


Figure 38. Case 1.1 - Position Error of 1000 Meters

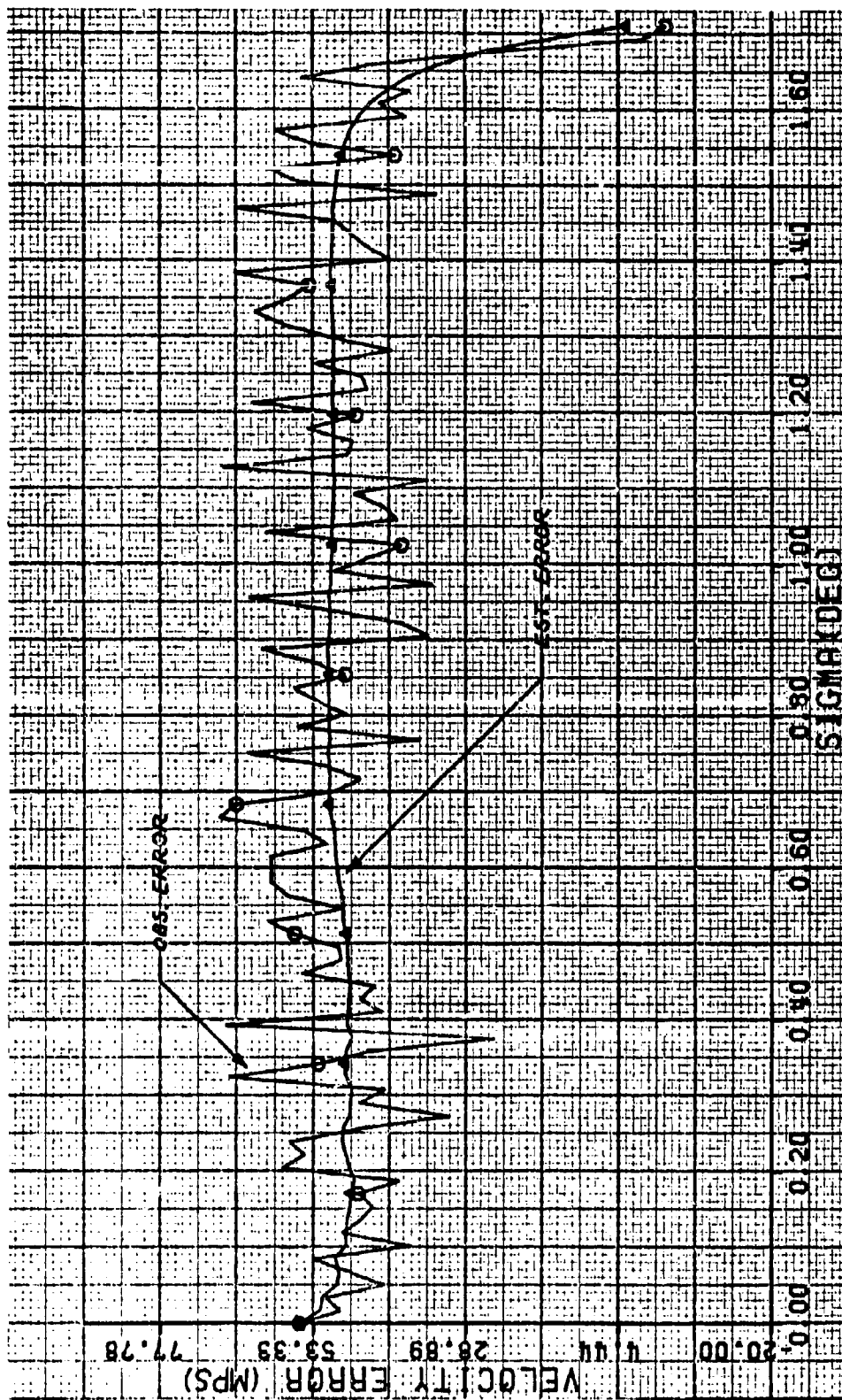


Figure 39. Case 1.1 - Velocity Error of 50 Meters/Second

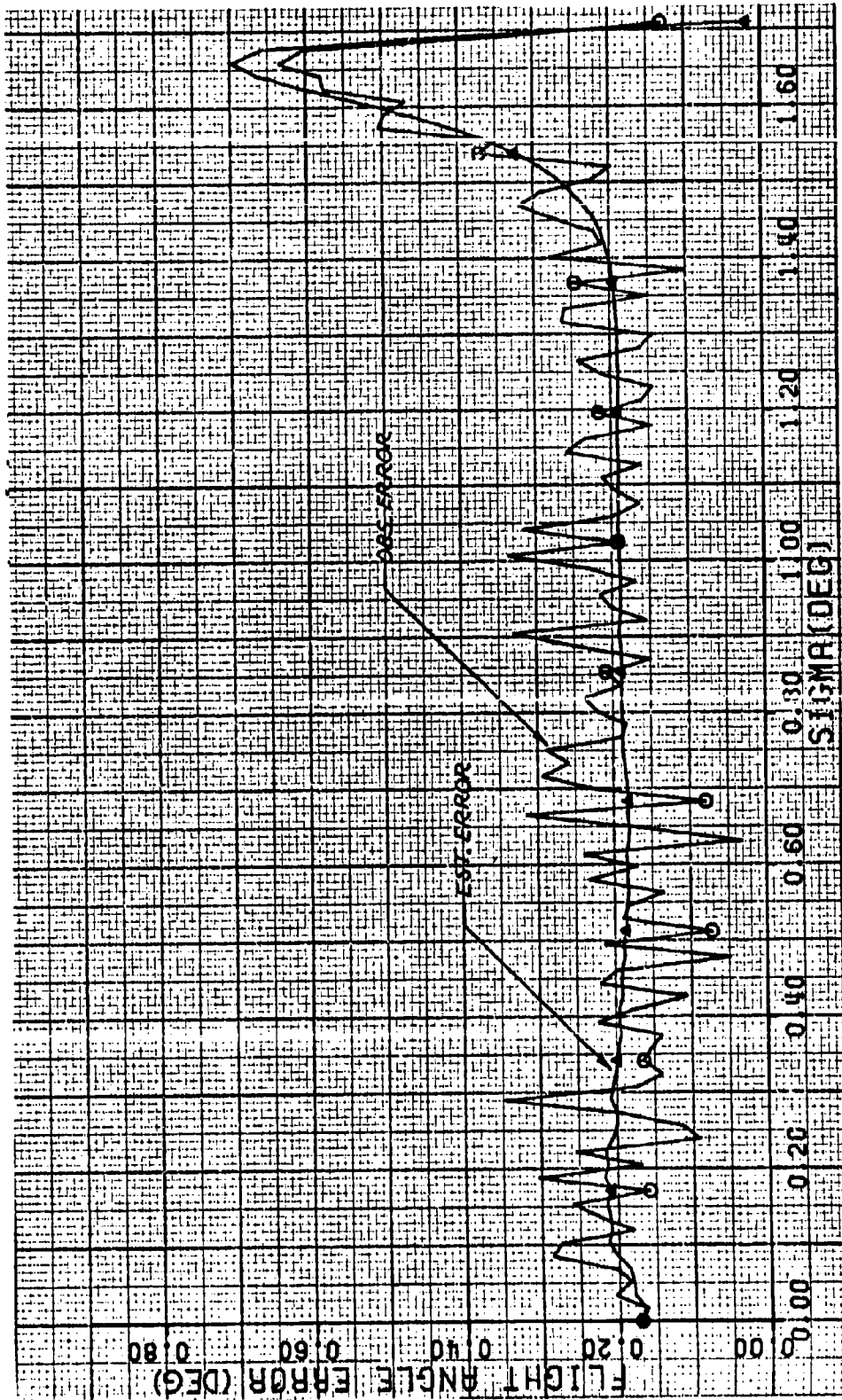


Figure 40. Case 1.1 - Flight Angle Error of .2 Degrees

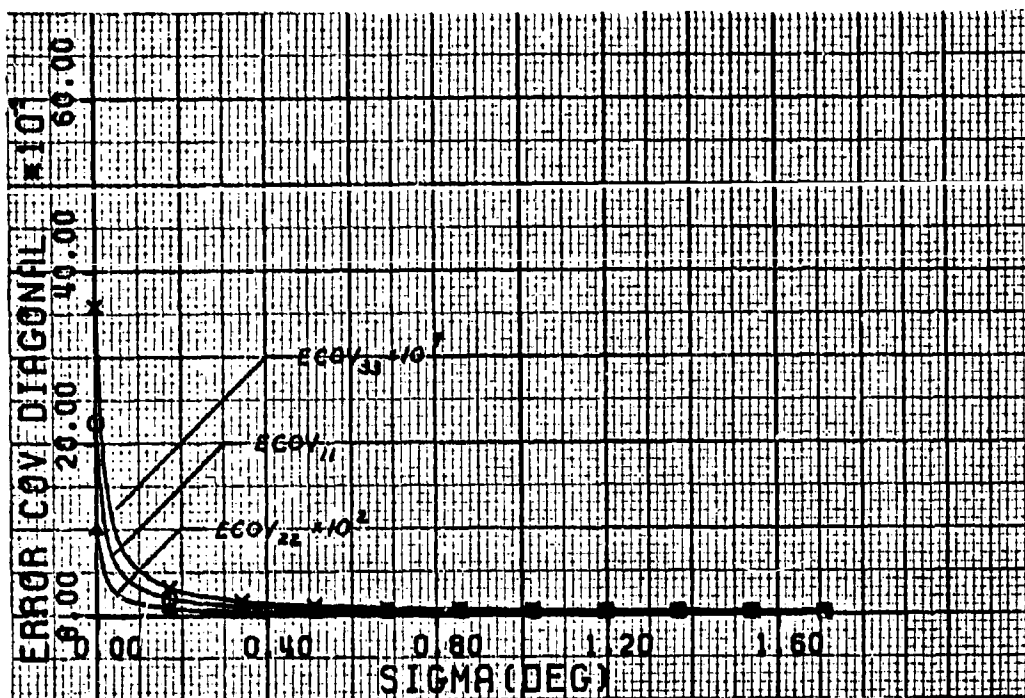


Figure 41. Case 1.1 - Diagonal Error Covariance Terms

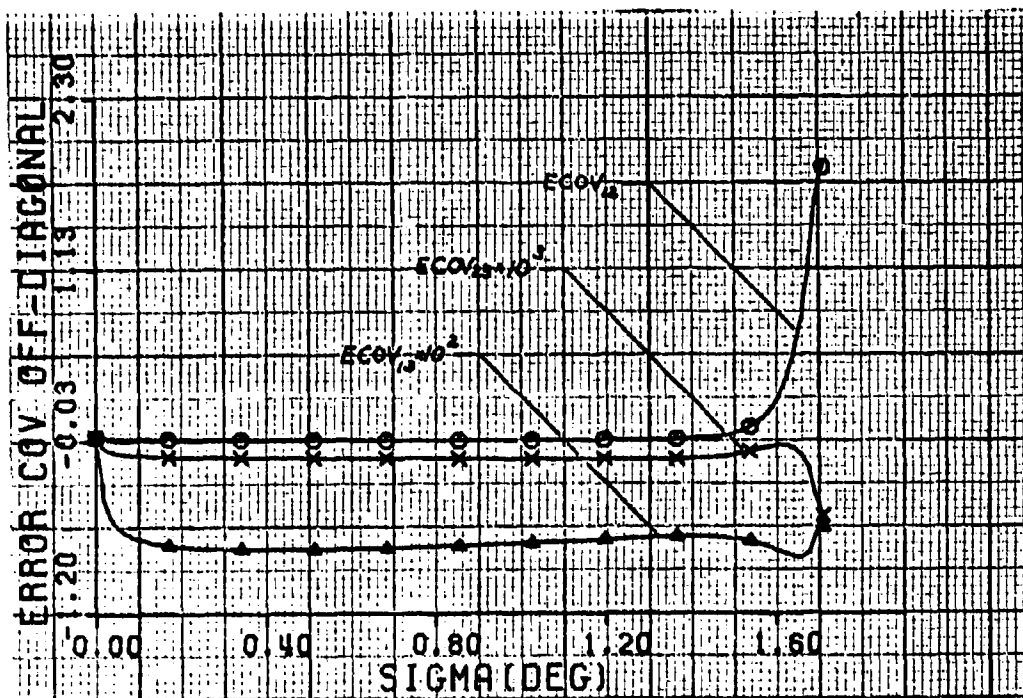


Figure 42. Case 1.1 - Off-Diagonal Error Covariance Terms



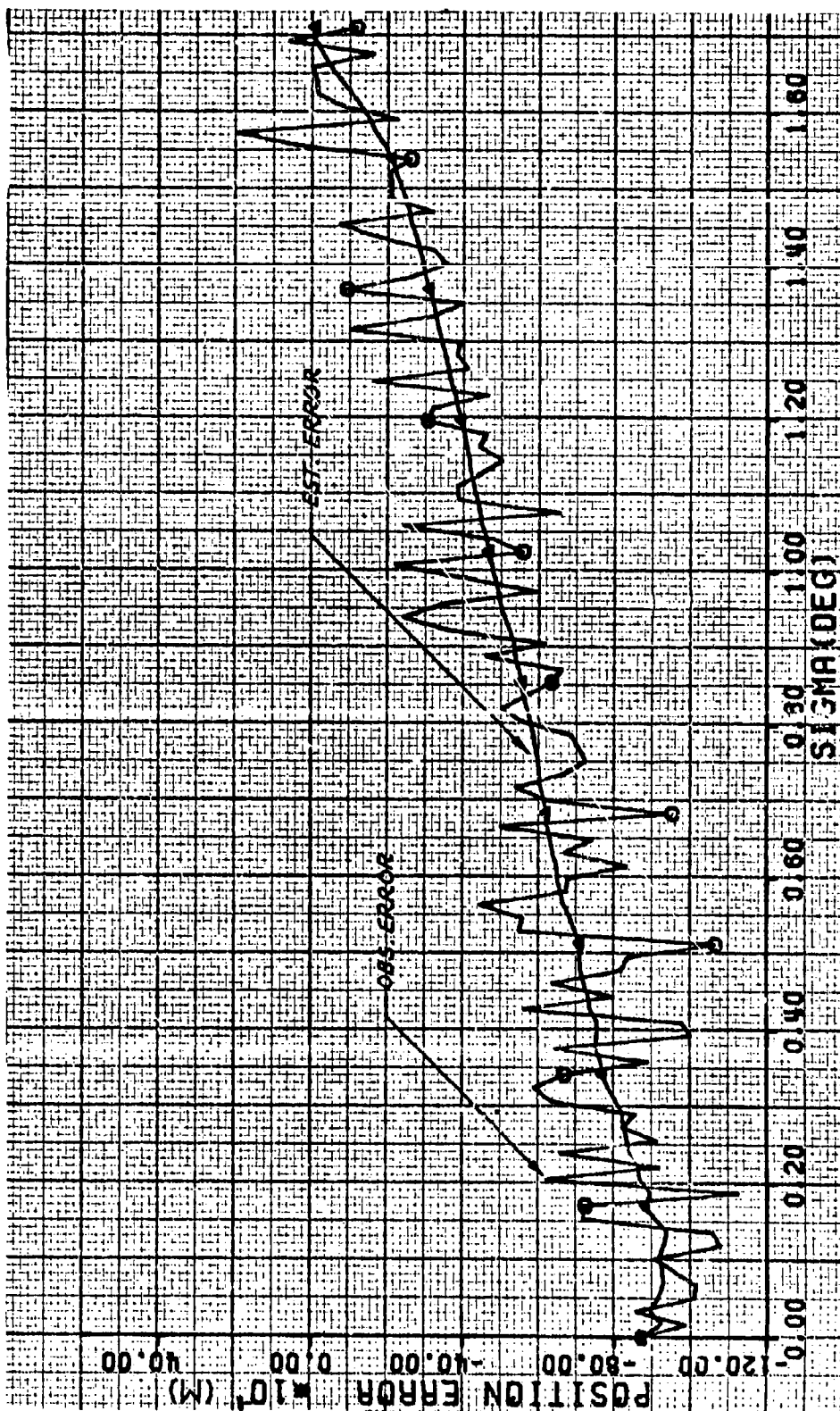


Figure 43. Case 1.2 - Position Error of -1000 Meters

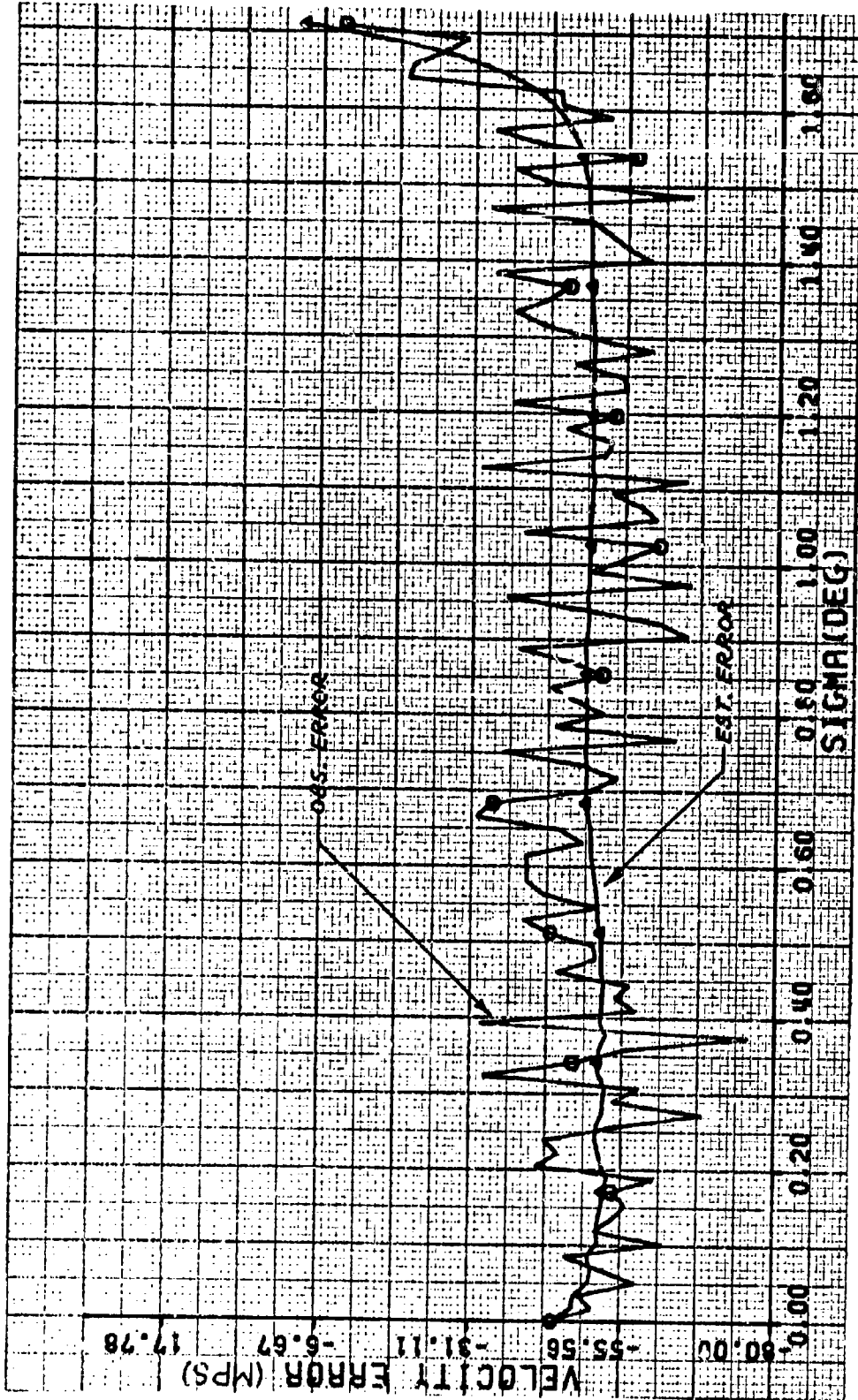


Figure 44. Case 1.2 - Velocity Error of -50 Meters/Second

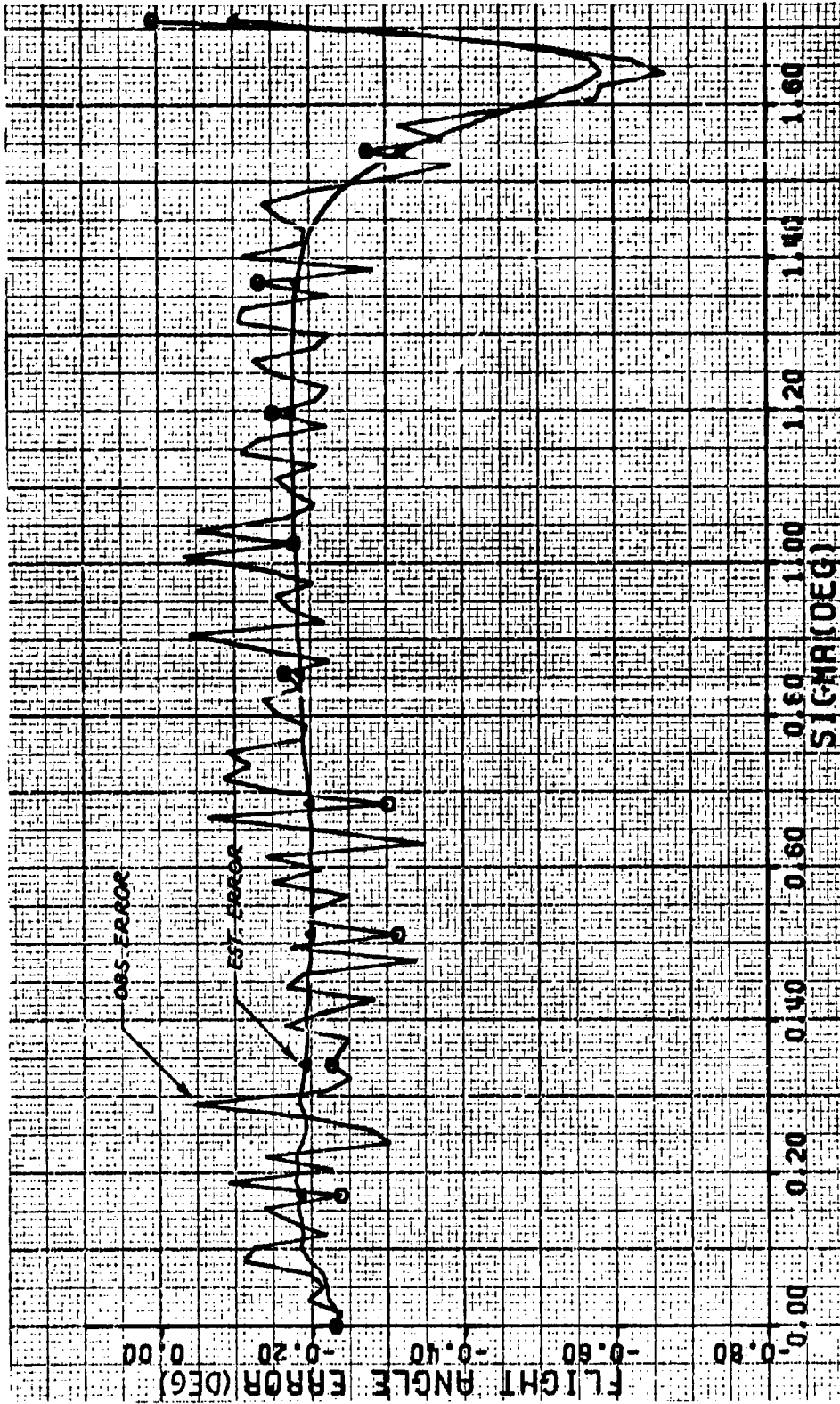


Figure 45. Case 1.2 - Flight Angle Error of -.2 Degrees

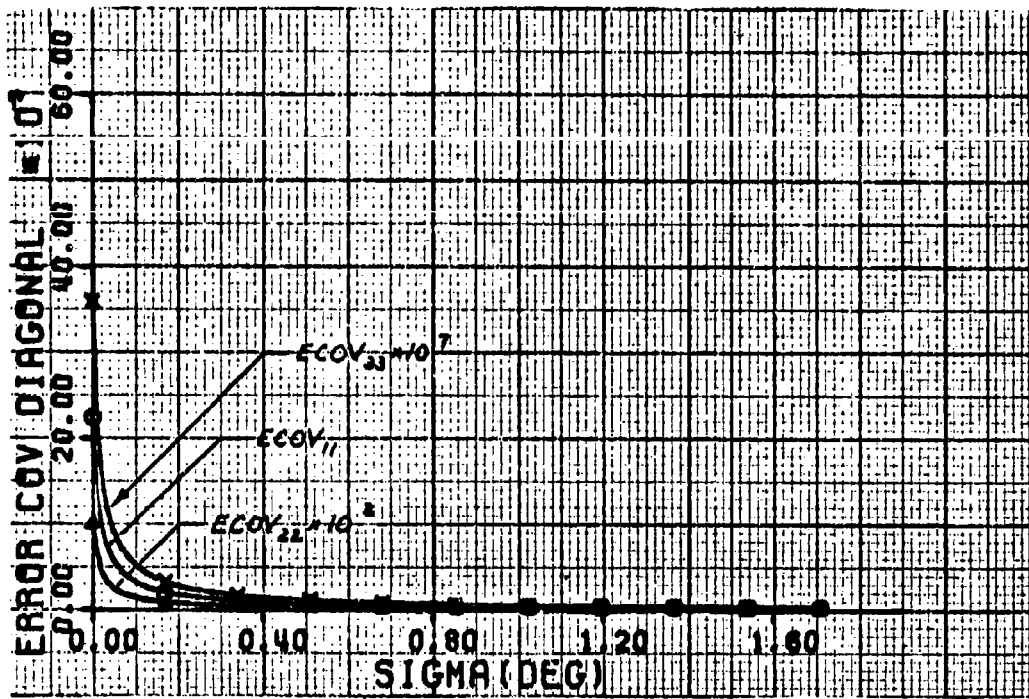


Figure 46. Case 1.2 - Diagonal Error Covariance Terms

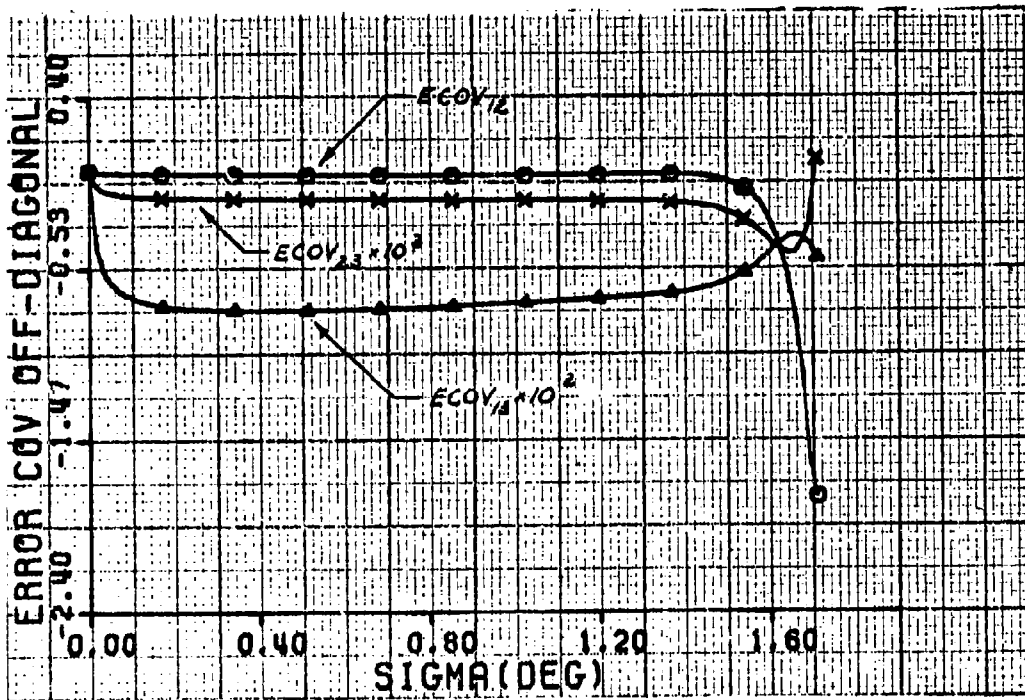


Figure 47. Case 1.2 - Off-Diagonal Error Covariance Terms

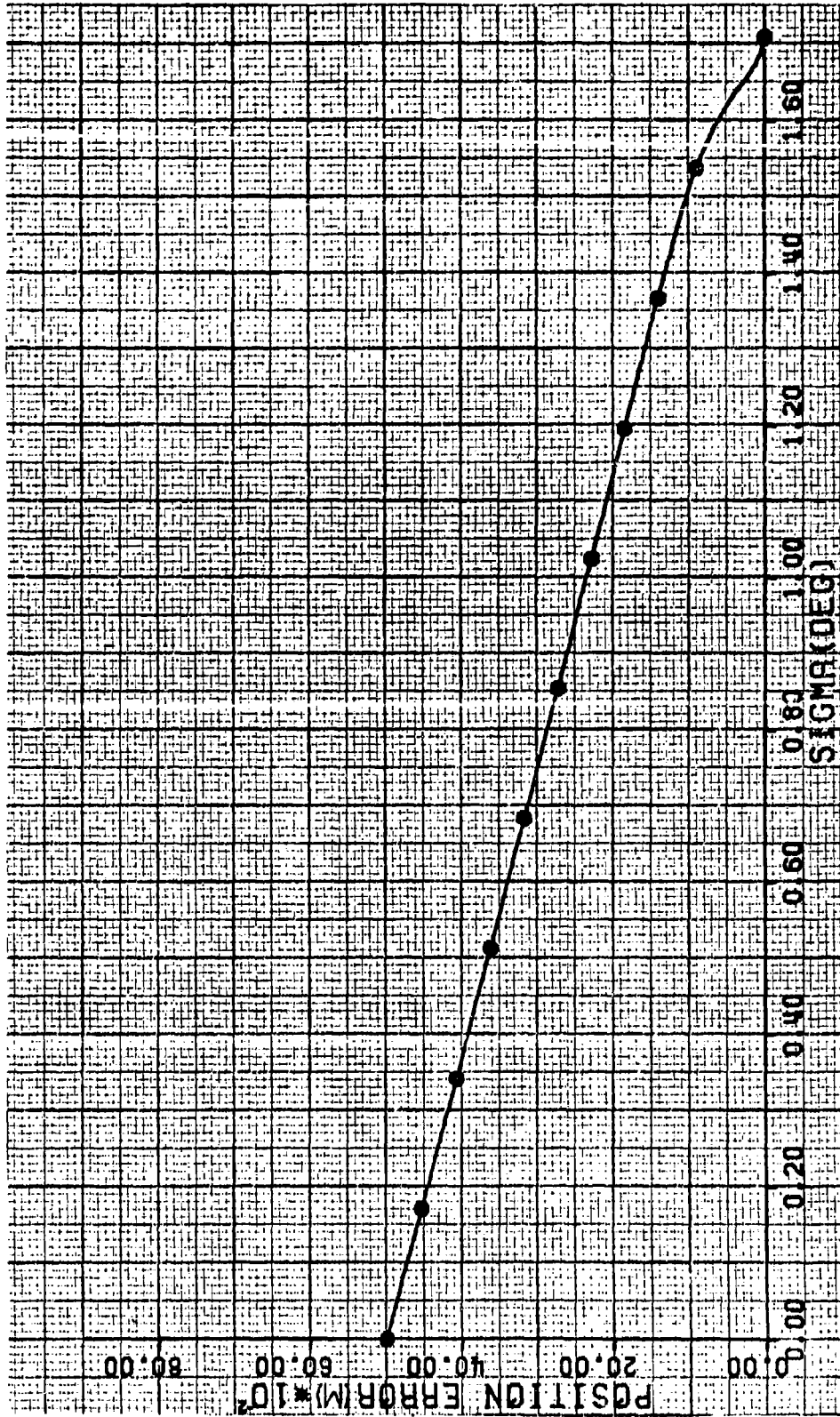


Figure 48. Case 1.3 - Position Error of 5000 Meters without Noise

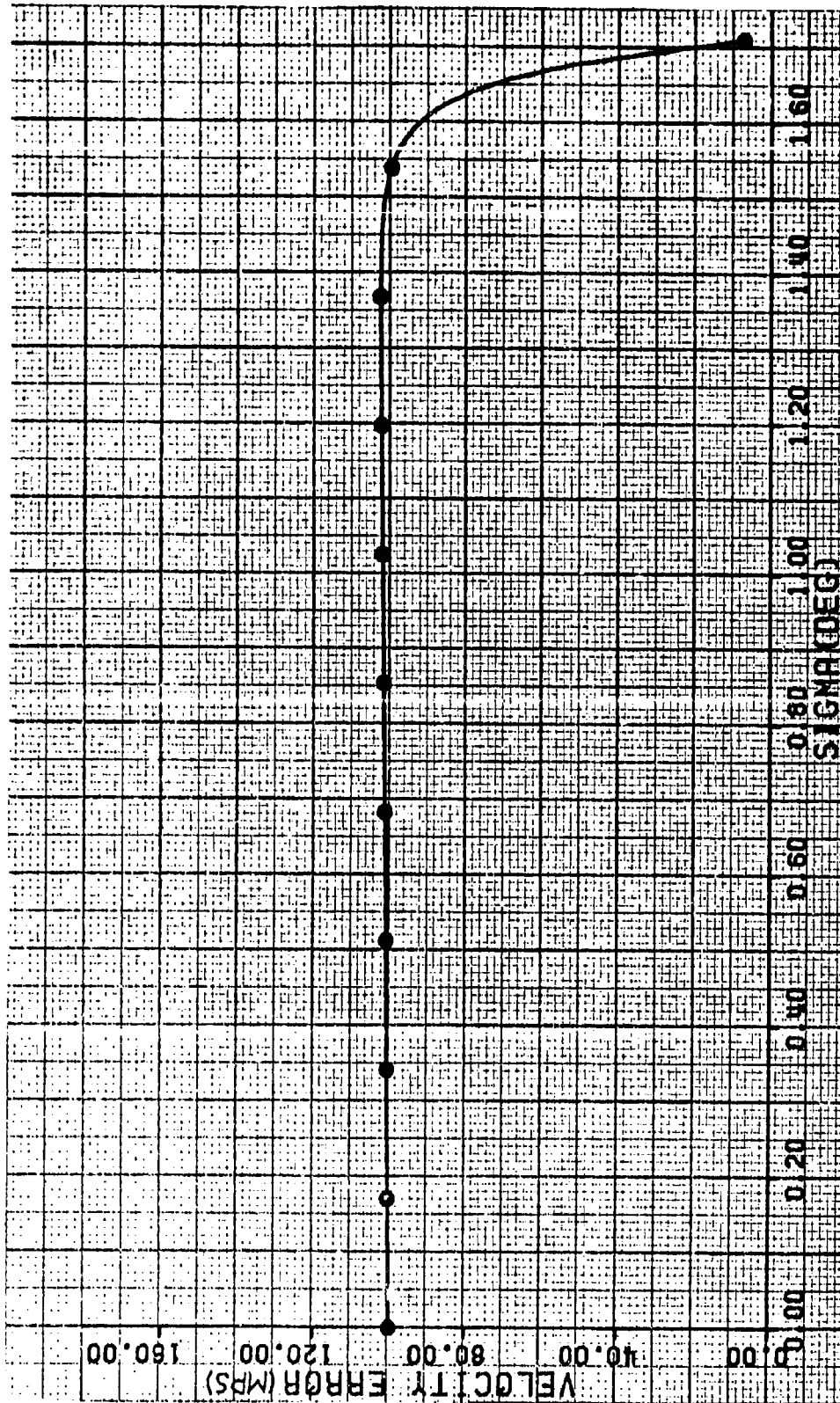


Figure 49. Case 1.3 - Velocity Error of 100 Meters/Second without Noise



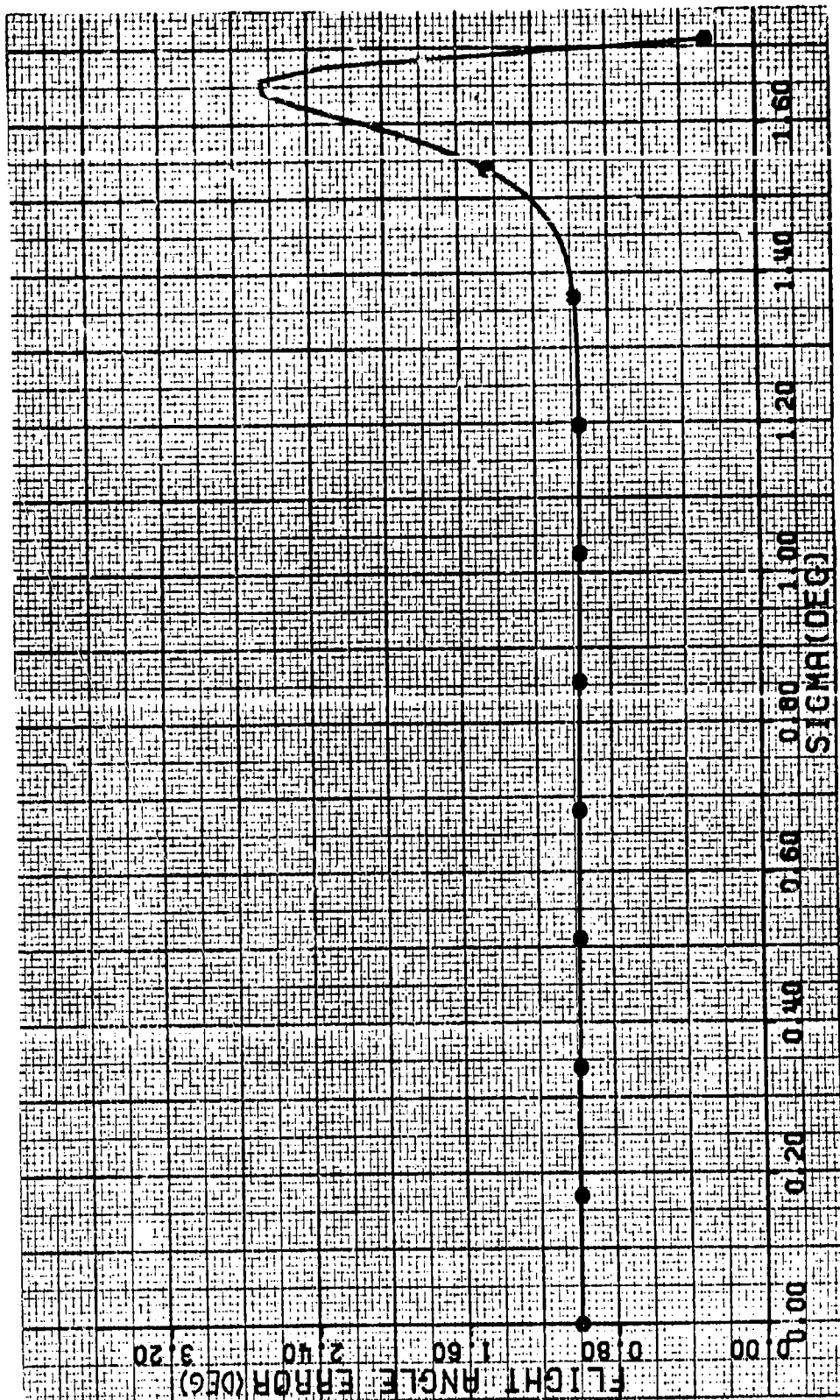


Figure 50. Case 1.3 - Flight Angle Error of 1.0 Degrees without Noise

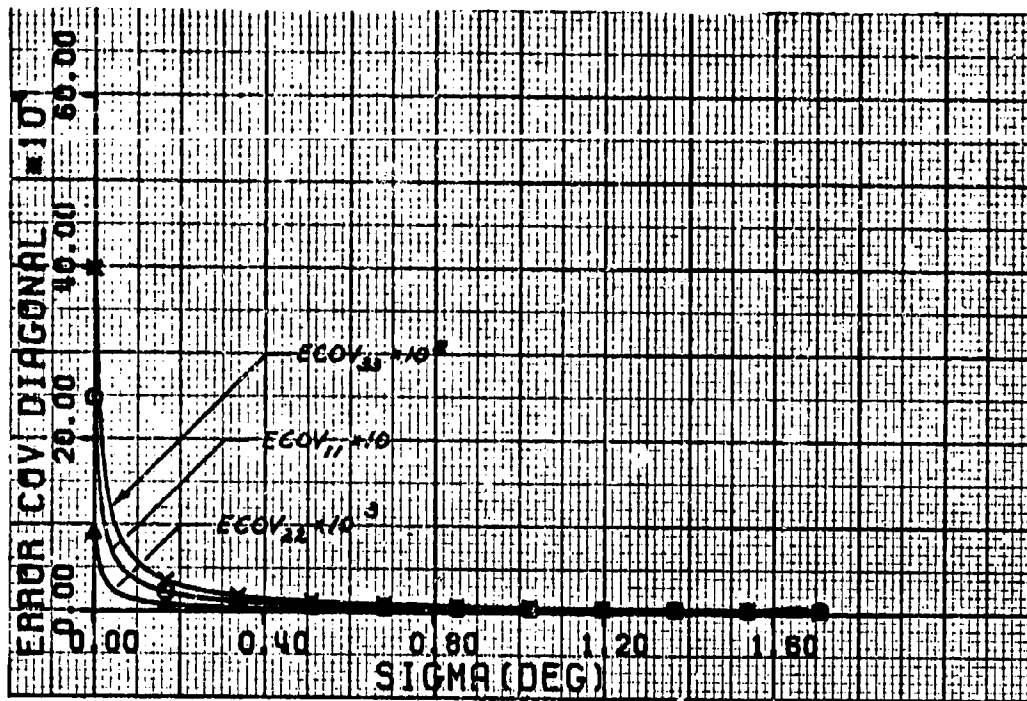


Figure 51. Case 1.3 - Diagonal Error Covariance Terms

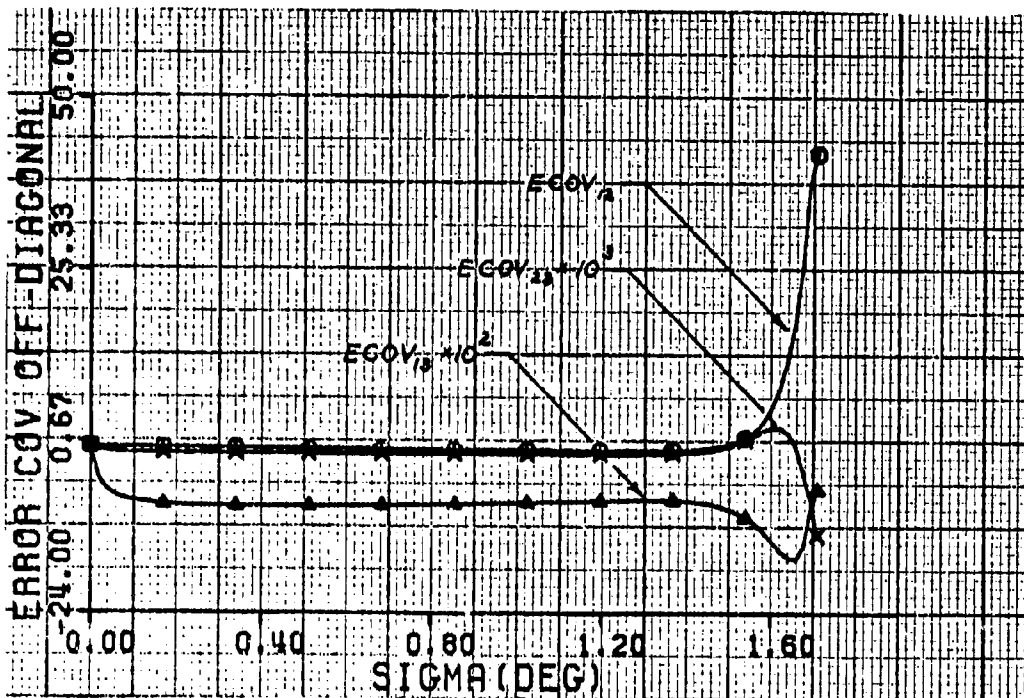


Figure 52. Case 1.3 - Off-Diagonal Error Covariance Terms



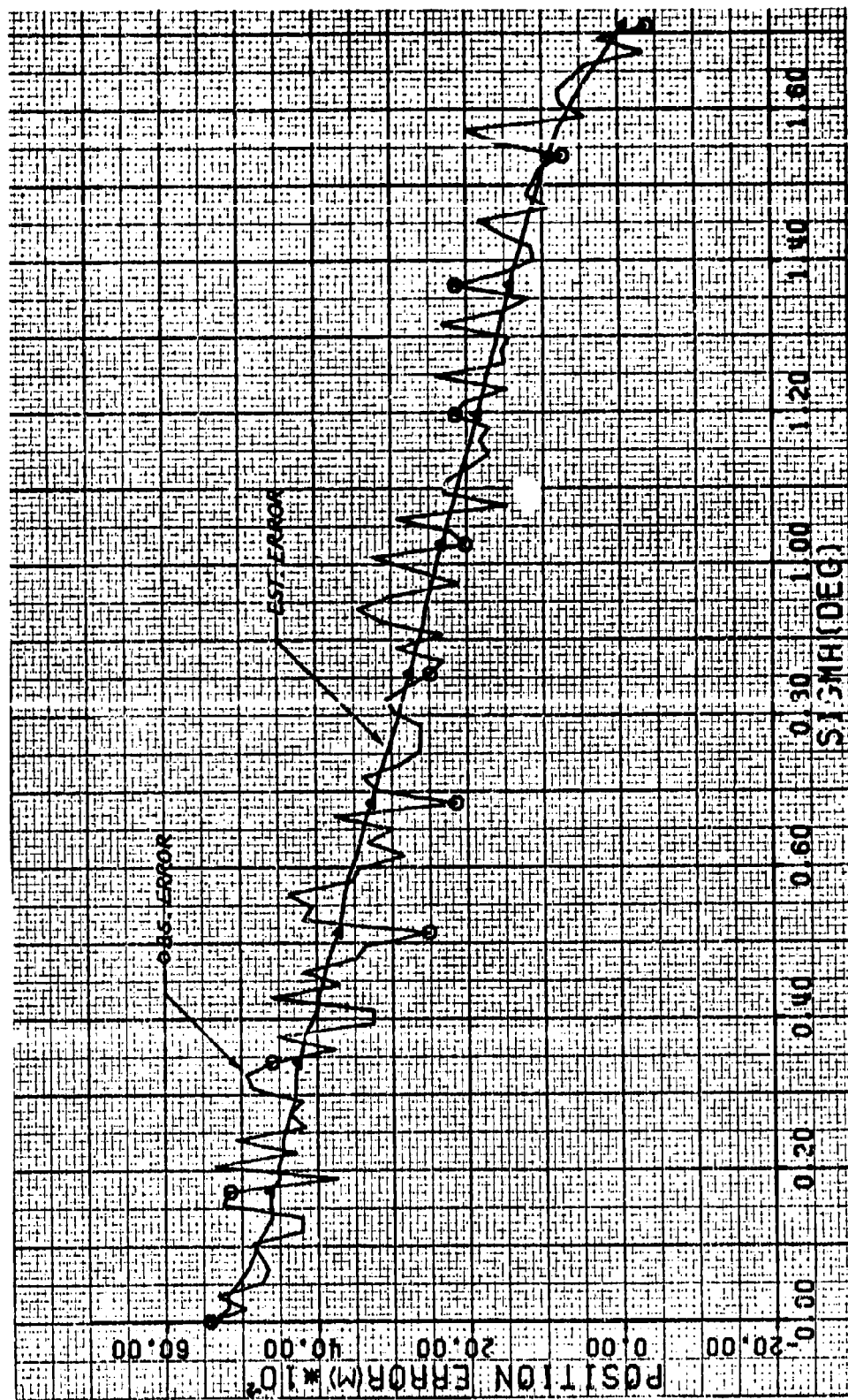


Figure 53. Case 1.4 - Position Error of 5000 Meters

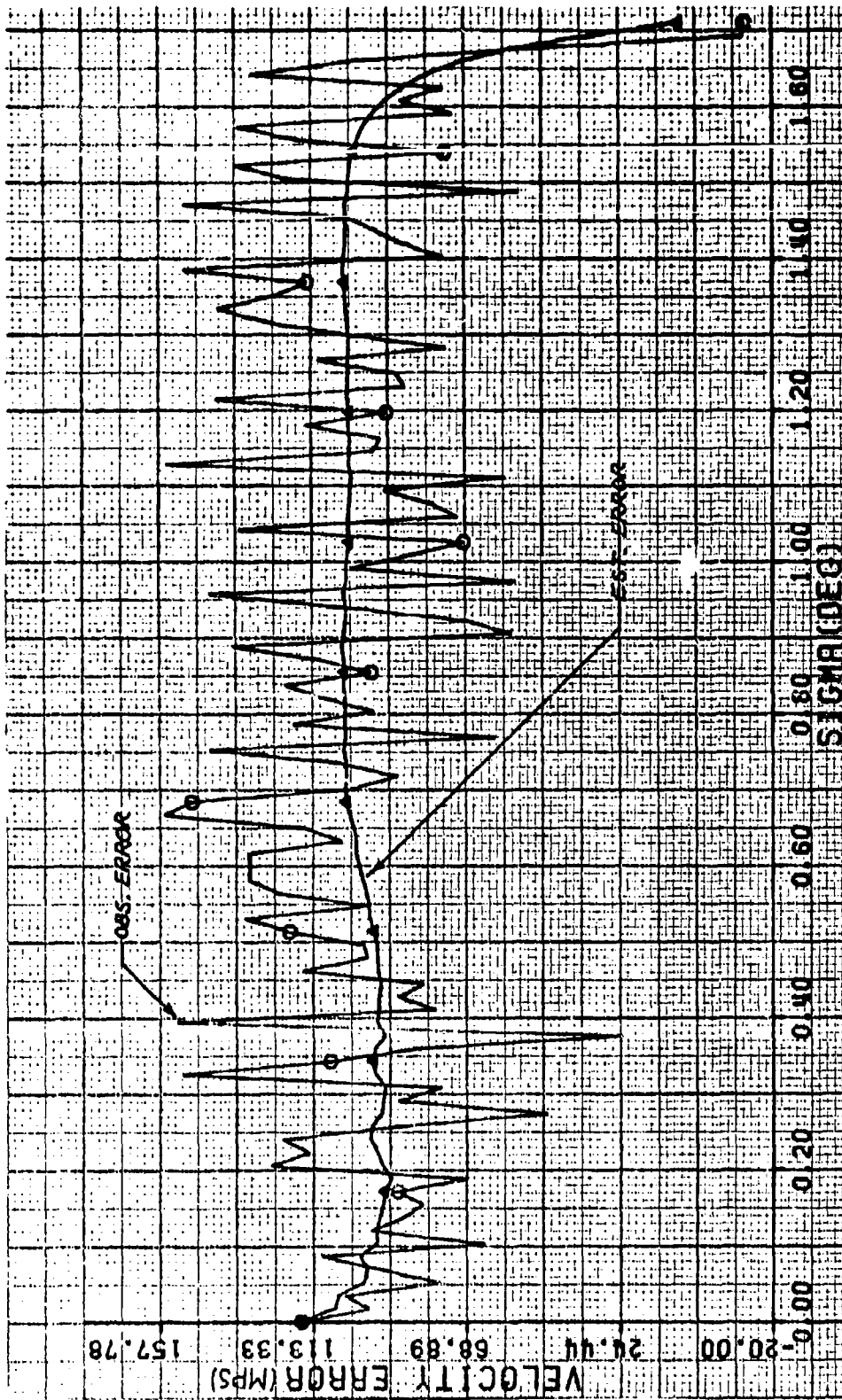


Figure 54. Case 1.4 - Velocity Error of 100 Meters/Second

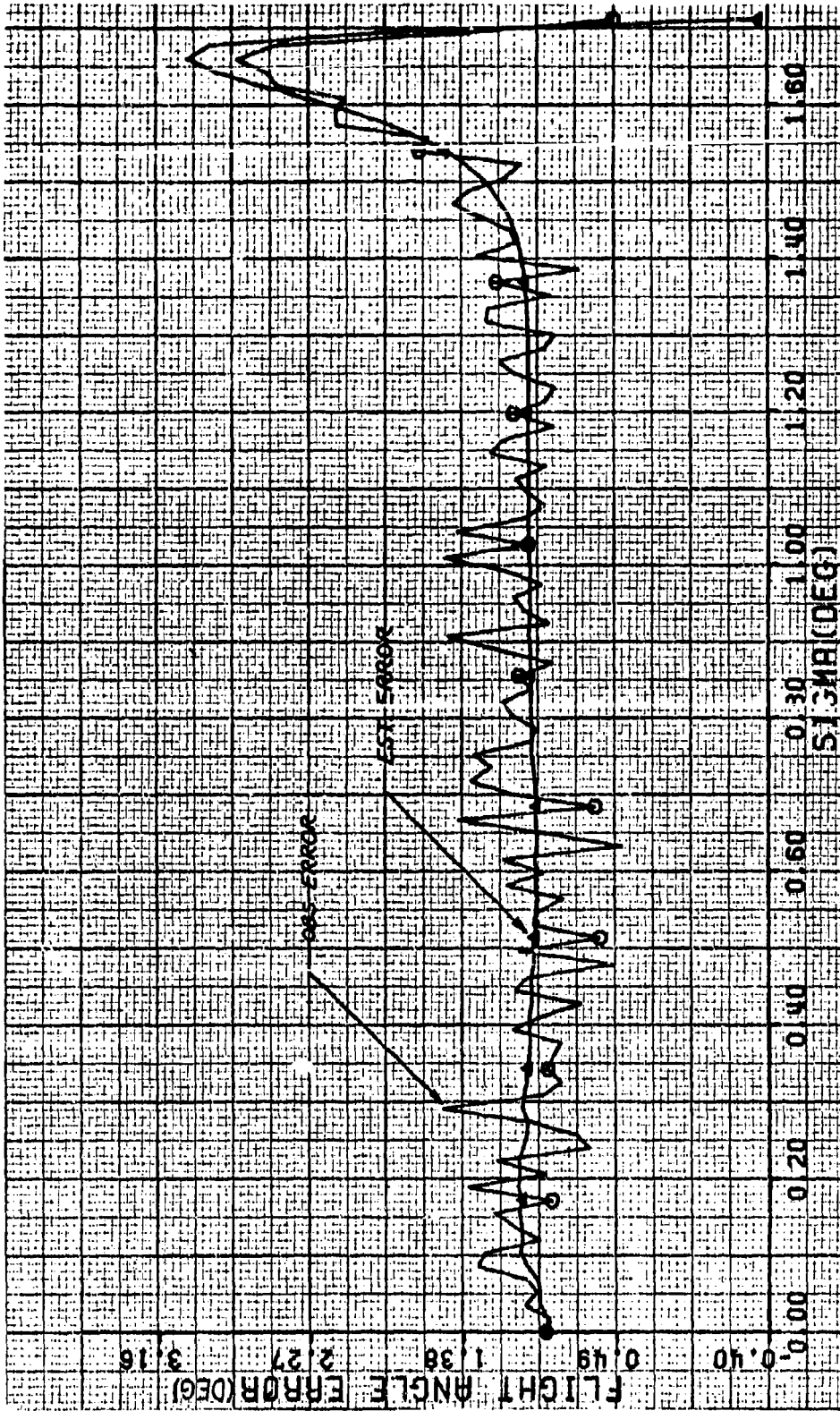


Figure 55. Case 1.4 - Flight Angle Error of 1.0 Degrees

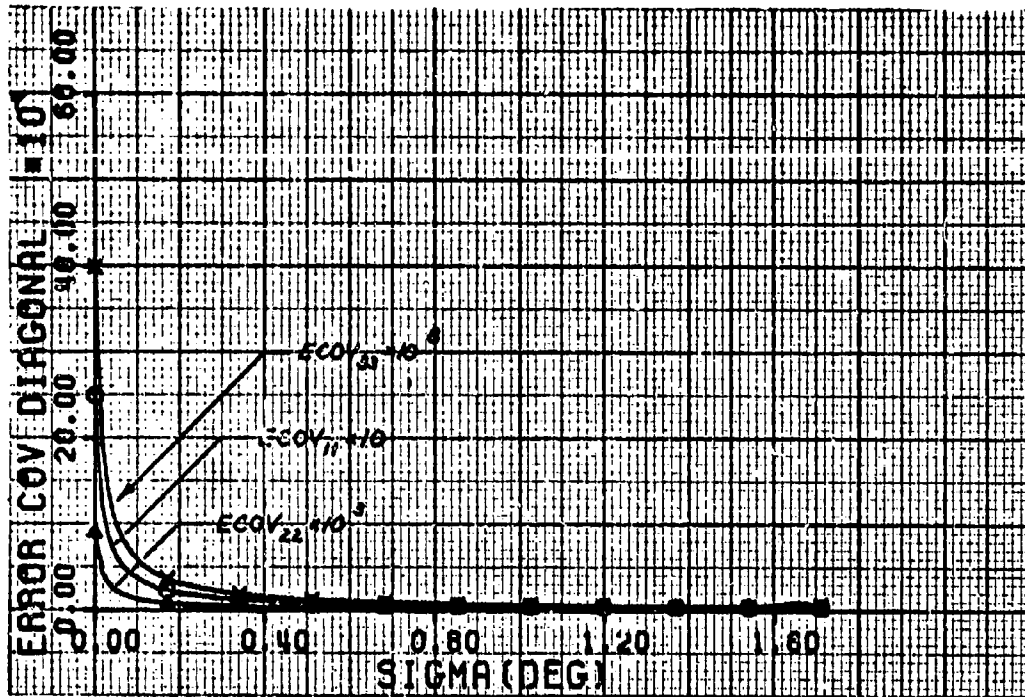


Figure 56. Case 1.4 - Diagonal Error Covariance Terms

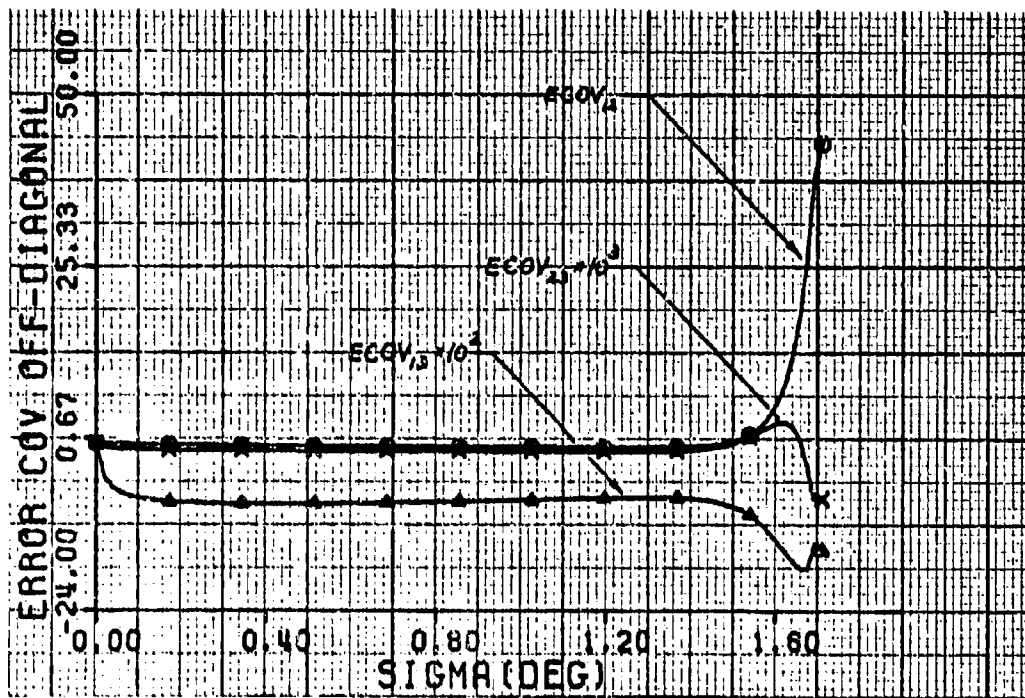


Figure 57. Case 1.4 - Off-Diagonal Error Covariance Terms

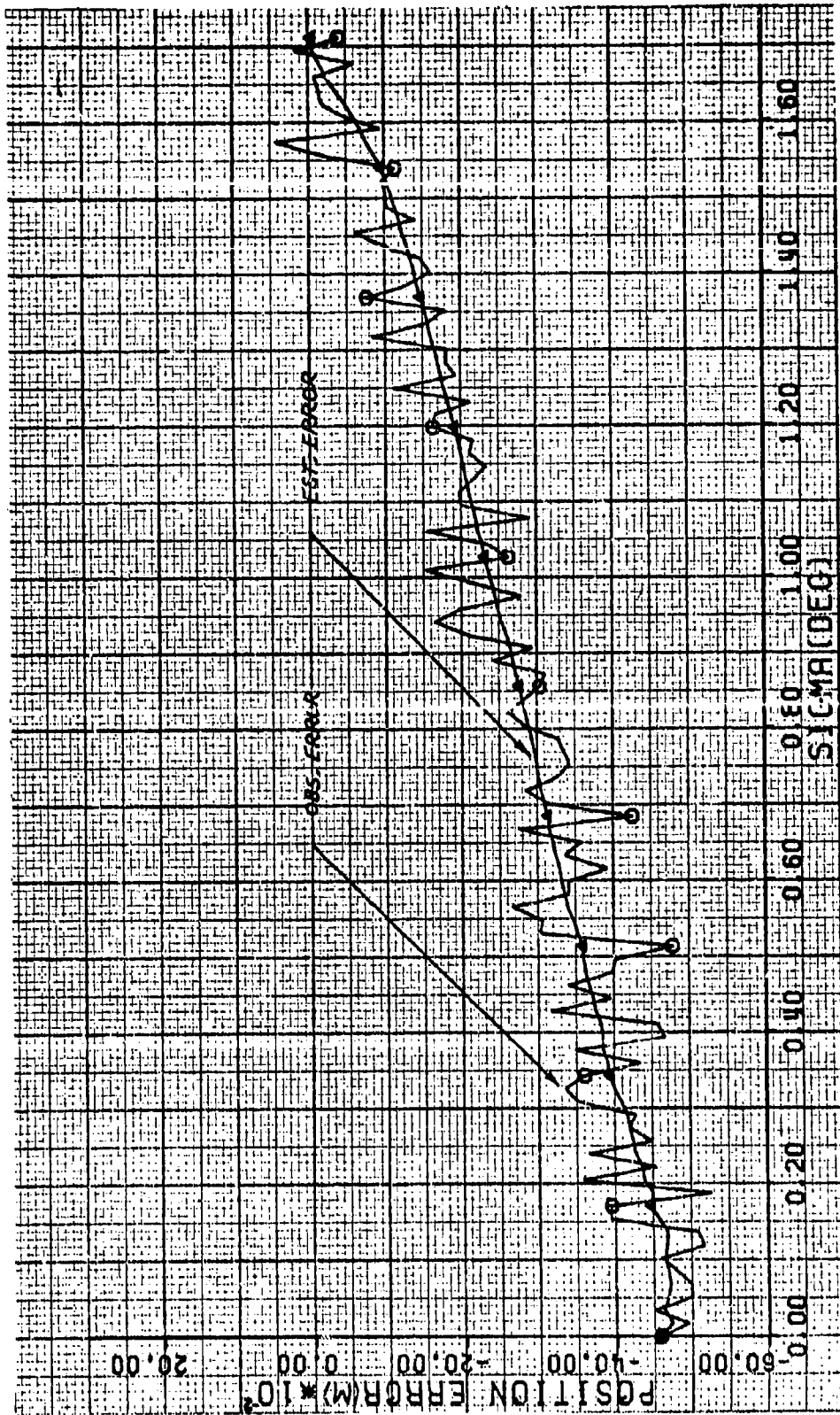


Figure 58. Case 1.5 - Position Error of -5000 Meters

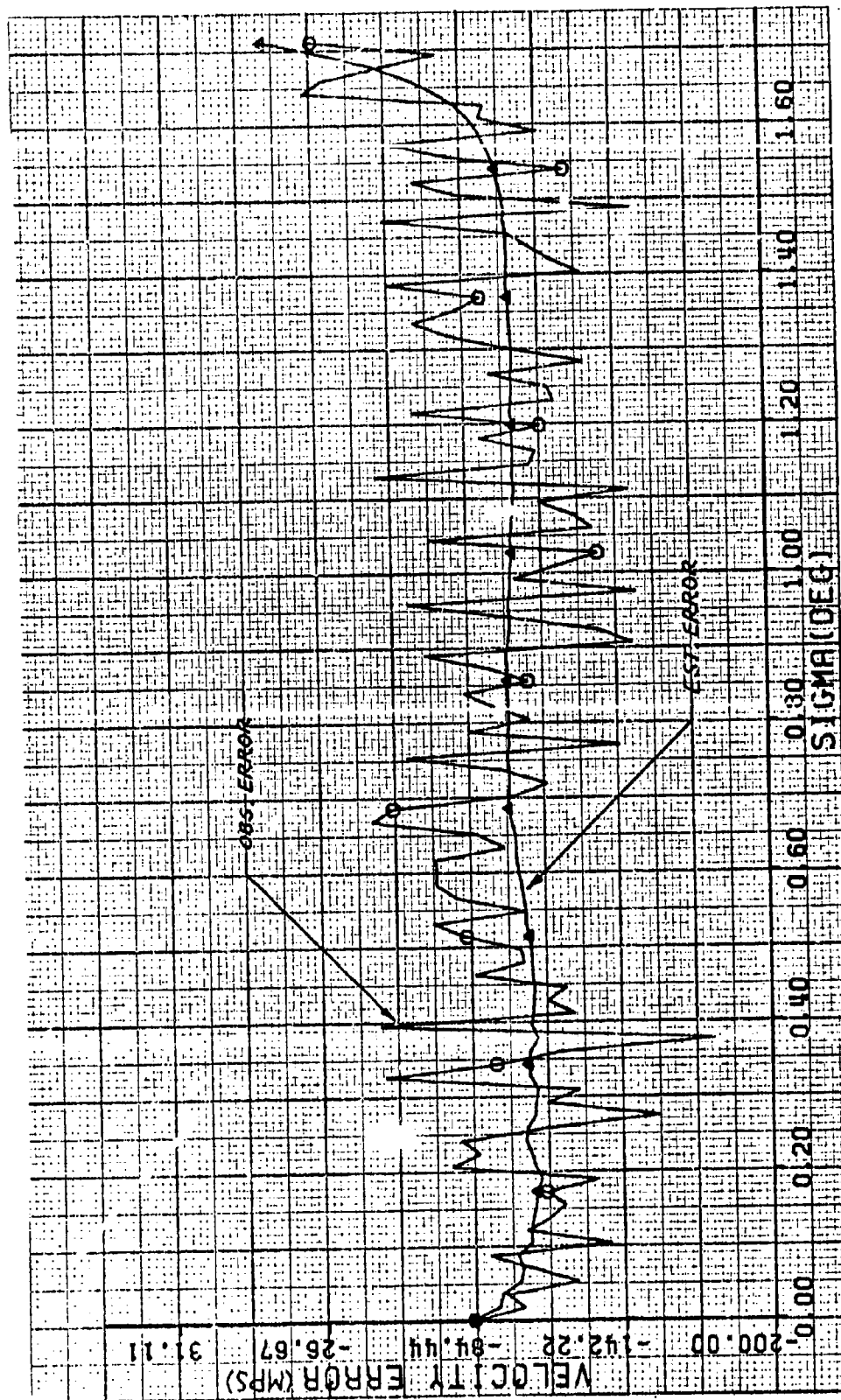


Figure 59. Case 1.5 - Velocity Error of -100 Meters/Second



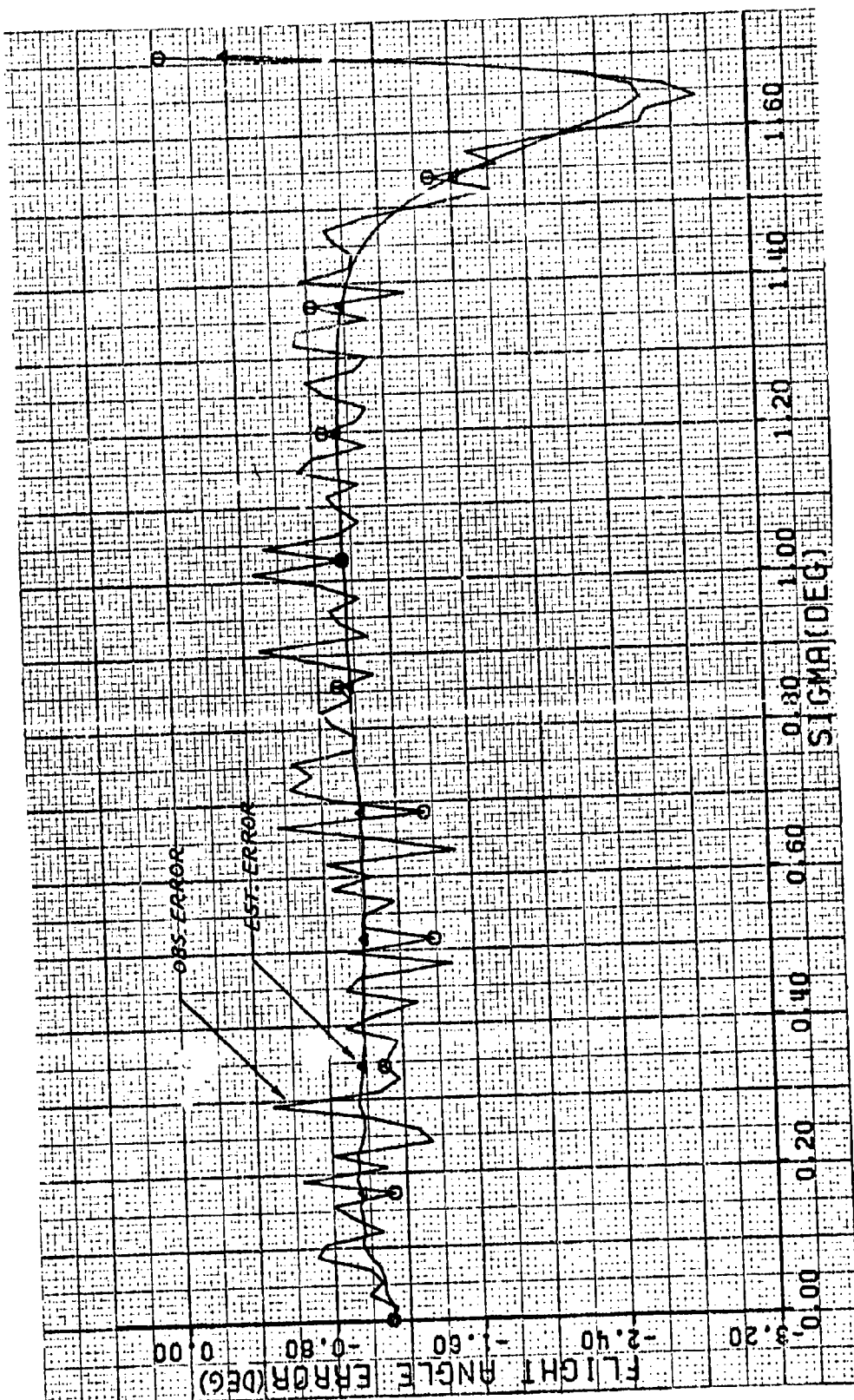


Figure 60. Case 1.5 - Flight Angle Error of -1.0 Degrees

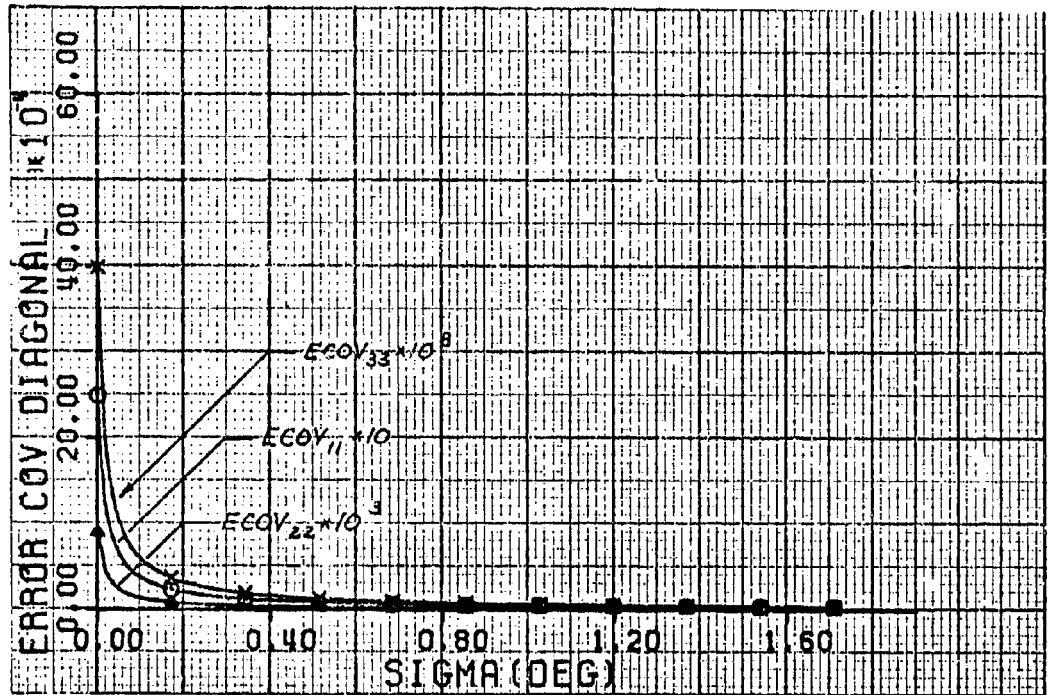


Figure 61. Case 1.5 - Diagonal Error Covariance Terms

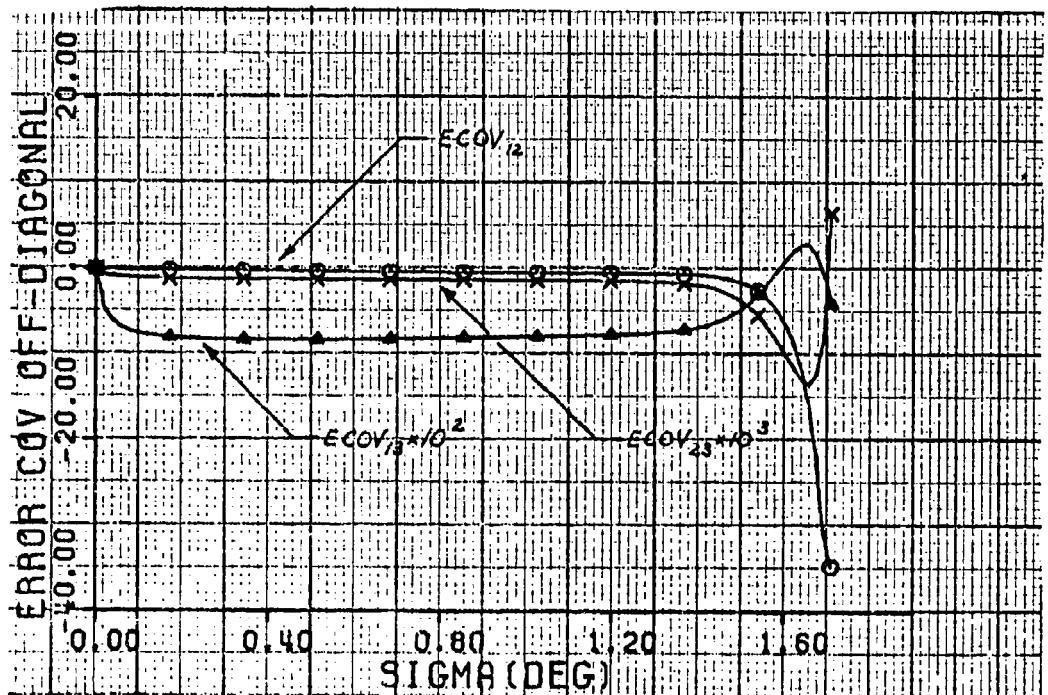


Figure 62. Case 1.5 - Off-Diagonal Error Covariance Terms



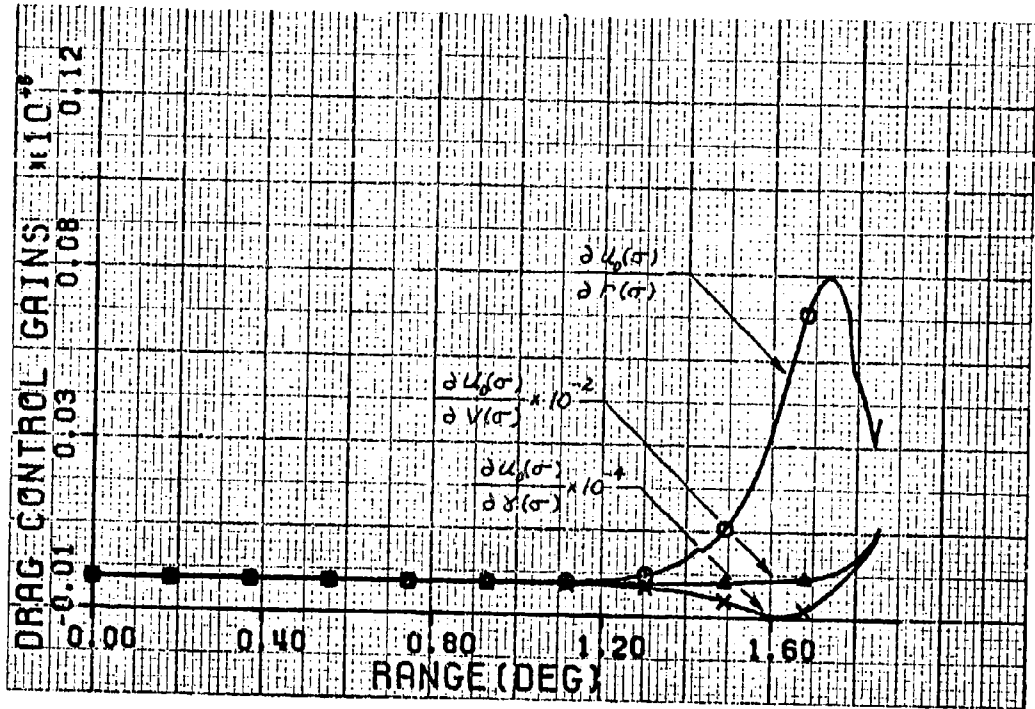


Figure 63. Case 7 - Drag Control Gains

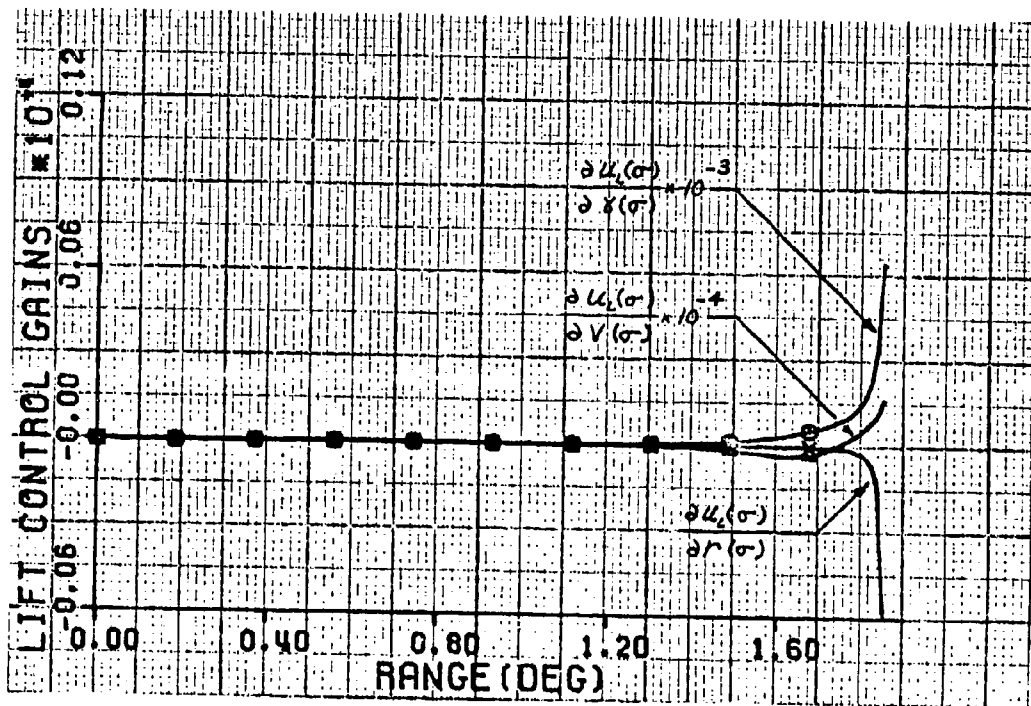


Figure 64. Case 7 - Lift Control Gains

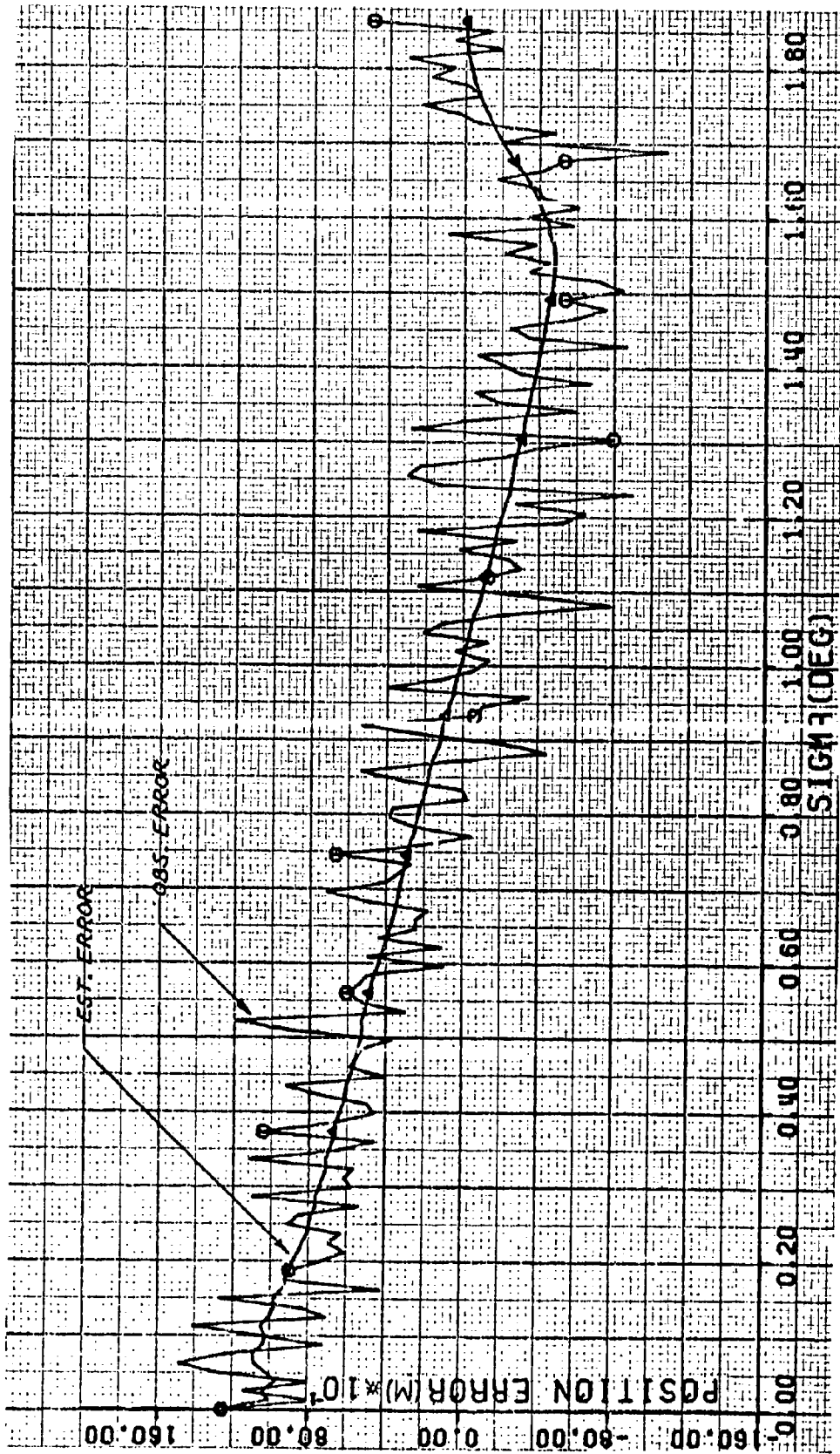


Figure 65. Case 7.1 - Position Error of 1000 Meters

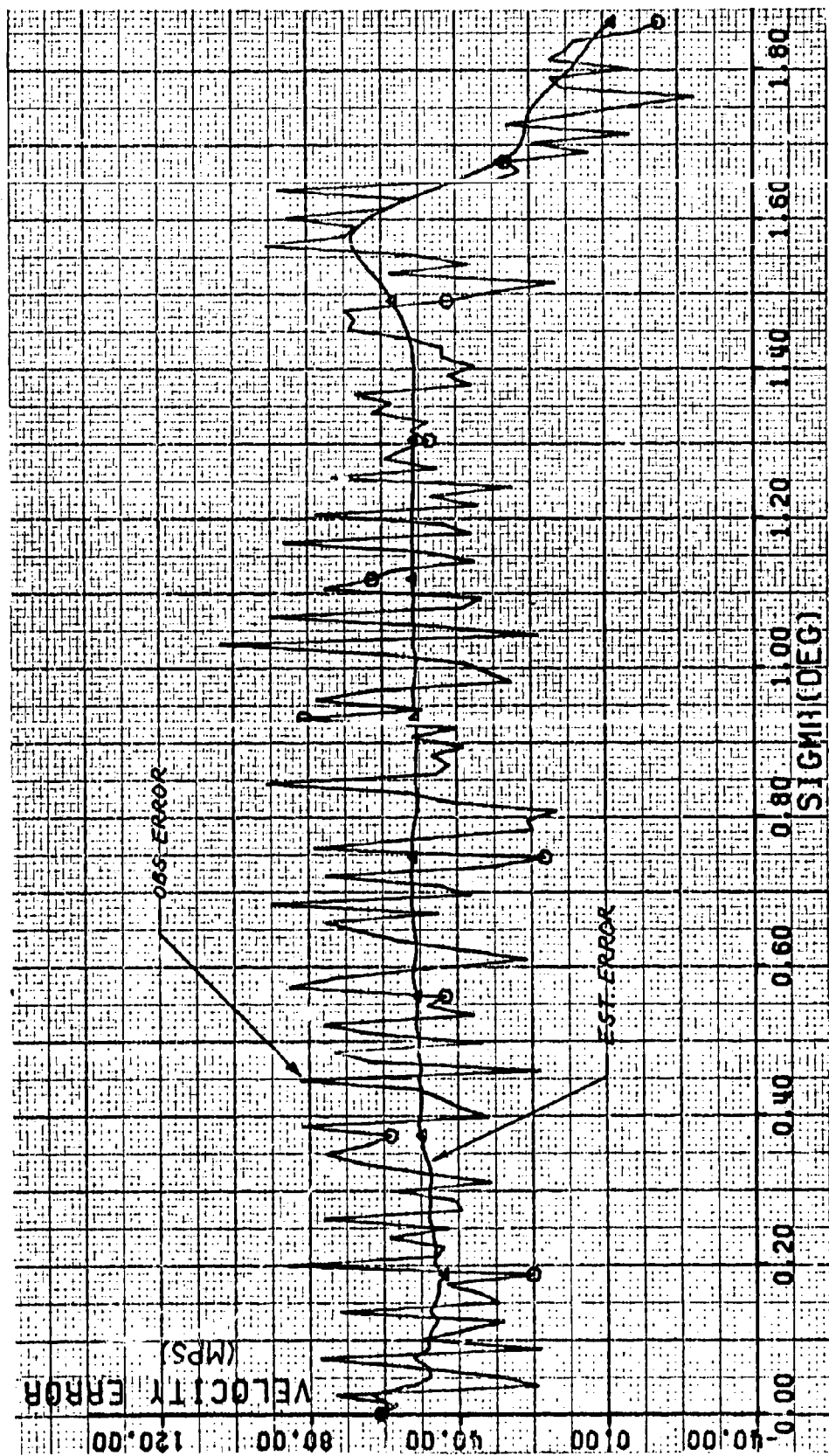


Figure 66. Case 7.1 - Velocity Error of 50 Meters/Second

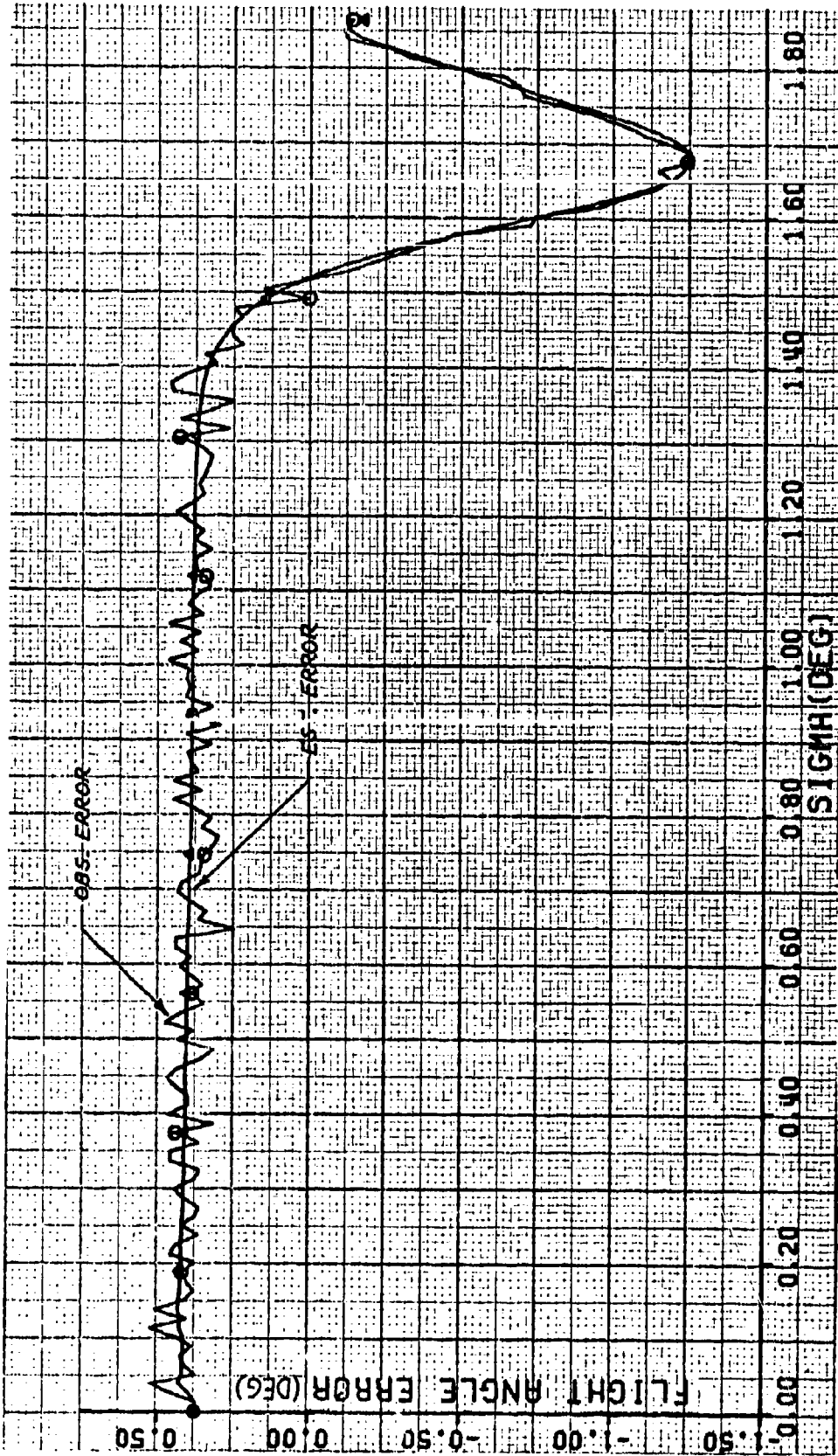


Figure 67. Case 7.1 - Flight Angle Error of .4 Degrees

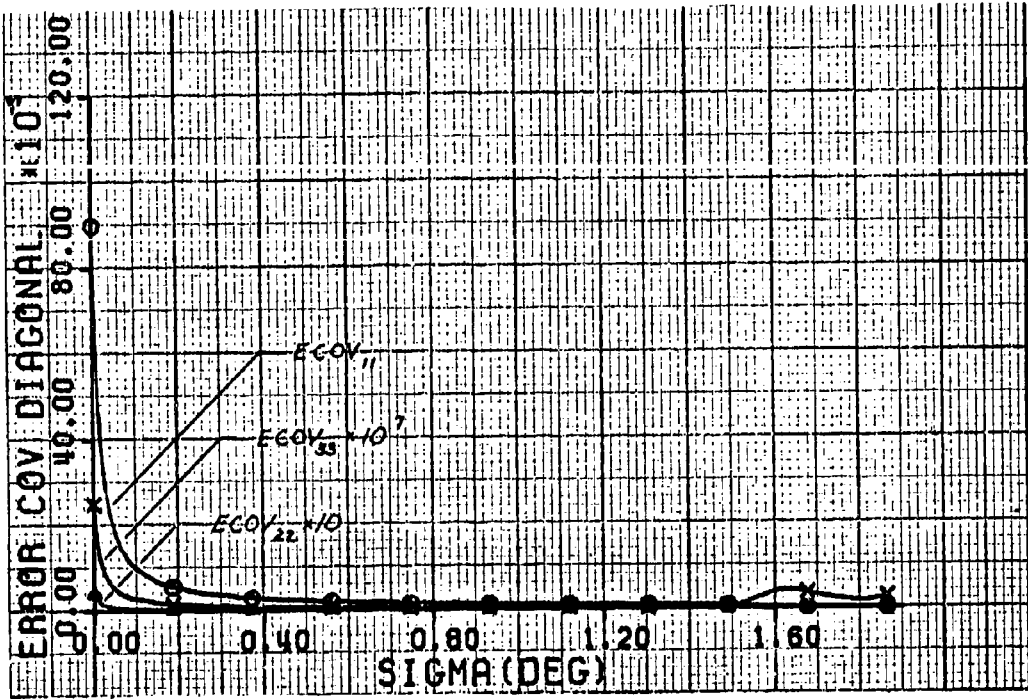


Figure 68. Case 7.1 - Diagonal Error Covariance Terms

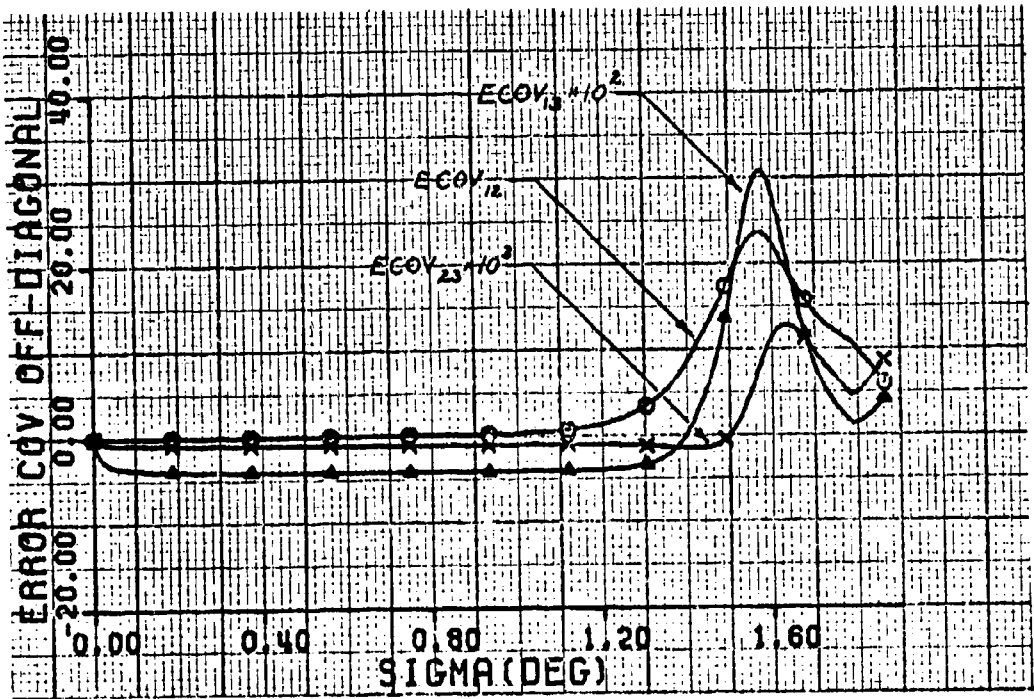


Figure 69. Case 7.1 - Off-Diagonal Error Covariance Terms

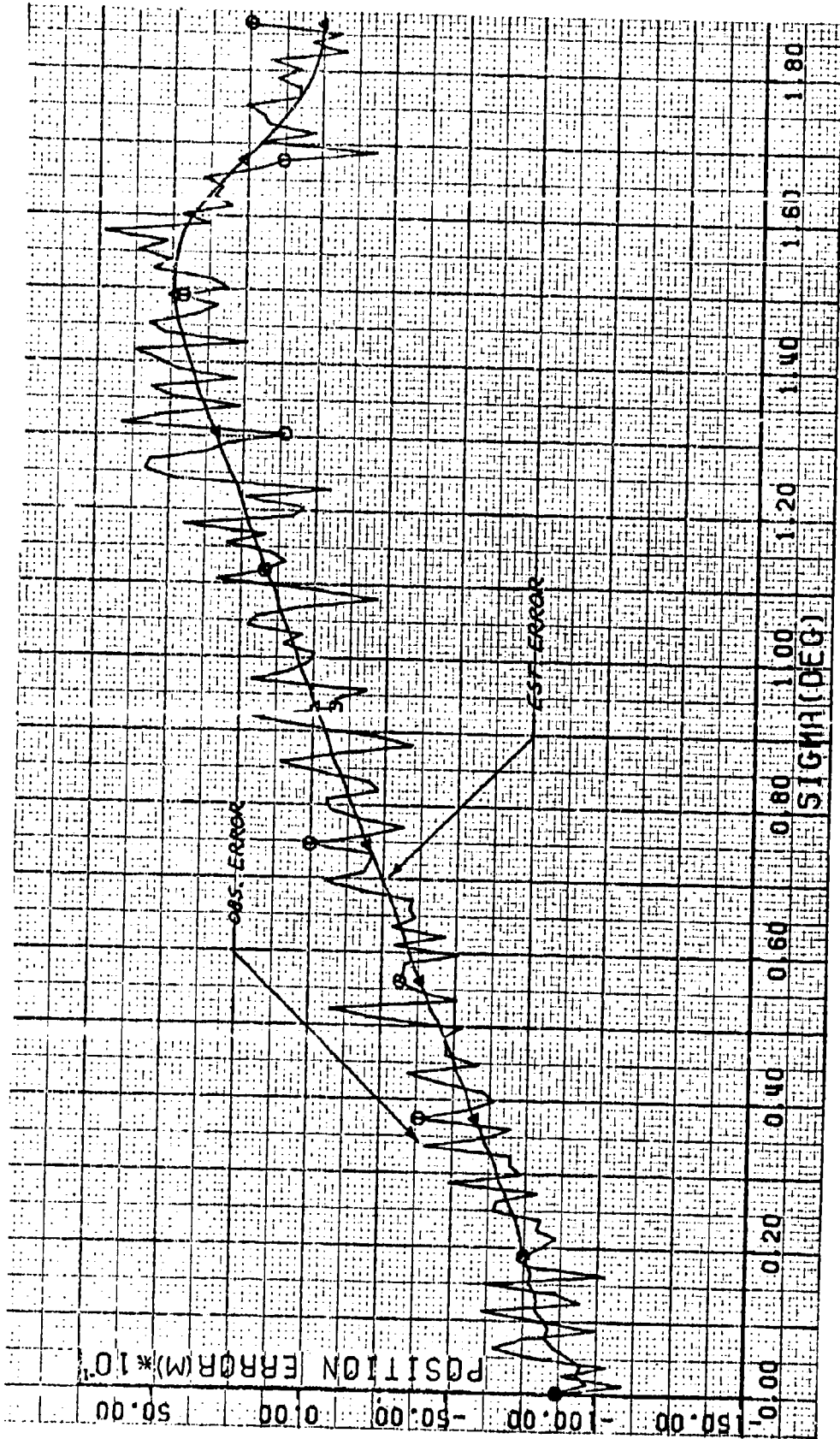


Figure 70. Case 7-2 - Position Error of ~1000 Meters

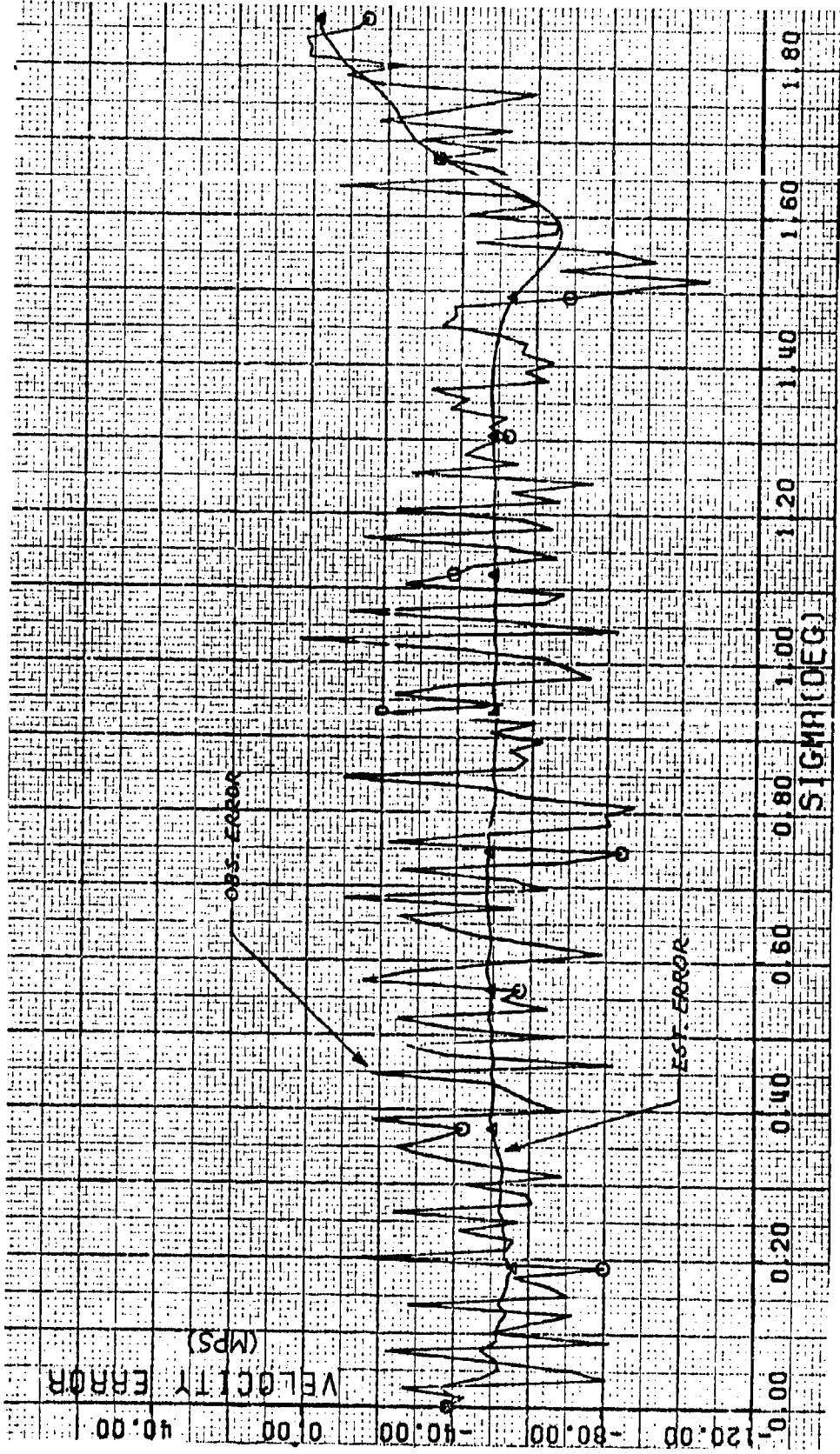


Figure 71. Case 7.2 - Velocity Error of -50 Meters/Second



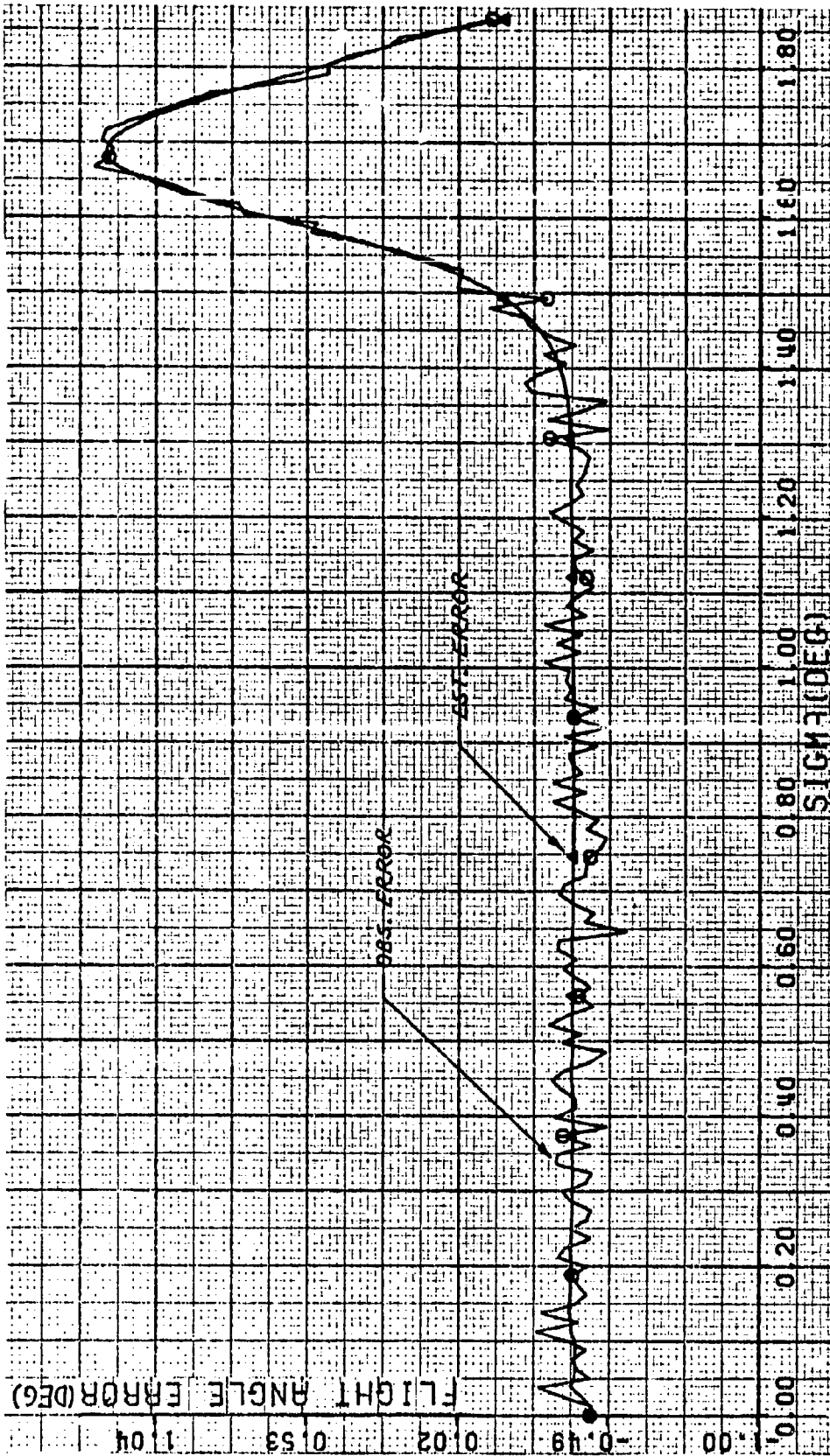


Figure 72. Case 7.2 - Flight Angle Error of -0.4 Degrees



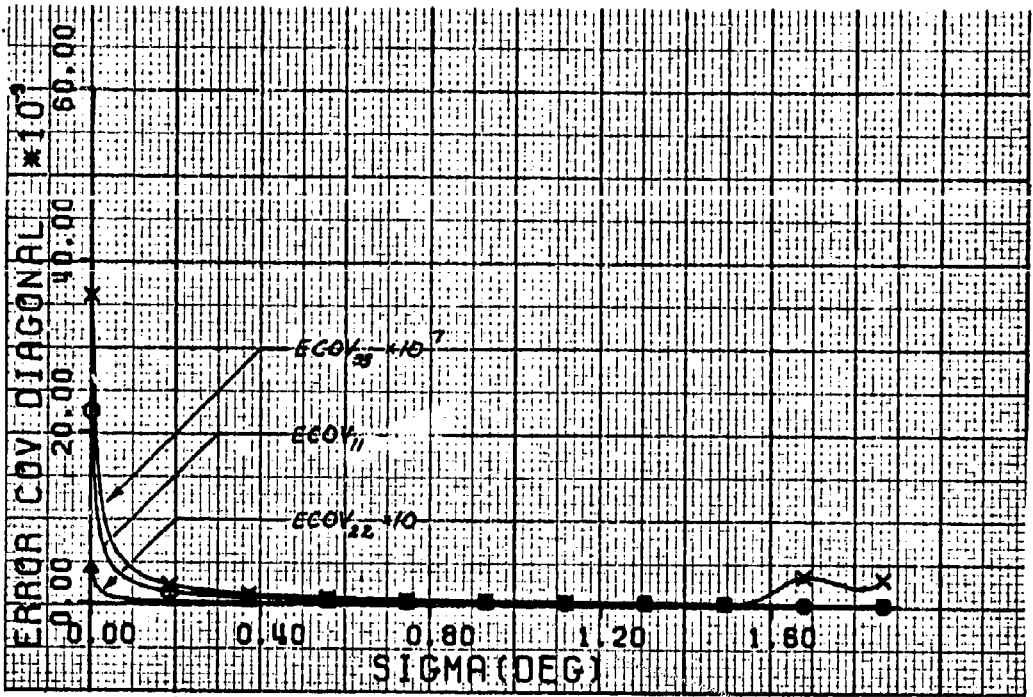


Figure 73. Case 7.2 - Diagonal Error Covariance Terms

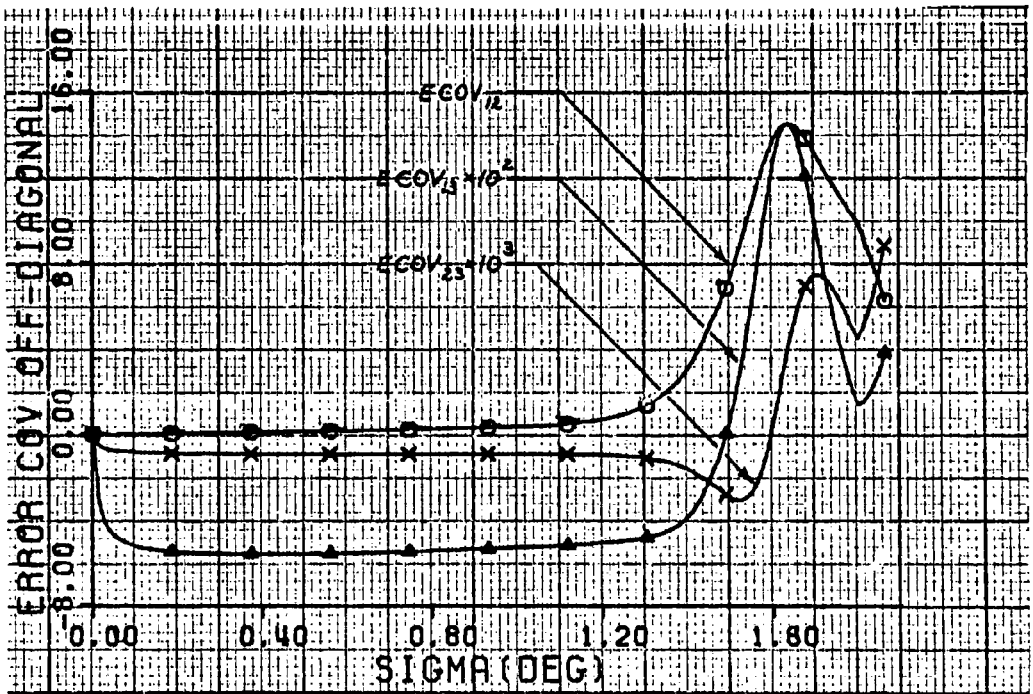


Figure 74. Case 7.3 - Off-Diagonal Error Covariance Terms

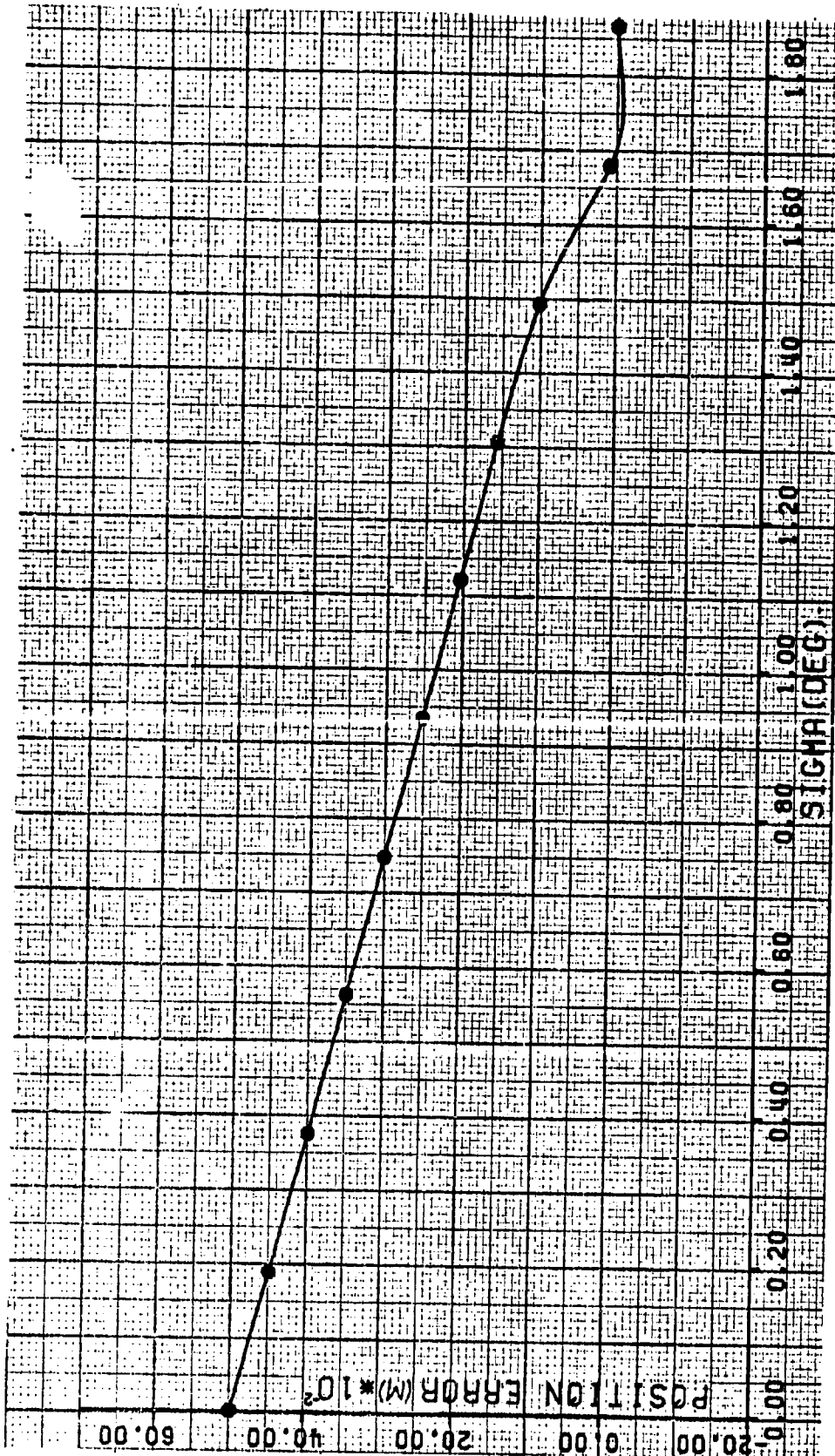


Figure 75. Case 7.3 - Position Error of 5000 Meters without Noise

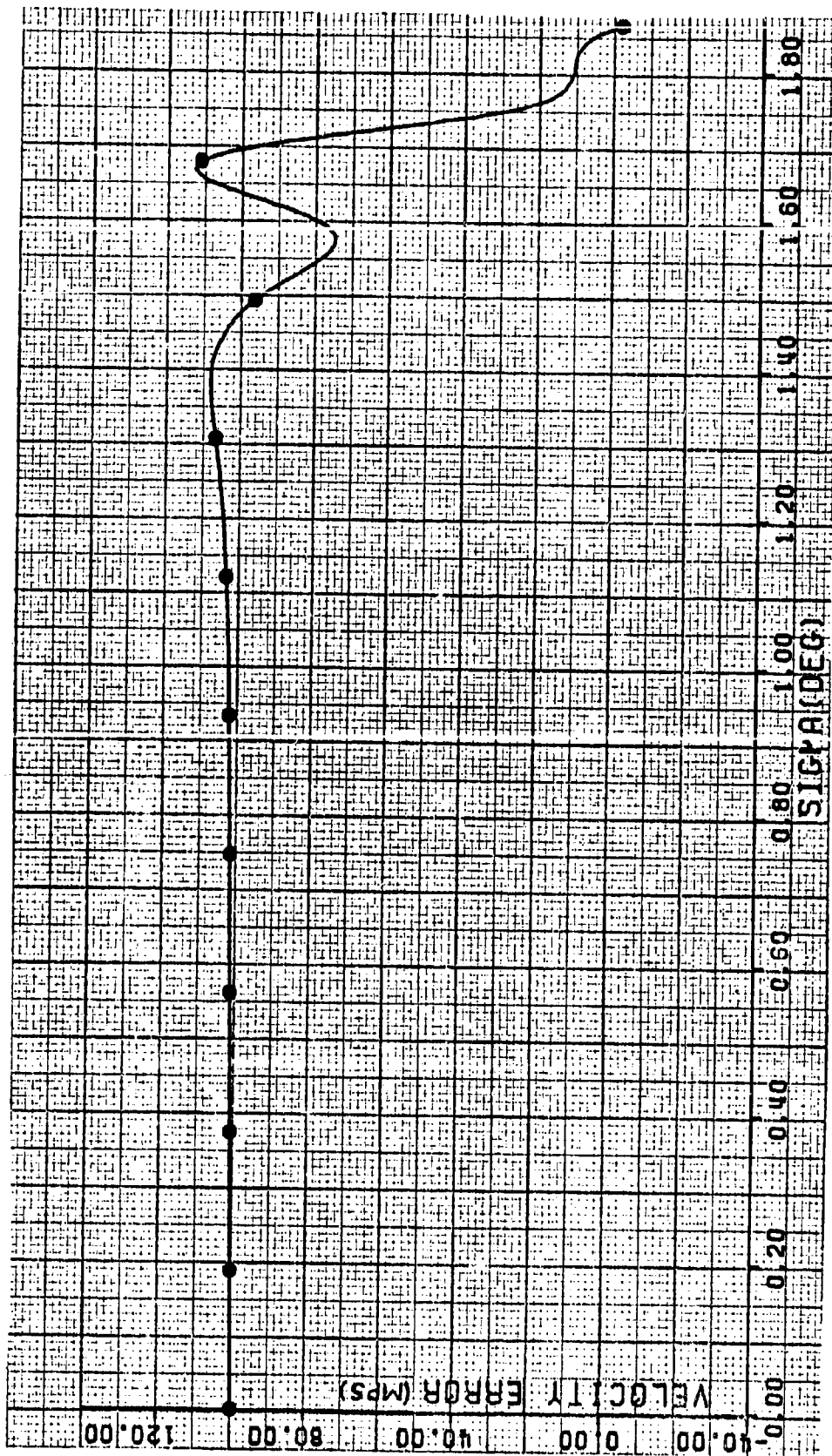


Figure 76. Case 7.3 - Velocity Error of 100 Meters/Second without Noise

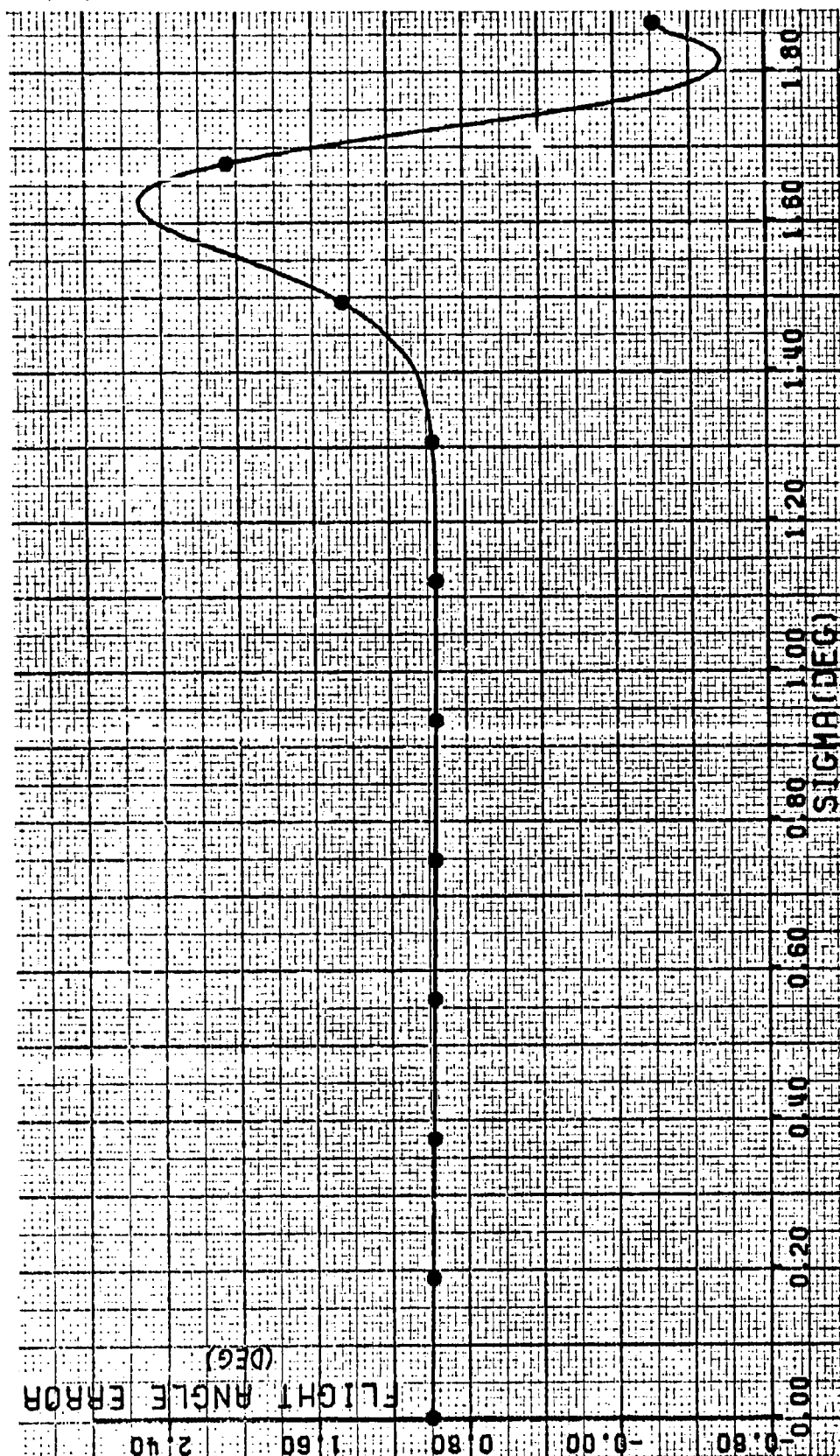


Figure 77. Case 7.3 - Flight Angle Error of 1.0 Degrees without Noise

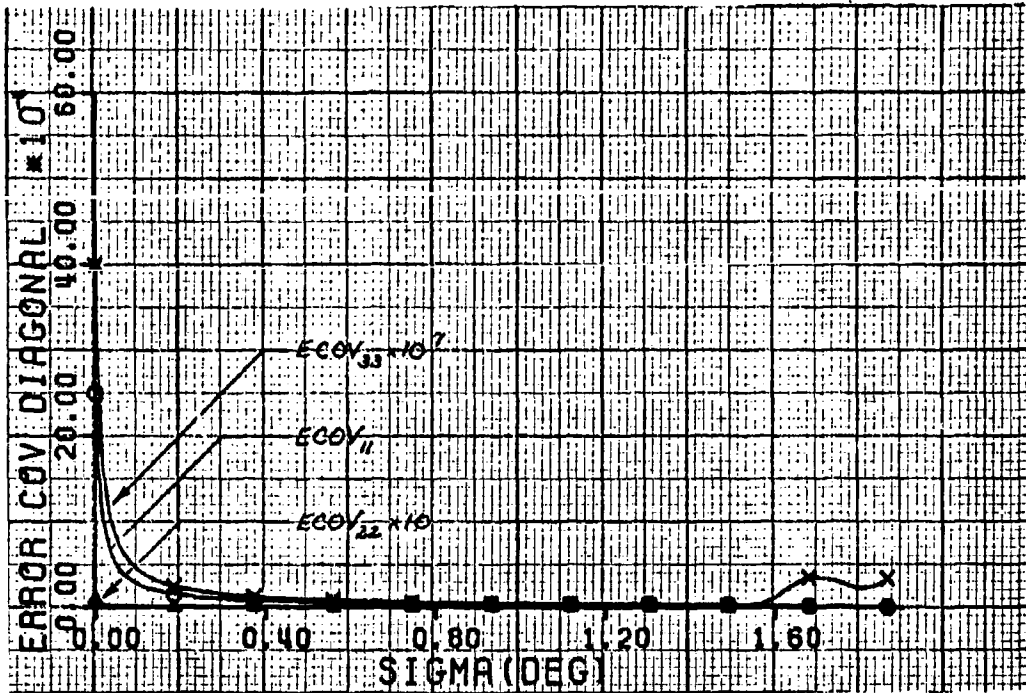


Figure 78. Case 7.3 - Diagonal Error Covariance Terms

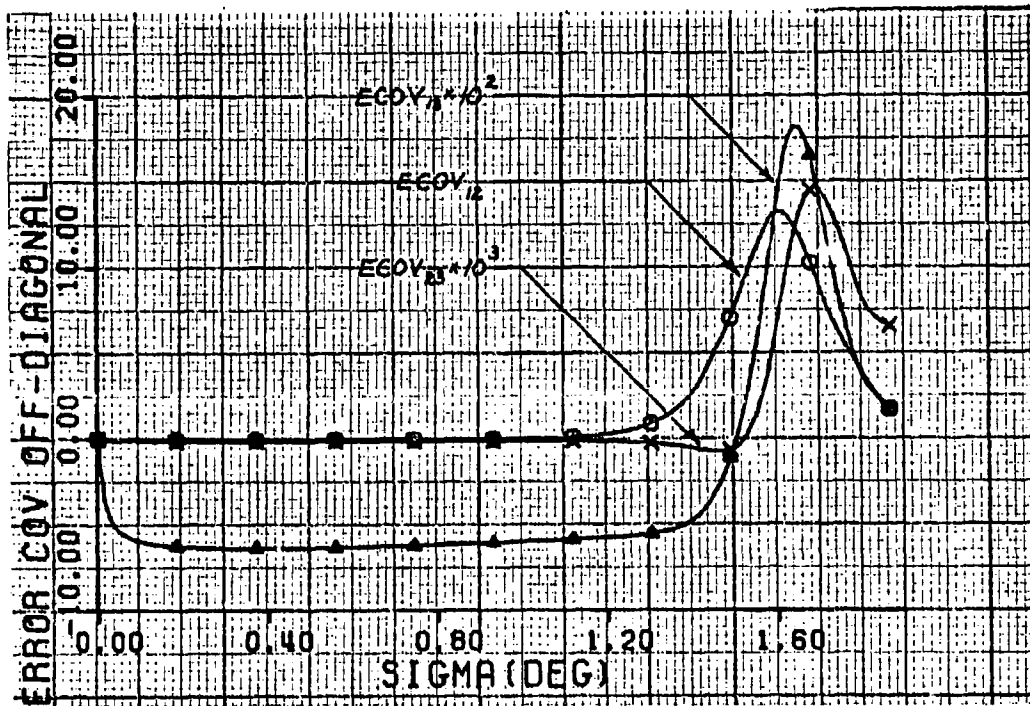


Figure 79. Case 7.3 - Off-Diagonal Error Covariance Terms

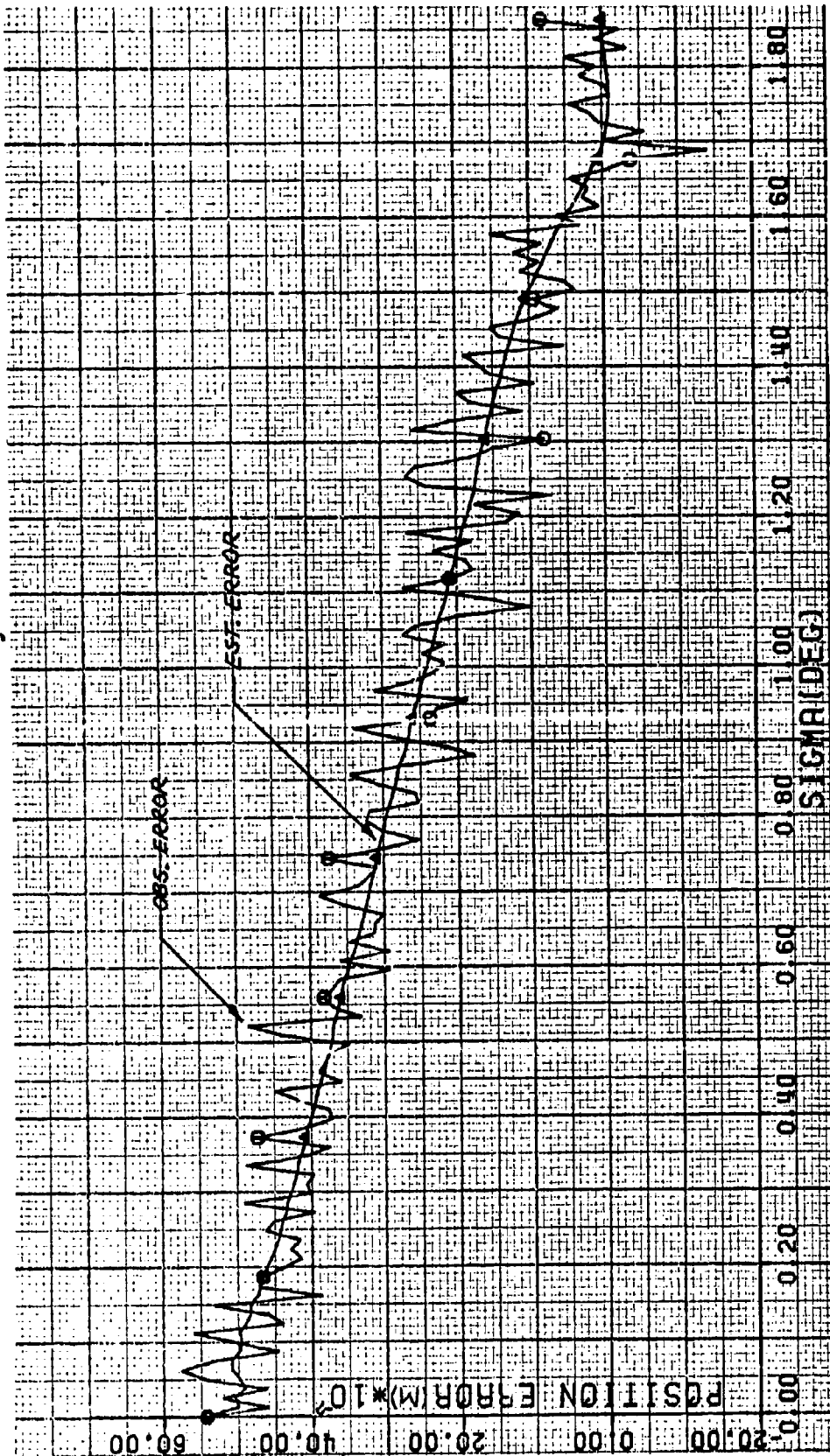


Figure 80. Case 7.4 - Position Error of 5000 Meters



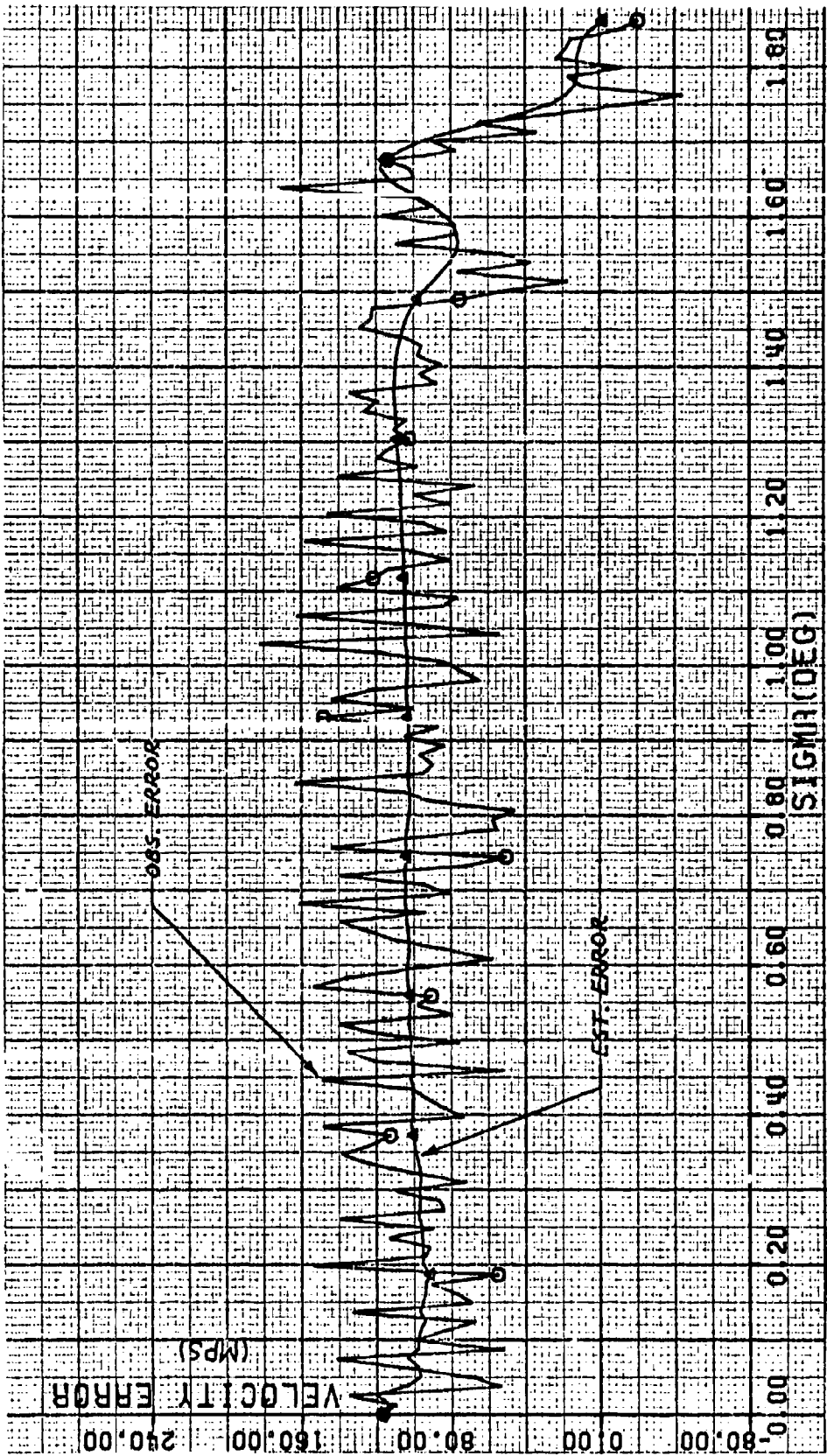


Figure 81. Case 7.4 - Velocity Error of 100 Meters/Second

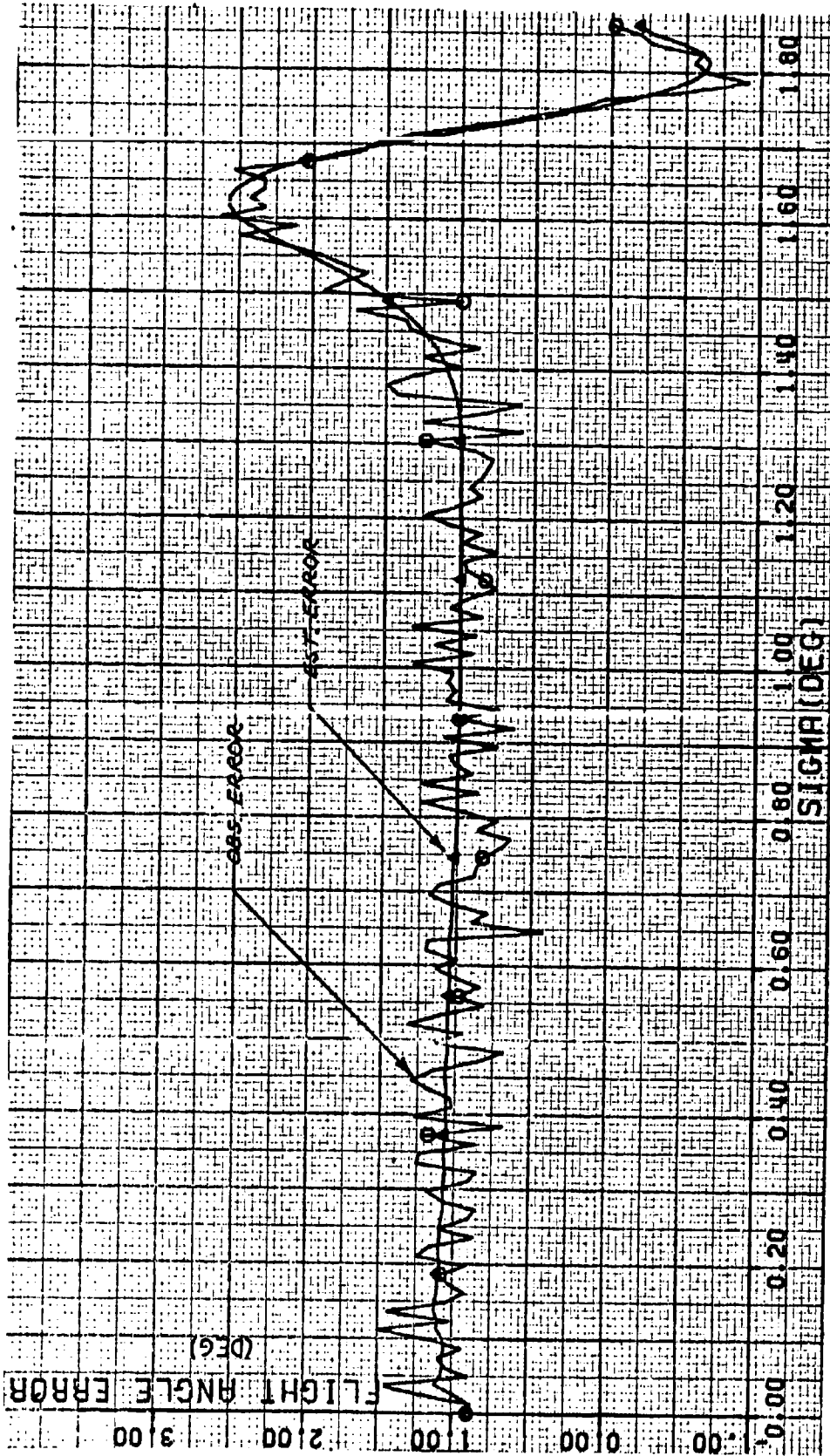


Figure 82. Case 7.4 - Flight Angle Error of 1.0 Degrees



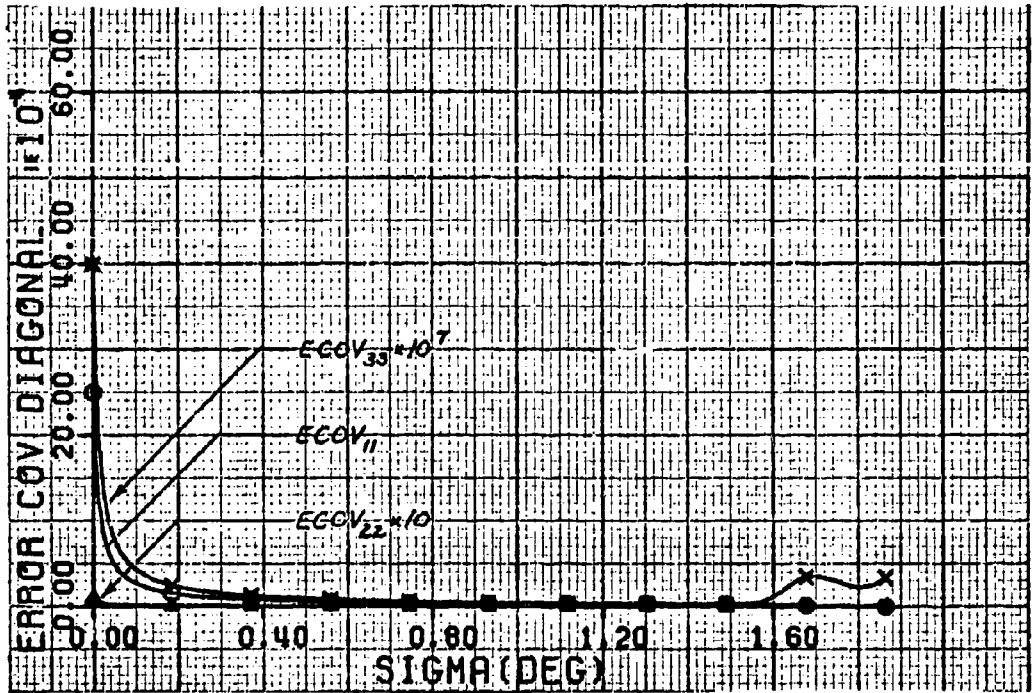


Figure 83. Case 7.4 - Diagonal Error Covariance Terms

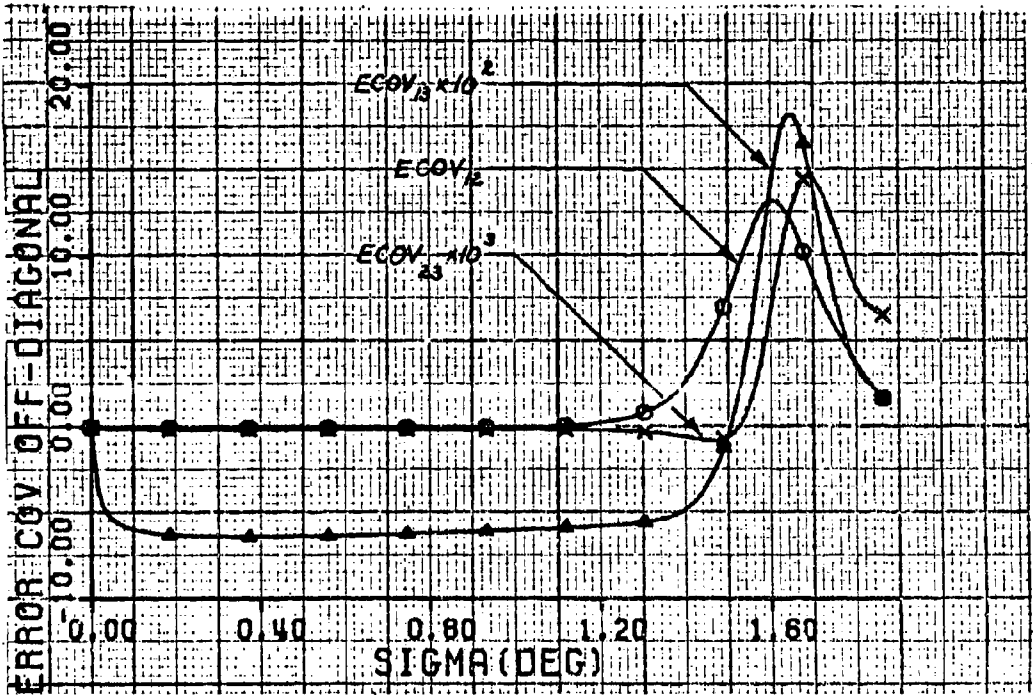


Figure 84. Case 7.4 - Off-Diagonal Error Covariance Terms

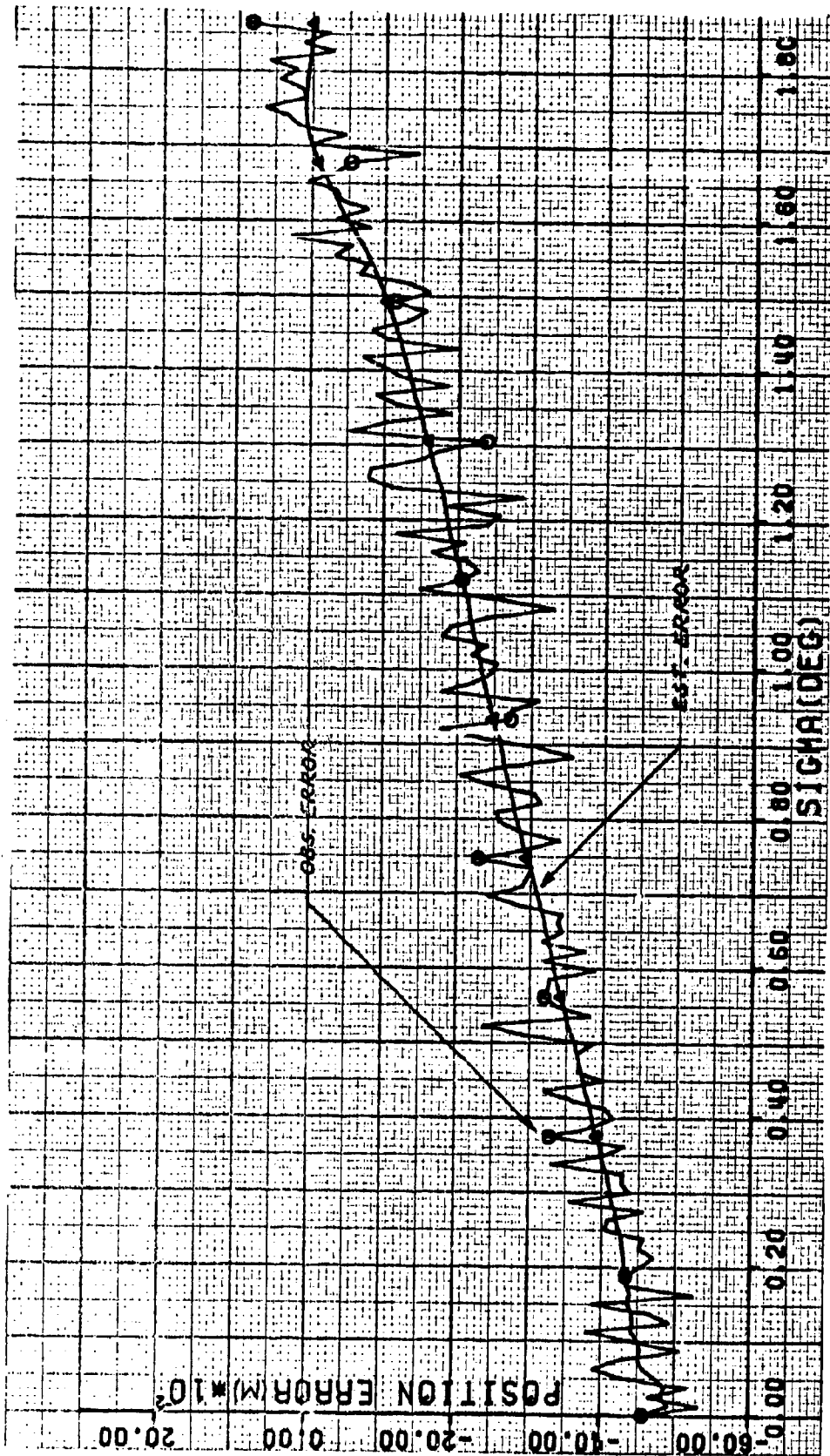


Figure 85. Case 7.5 - Position Error of -5000 Meters

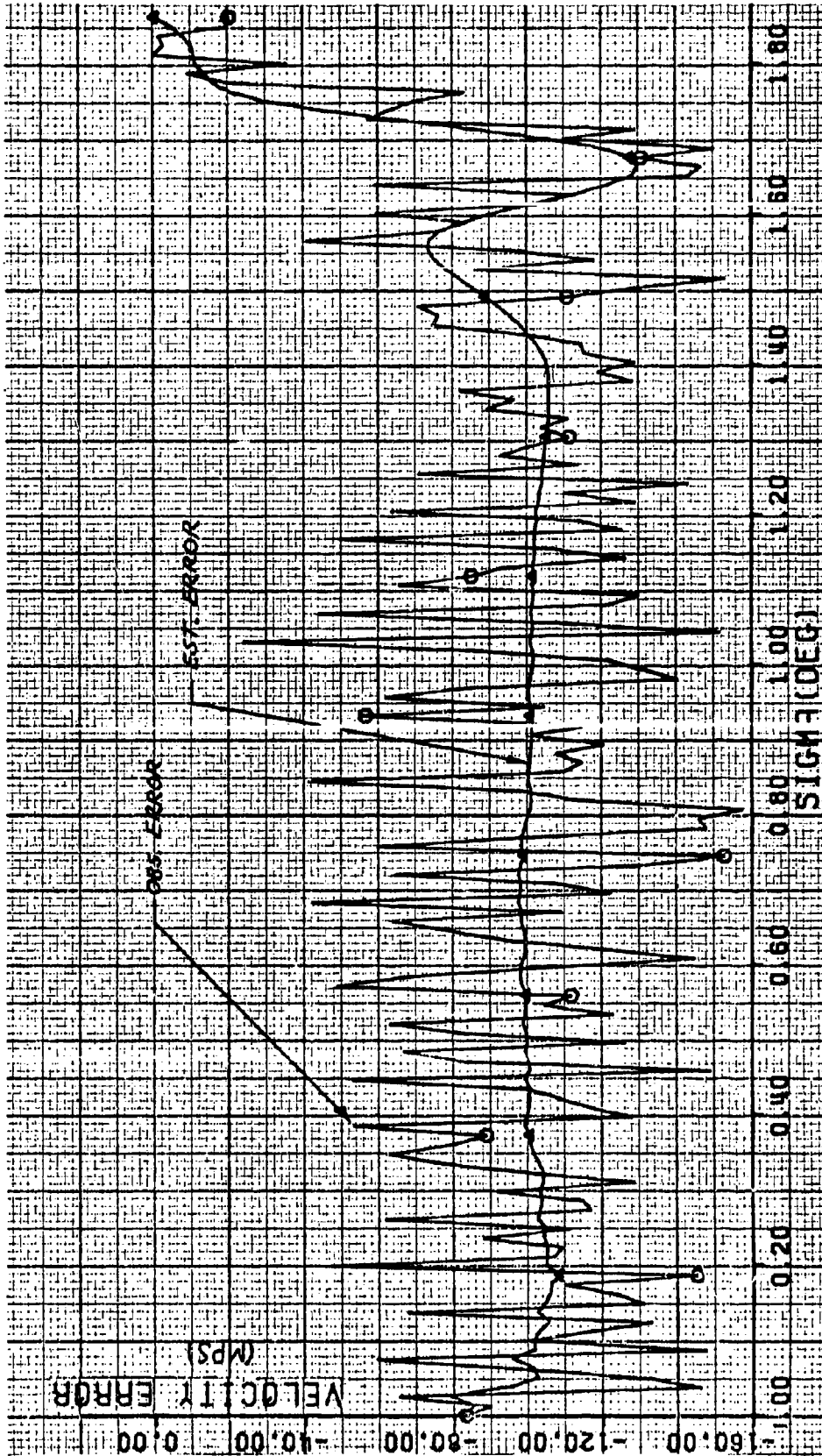


Figure 86. Case 7.5 - Velocity Error of -100 Meters/Second

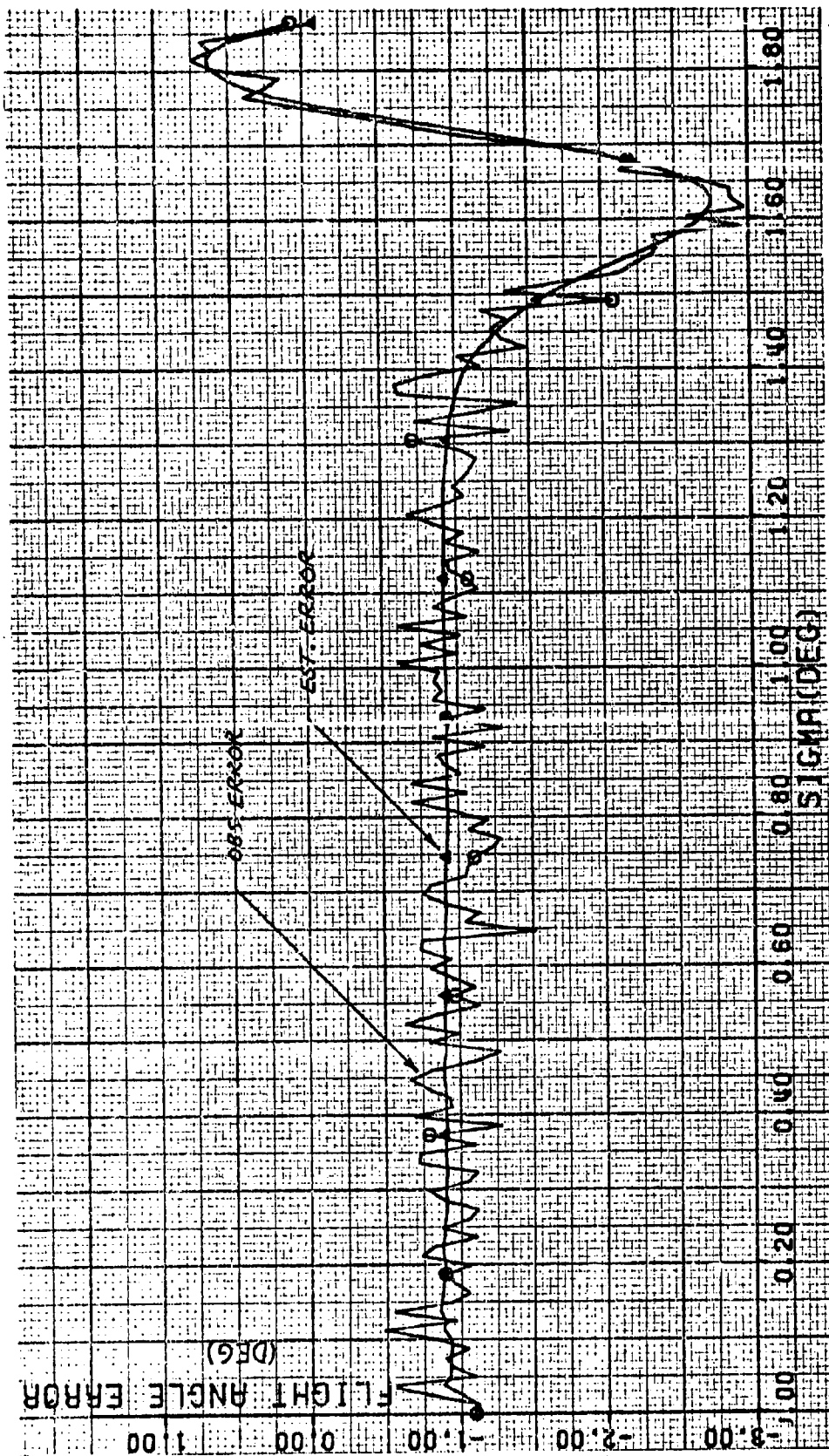


Figure 87. Case 7.5 - Flight Angle Error of -1.0 Degrees

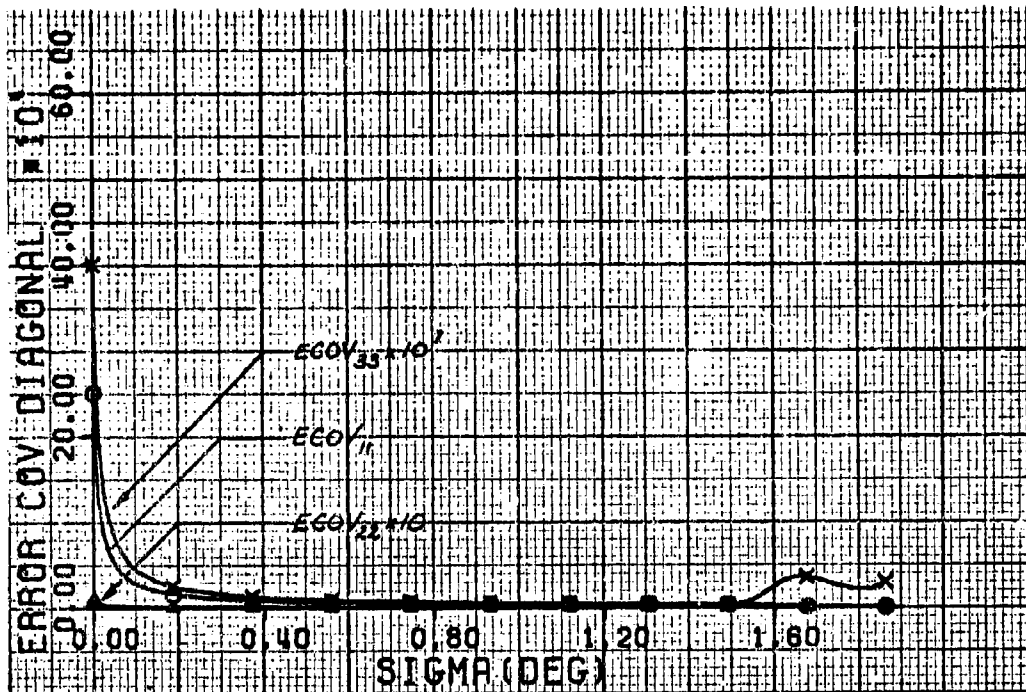


Figure 88. Case 7.5 - Diagonal Error Covariance Terms

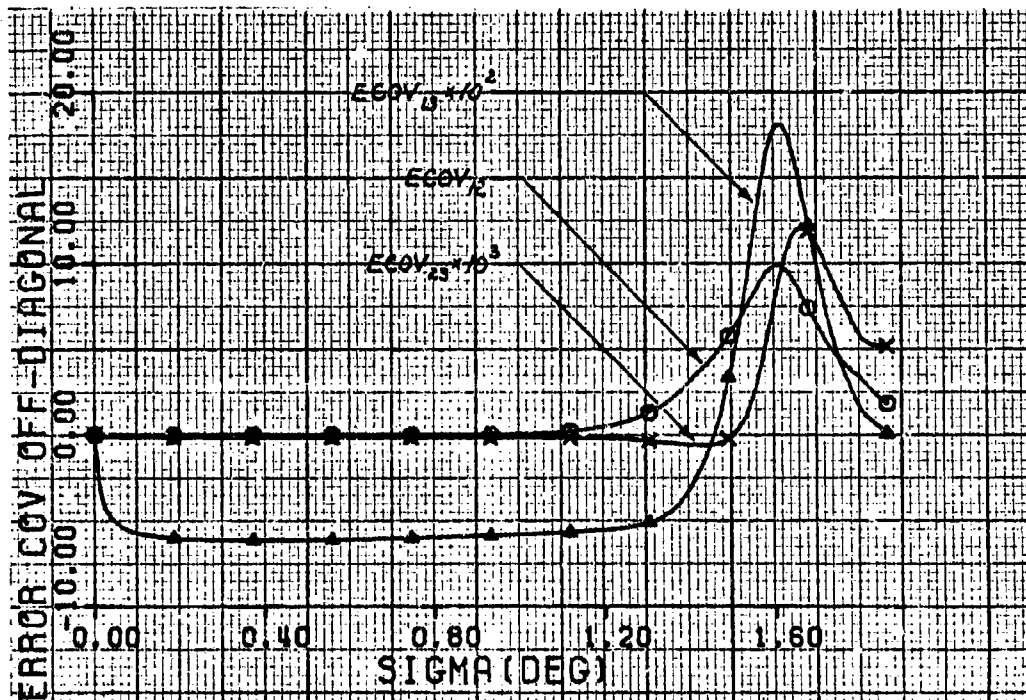


Figure 89. Case 7.5 - Off-Diagonal Error Covariance Terms

The flight angle is the most sensitive to initial condition errors from the nominal. This state variable is brought to near the terminal condition with the last two gain values. Up to this point, the flight angle error is allowed to deviate by large amounts from the nominal.

The flight angle error also appears to be the most sensitive to the addition of observation noise. This is shown by a comparison of the errors with and without noise present. Overall, the flight angle is most sensitive to any errors in state.

The position and velocity errors at the terminal point are relatively insensitive to the initial condition errors and to noise. In all the examples presented, the largest error in terminal position is about four meters and the largest error in terminal velocity is about six meters per second. Terminal position error appears to be almost completely insensitive to the magnitude of the initial errors.

A comparison of the graphs with positive and negative initial condition errors shows that the linear range of the feedback gains is very nearly the same on either side of the nominal trajectory with only a slightly higher peak error occurring in the flight angle when negative initial condition errors are present. The error curves with errors on both sides of the nominal are nearly mirror images.

The error covariance curves for the examples without noise present are shown for purposes of comparison. The same initial error covariance estimate is used in both cases along with the same noise covariance  $W$ . When no noise is present, the off-diagonal terms of the error covariance matrix simply reflect the coupling between the state equations and the validity of the linearizing assumptions. A comparison of these elements with and without noise present shows that the off-

diagonal terms have very nearly the same form. This indicates that the off-diagonal terms for this set of equations has very little relationship to the noise. They appear to be predominately due to the dynamics of the problem.

### VIII. Conclusions

The basic objectives of this thesis, to investigate a set of optimal solutions and to produce a suboptimal feedback scheme, have been accomplished. The conclusions drawn from the specific open- and closed-loop results presentation, as well as conclusions concerning the general problem are presented in this chapter.

#### Open-Loop Problem

The following conclusions are made concerning the open-loop results in Chapter V.

A. The amount of lift dominance at the end of the trajectory, and the length of range angle to go when the lift becomes dominant is a deciding factor in minimizing sensitivity coefficients. This conclusion is supported by observations 5 and 6 discussed at the end of Chapter V.

B. The appearance of minimum control for the first portion of the trajectory, stems from the presence of control in the criterion to be minimized.

#### Closed-Loop Problem

The following conclusions are made concerning the closed-loop results in Chapter VII.

C. The implicit guidance law simulation indicates that control for the trajectories tested can be maintained even with large initial condition errors, and will drive the vehicle along a neighboring trajectory to the boundary conditions with little error. In this simulation, the flight angle seems to be the most sensitive to



initial errors in the states. For the cases in which the velocity drops to less than 1700 mps at the terminal point, the feedback gains contain such high frequency content during the last of the flight, that the sampling rate is not high enough to allow the gains to be used.

D. The position error is least susceptible to both perturbation, and observation noise. This is attributable to the fact that the nominal trajectory is a minimum position sensitivity coefficient trajectory. This confirms the concept of minimizing sensitivity coefficients to achieve minimum terminal position error.

#### General Problem

The following conclusions are made concerning the overall problem:

E. The use of a passive, non-thrusting control in a classic optimal control problem is impractical unless it can be removed from the criterion function. In this problem, the cost of control was a deciding factor for the optimality of the trajectories.

F. The use of lift and drag for control requires a dense atmosphere, and thus a flat trajectory in the dense region, to achieve a well controlled entry.

G. The minimum sensitivity coefficient trajectory is one in which the vehicle begins a nominal entry angle, levels out to nearly horizontal flight, and then, during the last part of the trajectory, dives to meet the terminal angle condition. This appears to confirm conclusion F, and is illustrated by Case 7.

H. For each of the trajectories additional constraints, other than those contained here in, should be employed to make the trajectory usable. This is due, in part, to the type of control used,

which works only during, at best, the last quarter of the trajectory.  
For some trajectories, additional elements are necessary to achieve the  
magnitude and rate of change of magnitude necessary in the optimal  
control.

## IX. Recommendations

The recommendations concerning the general problem of sensitivity coefficient minimization for an entry trajectory and suggestions for areas of further study are presented in this chapter.

### Sensitivity Coefficient Minimization

The general problem of sensitivity coefficient minimization for an entry trajectory is highly dependent on the lift-to-drag ratio and the length of the trajectory during which control is exerted. The following recommendations are made in this area:

A. This problem should be eliminated as a problem in classical optimal control theory and cast as a parameter sweep problem. The purpose of this is to sweep only within a range of practical entry controllers.

- B. The parameters to be considered in the sweep include:
1. Lift-to-drag ratio
  2. Rate of change of lift-to-drag ratio
  3. The range angle arc for which the lift control is allowed to dominate the trajectory.

### Suggestions For Areas Of Further Study

In light of the recommendations given above, the following areas are suggested for further study:

- A. For the parameter sweep problem:
1. Use numerical analysis to describe, in a least square sense, smooth functions identified during the non-aerodynamic portion of the trajectory.

2. Also use numerical techniques to attempt to identify functions which may be used to describe the changes in the sensitivity coefficients during the aerodynamic portion of the trajectory.
3. Identify, using the relationships determined in 1 and 2 above, a relationship which describes the sensitivity coefficients throughout the trajectory.
4. Investigate the use of a hybrid computer for the parameter sweep problem and determine its value in solving an optimal control problem of this type with the primary objective of obtaining a practical controller.

NOT REPRODUCIBLE

B. Expand the present problem to include three degrees of freedom to determine the effects of cross-range motion on the sensitivity coefficients.

C. Investigate the present problem with constraints included on the following variables to achieve a practical controller:

1. Drag control for deceleration constraints
2. Lift-to-drag ratio for configuration constraints
3. Rate of change of drag control for maneuvering capability constraints.
4. Rate of change of lift-to-drag ratio for maneuvering capability constraints.
5. Velocity for heating constraints
6. Rate of change of velocity for deceleration constraints.

7. Rate of change of flight angle for deceleration constraints.

D. That the optimal implicit guidance scheme be investigated to determine the most practical method of implementing it and the simplest suboptimal estimation technique which can be used in an actual entry trajectory.

References

1. Johnson, R. W., Optimum Design and Linear Guidance Law Formulation of Entry Vehicles for Guidance Parameters and Temperature Accumulation Along Optimum Entry Trajectories. Dissertation, Report Number 66-2, UCLA, January 1966. AD 626636.
2. Brown, F. M., R. W. Johnson, and D. O. Norris, Short Course On Guidance and Control For Aerospace Vehicles. Report Number 131, Advisory Group for Aerospace Research and Development (AGARD), NATO, June 1969. AD 688334.
3. Henry, J. C. and R. L. Ringo, Optimal Guidance Laws for Maneuvering Entry Vehicles. Thesis. GGC/EE/69-10. Air Force Institute of Technology, Wright Patterson AFB, Ohio. June 1969.
4. Ward, B. D., Suboptimal Control Methods Applied To The Reentry Problem. Dissertation. Report Number 67-21, UCLA, June 1967. AD 824 050.
5. Gelb, A., and A. A. Sutherland, Application of the Kalman Filter To Aided Inertial Systems. Analytical Science Corporation Technical Publication 4652. August, 1968. AD 851052.
6. Payne, J. A., Computational methods in optimal control problems. AFFDL-TR-65-50. Wright Patterson AFB, Ohio: Air Force Flight Dynamics Laboratory. 1965.
7. Brattland, H. A., A Search for the Minimum Fuel Landing Trajectory of a Tilt Wing VTOL Aircraft. Thesis. GGC/EE/69-2. Air Force Institute of Technology, Wright Patterson AFB, Ohio. June, 1969.
8. Birta, L. G., and T. J. Trushel, "The Terminal Error Function/ Davidon-Fletcher Powell Method in Computation of Optimal Controls." JACC, Boulder, Colorado, 1969.
9. Breakwell, J. V., J. L. Speyer, and A. E. Bryson, "Optimization and Control of Nonlinear Systems Using The Second Variation", JSIAM on Control, Series A. 1963.
10. Sage, A. P., Optimum Systems Control. Englewood Cliffs, New Jersey, Prentice-Hall, Inc. 1968.
11. Bryson, A. E., and Y. C. Ho, Applied Optimal Control. Waltham, Mass., Blaisdell Publishing Co. 1969.
12. Aoki, M., Optimization of Stochastic Systems. New York, Academic Press. 1967.
13. Meditch, J.S., Stochastic Optimal Linear Estimation and Control. New York, McGraw-Hill. 1969.

14. Morrison, N., Introduction to Sequential Smoothing and Prediction. New York, McGraw-Hill. 1969.
15. Liepmann, H. W., and A. Roshko. Elements of Gas Dynamics. New York, John Wiley and Sons. 1957.
16. Olsen, R. M., Essentials of Engineering Fluid Mechanics. Scranton, Pa., International Textbook Co. 1961.
17. Elliot, G. E. and T. R. Filiatreau, An Application of the Kalman Filter to Orbit Determination. Thesis. GCC/EE/70-7. Air Force Institute of Technology, Wright Patterson AFB, Ohio. June, 1970.

## Appendix A

Open-Loop Optimal Control Equations For The Entry Problem

The purpose of this appendix is to present the detailed equations for both first and second variations of the optimal entry problem.

They are presented in order of development.

STATES

$$X_1' = \frac{X_1}{\tan X_3} \quad (A-1)$$

$$X_2' = \frac{-\mu}{X_1 X_2 \tan X_3} - \frac{X_1}{X_2 \sin X_3} C U_0 \quad (A-2)$$

$$X_3' = -1 + \frac{\mu}{X_1 X_2^2} - \frac{X_1}{X_2^2 \sin X_3} C U_2 \quad (A-3)$$

$$X_4' = -X_4 T_{11} - X_5 T_{21} - X_6 T_{31} \quad (A-4)$$

$$X_5' = -X_4 T_{12} - X_5 T_{22} - X_6 T_{32} \quad (A-5)$$

$$X_6' = -X_4 T_{13} - X_5 T_{23} - X_6 T_{33} \quad (A-6)$$

Where  $T_{11} = \frac{1}{\tan X_3} \quad (A-7)$

$$T_{12} = 0 \quad (A-8)$$

$$T_{13} = -\frac{X_1}{\sin^2 X_3} \quad (A-9)$$

$$T_{21} = \frac{\mu}{X_1^2 X_2 \tan X_3} - \frac{1}{X_2 \sin X_3} C U_0 - \frac{X_1}{X_2 \sin X_3} C_{x1} U_0 \quad (A-10)$$

$$T_{22} = \frac{\mu}{X_1 X_2^2 \tan X_3} + \frac{X_1}{X_2^2 \sin X_3} C U_0 - \frac{X_1}{X_2 \sin X_3} C_{x2} U_0 \quad (A-11)$$



$$T_{22} = \frac{\mu}{X_1 X_2 \sin^2 X_3} + \frac{X_1 \cos X_3}{X_2 \sin^2 X_3} C U_0 \quad (A-12)$$

$$T_{31} = -\frac{\mu}{X_1^2 X_2^2} - \frac{l}{X_2^2 \sin X_3} C U_1 - \frac{X_1}{X_2^2 \sin X_3} C_{x1} U_1 \quad (A-13)$$

$$T_{32} = -\frac{2\mu}{X_1 X_2^3} + \frac{2X_1}{X_2^3 \sin X_3} C U_1 - \frac{X_1}{X_2^2 \sin X_3} C_{x2} U_1 \quad (A-14)$$

and 
$$C = \frac{\rho X_2^2 C_{ps}}{2} \quad (A-15)$$

$$C_{x1} = \frac{X_2^2 C_{ps}}{2} \frac{\partial \rho}{\partial X_1} - \frac{\rho X_2^3}{2 \partial^2} \frac{\partial C_{ps}}{\partial M} \frac{\partial \partial}{\partial X_1} \quad (A-16)$$

$$C_{x2} = \rho X_2 C_{ps} + \frac{\rho X_2^2}{2 \partial} \frac{\partial C_{ps}}{\partial M} \quad (A-17)$$

where 
$$C_{ps} = \frac{238.87872 M^5}{7(2.8M^2 - 0.4)^2} \left[ \frac{l}{2(2.8M^2 - 0.4)} \right]^{\frac{1}{2}} - \frac{10}{7M^2} \quad (A-18)$$

$$\frac{\partial C_{ps}}{\partial M} = -\frac{2C_{ps}}{M} + \frac{238.87872 M^4}{(2.8M^2 - 0.4)^2} \left[ \frac{l}{2(2.8M^2 - 0.4)} \right]^{\frac{1}{2}} \left[ 1 - \frac{l}{0.6(2.8M^2 - 0.4)} \right] \quad (A-19)$$

$$M = \frac{X_2}{\partial} \quad (A-20)$$

### CRITERION

$$J = \frac{1}{2} \int_0^{\sigma} \left[ K_4 X_4^2 + K_5 X_5^2 + K_6 X_6^2 + K_{u_0} U_0^2 + K_{u_1} U_1^2 \right] d\sigma \quad (A-21)$$

### HAMILTONIAN

$$\begin{aligned} H = & \frac{1}{2} \left[ K_4 X_4^2 + K_5 X_5^2 + K_6 X_6^2 + K_{u_0} U_0^2 + K_{u_1} U_1^2 \right] + \lambda_1 F_1 + \lambda_2 F_2 \\ & + \lambda_3 F_3 - \lambda_4 \left[ X_4 T_{11} + X_5 T_{21} + X_6 T_{31} \right] \\ & - \lambda_5 \left[ X_5 T_{22} + X_6 T_{32} \right] - \lambda_6 \left[ X_4 T_{13} + X_5 T_{23} + X_6 T_{33} \right] \end{aligned} \quad (A-22)$$

$$T_{221} = -\frac{\mu}{x_1^2 x_2 \sin^2 x_3} + \frac{\cos x_3}{x_2 \sin^2 x_3} C_{U_0} + \frac{x_1 \cos x_3}{x_2 \sin^2 x_3} C_{x_1} U_0 \quad (A-33)$$

$$T_{311} = \frac{2\mu}{x_1^3 x_2^3} - \frac{2}{x_2^2 \sin x_3} C_{x_1} U_L - \frac{x_1}{x_2^2 \sin x_3} C_{x_1 x_1} U_L \quad (A-34)$$

$$T_{321} = \frac{2\mu}{x_1^2 x_2^3} + \frac{2}{x_2^3 \sin x_3} C_{U_L} + \frac{2x_1}{x_2^3 \sin x_3} C_{x_1} U_L \\ - \frac{x_1}{x_2^2 \sin x_3} C_{x_1 x_2} U_L - \frac{1}{x_2^2 \sin x_3} C_{x_2} U_L \quad (A-35)$$

$$T_{331} = \frac{\cos x_3}{x_2^2 \sin^2 x_3} C_{U_L} + \frac{x_1 \cos x_3}{x_2^2 \sin^2 x_3} C_{x_1} U_L \quad (A-36)$$

$$T_{112} = 0 \quad (A-37)$$

$$T_{122} = 0 \quad (A-38)$$

$$T_{132} = 0 \quad (A-39)$$

$$T_{212} = \frac{\mu}{x_1^2 x_2^2 \tan x_3} + \frac{1}{x_2^2 \sin x_3} C_{U_0} - \frac{1}{x_2 \sin x_3} C_{x_2} U_0 \\ - \frac{x_1}{x_2 \sin x_3} C_{x_1 x_2} U_0 + \frac{x_1}{x_2^2 \sin x_3} C_{x_1} U_0 \quad (A-40)$$

$$T_{222} = -\frac{2\mu}{x_1 x_2^3 \tan x_3} - \frac{2x_1}{x_2^3 \sin x_3} C_{U_0} + \frac{2x_1}{x_2^2 \sin x_3} C_{x_2} U_0 \\ - \frac{x_1}{x_2 \sin x_3} C_{x_2 x_2} U_0 \quad (A-41)$$

$$T_{232} = -\frac{\mu}{x_1 x_2^2 \sin^2 x_3} - \frac{x_1 \cos x_3}{x_2^2 \sin^2 x_3} C_{U_0} + \frac{x_1 \cos x_3}{x_2 \sin^2 x_3} C_{x_1} U_0 \quad (A-42)$$

$$T_{312} = \frac{2\mu}{x_1^2 x_2^3} + \frac{2}{x_2^3 \sin x_3} C_{U_L} - \frac{1}{x_2^2 \sin x_3} C_{x_2} U_L \\ - \frac{x_1}{x_2^2 \sin x_3} C_{x_1 x_2} U_L + \frac{2x_1}{x_2^3 \sin x_3} C_{x_1} U_L \quad (A-43)$$

ADJOINTS

$$\lambda_1' = - \left\{ \lambda_1 T_{11} + \lambda_2 T_{21} + \lambda_3 T_{31} - \lambda_4 [X_4 T_{111} + X_5 T_{211} + X_6 T_{311}] \right. \\ \left. - \lambda_5 [X_4 T_{121} + X_5 T_{221} + X_6 T_{321}] - \lambda_6 [X_4 T_{131} + X_5 T_{231} + X_6 T_{331}] \right\} \quad (A-22)$$

$$\lambda_2' = - \left\{ \lambda_1 T_{12} + \lambda_2 T_{22} + \lambda_3 T_{32} - \lambda_4 [X_4 T_{112} + X_5 T_{212} + X_6 T_{312}] \right. \\ \left. - \lambda_5 [X_4 T_{122} + X_5 T_{222} + X_6 T_{322}] - \lambda_6 [X_4 T_{132} + X_5 T_{232} + X_6 T_{332}] \right\} \quad (A-23)$$

$$\lambda_3' = - \left\{ \lambda_1 T_{13} + \lambda_2 T_{23} + \lambda_3 T_{33} - \lambda_4 [X_4 T_{113} + X_5 T_{213} + X_6 T_{313}] \right. \\ \left. - \lambda_5 [X_4 T_{123} + X_5 T_{223} + X_6 T_{323}] - \lambda_6 [X_4 T_{133} + X_5 T_{233} + X_6 T_{333}] \right\} \quad (A-24)$$

$$\lambda_4' = -K_4 X_4 + \lambda_4 T_{44} + \lambda_5 T_{45} + \lambda_6 T_{46} \quad (A-25)$$

$$\lambda_5' = -K_5 X_5 + \lambda_4 T_{54} + \lambda_5 T_{55} + \lambda_6 T_{56} \quad (A-26)$$

$$\lambda_6' = -K_6 X_6 + \lambda_4 T_{64} + \lambda_5 T_{65} + \lambda_6 T_{66} \quad (A-27)$$

where  $T_{11} = 0 \quad (A-28)$

$$T_{12} = 0 \quad (A-29)$$

$$T_{13} = - \frac{1}{\sin^2 X_3} \quad (A-30)$$

$$T_{21} = - \frac{2\mu}{X_1^3 X_2 \tan X_3} - \frac{2}{X_2 \sin X_3} C_{X1} U_0 - \frac{X_1}{X_2 \sin X_3} C_{X1X1} U_0 \quad (A-31)$$

$$T_{22} = - \frac{\mu}{X_1^2 X_2^2 \tan X_3} + \frac{X_1}{X_2^2 \sin X_3} C_{X1} U_0 + \frac{1}{X_2^2 \sin X_3} C U_0 \\ - \frac{X_1}{X_2 \sin X_3} C_{X1X2} U_0 - \frac{1}{X_2 \sin X_3} C_{X2} U_0 \quad (A-32)$$

$$T_{322} = \frac{6\mu}{X_1 X_2^4} + \frac{4X_1}{X_2^3 \sin X_3} C_{X2} U_L - \frac{6X_1}{X_2^4 \sin X_3} C U_L - \frac{X_1}{X_2^2 \sin X_3} C_{X2X2} U_L \quad (A-44)$$

$$T_{332} = -\frac{2X_1 \cos X_3}{X_2^3 \sin^2 X_3} C U_L + \frac{X_1 \cos X_3}{X_2^2 \sin^2 X_3} C_{X2} U_L \quad (A-45)$$

$$T_{113} = -\frac{1}{\sin^2 X_3} \quad (A-46)$$

$$T_{123} = 0 \quad (A-47)$$

$$T_{133} = \frac{2X_1 \cos X_3}{\sin^3 X_3} \quad (A-48)$$

$$T_{213} = -\frac{\mu}{X_1^2 X_2 \sin^2 X_3} + \frac{\cos X_3}{X_2 \sin^2 X_3} C U_0 + \frac{X_1 \cos X_3}{X_2 \sin^2 X_3} C_{X1} U_0 \quad (A-49)$$

$$T_{223} = -\frac{\mu}{X_1 X_2^2 \sin^2 X_3} - \frac{X_1 \cos X_3}{X_2^2 \sin^2 X_3} C U_0 + \frac{X_1 \cos X_3}{X_2 \sin^2 X_3} C_{X2} U_0 \quad (A-50)$$

$$T_{233} = -\frac{2\mu \cos X_3}{X_1 X_2 \sin^3 X_3} - \frac{2X_1 \cos^2 X_3}{X_2 \sin^3 X_3} C U_0 - \frac{X_1}{X_2 \sin X_3} C U_0 \quad (A-51)$$

$$T_{313} = \frac{\cos X_3}{X_2^2 \sin^2 X_3} C U_L + \frac{X_1 \cos X_3}{X_2^2 \sin^2 X_3} C_{X1} U_L \quad (A-52)$$

$$T_{323} = -\frac{2X_1 \cos X_3}{X_2^3 \sin^2 X_3} C U_L + \frac{X_1 \cos X_3}{X_2^2 \sin^2 X_3} C_{X2} U_L \quad (A-53)$$

$$T_{333} = -\frac{2X_1 \cos^2 X_3}{X_2^2 \sin^3 X_3} C U_L - \frac{X_1}{X_2^2 \sin X_3} C U_L \quad (A-54)$$

$$\text{where } C_{X1X1} = -\frac{X_2^3}{\partial^2} \frac{\partial \rho}{\partial X_1} \frac{\partial C_{PS}}{\partial M} \frac{\partial \theta}{\partial X_1} \quad (A-55)$$

$$C_{X1X2} = X_2 C_{PS} \frac{\partial \rho}{\partial X_1} - \frac{\rho X_2^2}{\partial^2} \frac{\partial C_{PS}}{\partial M} \frac{\partial \theta}{\partial X_1} + \frac{X_2^2}{2\theta} \frac{\partial C_{PS}}{\partial M} \frac{\partial \rho}{\partial X_1} \quad (A-56)$$

$$C_{X2X2} = \rho C_{PS} + \frac{2\rho X_2}{\theta} \frac{\partial C_{PS}}{\partial M} \quad (A-57)$$

GRADIENT

$$\begin{aligned}
 &K_{u_0} u_0 - \lambda_2 \frac{X_1 C}{X_2 \sin X_3} + \lambda_4 \frac{X_5}{X_2 \sin X_3} \left[ C + X_1 C_{X1} \right] \\
 &- \lambda_5 \frac{X_1 X_5}{X_2^2 \sin X_3} \left[ C - X_2 C_{X2} \right] - \lambda_6 \frac{X_1 X_5 C (\cos X_3)}{X_2 \sin^2 X_3} = 0 \triangleq G_1 \quad (A-58)
 \end{aligned}$$

$$\begin{aligned}
 &K_{u_L} u_L - \lambda_3 \frac{X_1 C}{X_2^2 \sin X_3} + \lambda_4 \frac{X_6}{X_2^2 \sin X_3} \left[ C + X_1 C_{X1} \right] \\
 &- \lambda_5 \frac{X_1 X_6}{X_2^3 \sin X_3} \left[ 2C - X_2 C_{X2} \right] - \lambda_6 \frac{X_1 X_6 C (\cos X_3)}{X_2^2 \sin^2 X_3} = 0 \triangleq G_2 \quad (A-59)
 \end{aligned}$$

DERIVATIVES OF GRADIENT

$$\left[ \frac{\partial G}{\partial u} \right]^{-1} = \begin{bmatrix} 1 & 0 \\ K_{u_0} & \\ 0 & \\ & 1 \\ & & K_{u_L} \end{bmatrix} \quad (A-60)$$

$$\frac{\partial G_i}{\partial \lambda_j} \triangleq G_{\lambda ij} \quad (A-61)$$

$$G_{\lambda 11} = 0 \quad (A-62)$$

$$G_{\lambda 12} = - \frac{X_1 C}{X_2 \sin X_3} \quad (A-63)$$

$$G_{\lambda 13} = 0 \quad (A-64)$$

$$G_{\lambda 14} = \frac{X_5}{X_2 \sin X_3} \left[ C + X_1 C_{X1} \right] \quad (A-65)$$

$$G_{\lambda 15} = - \frac{X_1 X_5}{X_2^2 \sin X_3} \left[ C - X_2 C_{X2} \right] \quad (A-66)$$

$$G_{\lambda 16} = - \frac{X_1 X_5 C (\cos X_3)}{X_2 \sin^2 X_3} \quad (A-67)$$

$$G\lambda_{21} = 0 \quad (A-68)$$

$$G\lambda_{22} = 0 \quad (A-69)$$

$$G\lambda_{23} = -\frac{X_1 C}{X_2 \sin X_3} \quad (A-70)$$

$$G\lambda_{24} = \frac{X_1 X_5}{X_2^2 \sin X_3} [C + X_1 C_{X1}] \quad (A-71)$$

$$G\lambda_{25} = -\frac{X_1 X_5}{X_2^3 \sin X_3} [2C - X_2 C_{X2}] \quad (A-72)$$

$$G\lambda_{26} = \frac{X_1 X_5 C (\cos X_2)}{X_2^2 \sin^2 X_3} \quad (A-73)$$

$$\frac{\partial G_i}{\partial X_j} \equiv GX_{ij} \quad (A-74)$$

$$GX_{11} = -\frac{\lambda_2}{X_2 \sin X_3} [C + X_1 C_{X1}] + \frac{\lambda_4 X_5}{X_2 \sin X_3} [2C_{X1} + X_1 C_{X1X1}]$$

$$- \frac{\lambda_5 X_5}{X_2^2 \sin X_3} [C + X_1 C_{X1} - X_1 X_2 C_{X1X2} - X_2 C_{X2}] - \frac{\lambda_6 X_5 \cos X_2}{X_2 \sin^2 X_3} [C + X_1 C_{X1}] \quad (A-75)$$

$$GX_{12} = \frac{\lambda_2 X_1}{X_2^2 \sin X_3} [C - X_2 C_{X2}] - \frac{\lambda_4 X_5}{X_2^2 \sin X_3} [C + X_1 C_{X1} - X_2 C_{X2} - X_1 X_2 C_{X1X2}]$$

$$+ \frac{\lambda_5 X_1 X_5}{X_2^3 \sin X_3} [2C - 2X_2 C_{X2} + X_2^2 C_{X2X2}] + \frac{\lambda_6 X_1 X_5 \cos X_2}{X_2^2 \sin^2 X_3} [C - X_2 C_{X2}] \quad (A-76)$$

$$GX_{13} = \frac{\lambda_2 X_1 C (\cos X_2)}{X_2 \sin^2 X_3} - \frac{\lambda_4 X_5 \cos X_2}{X_2 \sin^2 X_3} [C + X_1 C_{X1}]$$

$$- \frac{\lambda_5 X_1 X_5 \cos X_2}{X_2^2 \sin^2 X_3} [C - X_2 C_{X2}] + \frac{\lambda_6 X_1 X_5 (1 + \cos^2 X_2)}{X_2 \sin^3 X_3} \quad (A-77)$$

$$\begin{aligned}
 GX21 = & -\frac{\lambda_3}{X_2^2 \sin X_3} [C + X_1 C_{x1}] + \frac{\lambda_4 X_6}{X_2^2 \sin X_3} [2C_{x1} + X_1 C_{x1x1}] \\
 & -\frac{\lambda_5 X_6}{X_2^2 \sin X_3} [2C + 2X_1 C_{x1} - X_2 C_{x2} - X_1 X_2 C_{x1x2}] \\
 & -\frac{\lambda_6 X_6 \cos X_3}{X_2^2 \sin^2 X_3} [C + X_1 C_{x1}] \quad (A-78)
 \end{aligned}$$

$$\begin{aligned}
 GX22 = & \frac{\lambda_2 X_1}{X_2^3 \sin X_3} [2C - X_2 C_{x2}] - \frac{\lambda_4 X_6}{X_2^3 \sin X_3} [2C + 2X_1 C_{x1} - X_2 C_{x2} - X_1 X_2 C_{x1x2}] \\
 & + \frac{\lambda_5 X_1 X_6}{X_2^4 \sin X_3} [6C - 4X_2 C_{x2} + X_2^2 C_{x2x2}] + \frac{\lambda_6 X_1 X_6 \cos X_3}{X_2^3 \sin^2 X_3} [2C - X_2 C_{x2}] \quad (A-79)
 \end{aligned}$$

$$\begin{aligned}
 GX23 = & \frac{\lambda_3 X_1 C (\cos X_3)}{X_2^2 \sin^2 X_3} - \frac{\lambda_4 X_6 \cos X_3}{X_2^2 \sin^2 X_3} [C + X_1 C_{x1}] \\
 & + \frac{\lambda_5 X_1 X_6 \cos X_3}{X_2^3 \sin^2 X_3} [2C - X_2 C_{x2}] + \frac{\lambda_6 X_1 X_6 C (1 + \cos^2 X_3)}{X_2^2 \sin^3 X_3} \quad (A-80)
 \end{aligned}$$

$$GX14 = 0 \quad (A-81)$$

$$GX15 = \frac{\lambda_4}{X_2 \sin X_3} [C + X_1 C_{x1}] - \frac{\lambda_5 X_1}{X_2^2 \sin X_3} [C - X_2 C_{x2}] - \frac{\lambda_6 X_1 C (\cos X_3)}{X_2 \sin^2 X_3} \quad (A-82)$$

$$GX16 = 0 \quad (A-83)$$

$$GX24 = 0 \quad (A-84)$$

$$GX25 = 0 \quad (A-85)$$

$$GX26 = \frac{\lambda_4}{X_2^2 \sin X_3} [C + X_1 C_{x1}] - \frac{\lambda_5 X_1}{X_2^3 \sin X_3} [2C - X_2 C_{x2}] - \frac{\lambda_6 X_1 C (\cos X_3)}{X_2^2 \sin^2 X_3} \quad (A-86)$$

DERIVATIVES OF  $\lambda'$ 

$$\left[ \frac{\partial \lambda'}{\partial \mu} \right] = - \left[ \frac{\partial G}{\partial \mu} \right]^T \quad (A-87)$$

$$\left[ \frac{\partial \lambda'}{\partial \lambda} \right] = - \left[ \frac{\partial E}{\partial \lambda} \right]^T \quad (A-88)$$

$$T_{ijkl} \triangleq \frac{\partial T_{ijk}}{\partial x_l} \quad (A-89)$$

$$\frac{\partial \lambda'_i}{\partial x_j} = \frac{\partial \lambda'_j}{\partial x_i} \quad (A-90)$$

$$PDX_{ij} \triangleq \frac{\partial \lambda'_i}{\partial x_j} \quad (A-91)$$

$$PDX_{11} = - \left\{ \lambda_1 \overset{\circ}{V}_{111} + \lambda_2 T_{211} + \lambda_3 T_{311} - \lambda_4 [X_4 \overset{\circ}{V}_{111} + X_5 T_{211} + X_6 T_{311}] \right. \\ \left. - \lambda_5 [X_4 \overset{\circ}{V}_{211} + X_5 T_{221} + X_6 T_{321}] - \lambda_6 [X_4 \overset{\circ}{V}_{311} + X_5 T_{231} + X_6 T_{331}] \right\} \quad (A-92)$$

$$PDX_{12} = - \left\{ \lambda_1 \overset{\circ}{V}_{112} + \lambda_2 T_{212} + \lambda_3 T_{312} - \lambda_4 [X_4 \overset{\circ}{V}_{112} + X_5 T_{212} + X_6 T_{312}] \right. \\ \left. - \lambda_5 [X_4 \overset{\circ}{V}_{212} + X_5 T_{222} + X_6 T_{322}] - \lambda_6 [X_4 \overset{\circ}{V}_{312} + X_5 T_{232} + X_6 T_{332}] \right\} \quad (A-93)$$

$$PDX_{13} = - \left\{ \lambda_1 T_{113} + \lambda_2 T_{213} + \lambda_3 T_{313} - \lambda_4 [X_4 \overset{\circ}{V}_{113} + X_5 T_{213} + X_6 T_{313}] \right. \\ \left. - \lambda_5 [X_4 \overset{\circ}{V}_{213} + X_5 T_{223} + X_6 T_{323}] - \lambda_6 [X_4 T_{133} + X_5 T_{233} + X_6 T_{333}] \right\} \quad (A-94)$$

$$PDX_{14} = \lambda_4 \overset{\circ}{V}_{111} + \lambda_5 \overset{\circ}{V}_{121} + \lambda_6 T_{131} \quad (A-95)$$

$$PDX_{15} = \lambda_4 T_{211} + \lambda_5 T_{221} + \lambda_6 T_{231} \quad (A-96)$$

$$PDX_{16} = \lambda_4 T_{311} + \lambda_5 T_{321} + \lambda_6 T_{331} \quad (A-97)$$



$$\begin{aligned}
 PDX_{22} = & - \left\{ \lambda_1 \overset{\circ}{T}_{122} + \lambda_2 T_{222} + \lambda_3 T_{322} - \lambda_4 [\lambda_4 \overset{\circ}{T}_{1122} + \lambda_5 T_{2122} + \lambda_6 T_{3122}] \right. \\
 & \left. - \lambda_5 [\lambda_4 \overset{\circ}{T}_{1222} + \lambda_5 T_{2222} + \lambda_6 T_{3222}] - \lambda_6 [\lambda_4 \overset{\circ}{T}_{1222} + \lambda_5 T_{2222} + \lambda_6 T_{3222}] \right\} \quad (A-98)
 \end{aligned}$$

$$\begin{aligned}
 PDX_{23} = & - \left\{ \lambda_1 \overset{\circ}{T}_{123} + \lambda_2 T_{223} + \lambda_3 T_{323} - \lambda_4 [\lambda_4 \overset{\circ}{T}_{1123} + \lambda_5 T_{2123} + \lambda_6 T_{3123}] \right. \\
 & \left. - \lambda_5 [\lambda_4 \overset{\circ}{T}_{1223} + \lambda_5 T_{2223} + \lambda_6 T_{3223}] - \lambda_6 [\lambda_4 \overset{\circ}{T}_{1223} + \lambda_5 T_{2223} + \lambda_6 T_{3223}] \right\} \quad (A-99)
 \end{aligned}$$

$$PDX_{24} = \lambda_4 \overset{\circ}{T}_{112} + \lambda_5 \overset{\circ}{T}_{122} + \lambda_6 \overset{\circ}{T}_{132} = 0 \quad (A-100)$$

$$PDX_{25} = \lambda_4 T_{212} + \lambda_5 T_{222} + \lambda_6 T_{232} \quad (A-101)$$

$$PDX_{26} = \lambda_4 T_{312} + \lambda_5 T_{322} + \lambda_6 T_{332} \quad (A-102)$$

$$\begin{aligned}
 PDX_{33} = & - \left\{ \lambda_1 T_{133} + \lambda_2 T_{233} + \lambda_3 T_{333} - \lambda_4 [\lambda_4 T_{1133} + \lambda_5 T_{2133} + \lambda_6 T_{3133}] \right. \\
 & \left. - \lambda_5 [\lambda_4 \overset{\circ}{T}_{1233} + \lambda_5 T_{2233} + \lambda_6 T_{3233}] - \lambda_6 [\lambda_4 \overset{\circ}{T}_{1233} + \lambda_5 T_{2233} + \lambda_6 T_{3233}] \right\} \quad (A-103)
 \end{aligned}$$

$$PDX_{34} = \lambda_4 T_{113} + \lambda_5 T_{123} + \lambda_6 T_{133} \quad (A-104)$$

$$PDX_{35} = \lambda_4 T_{213} + \lambda_5 T_{223} + \lambda_6 T_{233} \quad (A-105)$$

$$PDX_{36} = \lambda_4 T_{313} + \lambda_5 T_{323} + \lambda_6 T_{333} \quad (A-106)$$

$$PDX_{44} = -K_4 \quad (A-107)$$

$$PDX_{45} = 0 \quad (A-108)$$

$$PDX_{46} = 0 \quad (A-109)$$

$$PDX_{55} = -K_5 \quad (A-110)$$

$$PDX_3 = 0 \quad (A-111)$$

$$PDX_4 = -K_6 \quad (A-112)$$

where

$$T_{211} = \frac{6K}{X_1^4 X_2 \tan X_3} - \frac{3}{X_2 \sin X_3} C_{X11} U_0 - \frac{X_1}{X_2 \sin X_3} C_{X111} U_0 \quad (A-113)$$

$$T_{311} = -\frac{6K}{X_1^3 X_2^3} - \frac{3}{X_2^2 \sin X_3} C_{X11} U_L - \frac{X_1}{X_2^2 \sin X_3} C_{X111} U_L \quad (A-114)$$

$$T_{221} = \frac{2K}{X_1^3 X_2^2 \tan X_3} + \frac{2}{X_2^2 \sin X_3} C_{X11} U_0 + \frac{X_1}{X_2^2 \sin X_3} C_{X111} U_0 \\ - \frac{2}{X_2 \sin X_3} C_{X112} U_0 - \frac{X_1}{X_2 \sin X_3} C_{X1112} U_0 \quad (A-115)$$

$$T_{321} = -\frac{4K}{X_1^3 X_2^3} + \frac{4}{X_2^3 \sin X_3} C_{X11} U_L + \frac{2X_1}{X_2^3 \sin X_3} C_{X111} U_L \\ - \frac{2}{X_2^2 \sin X_3} C_{X112} U_L - \frac{X_1}{X_2^2 \sin X_3} C_{X1112} U_L \quad (A-116)$$

$$T_{221} = \frac{2K}{X_1^3 X_2 \sin^2 X_3} + \frac{2 \cos X_3}{X_2 \sin^2 X_3} C_{X11} U_0 + \frac{X_1 \cos X_3}{X_2 \sin^2 X_3} C_{X111} U_0 \quad (A-117)$$

$$T_{321} = \frac{2 \cos X_3}{X_2^2 \sin^2 X_3} C_{X11} U_L + \frac{X_1 \cos X_3}{X_2^2 \sin^2 X_3} C_{X111} U_L \quad (A-118)$$

$$T_{212} = \frac{2K}{X_1^3 X_2^2 \tan X_3} + \frac{2}{X_2^2 \sin X_3} C_{X11} U_0 - \frac{2}{X_2 \sin X_3} C_{X112} U_0 \\ - \frac{X_1}{X_2^2 \sin X_3} C_{X111} U_0 - \frac{X_1}{X_2 \sin X_3} C_{X1112} U_0 \quad (A-119)$$

$$T_{312} = -\frac{6K}{X_1^3 X_2^4} + \frac{4}{X_2^3 \sin X_3} C_{X11} U_L - \frac{2}{X_2^2 \sin X_3} C_{X112} U_L \\ + \frac{2X_1}{X_2^3 \sin X_3} C_{X111} U_L - \frac{X_1}{X_2^2 \sin X_3} C_{X1112} U_L \quad (A-120)$$

$$T_{222} = \frac{2K_1}{X_1^2 X_2^3 \tan X_3} - \frac{2X_1}{X_2^3 \sin X_3} C_{X1} U_0 + \frac{2X_1}{X_2^2 \sin X_3} C_{X1X2} U_0$$

$$- \frac{2}{X_2^3 \sin X_3} C U_0 + \frac{2}{X_2^2 \sin X_3} C_{X2} U_0 - \frac{X_1}{X_2 \sin X_3} C_{X1X2X2} U_0$$

$$- \frac{1}{X_2 \sin X_3} C_{X2X2} U_0 \quad (A-121)$$

$$T_{222} = - \frac{6U_1}{X_1^2 X_2^4} - \frac{6}{X_2^4 \sin X_3} C U_L + \frac{4}{X_2^3 \sin X_3} C_{X2} U_L$$

$$- \frac{6X_1}{X_2^4 \sin X_3} C_{X1} U_L + \frac{4X_1}{X_2^3 \sin X_3} C_{X1X2} U_L - \frac{X_1}{X_2 \sin X_3} C_{X1X2X2} U_L$$

$$- \frac{1}{X_2^2 \sin X_3} C_{X2X2} U_L \quad (A-122)$$

$$T_{222} = \frac{K_1}{X_1^2 X_2^2 \sin^2 X_3} - \frac{\cos X_3}{X_2^2 \sin^2 X_3} C U_0 + \frac{\cos X_3}{X_2 \sin^2 X_3} C_{X2} U_0$$

$$- \frac{X_1 \cos X_3}{X_2^2 \sin^2 X_3} C_{X1} U_0 + \frac{X_1 \cos X_3}{X_2 \sin^2 X_3} C_{X1X2} U_0 \quad (A-123)$$

$$T_{222} = - \frac{2 \cos X_3}{X_2^3 \sin^2 X_3} C U_L + \frac{\cos X_3}{X_2^2 \sin^2 X_3} C_{X2} U_L - \frac{2X_1 \cos X_3}{X_2^3 \sin^2 X_3} C_{X1} U_L$$

$$+ \frac{X_1 \cos X_3}{X_2 \sin^2 X_3} C_{X1X2} U_L \quad (A-124)$$

$$T_{222} = \frac{2K_1}{X_1^2 X_2^3 \tan X_3} + \frac{2}{X_2^2 \sin X_3} C_{X2} U_0 - \frac{2}{X_2^3 \sin X_3} C U_0$$

$$- \frac{1}{X_2 \sin X_3} C_{X2X2} U_0 + \frac{2X_1}{X_2^2 \sin X_3} C_{X1X2} U_0$$

$$- \frac{X_1}{X_2 \sin X_3} C_{X1X2X2} U_0 - \frac{2X_1}{X_2^3 \sin X_3} C_{X1} U_0 \quad (A-125)$$

$$\begin{aligned}
 T_{3122} = & -\frac{6\mu}{X_1^2 X_2^4} + \frac{4}{X_2^3 \sin X_3} C_{x2} U_L - \frac{6}{X_2^4 \sin X_3} C U_L \\
 & - \frac{1}{X_2^2 \sin X_3} C_{x2x2} U_L + \frac{4X_1}{X_2^3 \sin X_3} C_{x1x2} U_L \\
 & - \frac{X_1}{X_2^2 \sin X_3} C_{x1x2x2} U_L - \frac{6X_1}{X_2^4 \sin X_3} C_{x1} U_L
 \end{aligned} \tag{A-126}$$

$$\begin{aligned}
 T_{2222} = & \frac{6\mu}{X_1 X_2^4 \tan X_3} - \frac{6X_1}{X_2^3 \sin X_3} C_{x2} U_0 + \frac{6X_1}{X_2^4 \sin X_3} C U_0 \\
 & + \frac{3X_1}{X_2^2 \sin X_3} C_{x2x2} U_0 - \frac{X_1}{X_2 \sin X_3} C_{x2x2x2} U_0
 \end{aligned} \tag{A-127}$$

$$\begin{aligned}
 T_{3222} = & -\frac{24\mu}{X_1 X_2^5} - \frac{18X_1}{X_2^4 \sin X_3} C_{x2} U_L + \frac{6X_1}{X_2^3 \sin X_3} C_{x2x2} U_L \\
 & - \frac{24X_1}{X_2^5 \sin X_3} C U_L - \frac{X_1}{X_2^2 \sin X_3} C_{x2x2x2} U_L
 \end{aligned} \tag{A-128}$$

$$\begin{aligned}
 T_{2222} = & \frac{2\mu}{X_1 X_2^3 \sin^4 X_3} - \frac{2X_1 \cos X_3}{X_2^2 \sin^4 X_3} C_{x2} U_0 + \frac{2X_1 \cos X_3}{X_2^3 \sin^4 X_3} C U_0 \\
 & + \frac{X_1 \cos X_3}{X_2 \sin^2 X_3} C_{x2x2} U_0
 \end{aligned} \tag{A-129}$$

$$T_{3222} = -\frac{4X_1 \cos X_3}{X_2^3 \sin^2 X_3} C_{x2} U_L + \frac{6X_1 \cos X_3}{X_2^4 \sin^2 X_3} C U_L + \frac{X_1 \cos X_3}{X_2^2 \sin^2 X_3} C_{x2x2} U_L \tag{A-130}$$

$$T_{1313} = \frac{2 \cos X_3}{\sin^3 X_3} \tag{A-131}$$

$$T_{2113} = \frac{2\mu}{X_1^3 X_2 \sin^4 X_3} + \frac{2 \cos X_3}{X_2 \sin^2 X_3} C_{x1} U_0 + \frac{X_1 \cos X_3}{X_2 \sin^2 X_3} C_{x1x1} U_0 \tag{A-132}$$

$$\begin{aligned}
 T_{2213} = & \frac{\mu}{X_1^2 X_2^2 \sin^2 X_3} - \frac{X_1 \cos X_3}{X_2^2 \sin^2 X_3} C_{x1} U_0 - \frac{\cos X_3}{X_2^2 \sin^2 X_3} C U_0 \\
 & + \frac{X_1 \cos X_3}{X_2 \sin^2 X_3} C_{x1x2} U_0 + \frac{\cos X_3}{X_2 \sin X_3} C_{x2} U_0
 \end{aligned} \tag{A-133}$$

$$T_{2313} = \frac{2\mu \cos X_3}{X_1^2 X_2 \sin^3 X_3} - \frac{(1 + \cos^2 X_3)}{X_2 \sin^3 X_3} C U_0 - \frac{X_1 (1 + \cos^2 X_3)}{X_2 \sin^3 X_3} C_{x1} U_0 \tag{A-134}$$

$$T_{3113} = \frac{2 \cos X_3}{X_2^2 \sin^2 X_3} C_{x1} u_L + \frac{X_1 \cos X_3}{X_2^2 \sin^2 X_3} C_{x1x1} u_L \quad (A-135)$$

$$T_{3213} = -\frac{2 \cos X_3}{X_2^3 \sin^2 X_3} C u_L - \frac{2X_1 \cos X_3}{X_2^3 \sin^2 X_3} C_{x1} u_L + \frac{X_1 \cos X_3}{X_2^2 \sin^2 X_3} C_{x1x2} u_L \\ + \frac{\cos X_3}{X_2^2 \sin^2 X_3} C_{x2} u_L \quad (A-136)$$

$$T_{3313} = -\frac{(1 + \cos^2 X_3)}{X_2^2 \sin^3 X_3} C u_L - \frac{X_1 (1 + \cos^2 X_3)}{X_2^2 \sin^3 X_3} C_{x1} u_L \quad (A-137)$$

$$T_{2113} = \frac{\mu}{X_1^2 X_2^2 \sin^2 X_3} - \frac{\cos X_3}{X_2^2 \sin^2 X_3} C u_0 + \frac{\cos X_3}{X_2 \sin^2 X_3} C_{x2} u_0 \\ + \frac{X_1 \cos X_3}{X_2 \sin^2 X_3} C_{x1x2} u_0 - \frac{X_1 \cos X_3}{X_2^2 \sin^2 X_3} C_{x1} u_0 \quad (A-138)$$

$$T_{2213} = \frac{2\mu}{X_1 X_2^3 \sin^2 X_3} + \frac{2X_1 \cos X_3}{X_2^3 \sin^2 X_3} C u_0 - \frac{2X_1 \cos X_3}{X_2^2 \sin^2 X_3} C_{x2} u_0 \\ + \frac{X_1 \cos X_3}{X_2 \sin^2 X_3} C_{x2x2} u_0 \quad (A-139)$$

$$T_{2313} = \frac{2\mu \cos X_3}{X_1 X_2^2 \sin^3 X_3} + \frac{X_1 (1 + \cos^2 X_3)}{X_2^2 \sin^3 X_3} C u_0 - \frac{X_1 (1 + \cos^2 X_3)}{X_2 \sin^3 X_3} C_{x2} u_0 \quad (A-140)$$

$$T_{3123} = -\frac{2 \cos X_3}{X_2^3 \sin^2 X_3} C u_L + \frac{\cos X_3}{X_2^2 \sin^2 X_3} C_{x2} u_L + \frac{X_1 \cos X_3}{X_2^2 \sin^2 X_3} C_{x1x2} u_L \\ - \frac{2X_1 \cos X_3}{X_2^3 \sin^2 X_3} C_{x1} u_L \quad (A-141)$$

$$T_{3223} = -\frac{4X_1 \cos X_3}{X_2^3 \sin^2 X_3} C_{x2} u_L + \frac{6X_1 \cos X_3}{X_2^4 \sin^2 X_3} C u_L + \frac{X_1 \cos X_3}{X_2^2 \sin^2 X_3} C_{x2x2} u_L \quad (A-142)$$

$$T_{3233} = \frac{2X_1 (1 + \cos^2 X_3)}{X_2^3 \sin^3 X_3} C u_L - \frac{X_1 (1 + \cos^2 X_3)}{X_2^2 \sin^3 X_3} C_{x2} u_L \quad (A-143)$$

$$T_{1133} = \frac{2 \cos X_3}{\sin^3 X_3} \quad (A-144)$$

$$T_{1333} = -\frac{2X_1 (1 + 2 \cos^2 X_3)}{\sin^4 X_3} \quad (A-145)$$

$$T_{2133} = \frac{2\mu \cos X_2}{X_1^2 X_2 \sin^3 X_3} - \frac{(1 + \cos^2 X_2)}{X_2 \sin^3 X_3} C_{110} - \frac{X_1 (1 + \cos^2 X_2)}{X_2 \sin^3 X_3} C_{X10} \quad (A-146)$$

$$T_{2233} = \frac{2\mu \cos X_2}{X_1 X_2^2 \sin^3 X_3} + \frac{X_1 (1 + \cos^2 X_2)}{X_2^2 \sin^3 X_3} C_{110} - \frac{X_1 (1 + \cos^2 X_2)}{X_2^2 \sin^3 X_3} C_{X20} \quad (A-147)$$

$$T_{2333} = \frac{2\mu (1 + 2 \cos^2 X_2)}{X_1 X_2 \sin^4 X_3} + \frac{2X_1 \cos X_2 (2 + \cos^2 X_2)}{X_2 \sin^4 X_3} C_{110} + \frac{X_1 \cos X_2}{X_2 \sin^2 X_3} C_{110} \quad (A-148)$$

$$T_{3133} = -\frac{(1 + \cos^2 X_2)}{X_2^2 \sin^3 X_3} C_{11L} - \frac{X_1 (1 + \cos^2 X_2)}{X_2^2 \sin^3 X_3} C_{X1L} \quad (A-149)$$

$$T_{3233} = \frac{2X_1 (1 + \cos^2 X_2)}{X_2^3 \sin^3 X_3} C_{11L} - \frac{X_1 (1 + \cos^2 X_2)}{X_2^2 \sin^3 X_3} C_{X2L} \quad (A-150)$$

$$T_{3333} = \frac{2X_1 \cos X_2 (2 + \cos^2 X_2)}{X_2^2 \sin^4 X_3} C_{11L} + \frac{X_1 \cos X_2}{X_2^2 \sin^2 X_3} C_{11L} \quad (A-151)$$

where

$$C_{X1X1} = 0 \quad (A-152)$$

$$C_{X1X1X2} = 2X_2 \frac{\partial \rho}{\partial X_1} \frac{\partial C_{PS}}{\partial M} \frac{\partial M}{\partial \theta} \frac{\partial \theta}{\partial X_1} \quad (A-153)$$

$$C_{X1X2X2} = C_{PS} \frac{\partial \rho}{\partial X_1} + \rho \frac{\partial C_{PS}}{\partial M} \frac{\partial M}{\partial \theta} \frac{\partial \theta}{\partial X_1} + \frac{2X_2}{\theta} \frac{\partial C_{PS}}{\partial M} \frac{\partial \rho}{\partial X_1} - \frac{2\rho X_2}{\theta^2} \frac{\partial C_{PS}}{\partial M} \frac{\partial \theta}{\partial X_1} \quad (A-154)$$

$$C_{X2X2X2} = \frac{3\rho}{\theta} \frac{\partial C_{PS}}{\partial M} \quad (A-155)$$

DERIVATIVES OF E(X, Y)

(A-56)

$T_{11}$	0	$T_{13}$	0	0	0	0
$T_{21}$	$T_{22}$	$T_{23}$	0	0	0	0
$T_{31}$	$T_{32}$	$T_{33}$	0	0	0	0
$-X_4 T_{11} - X_5 T_{211}$	$-X_4 T_{12} - X_5 T_{212}$	$-X_4 T_{13} - X_5 T_{213}$	$-T_{11}$	$-T_{21}$	$-T_{31}$	
$-X_6 T_{311}$	$-X_6 T_{312}$	$-X_6 T_{313}$				
$-X_4 T_{21} - X_5 T_{221}$	$-X_4 T_{22} - X_5 T_{222}$	$-X_4 T_{23} - X_5 T_{223}$	0	$-T_{22}$	$-T_{32}$	
$-X_6 T_{321}$	$-X_6 T_{322}$	$-X_6 T_{323}$				
$-X_4 T_{31} - X_5 T_{331}$	$-X_4 T_{32} - X_5 T_{332}$	$-X_4 T_{33} - X_5 T_{333}$	$-T_{13}$	$-T_{23}$	$-T_{33}$	
$-X_6 T_{331}$	$-X_6 T_{332}$	$-X_6 T_{333}$				

$$\left[ \frac{\partial E}{\partial X} \right] =$$

$$FU_{ij} \triangleq \frac{\partial F_i}{\partial u_j} \quad (A-157)$$

$$FU_{11} = 0 \quad (A-158)$$

$$FU_{12} = 0 \quad (A-159)$$

$$FU_{21} = - \frac{X_1 C}{X_2 \sin X_3} \quad (A-160)$$

$$FU_{22} = 0 \quad (A-161)$$

$$FU_{31} = 0 \quad (A-162)$$

$$FU_{32} = - \frac{X_1 C}{X_2^2 \sin X_3} \quad (A-163)$$

$$FU_{41} = \frac{X_5}{X_2 \sin X_3} [C + X_1 C_{x1}] \quad (A-164)$$

$$FU_{42} = \frac{X_6}{X_2^2 \sin X_3} [C + X_1 C_{x1}] \quad (A-165)$$

$$FU_{51} = - \frac{X_1 X_5}{X_2^2 \sin X_3} [C - X_2 C_{x2}] \quad (A-166)$$

$$FU_{52} = - \frac{X_1 X_6}{X_2^3 \sin X_3} [2C - X_2 C_{x2}] \quad (A-167)$$

$$FU_{61} = - \frac{X_1 X_5 \cos X_3}{X_2^2 \sin^2 X_3} C \quad (A-168)$$

$$FU_{62} = - \frac{X_1 X_6 \cos X_3}{X_2^2 \sin^2 X_3} C \quad (A-169)$$

$$END \Rightarrow BEER \quad (A-170)$$



Appendix B

Parameters for a Sample Trajectory

The purpose of this appendix is to present some sample parameters to be used in starting a trajectory solution. The general criterion function for the entry problem is (no control bias included):

$$J = \frac{1}{2} \int_{\sigma_0}^{\sigma_f} [K_4 X_4^2 + K_5 X_5^2 + K_6 X_6^2 + K_{u_D} U_D^2 + K_{u_L} U_L^2] d\sigma \quad (A-1)$$

For one particular case, that of Case 7 presented in Chapter V, the parameters after convergence are as follows:

$$K_4 = 1.0 \times 10^{-10}$$

$$K_5 = 1.0 \times 10^{-10}$$

$$K_6 = 1.0 \times 10^{-20}$$

$$K_{u_D} = 1.0 \times 10^3$$

$$K_{u_L} = 1.0 \times 10^3$$

No. Intervals = 150

$$\lambda_1(\sigma_0) = -0.21064992 \times 10^{-11}$$

$$\lambda_2(\sigma_0) = -0.21462654 \times 10^{-10}$$

$$\lambda_3(\sigma_0) = +0.59012141 \times 10^{-06}$$

$$\lambda_1(\sigma_f) = -0.53273489 \times 10^{-11}$$

$$\lambda_2(\sigma_f) = +0.26407696 \times 10^{-11}$$

$$\lambda_3(\sigma_f) = -0.56110516 \times 10^{-07}$$

$$\lambda_4(\sigma_f) = -0.59956528 \times 10^{-10}$$

$$\lambda_5(\sigma_f) = -0.54781552 \times 10^{-11}$$

$$\lambda_6(\sigma_f) = 0.83000869 \times 10^{-15}$$

Vita: Richard Eugene Holdeman

Richard Eugene Holdeman was born on November 30, 1937, in Dallas, Texas. He attended Will Rogers High School in Tulsa, Oklahoma and graduated in 1956. He then attended Oklahoma State University in Stillwater, Oklahoma, from 1956 until 1958, at which time he began work in a lumber yard. He attended West Texas State University in Canyon, Texas, from 1959 until his graduation in January, 1961, receiving a B.S. degree with majors in physics and mathematics. He was then employed by USAF civil service at Holloman AFB, New Mexico, as a guidance system performance analyst from 1961 until entrance into AFIT in 1968. Mr. Holdeman is a member of Tau Beta Pi, Eta Kappa Nu, Alpha Chi, Whos Who in American Colleges and Universities, and the American Institute of Aeronautics and Astronautics (AIAA). He is also co-author on two papers presented at the Symposium on Guidance Test at Holloman AFB, in 1966, and 1968.

Permanent Address: 600 Arnold Lane  
Alamogordo,  
New Mexico, 88310

Vita: Michael Walter Wynne

Michael Walter Wynne was born on 4 September 1944, in Hillsborough County, Florida, the son of Edward Patrick and Dorothy T. Wynne. His father was in service, and he moved several times prior to returning to Florida. He attended Melbourne High School, Melbourne, Florida, graduating in 1962. With only a month vacation, he entered the United States Military Academy that same year. He graduated in June 1966, receiving a Bachelor of Science Degree, and was immediately commissioned in the Air Force. He worked as a project engineer in charge of computer program procurement for the Secure Communications Project Office, Communications Directorate, Electronic Systems Division, Air Force Systems Command, from 1966 to June 1968. He entered the Air Force Institute of Technology as a resident student in July 1968.

Permanent Address: 305 Glenwood Ave.  
Satellite Beach,  
Florida, 32935

This thesis typed by Barbara Wynne.



14. KEY WORDS	LINK A		LINK B		LINK C	
	ROLE	WT	ROLE	WT	ROLE	WT
Optimization Optimal Control Entry Trajectories Reentry Trajectories Re-Entry Trajectories Sensitivity Coefficients Influence Coefficients Terminal Error Function Second Variation Kalman Filter Implicit Guidance Suboptimal Feedback Control						